ARMOUR RESEARCH FOUNDATION
of
ILLINOIS INSTITUTE OF TECHNOLOGY
Technology Center
Chicago 16, Illinois

ARF Project B 095
Subcontract No. 73-(14-432)
Prime Contract No. AT-11-1 GEN-14

TRANSFORMATIONS IN URANIUM-BASE ALLOYS

Summary Report
December 14, 1955 - March 31, 1957

for
Westinghouse Electric Corporation
Bettis Plant
Pittsburgh 30, Pennsylvania

June 28, 1957

ARMOUR RESEARCH FOUNDATION OF ILLINOIS INSTITUTE OF TECHNOLOGY

DISCLAIMER

DISCLAIMER

Portions of this document may be illegible in electronic image products. Images are produced from the best available original document.

TRANSFORMATIONS IN URANIUM-BASE ALLOYS

ABSTRACT

Transformation kinetics of binary U-Nb and ternary U-Nb-base alloys have been investigated. Additions included zirconium, chromium, titanium, silicon, nickel, ruthenium and vanadium. Encapsulated samples were given a homogenization anneal at 1000° or 1100°C, water-quenched from 900°C to retain the gamma phase, and reheated to temperatures between 360° and 600°C. The metastability of the gamma phase was examined by metallographic, hardness, resistometric, dilatometric and X-ray diffraction techniques.

The U-Nb system is characterized by a monotectoid decomposition of the high temperature gamma allotrope at about 645°C to form alpha and γ_2, a niobium-rich cubic structure. Decomposition in U-Nb and in most U-Nb-X alloys occurred by a continuous precipitation of alpha from the body-centered cubic gamma phase with a resultant enrichment in niobium of gamma until the equilibrium γ_2 composition was reached. In the U-Nb-Ti and U-Nb-V systems, alpha and γ_2 were co-precipitated. Annealing at 550° and 600°C produced decomposition products which, in most materials, originated at the grain boundaries; a fine precipitate which initiated throughout the matrix was observed at lower annealing temperatures.

Increasing the niobium content resulted in greatly increased stability. The following elements added to a U-Nb base were found to retard transformation of the gamma phase: zirconium, chromium, ruthenium and vanadium. Additions of titanium, silicon, and nickel produced alloys which were less stable than the U-Nb base to which they were added. Cold-working a U-7w/o Nb-2w/o Zr composition caused a more rapid transformation upon annealing at 360° and 450°C, and the resulting microstructures were different.

ARMOUR RESEARCH FOUNDATION OF ILLINOIS INSTITUTE OF TECHNOLOGY

Continuous cooling transformation studies were conducted on U-10w/o Nb materials, solution annealed at 700° and 950°C, and cooled at various linear rates to temperatures between 300° and 600°C. Cooling rates between 8.5° and 14.5°C per minute were required to prevent transformation of the gamma phase, depending upon the prior melting techniques and thermal history.

253-2

TABLE OF CONTENTS

LIST OF ILLUSTRATIONS

TRANSFORMATIONS IN URANIUM-BASE ALLOYS

I. INTRODUCTION

This report summarizes a major portion of the work performed during the interval December 14, 1955 to March 31, 1957 under Subcontract 73 - (14-432) for the Bettis Plant of Westinghouse Electric Corporation. The investigations reported herein include isothermal transformation and continuous cooling studies of uranium-base alloys. In addition, preliminary corrosion studies of these alloys were performed under this program; these results are presented in the separately classified Part II of this report.

A previous Foundation research program indicated the effectiveness of niobium additions to uranium in stabilizing the gamma phase [1]. The alloys selected for transformation kinetics studies consisted of eighteen U-Nb and U-Nb-X compositions. The effects of niobium and the various ternary additions to a U-Nb base on the metastability of the gamma phase were investigated at temperatures between 600° and 360°C. Hardness, metallographic, resistometric and dilatometric techniques were used to determine initiation of transformation in specimens which had been quenched from the gamma field to room temperature and reheated for varying lengths of time. X-ray diffraction studies were conducted to identify the phases present in the decomposition products and to compare mechanisms of transformation. The effects of cold work on transformation of a U-Nb-Zr alloy were studied by metallographic examination and hardness tests. Continuous cooling transformation studies were conducted on a U-10w/o Nb alloy to determine critical cooling rates required to prevent decomposition of the gamma phase.

ARMOUR RESEARCH FOUNDATION OF ILLINOIS INSTITUTE OF TECHNOLOGY

Material preparation and thermal treatments required the use of special techniques due to the toxic and reactive nature of uranium.

II. EXPERIMENTAL PROCEDURES

A. Materials

The alloys under investigation in this program were prepared from natural derby uranium, supplied by Westinghouse Electric Corporation in rod form about one inch in diameter. Some of this material was "warm" rolled prior to cutting into small pieces suitable for accurately weighed charges. A number of specimens were analyzed for carbon and other impurities. The samples contained 0.01 to 0.02w/o carbon, and the hydrogen content was in the range of 7 to 15 ppm. The alloy additions were made with high purity commercial grade materials as follows:

Alloy Addition	Form	Purity (w/o)
Niobium	Sintered bar (Grade 1)	~ 99.5
Zirconium	Iodide bar	99.9
Chromium	Electrolytic plate	99 +
Titanium	Sponge	99.7
Silicon	Purified Powder	99.8
Nickel	Pellets	99.9
Ruthenium	Powder	~ 99.5
Vanadium	Metal Chips	99.7

B. Preparation of Alloys

A nonconsumable tungsten electrode arc furnace was used for melting of the uranium-base alloys. The procedure described below yielded ingots which were homogeneous and free from contamination. The furnace atmosphere was tested by remelting small ingots of titanium; the uniform hardness of these control melts assured the absence of contamination. Two ingots of each

ARMOUR RESEARCH FOUNDATION OF ILLINOIS INSTITUTE OF TECHNOLOGY

Project No. B 095
Summary Report

composition, weighing 100 grams each, were first prepared using a 2-1/4 in. diameter, water-cooled copper crucible, and a helium atmosphere. Melting was accomplished using a current of 500 amperes at 40 volts and a melting time of about 3 minutes. The ingots were inverted and remelted four times. Following melting, the ingots were accurately weighed to insure that no contamination from electrode or crucible had occurred.

The two 100-gram ingots for each alloy were consolidated by melting in a 2-3/4 in. crucible, following the procedures described above. The resultant 200-gram "pancake" ingots, about 1/4 in. thick, were machined into test specimens for the various phases of these investigations.

Polished and etched sections of ingots were examined; the material was found to be uniform except for a thin layer containing a gray "slag" on the top surface. This layer was subsequently removed during machining of test specimens. Extremely small weight losses occurred during melting, indicating that compositions of the ingots were very close to nominal. Chemical analyses of the U-12.5w/o Nb and U-15w/o Nb alloys showed these materials to be of reasonably uniform composition. Four samples from the U-12.5w/o Nb alloy, taken from extreme portions of the ingot, ranged in niobium content from 12.43w/o to 12.74w/o; four samples from the U-15% Nb composition varied from 15.11w/o to 15.36w/o of niobium. All of the other minor alloying additions have been analyzed in ingots prepared for this and previous programs. In all cases, the material was homogeneous and close to the nominal composition.

C. Annealing Treatments

All of the materials were thermally homogenized prior to solution treatment. Because of the high temperatures used, the samples were wrapped in molybdenum foil and encapsulated in quartz or Vycor bulbs under an inert

atmosphere. For most compositions, a homogenization treatment of 24 hours at 1100°C produced microstructures free from coring and incipient melting. Alloys containing 3a/o chromium exhibited incipient melting at this temperature; these materials were successfully homogenized at 1000°C. The U-8w/o Nb-0.84w/o Ni composition showed melting at temperatures as low as 750°C, and no additional work was done on this alloy.

Following the homogenization anneal at 1100° or 1000°C, the samples were furnace cooled to the solution treating temperature of 900°C. After 24 hours at this temperature, the specimens were water quenched. In order to obtain more rapid cooling rates, the bulbs were broken during the quenching operation. This procedure resulted in retention of the metastable gamma phase. Samples for isothermal annealing treatments were also wrapped in molybdenum foil and encapsulated. Heat treatments requiring annealing times up to 100 hours were conducted in lead or lead-tin baths. For long-time annealing treatments, precision controlled resistance type tube furnaces were used. All specimens were water quenched following the annealing treatments.

Homogenization and annealing treatments differing from the above were employed in the continuous cooling studies and in the investigation of the effects of cold work on transformation. Descriptions of these operations will be included under the sections which discuss these phases of the program.

D. Metallographic Techniques

Specimens for metallographic examination were mounted in phenolic resin (Bakelite); the surface examined was a vertical section (top to bottom) of the ingot. Some additional solution-treated materials were also mounted in a plastic setting at room temperature to insure that the heat and pressure during Bakelite mounting had no effect on the microstructures.

Grinding was done on silicon carbide papers, with 120, 240, 320, 400 and 600 grits, water being the lubricant. Rough polishing was accomplished using Elgin Grade 9 diamond paste with kerosene on an A.B. Metcloth wheel. A second polishing operation utilized a 1 micron diamond paste on an A.B. Microcloth wheel, with kerosene as a lubricant. The final polishing operation consisted of a combined etch-polish with a 1% hydrofluoric acid solution and Linde B abrasive on a Microcloth wheel. This combination of chemical etching and mechanical polishing action was found to be effective in removing flowed metal from the surfaces of the samples. In addition, scratch-free surfaces were produced in less time than was required when water alone was the lubricant with the Linde B abrasive.

The etchant most commonly applied during these investigations was a solution of 10% CrO_3, 2% HF, and water. This chemical etchant was used at room temperature and produced satisfactory results for most of the transformation structures. An electrolytic etchant was also employed. The composition was 8 parts orthophosphoric acid, 5 parts ethylene glycol and 5 parts ethyl alcohol. A current density of about 30 ma/sq cm was found to be effective. The polished and etched metallographic samples also served for hardness determinations.

E. Resistometric Techniques

Significant changes of electrical resistivity occur upon transformation of the metastable gamma phase. Measurements of resistivity were taken at room temperature on machined samples which were approximately 2 in. long by 0.2 in. square. A schematic diagram of the apparatus is shown in Figure 1. The current-potential method was employed, using an accurately calibrated series standard resistance. Prior to measurements, the specimens were sanded
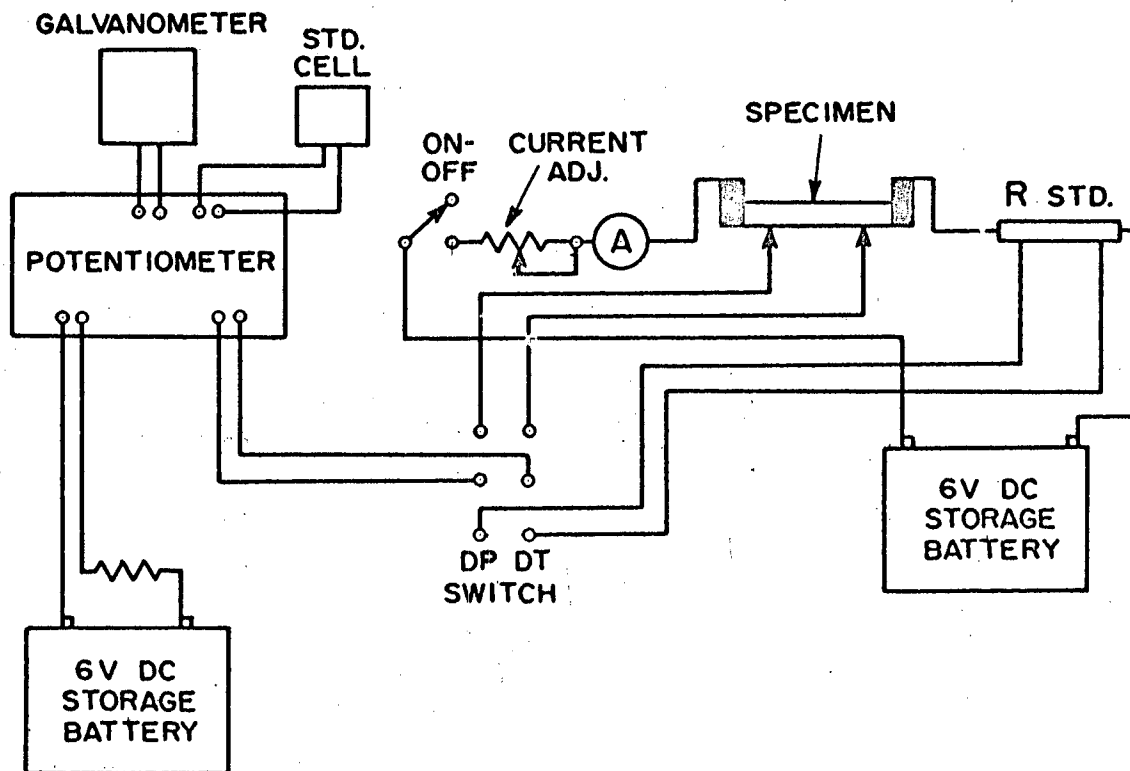
GALVANOMETER STD. CELL ON-OFF CURRENT ADJ. SPECIMEN R STD.

POTENTIOMETER

A

DP DT SWITCH

6V DC STORAGE BATTERY

6V DC STORAGE BATTERY

FIG. 1 — SCHEMATIC DIAGRAM OF RESISTIVITY APPARATUS

to remove any scale, and good contact with the copper knife edges was insured by spring-loading.

Resistivity values were first obtained for materials in the solution-treated and quenched condition. Four or more specimens were used for each composition, and variations in these solution-treated values for an alloy were very small. After isothermal annealing, resistivity measurements were taken, and the samples were re-solution-treated prior to subsequent annealing. Resistivity values on materials which had been transformed and re-solution-treated were found to be substantially constant. Several duplicate thermal treatments were conducted on specimens of the same alloy to insure the reproducibility of results.

F.   Dilatometric Techniques

The increase in density which accompanies transformation of the gamma phase was measured by dilatometric techniques. Figure 2 is a schematic diagram of the apparatus used to measure changes in length at the various annealing temperatures. Test specimens, approximately 2 in. long by 0.2 in. square were water quenched from 900°C to retain the metastable gamma phase. The sample was placed in the bottom of the outer tube; the inner quartz tube rested on top of the specimen and was free to move vertically. Due to the highly reactive nature of these uranium-base alloys, an inert atmosphere was provided. Helium gas, admitted through the inner tube, flowed out through the holes above the specimen and was exhausted through the small space between the two tubes. It was found that a flowing gas caused some oxidation due to the continuous introduction of small amounts of impurities. Much of this scaling was prevented by the use of a static atmosphere, which was obtained by means of the thin rubber seal illustrated in Figure 2. This arrangement permitted

ARMOUR RESEARCH FOUNDATION OF ILLINOIS INSTITUTE OF TECHNOLOGY
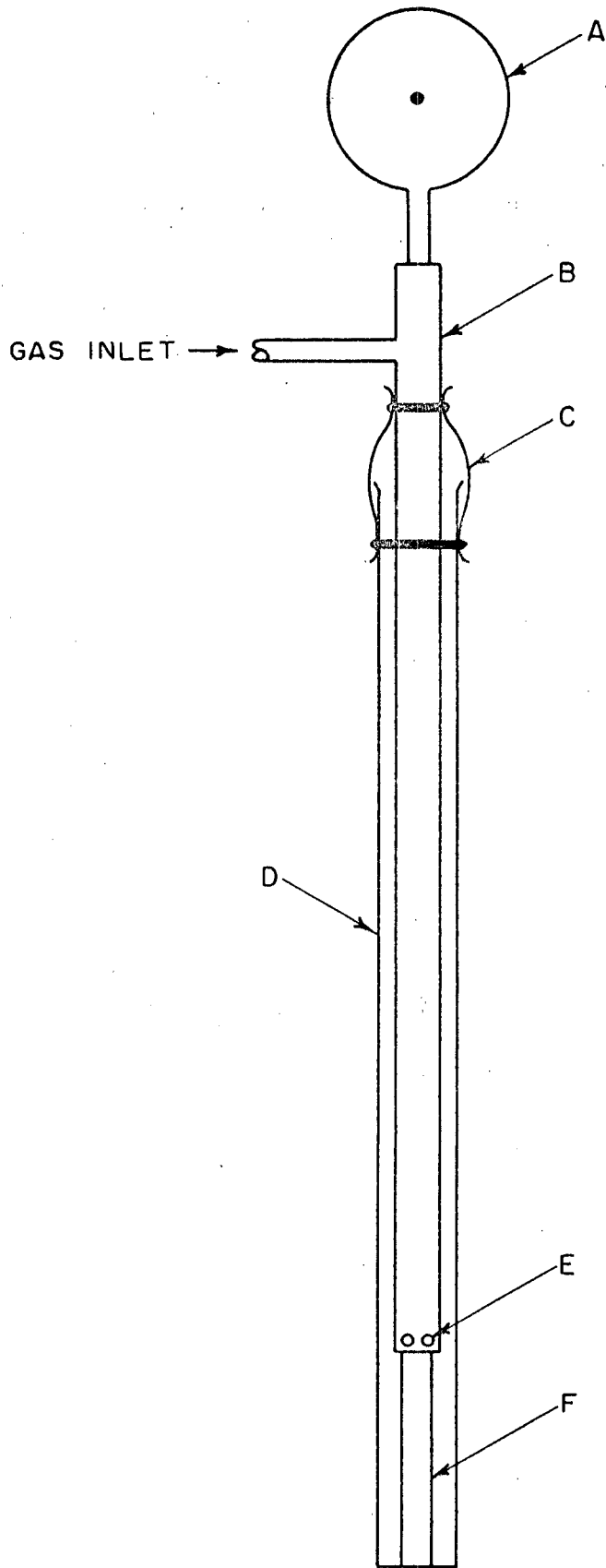
A. DIAL GAUGE
B. INNER QUARTZ TUBE
C. RUBBER MEMBRANE
D. OUTER QUARTZ TUBE
E. GAS EXIT HOLES
F. SAMPLE BAR

GAS INLET →

FIG. 2 - SCHEMATIC DIAGRAM OF DILATOMETRIC APPARATUS
USED FOR ISOTHERMAL TRANSFORMATION DETERMINATIONS

the inner quartz tube to follow changes in length of the test specimen. The system was first thoroughly purged with helium before inserting the quartz tubes and sample into a lead bath furnace. A dial gauge graduated in intervals of ten-thousandths of an inch measured the changes in length as transformation proceeded.

The use of this dilatometric apparatus was limited to the higher annealing temperatures where transformation was initiated in short annealing times and produced relatively large changes in length. Results at the lower annealing temperatures were less accurate, as very long annealing times produced only slight length variations. Data for change in length at these lower temperatures were obtained by measurements of length of specimens taken before and after isothermal annealing.

G.   X-Ray Diffraction Techniques

X-ray diffraction studies were conducted primarily for the purpose of identifying the phases present in the decomposition products. Solid samples, measuring about 5/8 in. square by 0.2 in. thick, were used in this investigation. Diffraction patterns were obtained using a Norelco Geiger-counter spectrometer, with nickel-filtered copper radiation. The chart speed was 1/2 degree per minute.

For each alloy, one X-ray specimen was transformed at the longest scheduled annealing interval for each of the four principal annealing temperatures under investigation. In addition, the modes of transformation for several compositions were studied at various temperatures, obtaining a series of patterns for each annealing temperature. This was accomplished by reheating the same samples for progressively longer times and obtaining a diffraction pattern at each annealing interval. These series were not used to determine

the annealing time required for initiation of transformation, as an appreciable
amount of decomposition product is required for detection by this method.
However, such series were found to be of value in comparing rates and mecha-
nisms of transformation of several compositions.

III. DISCUSSION OF RESULTS

A.   Isothermal Transformation Kinetics

1.   Introduction

Transformation kinetics have been investigated for three binary
U-Nb alloys and ternary U-Nb base compositions with additions of zirconium,
chromium, titanium, silicon, nickel, ruthenium and vanadium. With the exception
of the material containing zirconium, the ternary elements were added to a 8 or
10w/o niobium composition on the basis of atomic percentages. A list of these
alloys is presented in Table I; the ternary additions are expressed in both
weight and atomic percent although weight percent will be used throughout the
report.

In discussing data for the various alloys, two modes of presen-
tation have been employed. The first consists of grouping the alloys in
sections according to composition: U-Nb, U-Nb-Zr, U-Nb-Cr, U-Nb-Ti, U-Nb-Si,
U-Nb-Ni, U-Nb-Ru and U-Nb-V. Under each section, data from the various methods
of studying transformation will be presented. This information includes
hardness, electrical resistivity and dilatometric curves, and also metallo-
graphic results with accompanying photomicrographs for each composition. For
some alloys X-ray diffraction patterns will be illustrated to demonstrate
mechanisms of transformation. As most of the ternary additions are present
at two percentage levels, the effects of these elements on initiation of
transformation will be apparent.

TABLE I

URANIUM-BASE ALLOYS INVESTIGATED

Alloy Weight Per Cent	Alloy Additions Atomic Per Cent
U-7 Nb	16.2 Nb
U-12.5 Nb	26.8 Nb
U-15 Nb	31.2 Nb
U-7 Nb-1 Zr	16.0 Nb-2.32 Zr
U-7 Nb-2 Zr	15.7 Nb-4.57 Zr
U-8 Nb-0.12 Cr	18.2 Nb-0.5 Cr
U-8 Nb-0.74 Cr	17.8 Nb-3.0 Cr
U-10 Nb-0.13 Cr	22.1 Nb-0.5 Cr
U-10 Nb-0.78 Cr	21.7 Nb-3.0 Cr
U-8 Nb-0.90 Ti	17.7 Nb-4.0 Ti
U-8 Nb-1.94 Ti	17.1 Nb-8.0 Ti
U-8 Nb-0.14 Si	18.1 Nb-1.0 Si
U-8 Nb-0.68 Si	17.4 Nb-5.0 Si
U-8 Nb-0.14 Ni	18.2 Nb-0.5 Ni
U-8 Nb-0.84 Ni	17.8 Nb-3.0 Ni
U-8 Nb 0.49 Ru	18.1 Nb-1.0 Ru
U-8 Nb-0.98 V	17.7 Nb-4.0 V
U-8 Nb-2.02 V	17.1 Nb-8.0 V

A second method of presenting the findings will be found under the "Comparative Data" section. This part of the report compares the relative stability of the gamma phase of all of the materials under investigation. TTT diagrams based on initial changes in hardness, metallographically observed transformation and electrical resistivity for each group of alloys are included in a single section for easy reference. In order to demonstrate more readily the effects of alloy additions, TTT curves for a number of compositions are presented on a single page for each of the above three methods of transformation study.

The "Comparative Data" section presents in tabular form the results of X-ray diffractometer studies of all the compositions, and also shows the effects of the various alloy additions on lattice parameters and other properties of solution-treated materials.

2. U-Nb Alloys

Three binary uranium-niobium alloys (U-7, 12.5, 15w/o Nb) are included among the compositions under investigation. In addition, limited data were obtained for a U-8w/o Nb material in order to permit a more complete evaluation of the effects of ternary additions to this base composition.

The phase diagram for the uranium-niobium system (Figure 3) shows that the decomposition products of the gamma phase in the region under study are alpha, with a low solubility of niobium, and a niobium-rich gamma phase.[2] More recent work on this system indicates that the monotectoid point is located at a higher niobium content.[3] A portion of this diagram is presented in Figure 4; the monotectoid point occurrs at about 8 weight per cent niobium.

ARMOUR RESEARCH FOUNDATION OF ILLINOIS INSTITUTE OF TECHNOLOGY

Project No. B 095
                              Summary Report

a. Metallographic Results

Water quenching the U-7w/o Nb alloy from 900°C retained the metastable gamma phase. This structure is illustrated in Figure 5. Annealing this solution-treated material at 600° and 550°C produced a dark-etching decomposition product which originated at the grain boundaries and around the impurity particles. Figure 6 shows a typical microstructure of a sample partially transformed at these temperatures. After 0.4 hour at 550°C, the transformation product covers over half of the area; the light matrix is the gamma phase. Continued annealing resulted in further growth of the decomposition product until no areas of gamma were visible. Such a structure is illustrated in Figure 7; this U-7w/o Nb material was annealed for 4 hours at 550°C. Annealing at this temperature for 100 hours produced a slight coarsening of the transformation products.

Annealing at U-7w/o Nb alloy at 450°C produced microstructures which differed considerably from those observed at the higher temperatures. After 1 hour at 450°C, the specimen was found to be covered with a dark "stain" which was uniform and continuous over most of the sample. A few areas, however, showed the presence of retained gamma; in these areas, the staining was observed to occur in small, angular particles. Merging of these particles resulted in the uniformly stained areas which had no resolvable structure at magnification of 1000X. Figure 8 illustrates this stained structure at the grain boundaries and within the gamma grains. None of the darker etching transformation product that originates at the grain boundaries upon annealing at higher temperatures was found in this sample. The presence of the darker grain-boundary transformation was first detected upon annealing for 4 hours at 450°C. After 10 hours at 450°C, Figure 9, the matrix is uniformly stained

by the etchant employed and has the appearance of a fine precipitate. The darker etching transformation product is present in most of the grain boundaries.

Microstructures differing from those described above were observed in samples annealed at 360°C. After relatively short annealing times (less than 1 hour), oriented fine structures appeared within the grains. Such samples exhibited a tendency to stain lightly after etching, and repeated metallographic preparation produced some variations in the appearance of these structures. An example is illustrated in Figure 10, which shows the staining and oriented pattern observed after annealing at 360°C for 10 hours. The light staining noted at this annealing temperature did not resemble a fine precipitate as had been noted at the 450°C temperature. Hardness increases and changes in other properties are associated with the presence of this fine oriented structure and indicate incipient decomposition.

The dark-etching grain boundary transformation product was first observed in the U-7w/o Nb material after annealing for 100 hours at 360°C. Less than 5% of this product was present after 1000 hours at this annealing temperature.

A limited number of isothermal annealing treatments were conducted on a U-8w/o Nb alloy in order to obtain data on the initiation of transformation. Annealing this composition for 4 hours at 450°C resulted in the simultaneous appearance of both the grain boundary type of transformation and the stained matrix, or fine decomposition product. In this sample (Figure 11) the stained matrix is initiated in small, angular particles especially along sub-grain boundaries. In some areas, these particles have merged to produce continuous lines or uniformly stained areas. The darker etching product is found in a few grain boundaries throughout the specimen.

The binary alloys containing 12.5 and 15w/o niobium exhibited the dark-etching product upon annealing at 600° and 550°C, as had been observed in the U-7w/o Nb material although much longer annealing times were required for its initiation. The stained matrix or fine decomposition product was first observed in the U-12.5w/o Nb composition after annealing for 100 hours at 450°C. None was found in the U-15w/o Nb alloy at the 450°C annealing temperature. Figure 12 shows the dark etching grain boundary product and the gamma matrix present after 100 hours at 450°C. This structure resembles those found on samples partially transformed at 600° and 550°C. Annealing the U-(12.5, 15)w/o niobium compositions at 360°C resulted in only a few traces of the oriented pattern, and no decomposition was detected at the grain boundaries after 1000 hours at this temperature.

TTT curves showing initiation of metallographically observed transformation for the binary U-Nb alloys are presented in Figures 13 to 16. These curves are based on annealing times required to produce the dark-etching transformation product which originates in the grain boundaries. Data included in these figures show the estimated percentage of this transformation product, and also indicate the presence of the fine decomposition product observed upon annealing at 450°C. In addition, the oriented structure found at 360°C is denoted as "gamma or transition structure".

These TTT diagrams readily demonstrate the stabilizing effect of niobium on retention of the gamma phase. As the niobium content was increased, progressively longer annealing times were required to initiate transformation at the grain boundaries.

b.   Hardness Results

Results of Vickers (10 Kg) hardness measurements on the U-7w/o Nb alloy are presented in Figure 17. Hardness values increased in 0.1 hour or

ARMOUR RESEARCH FOUNDATION OF ILLINOIS INSTITUTE OF TECHNOLOGY

less upon annealing at 550° and 360°C. Overaging occurred in less than 4 hours at 550°C. Hardness values were increasing after 1000 hours at 360°C, and the extremely rapid increase at this annealing temperature is believed to be due to pre-precipitation hardening. The hardness curve reached a maximum in less than 100 hours at 450°C and in about 10 hours at 600°C.

Considerably longer annealing times were required to produce hardness increases in the U-12.5w/o Nb alloy. Hardness curves (Figure 18) show an initial rise in about 3 hours at 550°C, in approximately 4 hours at 600° and 360°C, and in slightly less than 10 hours at 450°C.

Increasing the niobium content to 15 per cent resulted in additional stability of the gamma phase. Hardness curves for the U-15w/o Nb alloy (Figure 19) show that at all annealing temperatures, longer times are required to produce increases than were noted for the U-12.5w/o Nb material.

The variation of hardness with niobium content for solution-treated alloys is illustrated in Figure 20. Hardness values rise sharply with increasing niobium content up to about 10 per cent niobium; above this amount the hardness curve becomes asymptotic.

c.   Electrical Resistivity Results

Transformation of the gamma phase in these uranium-niobium alloys is accompanied by a decrease in electrical resistivity. Extremely short annealing times produced resistivity changes in the U-7w/o Nb composition at all temperatures (Figure 21). Transformation, as indicated by the curve for 550°C, progresses rapidly. In 4 hours, the resistivity value was about 24 microhm-cm below that for the solution-treated material. Annealing for 100 hours produced a slight additional decrease of 3 microhm-cm. This further decrease may be due to continued transformation or agglomeration and coarsening of the decomposition products.

ARMOUR RESEARCH FOUNDATION OF ILLINOIS INSTITUTE OF TECHNOLOGY

Annealing at 450°C resulted in a more gradual decrease in resistivity. A major portion of this decrease occurred in 8 hours, at which time only very small amounts of the dark etching grain boundary decomposition transformation were present in the microstructures. The fine decomposition product observed at this annealing temperature is associated with the decrease in resistivity.

Electrical resistivity results for samples of the U-7w/o Nb material annealed at 360°C show that, although the initial decrease occurred in less than 0.15 hour, subsequent heat treatment caused very small additional changes. After 400 hours at 360°C, the resistivity value had decreased only 6.5 microhm-cm below the solution-treated value, indicating a relatively small amount of transformation.

The effect of increased amounts of niobium on transformation is demonstrated by the resistivity curves for the U-12.5w/o Nb and U-15w/o Nb alloys, Figures 22 and 23. The 550°C annealing temperature produced the first decreases in resistivity in these compositions, placing the nose of TTT curves at this temperature. Longer annealing times were required for changes in resistivity at 450°C; about 5 hours for the U-12.5w/o Nb material, and slightly over 10 hours for the U-15w/o Nb alloy. Very slight decreases in resistivity were noted in both compositions after annealing for 400 hours at 360°C. The U-15w/o Nb material required longer annealing times to produce changes in resistivity than were noted for the U-12.5w/o Nb alloy at all annealing temperatures. Both compositions showed a great increase in stability of the gamma phase over that of the U-7w/o Nb material.

d.   Dilatometric Results

All of the materials under investigation exhibited an increase in density upon transformation of the metastable gamma phase. The rapidity of

ARMOUR RESEARCH FOUNDATION OF ILLINOIS INSTITUTE OF TECHNOLOGY

Project No. B 095
Summary Report

transformation of the U-7w/o Nb alloy at 550°C, as determined by dilatometric measurements, is demonstrated in Figure 24. The curve shows that decomposition is initiated in about 0.2 hour, and is substantially complete in 4 hours. These findings are in approximate agreement with results of hardness, metallographic and electrical resistivity determinations for this material at 550°C.

Annealing the U-7w/o Nb material at 450°C also produced a rapid increase in density. Length measurements of samples before and after annealing indicate that a considerable amount of transformation had taken place after 1 hour at 450°C. Smaller changes in length occurred at 360°C; after 400 hours, the decrease in length was about 50 per cent of the maximum change measured on a sample transformed at 550°C for 100 hours. While these results are only approximate, due to measurement errors introduced by oxide formation and slight warpage, the data indicate that at 360°C transformation is associated with the stained, oriented structure observed in the microstructures.

e. X-Ray Diffraction Results

Decomposition of the gamma phase has been investigated by X-ray diffraction techniques on samples which were water-quenched from 900°C, followed by annealing at 600°, 550°, 450° and 360°C. The mechanism of transformation of the U-7w/o Nb alloy at 450°C is illustrated by the spectrometer traces shown in Figures 25 to 28. Solution annealing for 24 hours at 900°C followed by water-quenching resulted in the single (110) peak for retained gamma (Figure 25). Annealing for 1 hour at 450°C produced the changes shown in Figure 26. The (111) reflection for alpha is distinct and there are rises in the vicinity of the three alpha peaks found at 2θ values lower than that for gamma. This annealing treatment resulted in formation of the fine decomposition product illustrated in Figure 8. After 10 hours at 450°C (Figure 27), the

Project No. B 095
Summary Report

gamma peak has shifted to a higher 2θ value, indicating niobium enrichment, and the (110), (021), and (002) peaks for alpha are more distinct. The microstructure from this annealing treatment (Figure 9) exhibited the stained matrix, or fine decomposition product, with initial transformation in the grain boundaries. This small amount of grain boundary transformation would not be sufficient to produce the strong alpha peaks observed in the diffractometer pattern. Therefore, it is believed that the structure is a fine precipitate of the alpha phase. Subsequent annealing produced a further change of the gamma, as well as increased amount and sharpness of the alpha peaks, as shown in the diffractometer pattern for a sample annealed at 450°C for 1000 hours (Figure 28).

The shifting of the peak for gamma to higher 2θ values is a result of niobium enrichment of this phase. As alpha is precipitated, the composition of gamma varies continuously between that for γ_1 (the metastable phase retained on quenching from 900°C) and γ_2 (the equilibrium, niobium-rich phase).

A similar mode of decomposition was found for the U-12.5w/o Nb and U-15w/o Nb compositions. Much longer annealing times were required to produce structural changes in these compositions having higher niobium contents. No alpha was detected in the patterns of either material after annealing at 360°C for 1000 hours. However, the peaks for gamma had shifted to 2θ values which were slightly higher than the solution-treated values, indicating that a small amount of transformation had occurred.
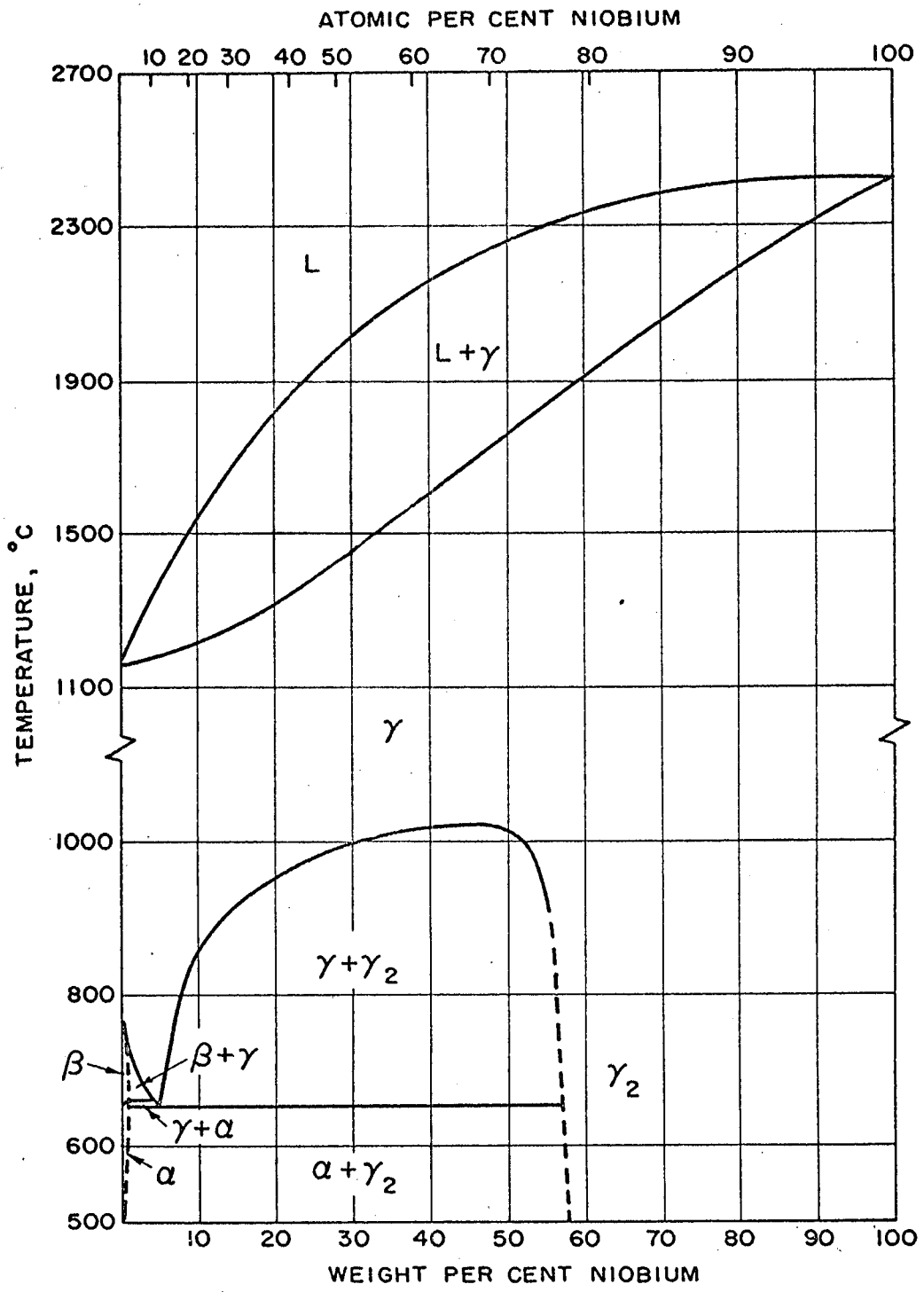
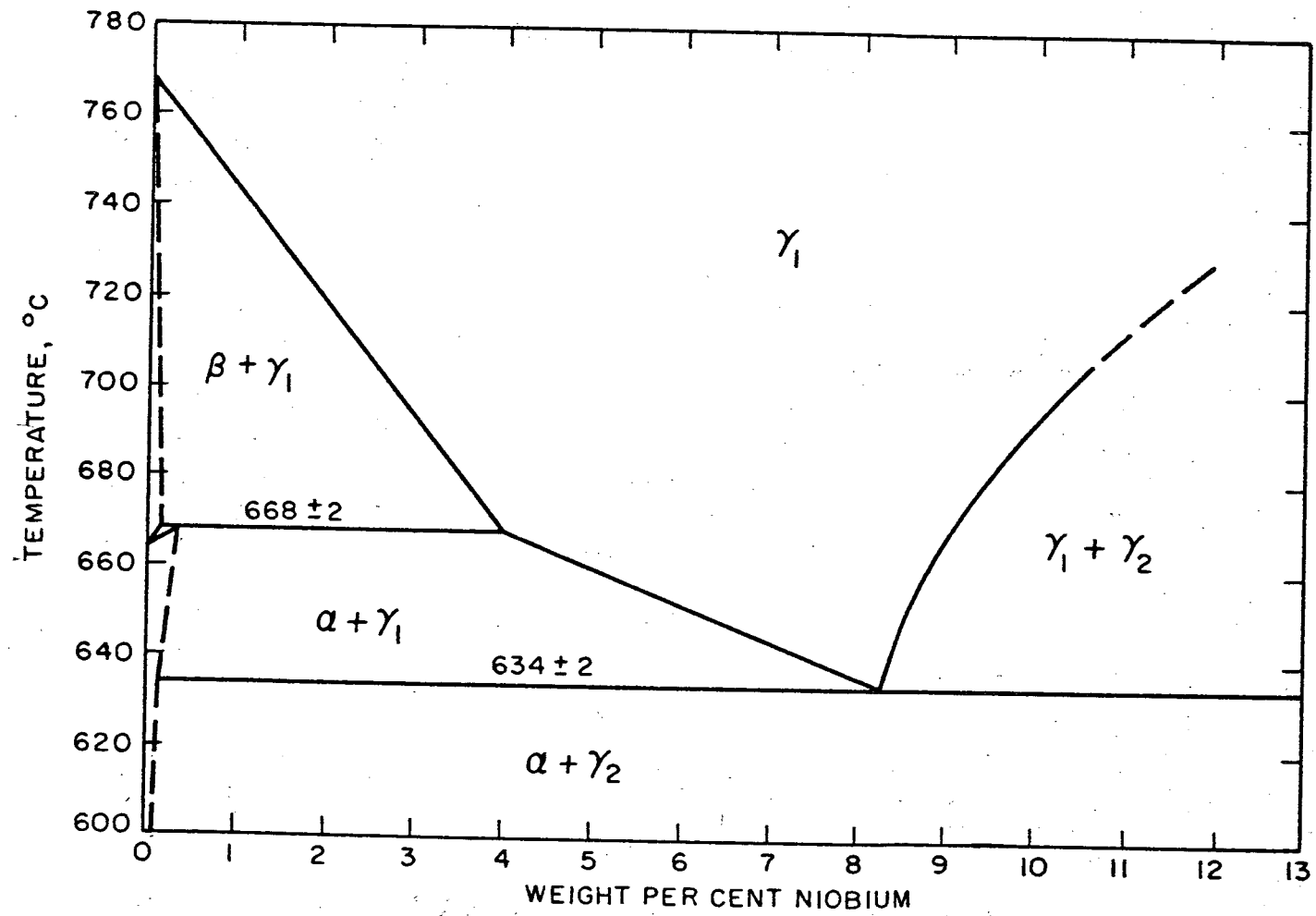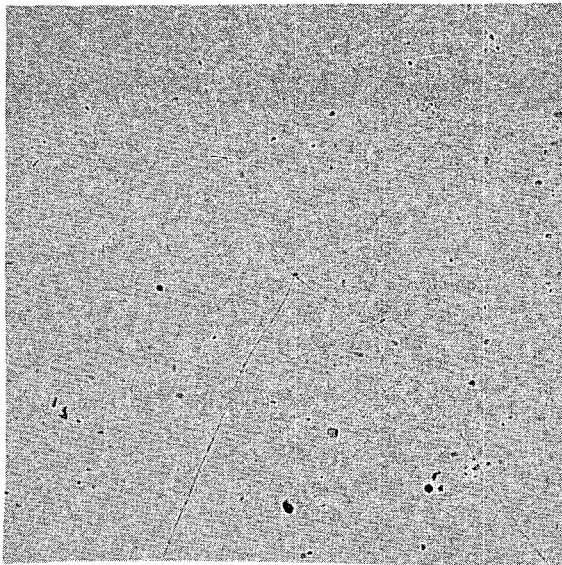FIG. 3 - THE URANIUM-NIOBIUM SYSTEM

FIG. 4. - PARTIAL DIAGRAM OF THE URANIUM-NIOBIUM
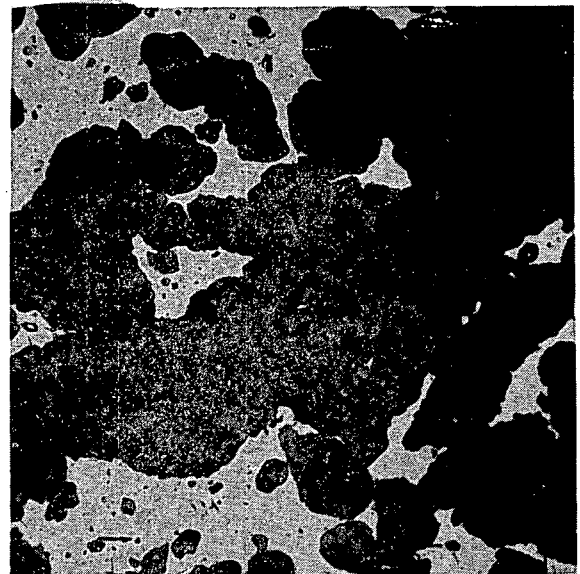SYSTEM (DWIGHT)

Neg. No. 14710   X 250

Fig. 5

Alloy: U-7w/o Nb.
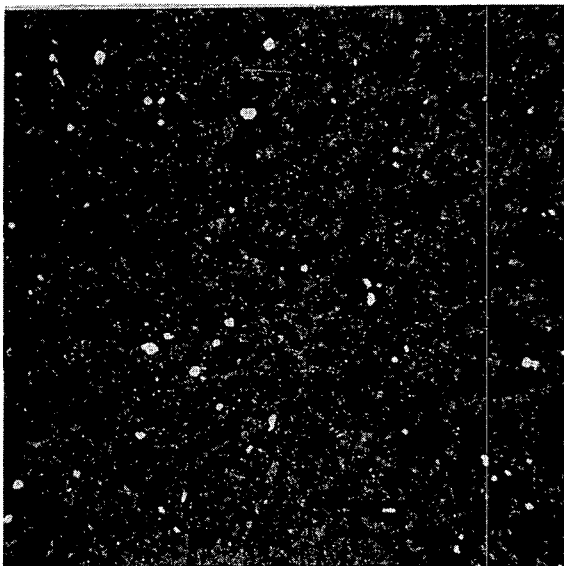Treatment: 900°C-WQ.
Retained γ and impurity phase.

Neg. No. 13808   X 250

Fig. 6

Alloy: U-7w/o Nb.
Treatment: 900°C-WQ; 550°C-0.4 hr-
WQ. Retained γ with transformation
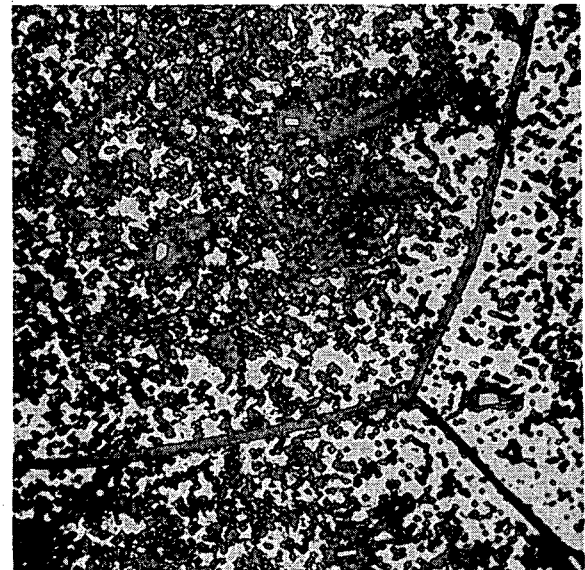product at grain boundaries and
around impurity particles.

Neg. No. 14714   X 250

Fig. 7

Alloy: U-7w/o Nb.
Treatment: 900°C-WQ; 550°C-4 hrs-
WQ. Transformation product and im-
purities. No areas of γ are evident.

Etchant: 10% CrO_3 + 2% HF + H_2O.

Neg. No. 13721   X 1000

Fig. 8

Alloy: U-7w/o Nb.
Treatment: 900°C-WQ; 450°C-1 hr-
WQ. Retained γ plus structure
originating in grain boundaries and
within grains.

- 22 -
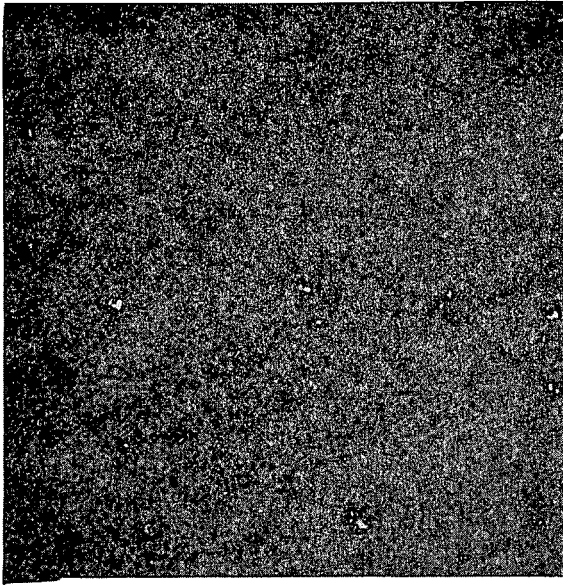
Neg. No. 13831   X 250

Fig. 9

Alloy: U-7w/o Nb.
Treatment: 900°C-WQ; 450°C-10 hrs-
WQ. Fine decomposition product, in-
itial grain boundary transformation,
and impurities.
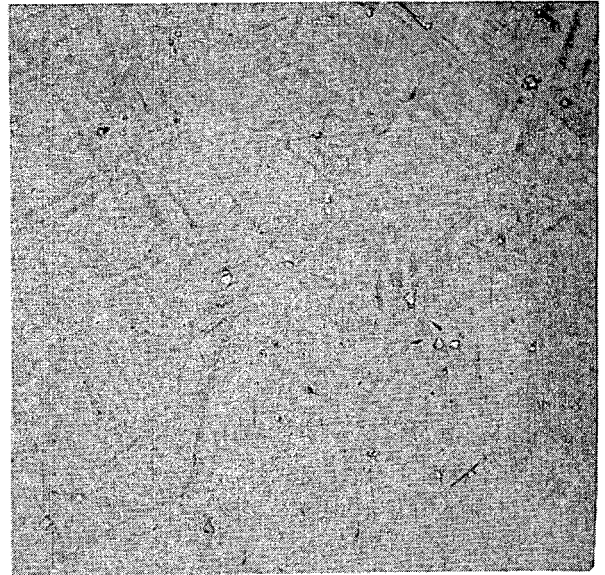
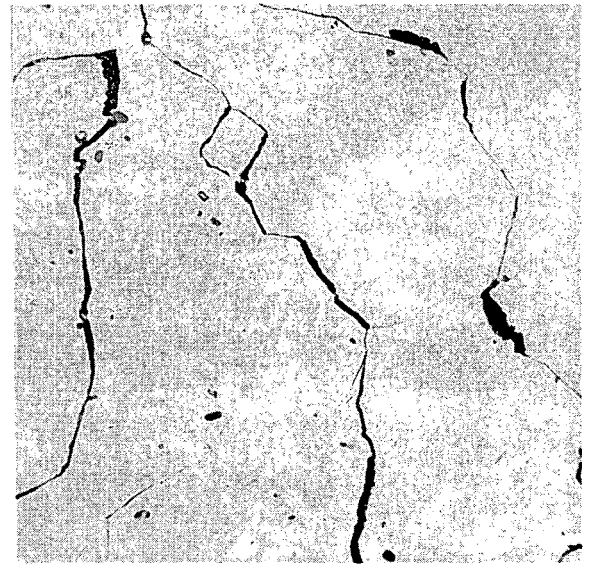Neg. No. 14724   X 250

Fig. 10

Alloy: U-7w/o Nb.
Treatment: 900°C-WQ; 360°C-10 hrs-
WQ. Lightly stained, oriented
pattern.

Neg. No. 14148   X 1000

Fig. 11

Alloy: U-8w/o Nb.
Treatment: 900°C-WQ; 450°C-4 hrs-WQ.
Retained γ, grain boundary decompo-
sition, and stained structure origi-
nating within the grains.

Etchant: 10% CrO_3 + 2% HF + H_2O.   - 23 -

Neg. No. 14712   X 250

Fig. 12

Alloy: U-15w/o Nb.
Treatment: 900°C-WQ; 450°C-100 hrs-
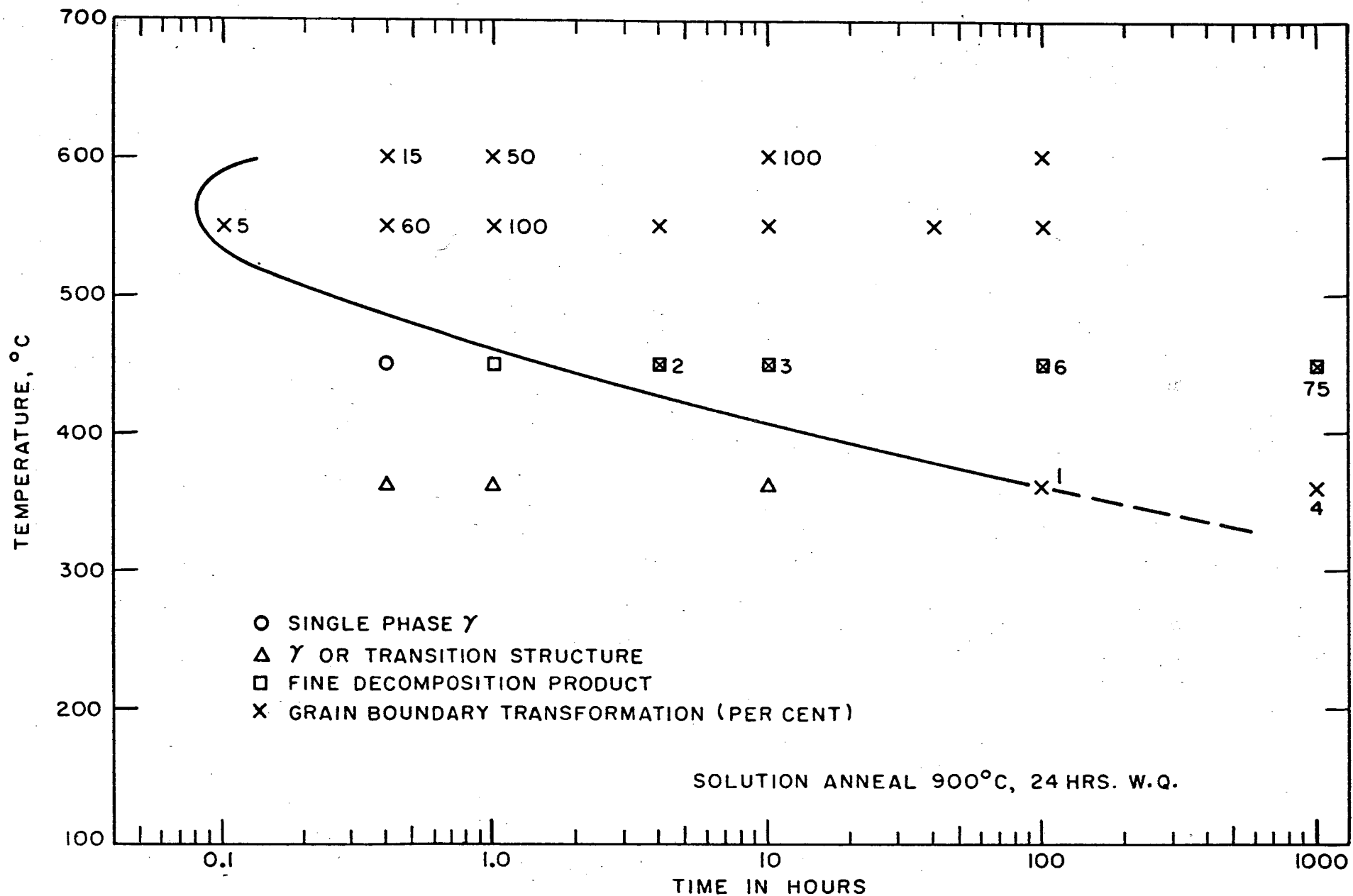WQ. Retained γ with transformation
at the grain boundaries.

FIG. 13 - TTT DIAGRAM FOR A U-7w/o Nb ALLOY ILLUSTRATING INITIAL METALLOGRAPHIC OBSERVATION OF GRAIN BOUNDARY TRANSFORMATION
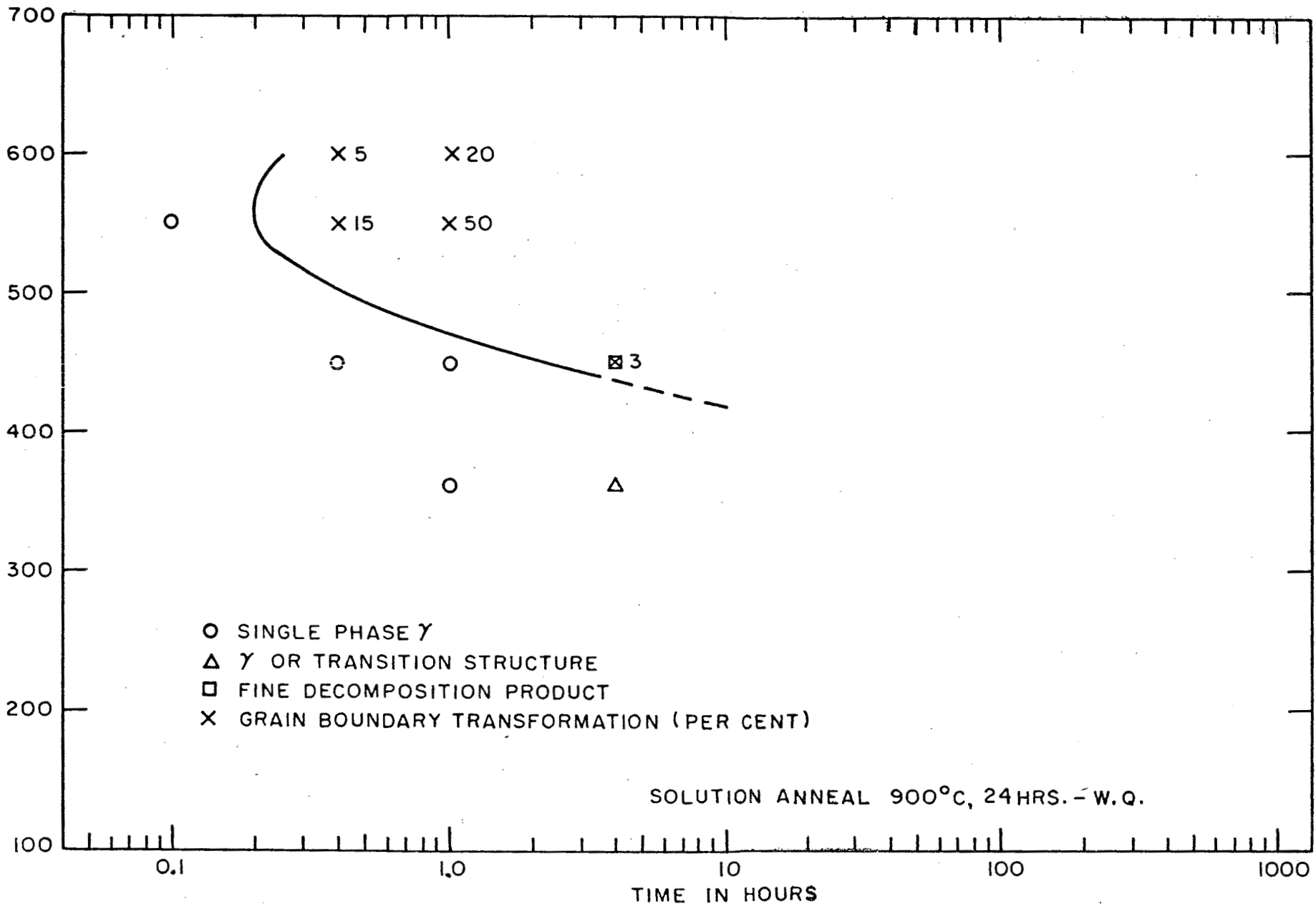
FIG. 14 - TTT DIAGRAM FOR A U-8w/o Nb ALLOY ILLUSTRATING INITIAL METALLOGRAPHIC OBSERVATION OF GRAIN BOUNDARY TRANSFORMATION
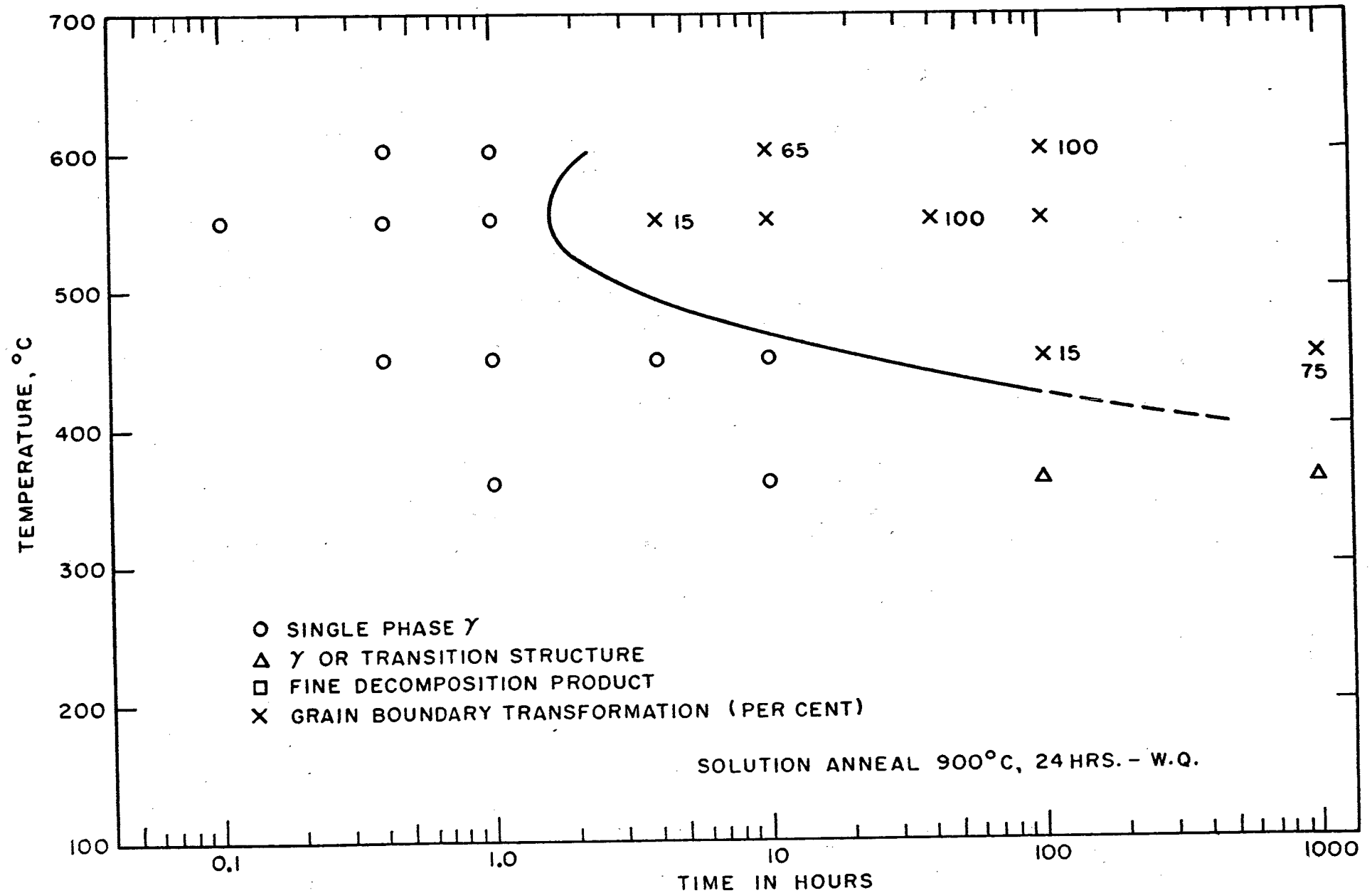
FIG. 15 - TTT DIAGRAM FOR A U-12.5w/o Nb ALLOY ILLUSTRATING INITIAL METALLOGRAPHIC OBSERVATION OF GRAIN BOUNDARY TRANSFORMATION
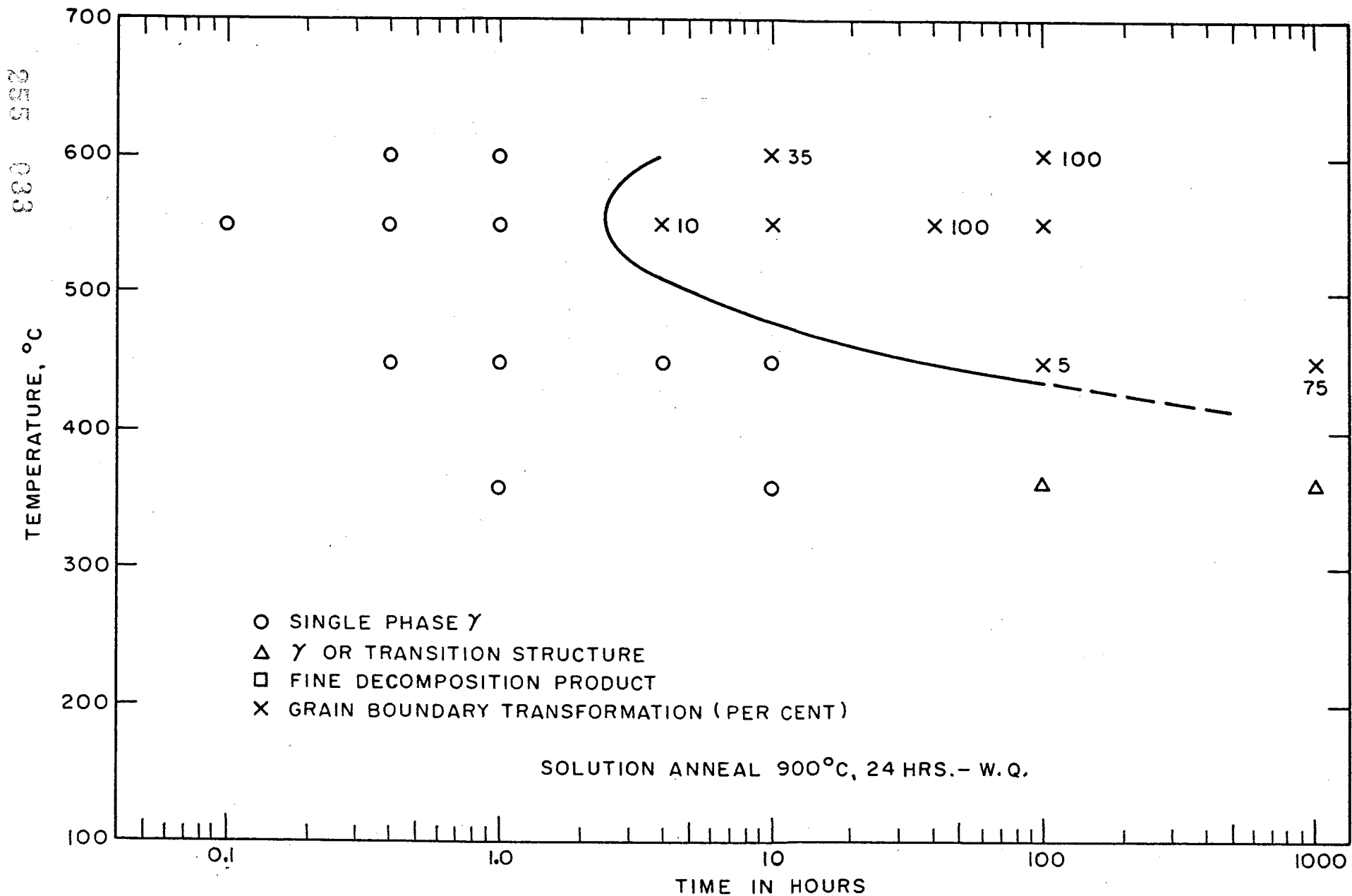
Legend within figure:

O SINGLE PHASE γ
△ γ OR TRANSITION STRUCTURE
□ FINE DECOMPOSITION PRODUCT
X GRAIN BOUNDARY TRANSFORMATION (PER CENT)

SOLUTION ANNEAL 900°C, 24 HRS. – W.Q.

700

600 — ○ — ○ — ✕ 35 — ✕ 100

✕ 10 — ✕ — ✕ 100 — ✕

○ — ○

500

TEMPERATURE, °C

○ — ○ — ○ — ○ — ✕ 5 — ✕ 75

400

○ — ○ — △ — △

300

○ SINGLE PHASE γ
△ γ OR TRANSITION STRUCTURE
□ FINE DECOMPOSITION PRODUCT
✕ GRAIN BOUNDARY TRANSFORMATION (PER CENT)

200

SOLUTION ANNEAL 900°C, 24 HRS.— W.Q.

100
0.1   1.0   10   100   1000

TIME IN HOURS

FIG. 16 - TTT DIAGRAM FOR A U-15w/o Nb ALLOY ILLUSTRATING INITIAL METALLOGRAPHIC OBSERVATION OF GRAIN BOUNDARY TRANSFORMATION
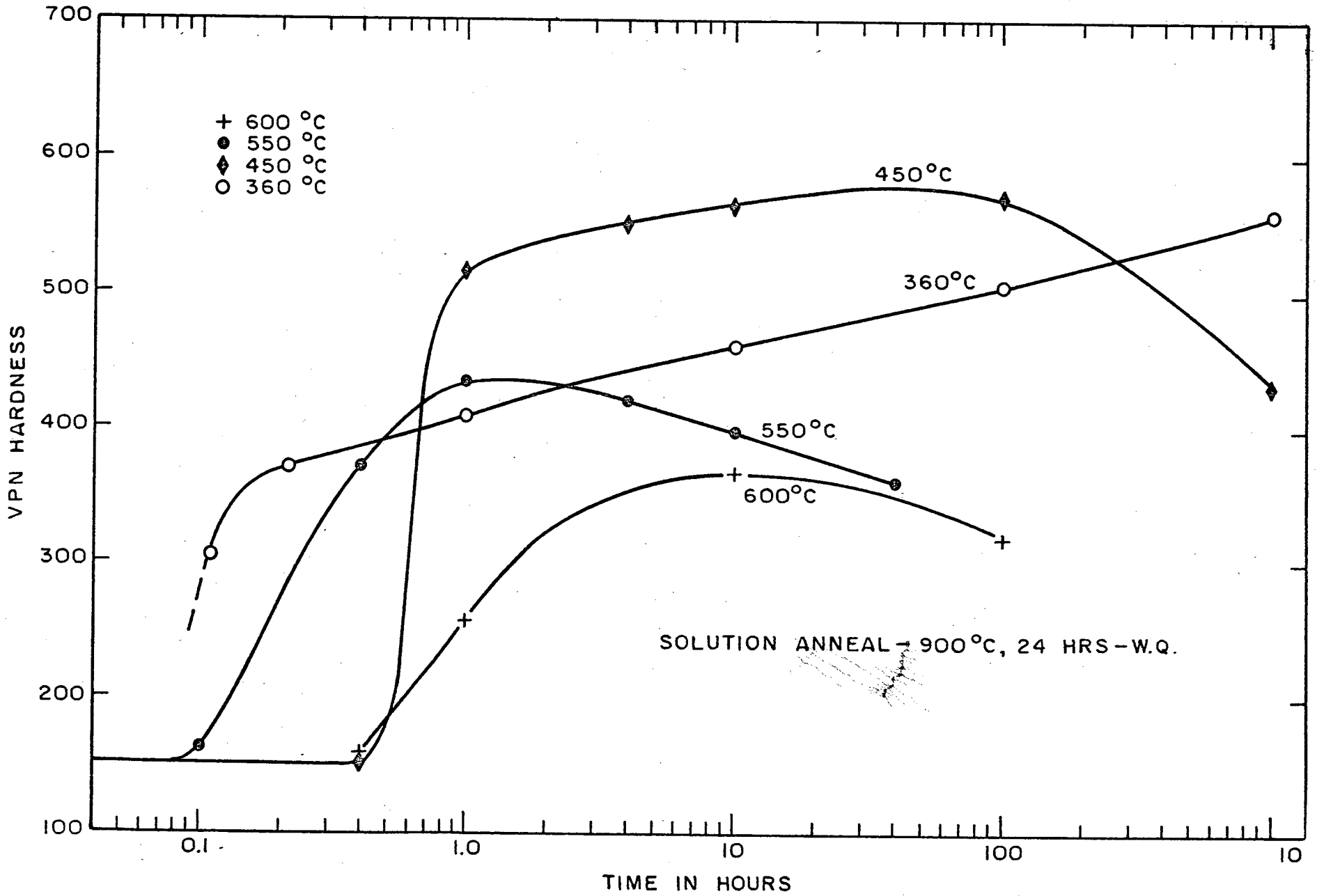
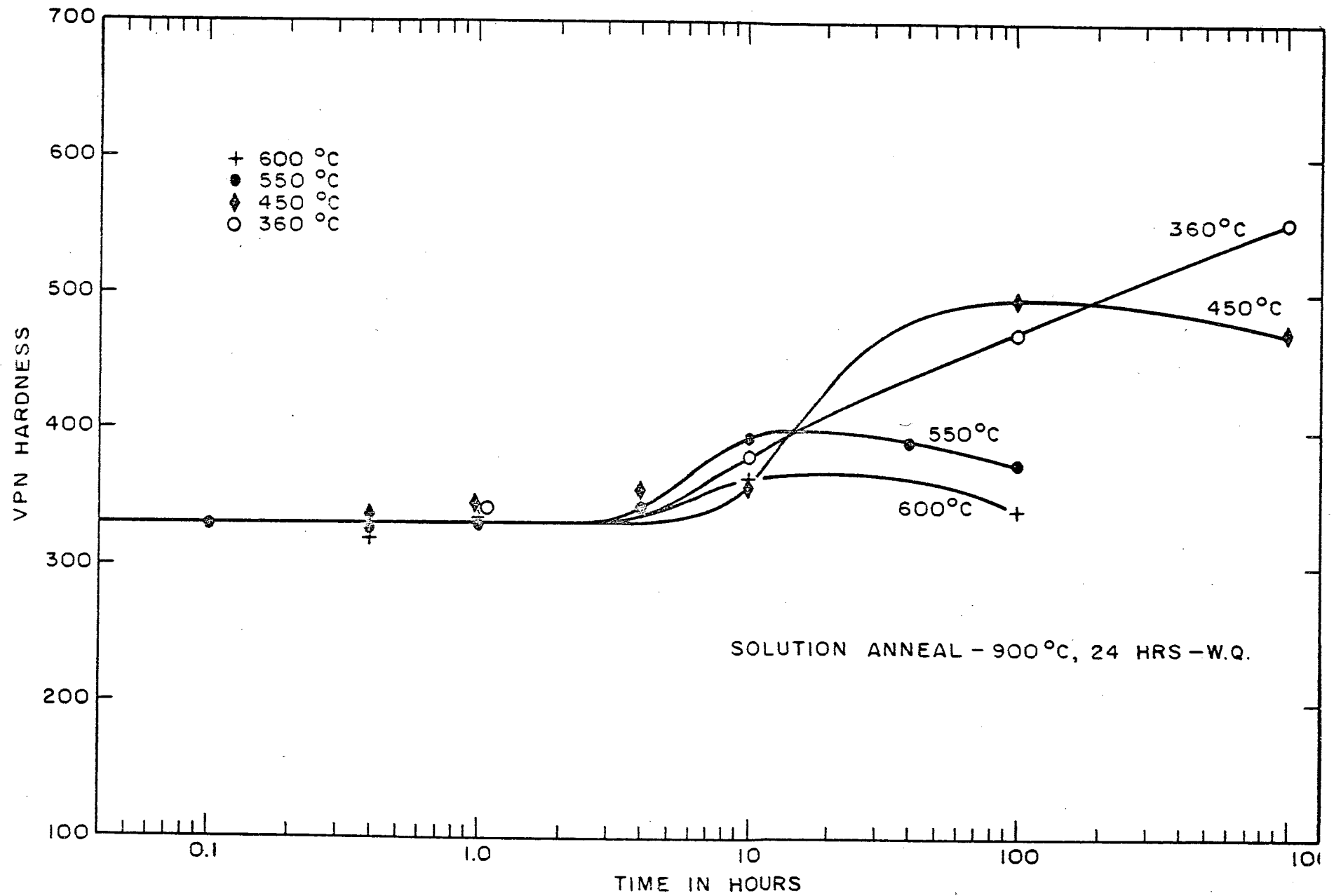FIG. 17- HARDNESS DATA FOR AN ISOTHERMALLY ANNEALED U-7w/o Nb ALLOY

FIG. 18 - HARDNESS DATA FOR AN ISOTHERMALLY ANNEALED U-12.5w/o Nb ALLOY
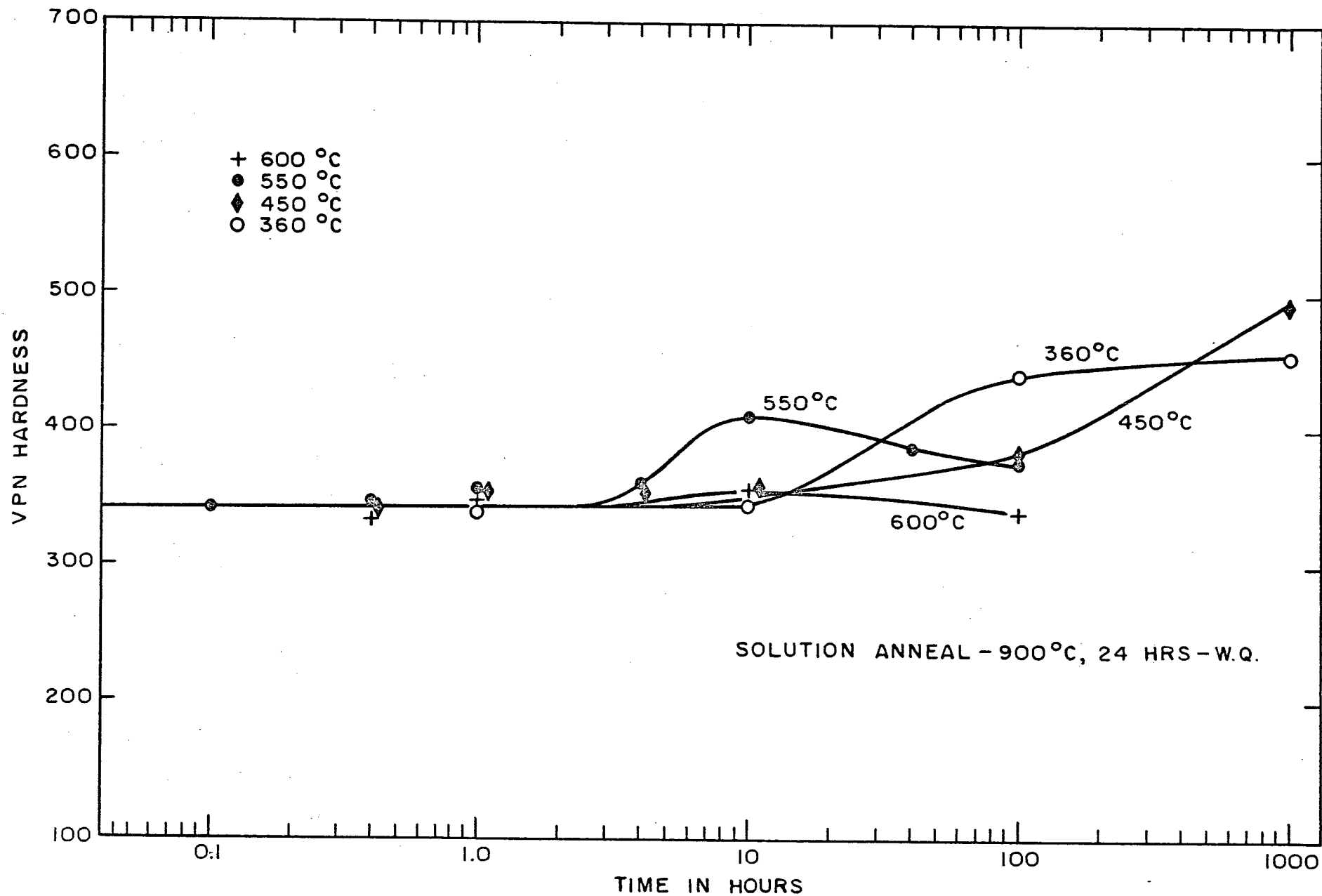
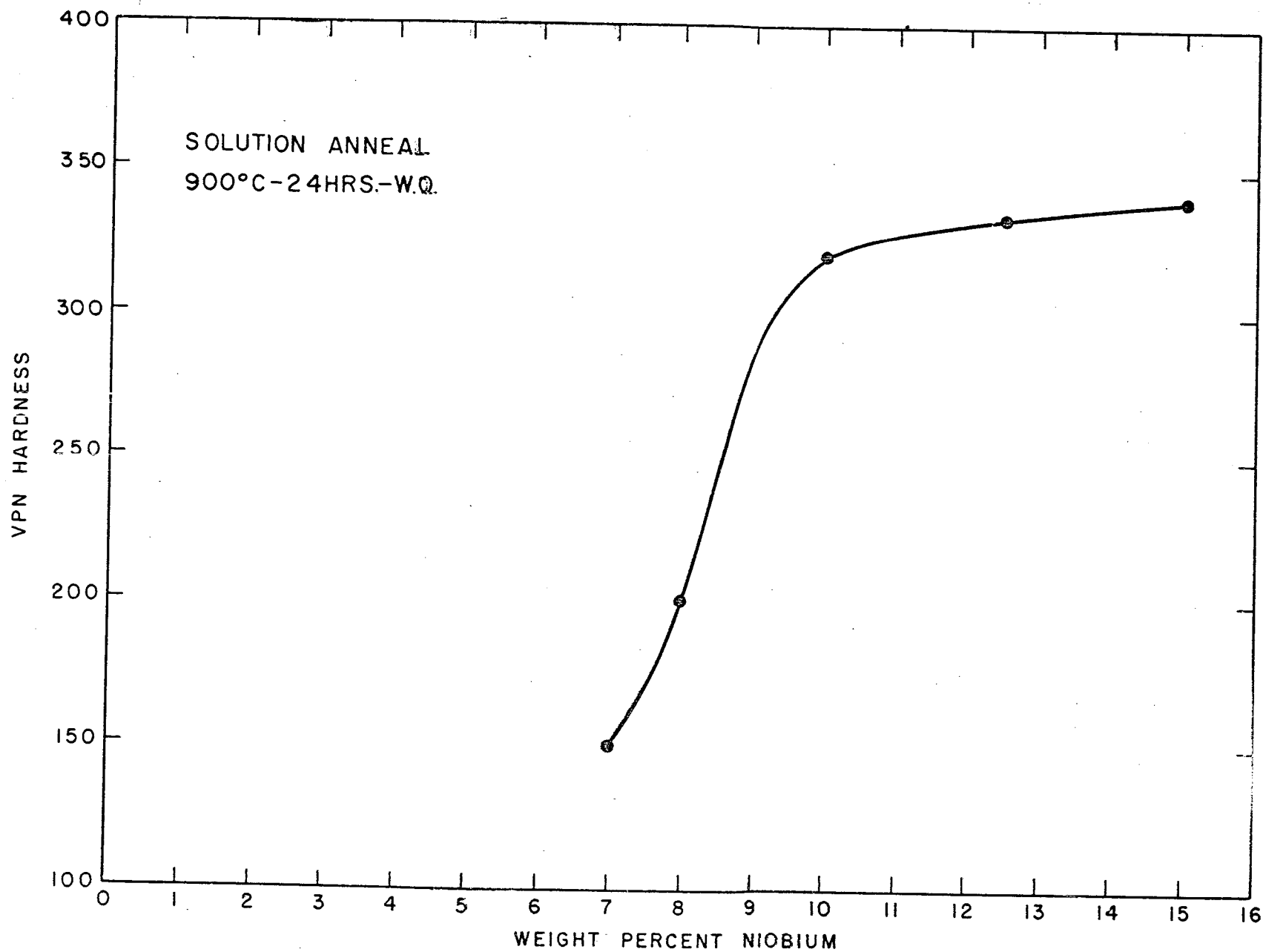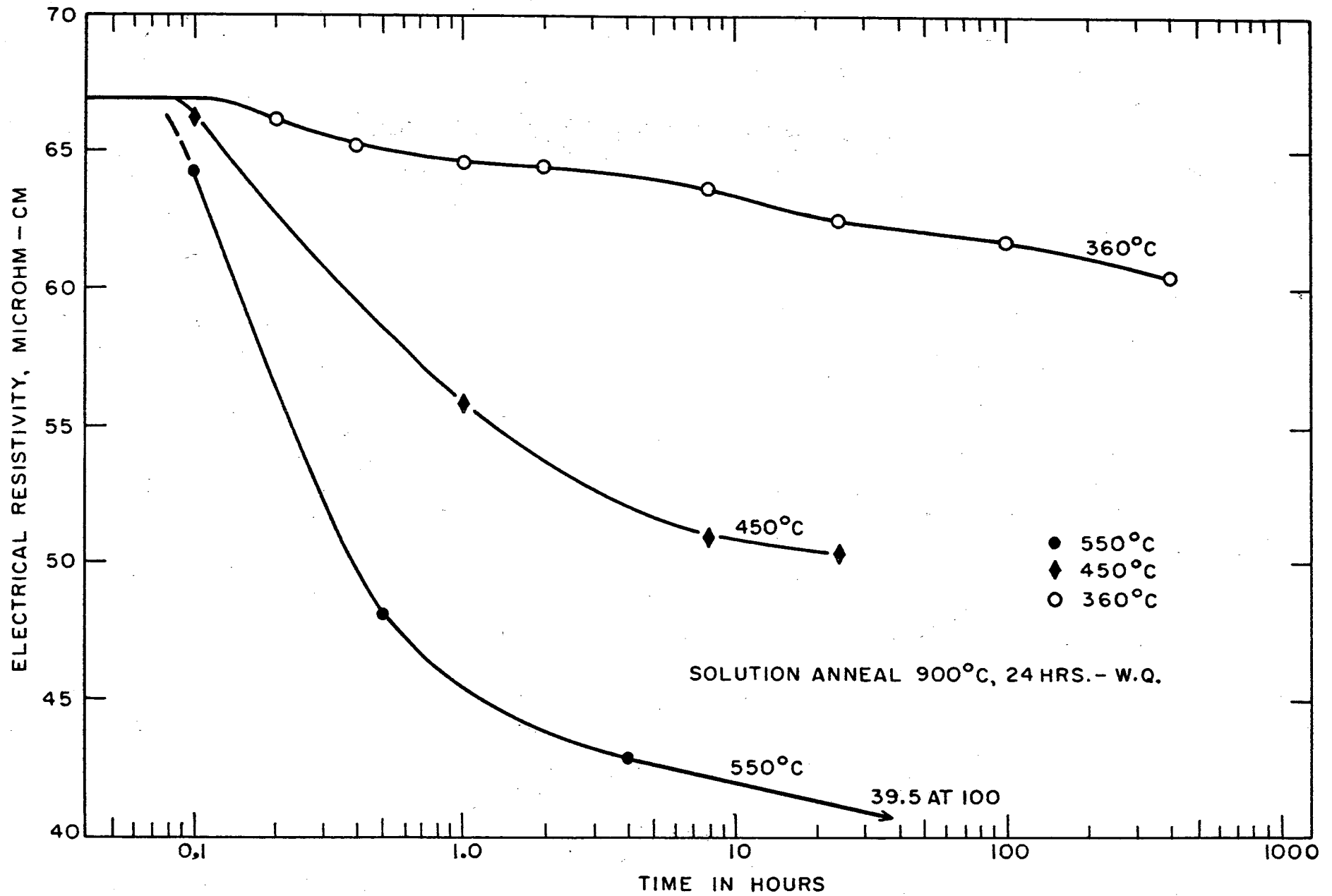FIG. 19 - HARDNESS DATA FOR AN ISOTHERMALLY ANNEALED U-15w/o Nb ALLOY

FIG. 20 - HARDNESS OF U-Nb ALLOYS

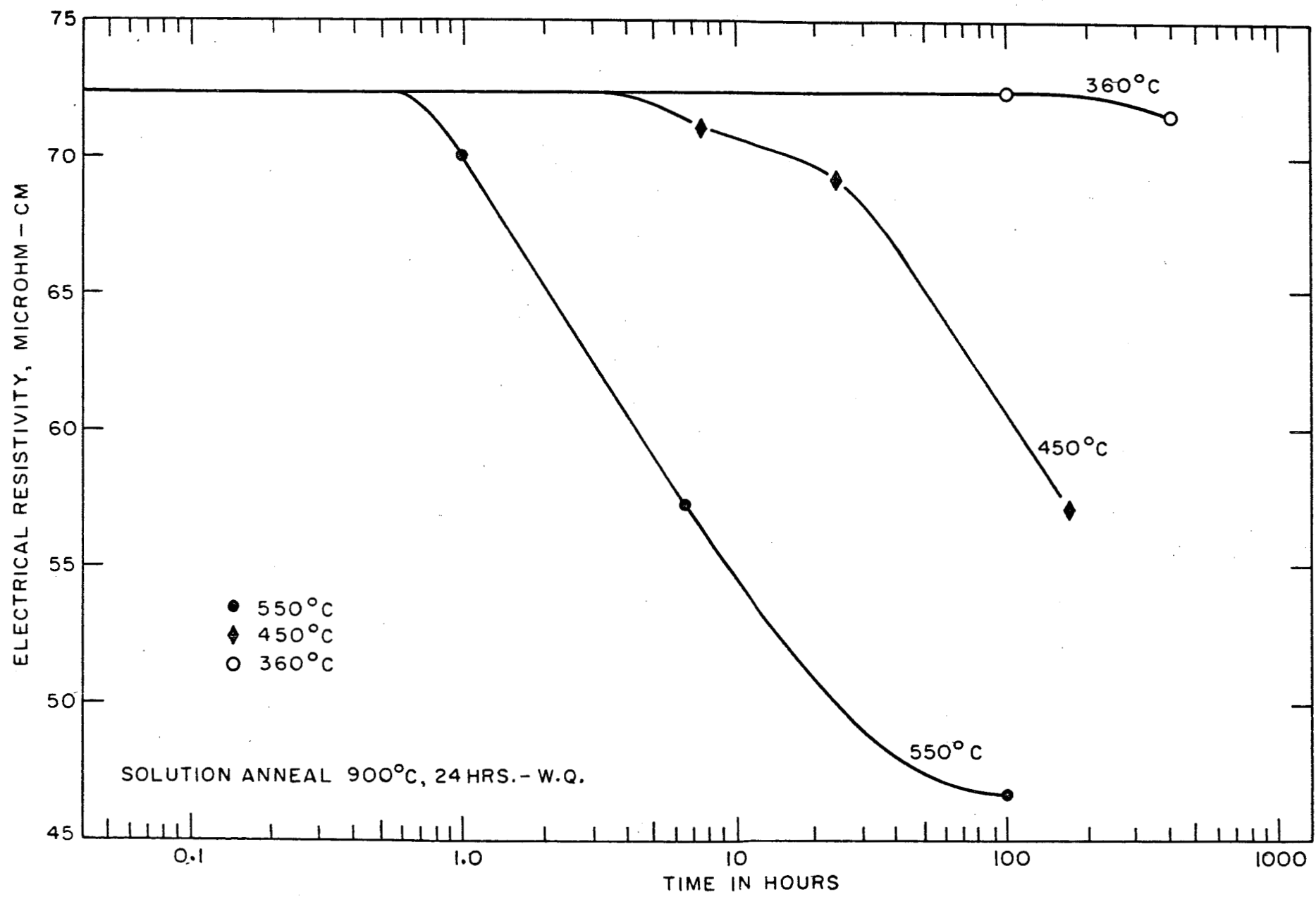FIG. 21 - ROOM TEMPERATURE ELECTRICAL RESISTIVITY DATA FOR AN ISOTHERMALLY ANNEALED U-7w/o Nb ALLOY

FIG. 22 - ROOM TEMPERATURE ELECTRICAL RESISTIVITY DATA FOR AN
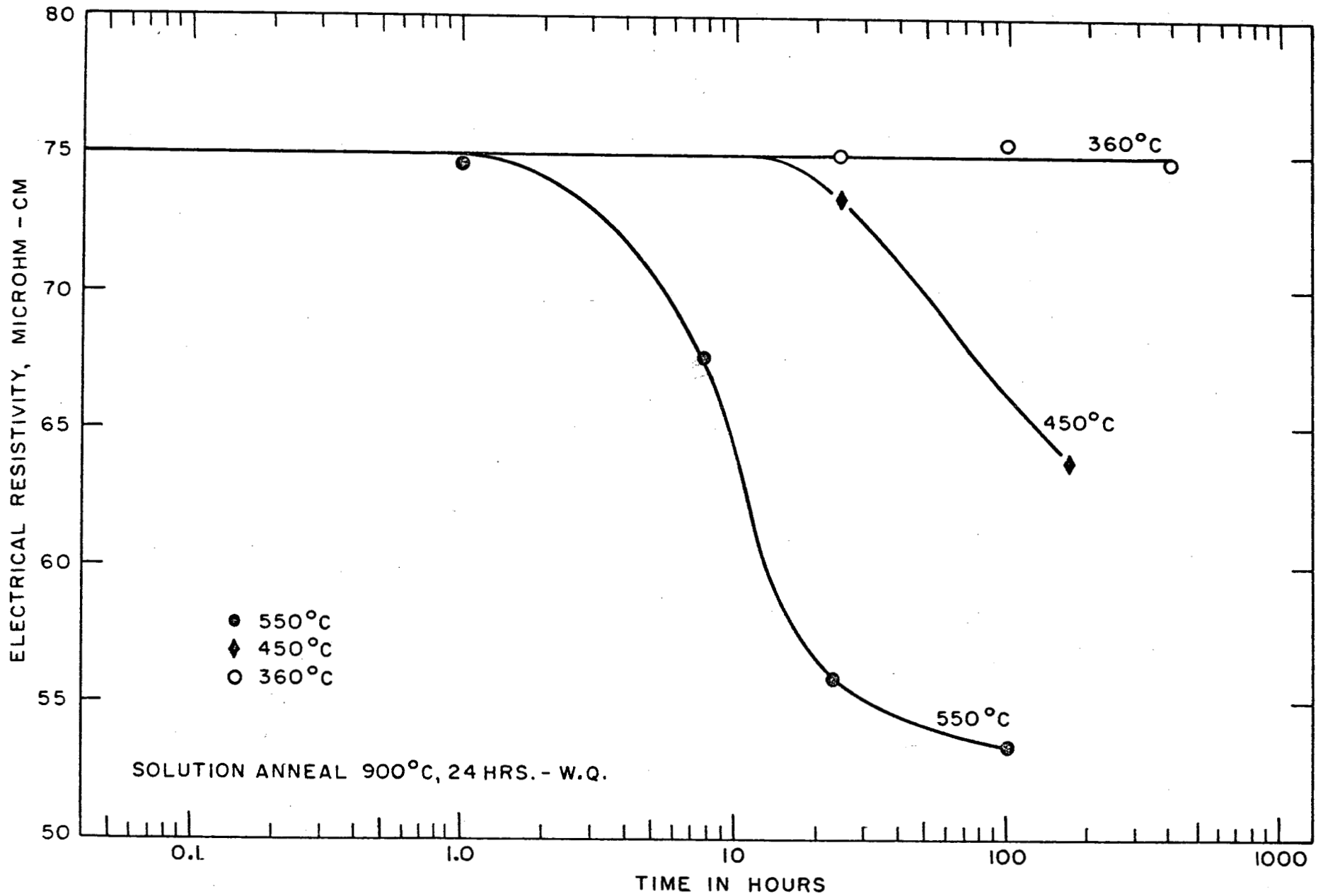ISOTHERMALLY ANNEALED U-12.5w/o Nb ALLOY

FIG. 23 - ROOM TEMPERATURE ELECTRICAL RESISTIVITY DATA FOR AN
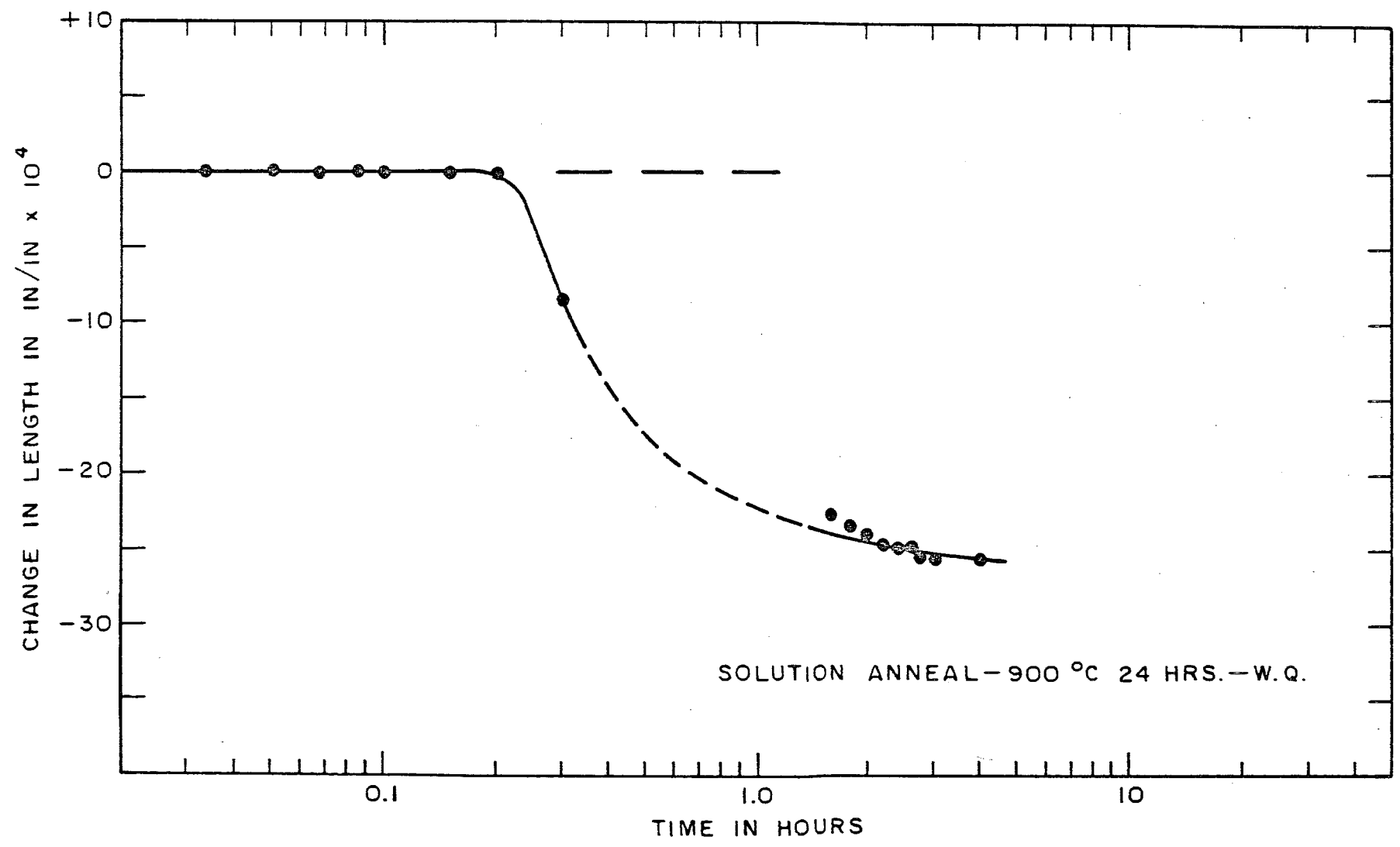ISOTHERMALLY ANNEALED U-15w/o Nb ALLOY

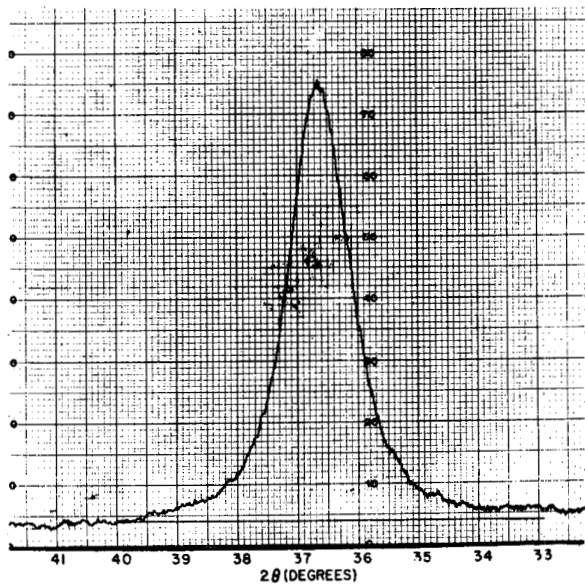FIG. 24 - DILATOMETRIC DATA FOR A U-7 $^W/o$Nb ALLOY
ISOTHERMALLY ANNEALED AT 550°C

Fig. 25

X-ray diffractometer pattern.
Alloy: U-7w/o Nb.
Treatment: 900°C-WQ
Retained γ(2θ=36.6°).
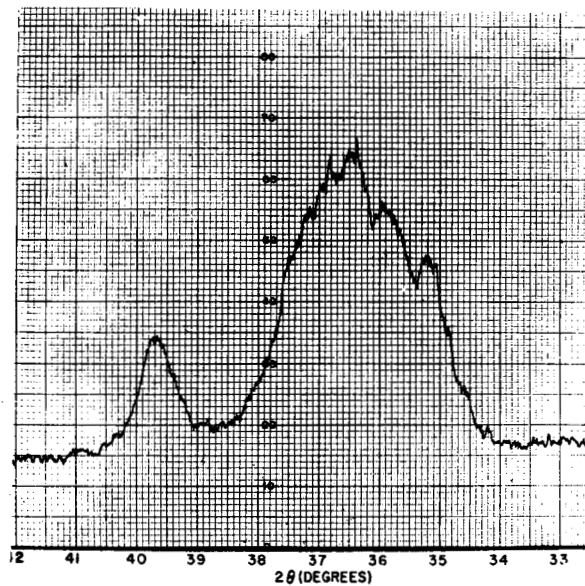
Fig. 26

X-ray diffractometer pattern.
Alloy: U-7w/o Nb.
Treatment: 900°C-WQ; 450°C -
1 hr-WQ. Peak for α (39.7°) and
the other indistinct reflections
for α and γ.
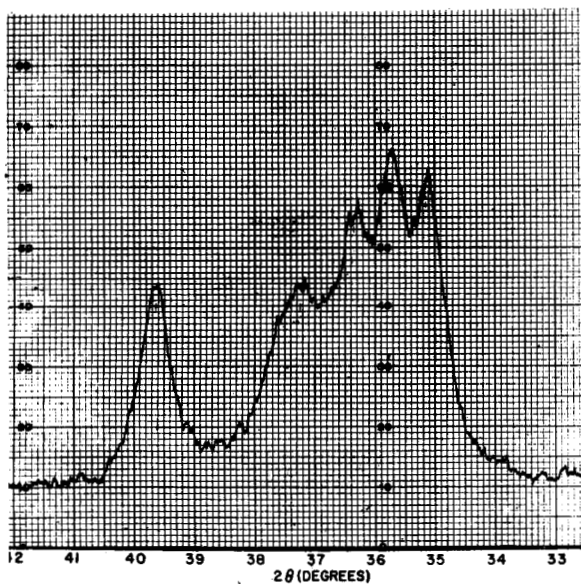

Fig. 27

X-ray diffractometer pattern.
Alloy: U-7w/o Nb.
Treatment: 900°C-WQ; 450°C -
10 hrs-WQ. α and γ, with shift
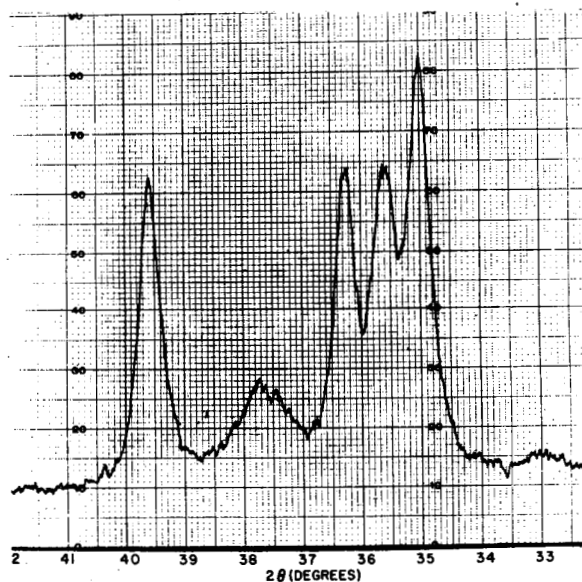of γ to higher 2θ value (37.2°).

Fig. 28

X-ray diffractometer pattern.
Alloy: U-7w/o Nb.
Treatment: 900°C-WQ; 450°C-1000
hrs-WQ. Increased sharpness of α
peaks and further shift of γ peak
to 37.7°.

- 36 -

3.   U-Nb-Zr Alloys

a.   Metallographic Results

        Zirconium was added to a U-7w/o Nb base at levels of 1 and 2 w/o.
Microstructures of these alloys which were transformed at 600° and 550°C
resembled those of the U-7w/o Nb material, illustrated in the previous section.
The dark-etching decomposition product originated at the grain boundaries and
around impurity particles; subsequent annealing resulted in the growth of this
product until no observable areas of gamma were present.

        As noted for the U-7w/o Nb composition, the alloys containing
zirconium also exhibited the fine decomposition product after relatively short
annealing times at 450°C. This structure, however, was not observed to origi-
nate in the small angular particles which were illustrated in the previous
section. Instead, this product appeared to initiate throughout the grains as
a light stain; some grains etched darker than adjacent grains, as may be seen
in Figure 29. This sample, U-7w/o Nb-2w/o Zr, was annealed for 1 hour at 450°C,
and several of the grains show initiation of this fine product. Further
annealing resulted in a uniform appearance of this product throughout the
sample, and after 10 hours at 450°C traces of the dark-etching transformation
product were observed at the grain boundaries (Figure 30). Prolonged annealing
resulted in very slow growth of this material in the grain boundaries. After
1000 hours at 450°C this product covered about 6% of the area of the U-7w/o Nb -
2w/o Zr alloy, and about 10% was found in the 1w/o zirconium composition.

        Microstructures produced upon annealing at 360°C were similar to
those observed in the U-7w/o Nb alloy. The oriented pattern was noted after
relatively short annealing times, and these structures generally coincided with
hardness increases. Small amounts of decomposition at the grain boundaries

were noted in the U-7w/o Nb-1w/o Zr material after 1000 hours at 360°C, as illustrated in Figure 31. The lightly stained, oriented pattern is evident within the grains. No grain boundary transformation was observed in the alloy containing 2w/o zirconium after this annealing treatment.

Metallographic data for the U-Nb-Zr compositions are summarized in Figures 32 and 33. These results reveal that, at all temperatures, longer annealing times were required to initiate grain boundary decomposition in the material having the higher zirconium content.

b.   Hardness Results

Hardness data for the U-Nb-Zr alloys are presented in Figures 34 and 35. The U-7w/o Nb-2w/o Zr material was more stable than the alloy containing 1w/o zirconium at 600°C and 550°C. Longer annealing times were required to produce an increase in hardness, and the peaks of these hardness curves occurred at considerably longer annealing times. At 450° and 300°C, the U-7w/o Nb-1w/o Zr alloy appeared to be the more stable, and both materials exhibited initial hardness increases in the extremely short time of 0.1 hour at 360°C. The curves for 360°C show that hardness values were still rising at 1000 hours; and, as was noted for the U-Nb alloys, the rapid initial increase at this temperature was probably the result of pre-precipitation hardening effects.

c.   Electrical Resistivity Results

Initial decreases in resistivity occurred in short times at all annealing temperatures in the two alloys containing zirconium (Figures 36 and 37). Annealing at 550°C produced changes in less than 0.1 hour, and the curves for this temperature show that the major portion of decrease in resistivity had taken place in less than 10 hours. Additional annealing produced a small but

continuing drop in resistivity up to 100 hours. These further changes may result from slight additional decomposition and a coarsening of the transformation product; microstructures of samples annealed for 100 hours at 550°C appear to be coarser than those annealed for shorter lengths of time.

Both U-Nb-Zr alloys exhibited a change of resistivity in slightly less than 0.1 hour at 450°C. After 10 hours at this temperature, a substantial decrease had occurred, although only traces of the grain boundary decomposition were found in the microstructures (Figure 30). This significant drop in resistivity may be attributed to the fine decomposition product.

Annealing at 360°C also produced rapid initial changes in resistivity. These decreases were very small; after 400 hours the resistivity values were only 4 to 5 microhm-cm below the values for solution treated materials. These results indicate that only slight amounts of transformation had taken place.

d.   Dilatometric Results

Results of dilatometric measurements on a U-7w/o Nb-1w/o Zr alloy annealed at 550°C are presented in Figure 38. A decrease in length occurred in about 0.2 hour, and transformation appeared to be complete in less than 3 hours. These results are in substantial agreement with hardness measurements and metallographic observations.

Initiation of transformation in the U-7w/o Nb-2w/o Zr composition, as shown by the dilatometric curve, Figure 39, took place in less than 0.2 hour at 550°C. The change in length appeared to be complete in less than 7 hours, which indicates that the rate of transformation was slower than in the 1w/o zirconium material.

Annealing the alloys containing zirconium at 450°C produced very large decreases in length in 4 hours. These results, based on length measurements

taken on samples before and after annealing, show that this increase in density is approaching the maximum value. Transformation, as determined by increases in density, initiated and progressed rapidly at this annealing temperature.

Much smaller changes in length were found upon annealing at 360°C. After 400 hours at this temperature, the change was about one third of the maximum decrease in length observed at the higher annealing temperatures.

e. X-Ray Diffraction Results

Figures 40 to 43 illustrate diffractometer charts obtained from the U-7w/o Nb-2w/o Zr alloy annealed for varying times at 550°C. In Figure 40, after 0.4 hour the single gamma peak ($2\theta = 36.8°$) has shifted to a slightly higher 2θ value than was noted in the solution-treated sample. This shift is due to the precipitation of a small amount of alpha, resulting in an enrichment of the gamma phase in niobium content. Some grain boundary decomposition is observed metallographically for this treatment, although the alpha present was not detected by the X-ray diffractometer. After 4 hours, Figure 41, four distinct alpha reflections are observed; the gamma peak has broadened and the average value indicates a continued shift in composition. In Figure 42 the alpha peaks are unchanged after 46 additional hours, but the gamma peak is now broad and poorly defined, probably the result of a finely dispersed gamma structure having a range of compositions. After a total of 100 hours at 550°C (Figure 43) the alpha peaks are more predominant. The single gamma peak has markedly shifted ($2\theta = 37.7°$) and has become sharply defined. Samples annealed for times up to 500 hours show that this sharpening of the γ_2 peak continues but that the 2θ value is unchanged.

These results indicate that as alpha precipitates, the composition of gamma varies continuously between that for γ_1 and γ_2. As decomposition

proceeds, the equilibrium compositions of alpha and γ_2 are approached. This type of mechanism is noted at both 450° and 550°C, for the 1w/o and 2w/o zirconium alloys, and is similar to that observed in the U-Nb alloys. The binary compositions, however, did not exhibit the broadened, poorly defined gamma peak during the intermediate stages of transformation as illustrated in Figure 42.

X-ray diffraction patterns for the U-Nb-Zr alloys annealed at 360°C for 1000 hours show that incipient transformation had taken place. The gamma peak was broadened, and indistinct rises in the vicinity of alpha peaks were noted. Both patterns showed less evidence of alpha than was found in the U-7w/o alloy after the same annealing treatment.
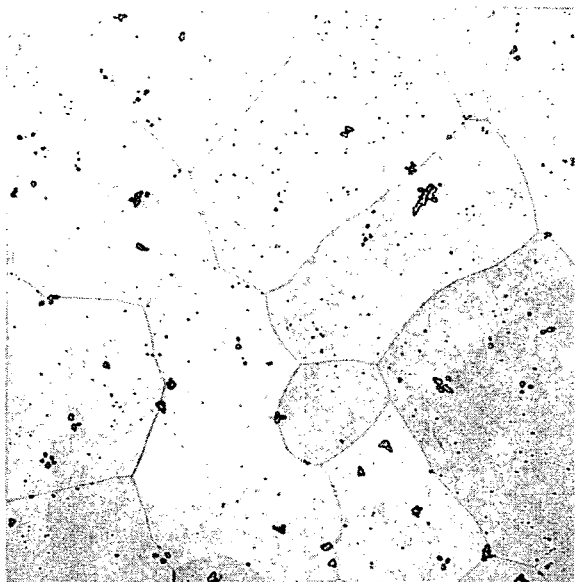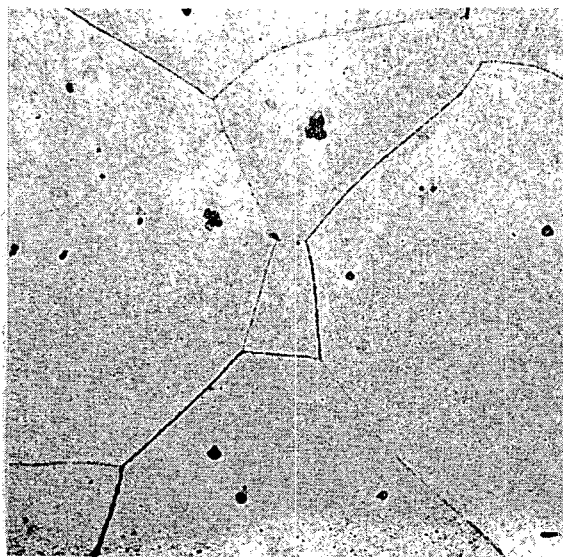
Neg. No. 12905   X 250

Fig. 29

Alloy: U-7w/o Nb-2w/o Zr.
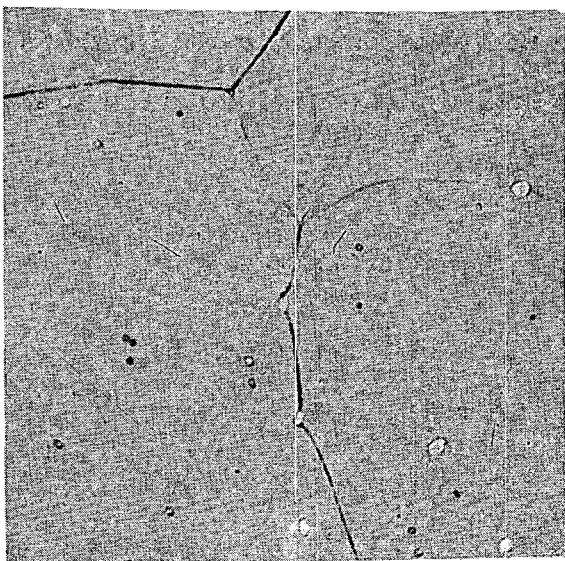Treatment: 900°C-WQ; 450°C-1 hr-
WQ. Light staining in some grains.

Neg. No. 14082   X 250

Fig. 30

Alloy: U-7w/o Nb-2w/o Zr.
Treatment: 900°C-WQ; 450°C-10 hrs-
WQ. Fine precipitate throughout
matrix; small amounts of transfor-
mation at some grain boundaries.

Neg. No. 13832   X 1000

Fig. 31

Alloy: U-7w/o Nb-1w/o Zr.
Treatment: 900°C-WQ; 360°C-1000
hrs-WQ. Oriented pattern within
grains; initial transformation at
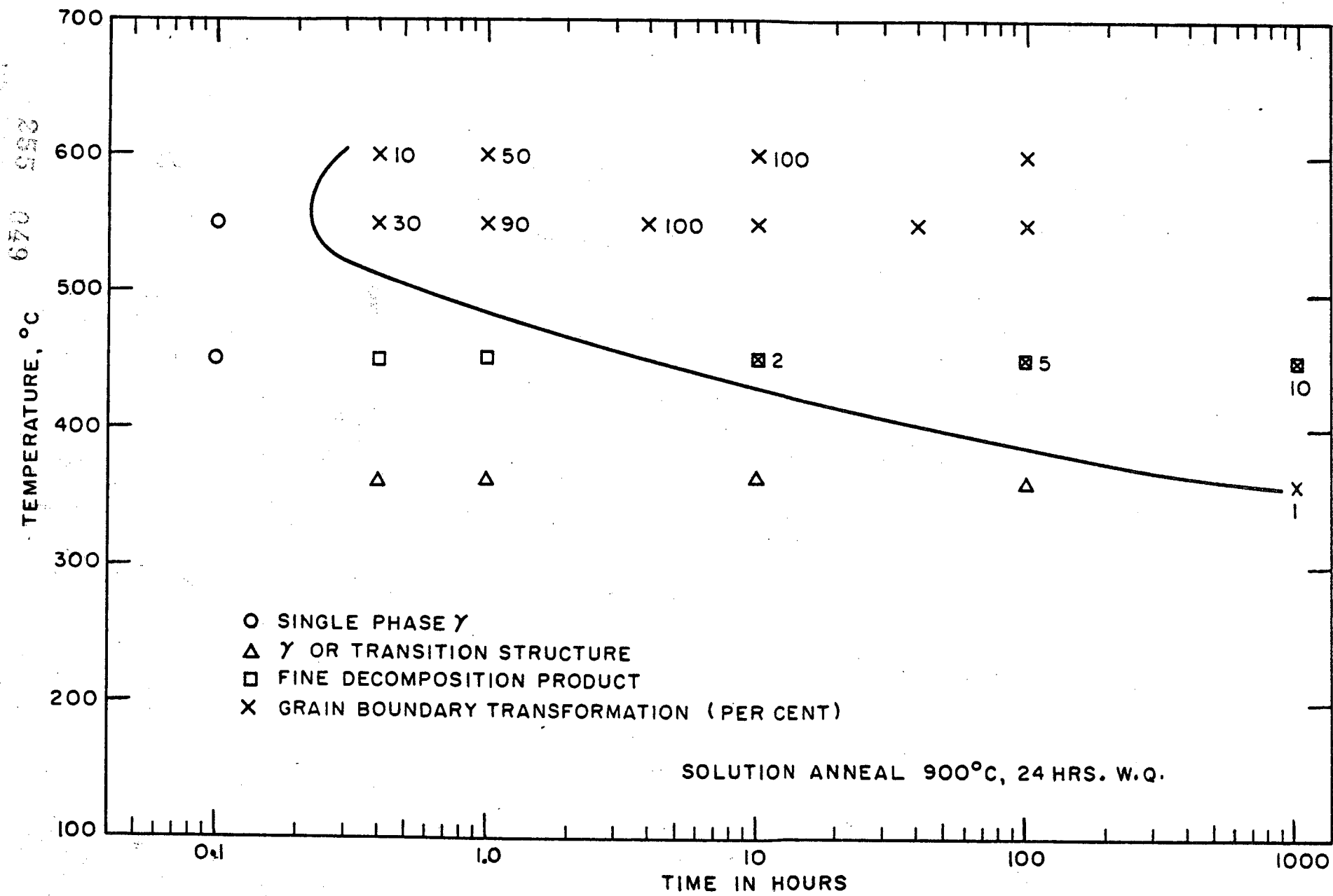grain boundaries.

Etchant: 10% CrO_3 + 2% HF + H_2O

FIG. 32 - TTT DIAGRAM FOR A U-7w/o Nb-1w/o Zr ALLOY ILLUSTRATING INITIAL METALLOGRAPHIC OBSERVATION OF GRAIN BOUNDARY TRANSFORMATION

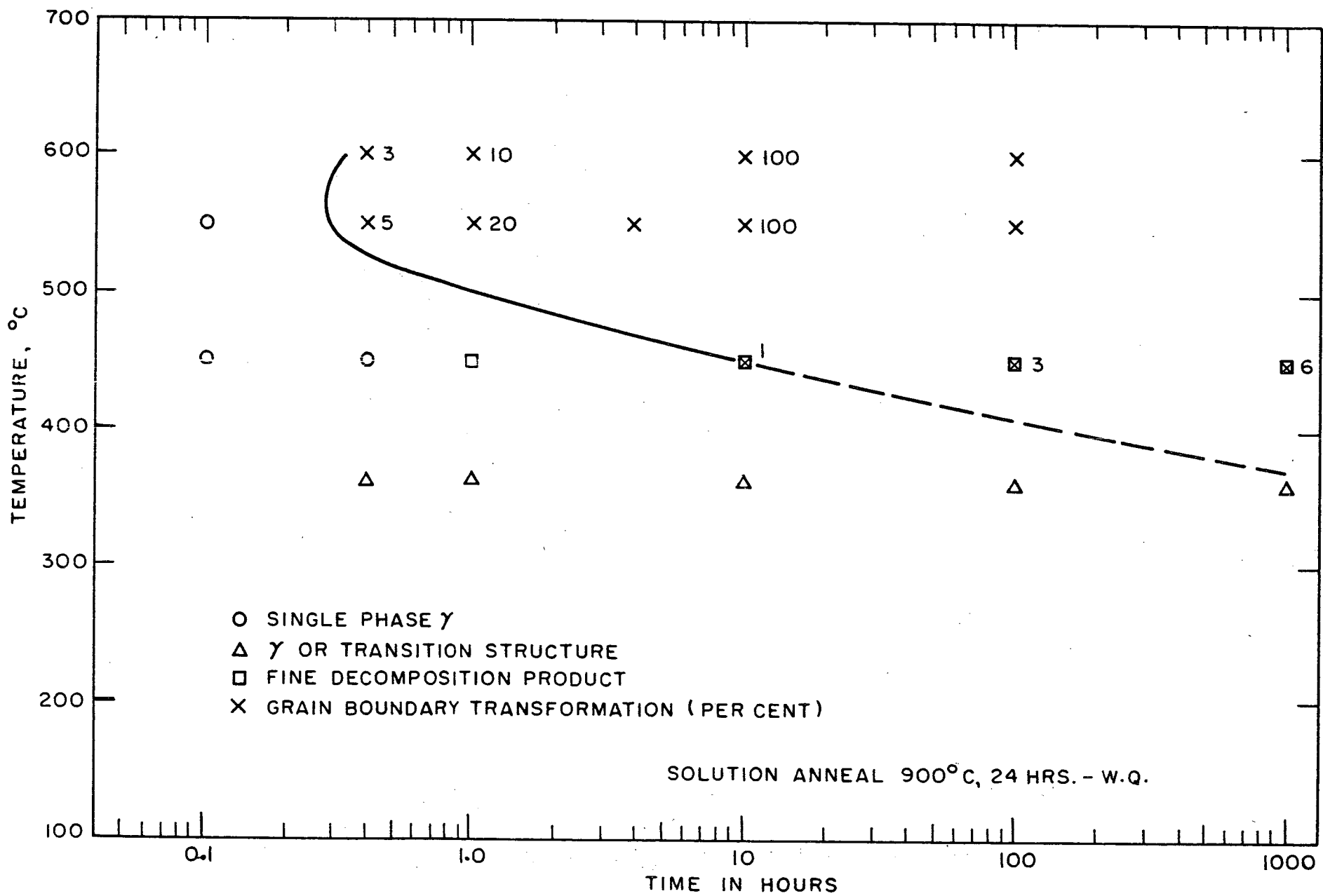FIG. 33 - TTT DIAGRAM FOR A U-7w/o Nb-2w/o Zr ALLOY ILLUSTRATING INITIAL
METALLOGRAPHIC OBSERVATION OF GRAIN BOUNDARY TRANSFORMATION

700

600

VPN HARDNESS

500

400

300

200

100

450°C

360°C

550°C

300°C

600°C

+ 600 °C
● 550 °C
◆ 450 °C
○ 360 °C
▣ 300 °C

SOLUTION ANNEAL   900°C, 24 HRS. – W.Q.
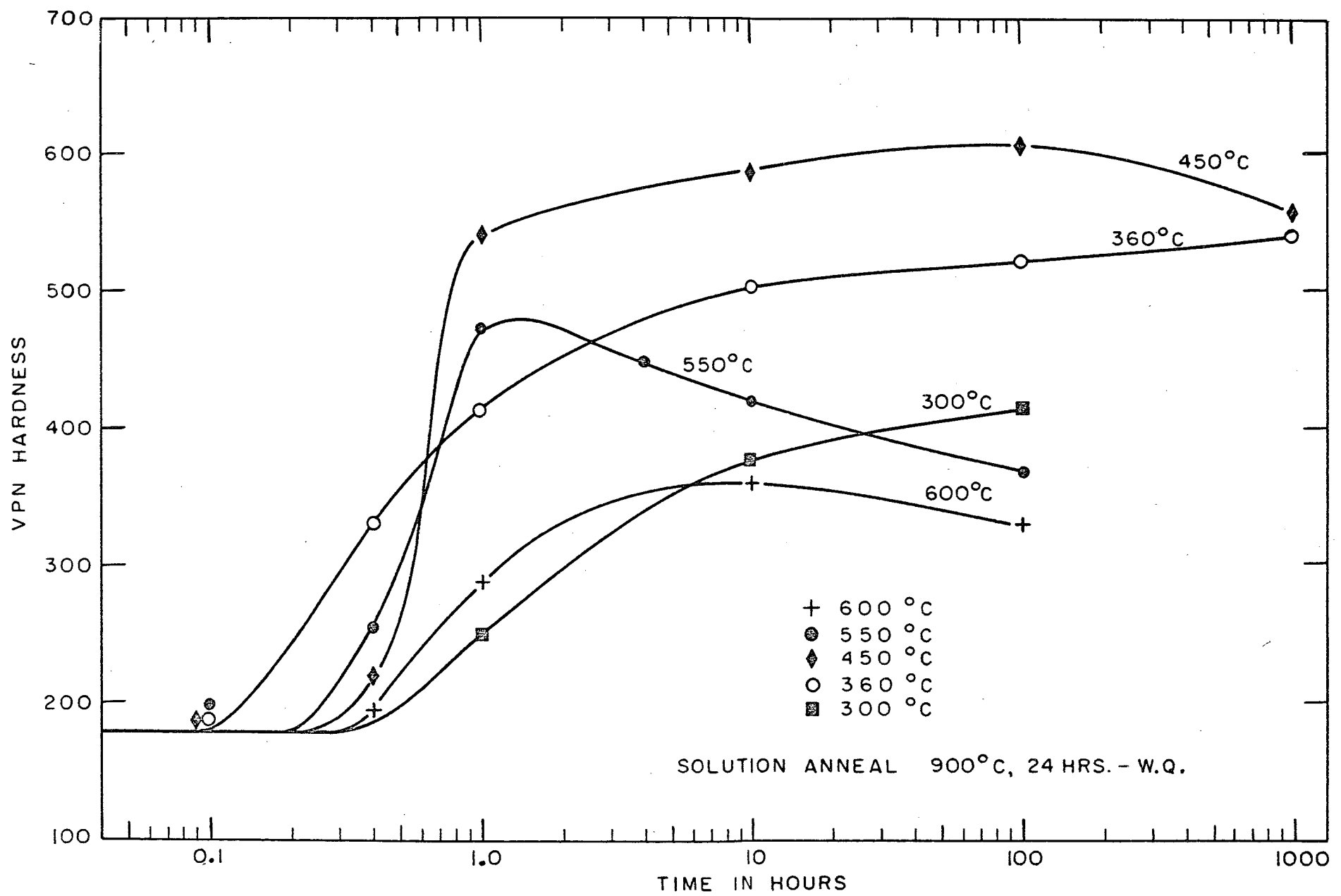
0.1   1.0   10   100   1000

TIME IN HOURS

FIG. 34 – HARDNESS DATA FOR AN ISOTHERMALLY ANNEALED U-7w/o Nb-1w/o Zr ALLOY

FIG. 35 - HARDNESS DATA FOR AN ISOTHERMALLY ANNEALED U-7w/o Nb-2w/o Zr ALLOY

SOLUTION ANNEAL 900°C, 24 HRS. - W.Q.

Legend:
+ 600 °C
● 550 °C
♦ 450 °C
○ 360 °C
▣ 300 °C

FIG. 36 - ROOM TEMPERATURE ELECTRICAL RESISTIVITY DATA FOR AN
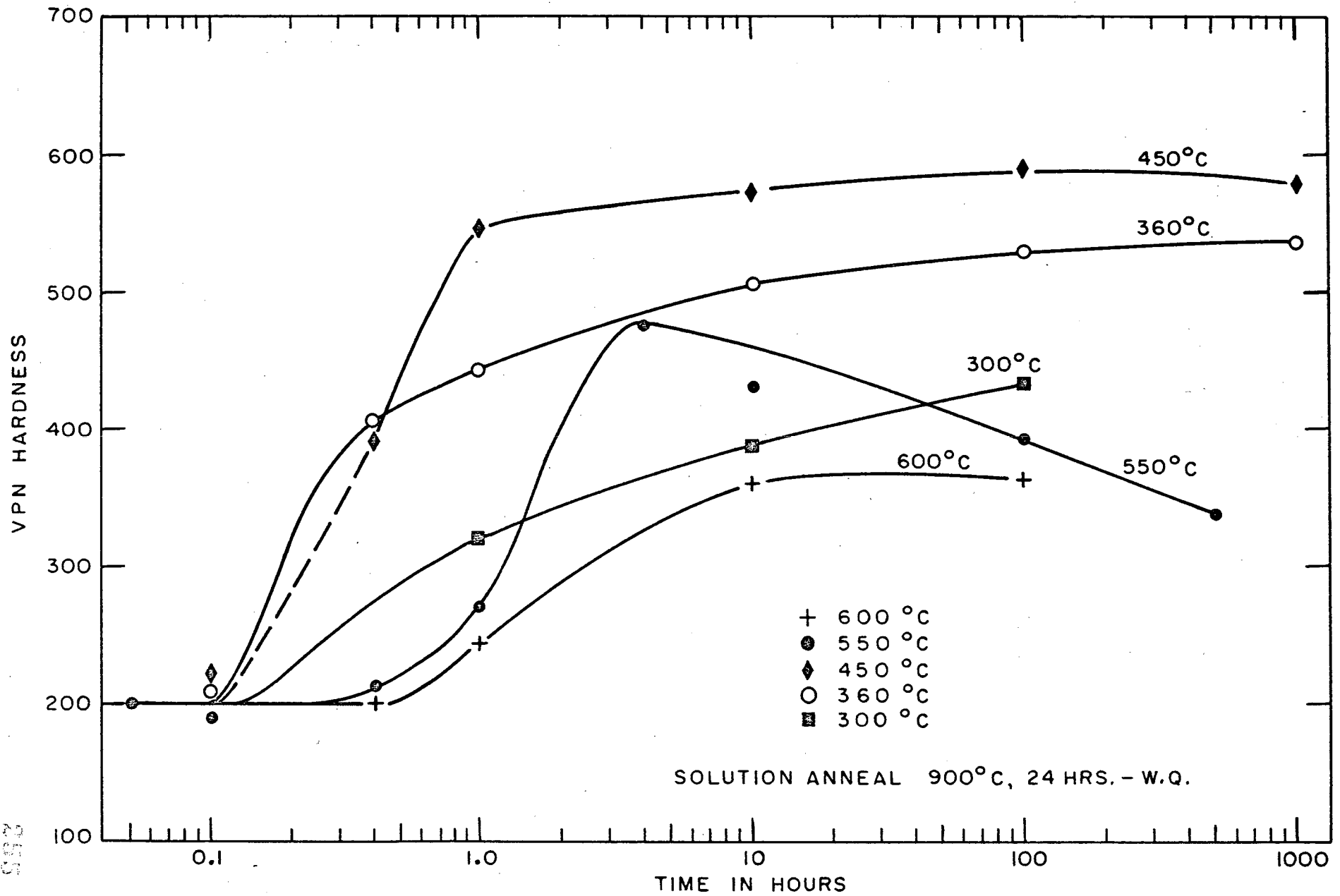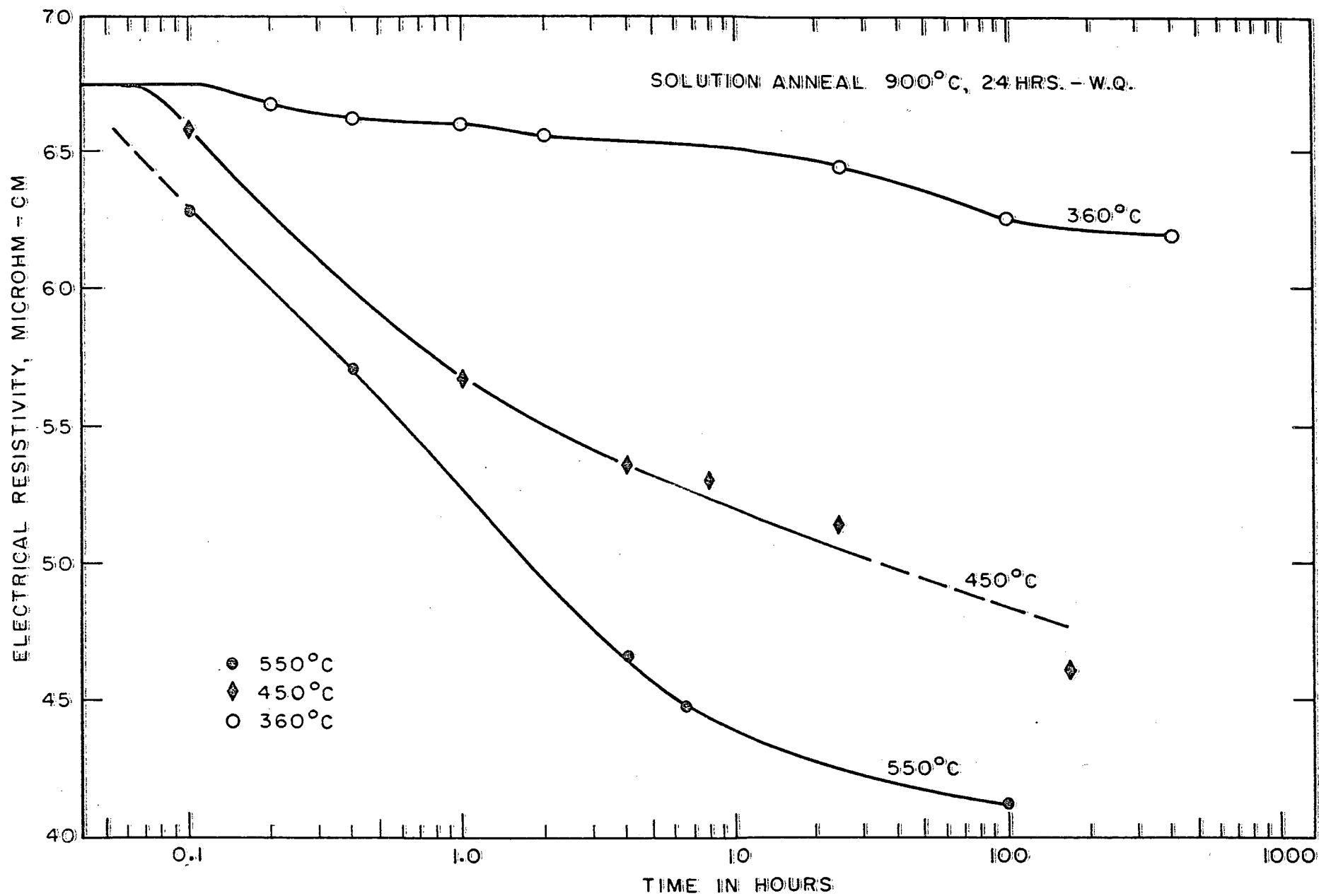ISOTHERMALLY ANNEALED U-7w/o Nb-1w/o Zr ALLOY

FIG. 37 - ROOM TEMPERATURE ELECTRICAL RESISTIVITY DATA FOR AN
ISOTHERMALLY ANNEALED U-7w/o Nb-2w/o Zr ALLOY

CHANGE IN LENGTH IN IN/IN × 10^4

TIME IN HOURS

+10

0

−10

−20

−30

0.1

1.0

10

SOLUTION ANNEAL − 900 °C 24 HRS. − W. Q.
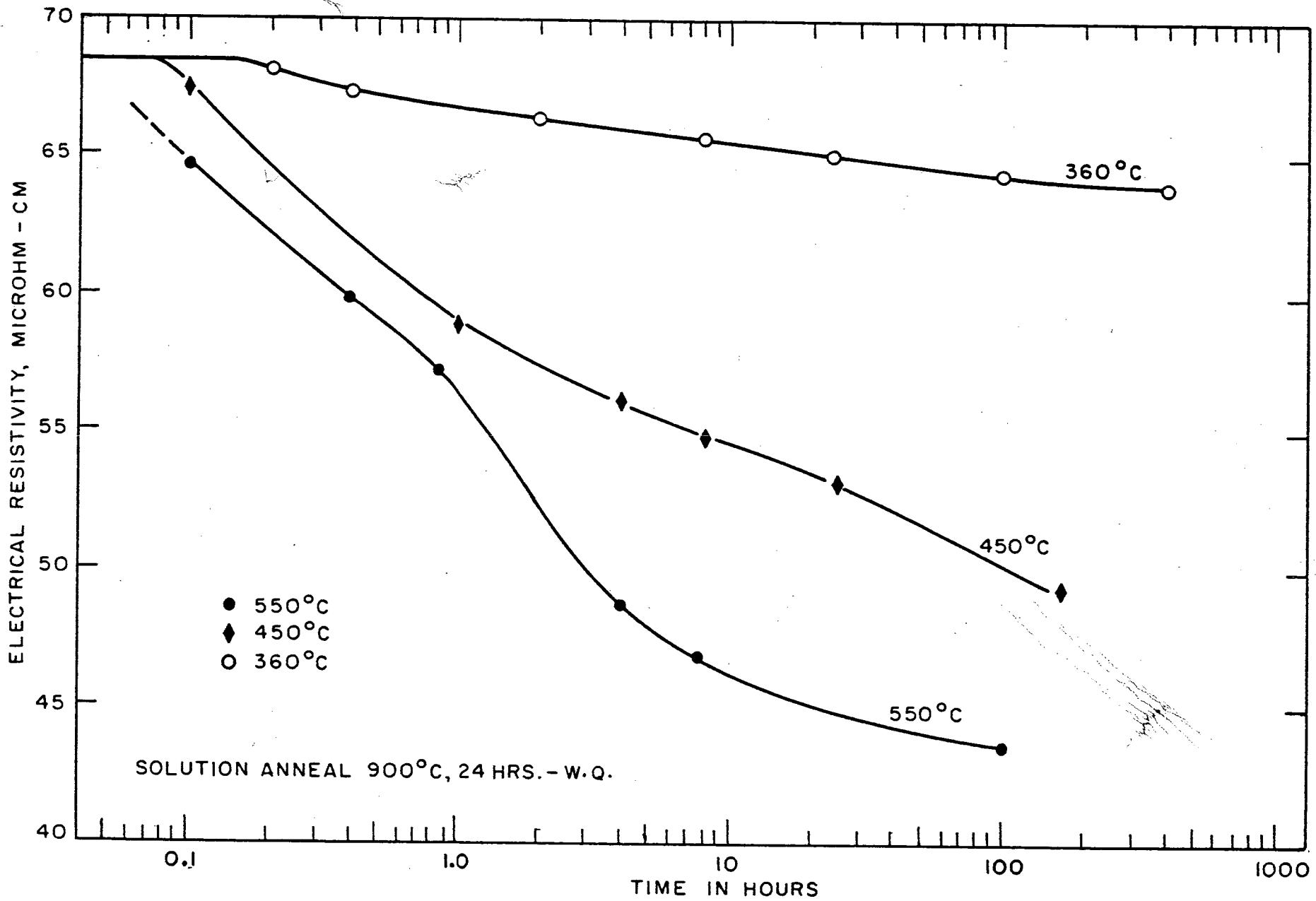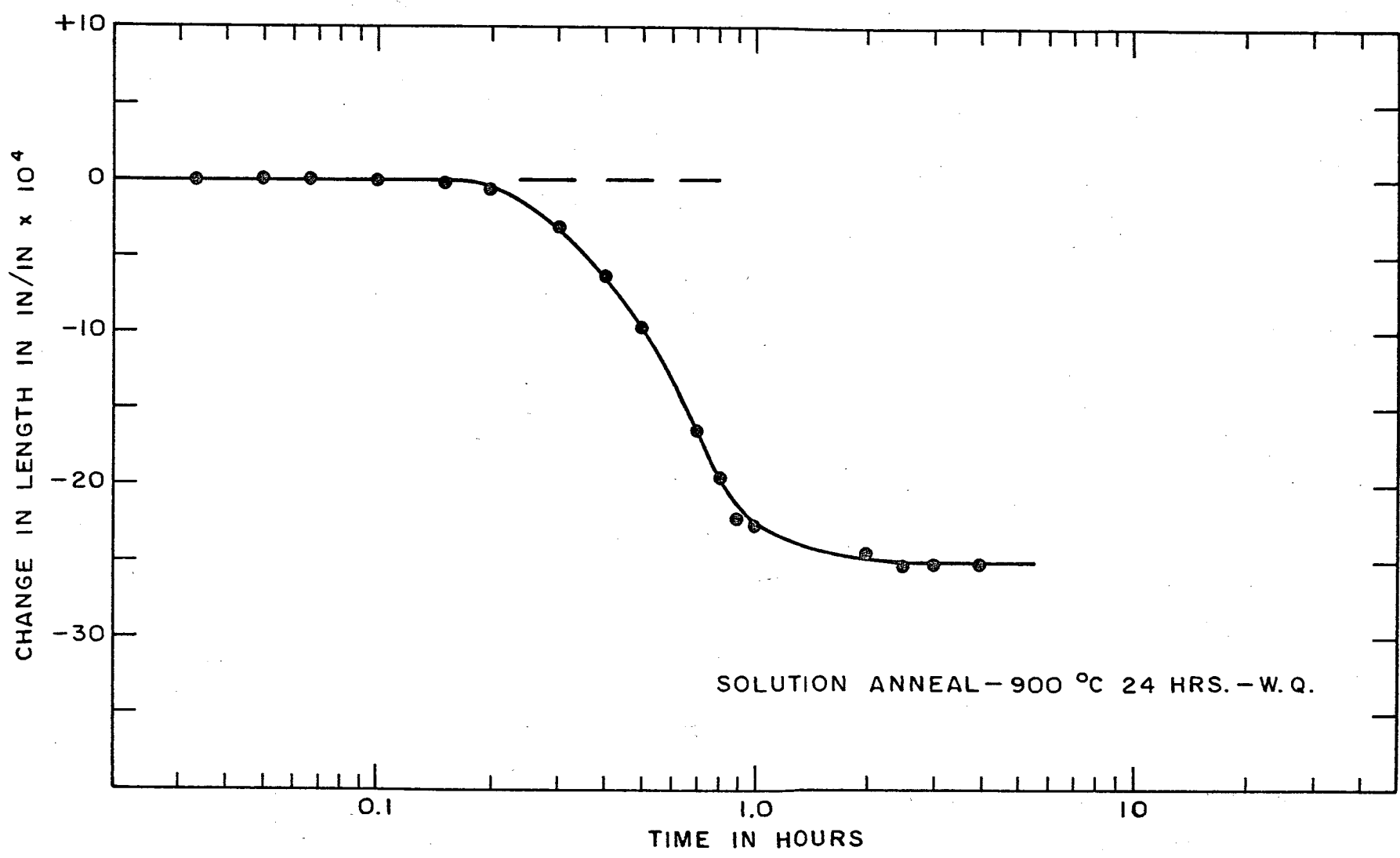
FIG. 38 − DILATOMETRIC DATA FOR A U-7 ^{W}/o Nb -1 ^{W}/o Zr ALLOY
ISOTHERMALLY ANNEALED AT 550 °C
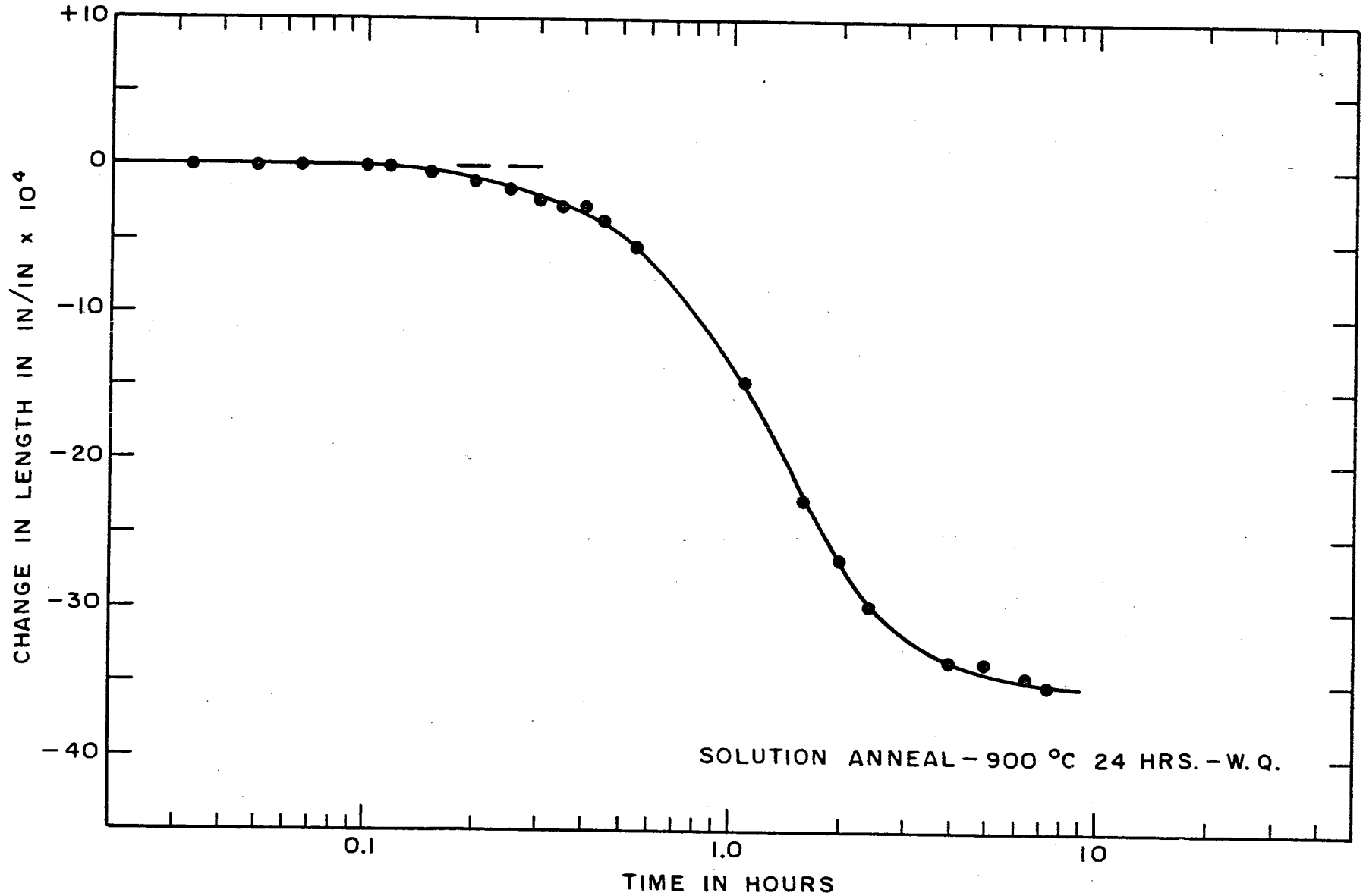
FIG. 39 - DILATOMETRIC DATA FOR A U-7 ^{W}/o Nb-2 ^{W}/o Zr ALLOY
ISOTHERMALLY ANNEALED AT 550°C
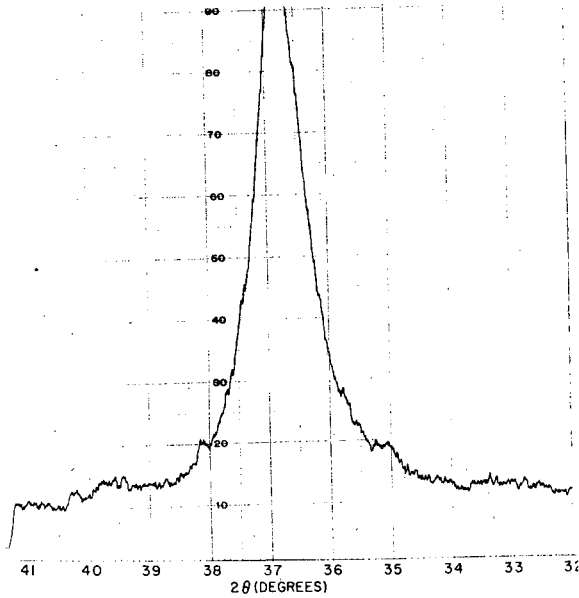
Fig. 40

X-ray diffractometer pattern.
Alloy: U-7w/o Nb-2w/o Zr.
Treatment: 900°C-WQ; 550°C-0.4
hr-WQ. γ (2θ = 36.8°).

Fig. 41

X-ray diffractometer pattern.
Alloy: U-7w/o Nb-2w/o Zr.
Treatment: 900°C-WQ; 550°C-4 hrs-
WQ. 4 peaks for α. γ at 37.2°.

Fig. 42

X-ray diffractometer pattern.
Alloy: U-7w/o Nb-2w/o Zr.
Treatment: 900°C-WQ; 550°C-50
hrs WQ. Diffuse γ reflection
+ α.

Fig. 43

X-ray diffractometer pattern.
Alloy: U-7w/o Nb-2w/o Zr.
Treatment: 900°C-WQ; 550°C-100
hrs-WQ. Increased amount of α
with γ peak at 37.7°.

- 51 -

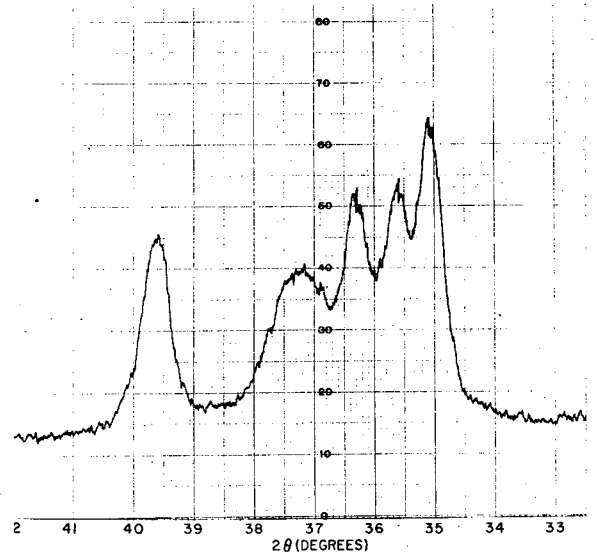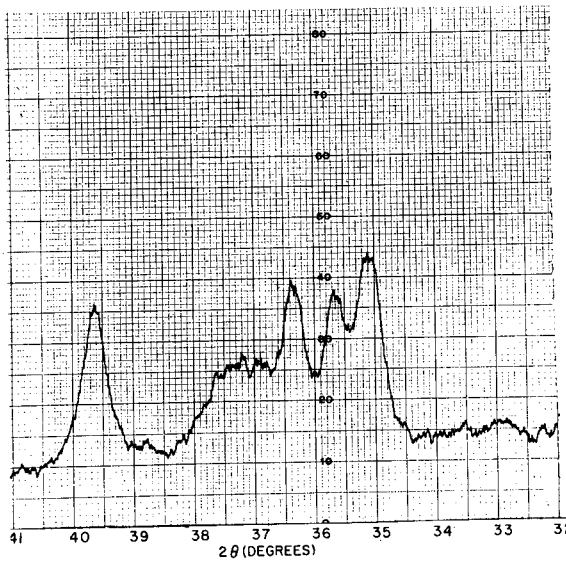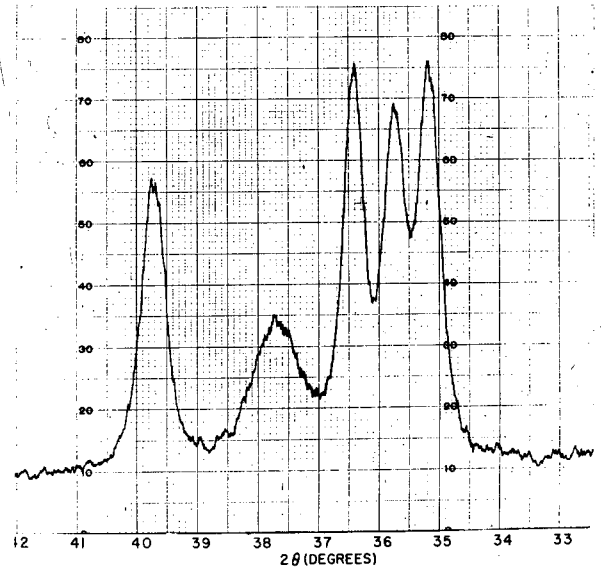4.   U-Nb-Cr Alloys

        Four uranium-base alloys containing niobium and chromium were
studied. These consisted of U-8w/o Nb and U-10w/o Nb base materials to which
chromium was added at two levels, 0.5 and 3 a/o. From this range of combi-
nations, it was possible to demonstrate the effects of increasing amounts of
both niobium and chromium.

a.   Metallographic Results

        The two U-Nb base alloys containing 3 a/o chromium exhibited in-
cipient meltingafter a homogenization anneal at 1100°C and 1050°C. No melting
was observed in the microstructures of samples held for 48 hours at 1000°C.
The 0.5 a/o chromium compositions did not exhibit incipient melting at 1100°C
and were consequently homogenized at this temperature.

        Transformation structures of the U-Nb-Cr alloys annealed at 600° and
550°C were similar to those for materials previously described in that decom-
position originated at the grain boundaries and continued to grow until no
massive areas of gamma remained. The decomposition products in the U-10w/o Nb-
Cr alloys were somewhat lamellar at these annealing temperatures. Figure 44
shows the product obtained upon annealing the U-10w/o Nb-0.13w/o Cr material
for 10 hours at 600°C. No large patches of gamma are visible, and most areas
are lamellar. Further annealing resulted in the change of this lamellar
structure, as illustrated in Figure 45 for the same material annealed for 100
hours at 600°C.

        Annealing the alloys containing chromium at 450°C produced trans-
formation at the grain boundaries and also the fine decomposition product
throughout the grains. In most instances, the fine precipitate was initiated
first, at annealing times which produced changes in hardness, electrical

resistivity and density. Relatively small amounts of the grain boundary transformation were present in the U-Nb-Cr materials after 1000 hours at 450°C. Annealing at 360°C produced the oriented structures similar to those described for other compositions at this temperature.

The effects of increasing amounts of chromium and niobium on grain boundary transformation are illustrated in the TTT diagrams of Figures 46 to 49. The U-10w/o Nb-Cr alloys required considerably longer annealing times to initiate transformation than were required for the U-8w/o Nb-Cr materials. In addition, compositions having the higher chromium content (3 a/o) were more stable than those with 0.5 a/o for both the U-8w/o Nb and U-10w/o Nb base materials.

b. Hardness Results

The U-8w/o Nb-0.12w/o Cr and U-8w/o Nb-0.74w/o Cr alloys exhibited increases in hardness in less than 1 hour at all annealing temperatures. Relatively small differences were noted between the curves for the two compositions, Figures 50 and 51, although the increased chromium content resulted in slight added stability of the gamma phase, and a considerably higher base hardness.

Curves for the two alloys containing 10w/o niobium are presented in Figures 52 and 53. The effect of increased niobium content is evident from a comparison with the two previous curves. The U-10w/o Nb-0.78w/o Cr material showed initial changes in hardness in times ranging from about 0.6 hour at 550°C to approximately 8 hours at 450°C. The U-10w/o Nb composition having the lower chromium content displayed hardness increases in shorter annealing times at all temperatures. Hardness values for both alloys at the lower annealing temperature were somewhat variable. Such variations usually

occurred as transformation was initiated and may have been due to slight localized variations in composition within the samples.

c. Electrical Resistivity Results

Resistivity curves for the four U-Nb-Cr alloys are presented in Figures 54 to 57. As noted for other materials, the initial and most rapid decreases occurred at the 550°C annealing temperature. Relatively small decreases in resistivity were recorded at the 360°C temperature for times up to 400 hours. The U-10w/o Nb-0.78w/o Cr composition was the most stable of the group; the least stable was the U-8w/o Nb-0.12w/o Cr material. The results verify the findings of hardness tests and metallographic examination which demonstrated the effectiveness of both niobium and chromium as gamma-phase stabilizers.

d. Dilatometric Results

Initiation of transformation in the U-8w/o Nb-0.12w/o Cr alloy occurred in slightly less than 0.2 hour at 550°C, as determined by the dilatometric curves shown in Figure 58. This value is in fair agreement with the annealing times required to produce changes in other properties at this annealing temperature. The initial hardness increase and metallographically observed transformation occurred in 0.3 hour or less; resistivity values decreased in less than 0.1 hour. These variations in annealing times as determined by the several methods used to study transformation will be discussed under the "Comparative Data" section of this report.

Dilatometric data for this U-8w/o Nb-0.12w/o Cr material at 450°C show that transformation started in slightly over 1 hour. After 8 hours at this temperature, the change in length was about half the value measured on

255   060

a sample which had been completely transformed at 550°C. These results indicate that a considerable amount of transformation had taken place before the dark-etching grain boundary product was present in the microstructure. Similar observations were noted for the other U-Nb-Cr compositions annealed at 450°C.

Annealing the alloys containing chromium at 360°C produced significant increases in density after 400 hours at temperature. The U-8w/o Nb-Cr materials showed greater changes in length than were measured for the U-10w/o Nb-Cr compositions, reflecting the stabilizing value of increased amounts of niobium.

e. X-Ray Diffraction Results

Spectrometer patterns for both U-8w/o Nb-Cr alloys indicate that transformation was complete after annealing for 100 hours at 600°C or 550°C. The phases present were α and γ_2. After 1000 hours at 450°C, the gamma peak for the U-8w/o Nb-0.12w/o Cr material was approaching the 2θ value for γ_2, indicating a relatively large amount of decomposition. Less transformation occurred during this annealing treatment for the U-8w/o Nb-0.74w/o Cr composition; although the four alpha peaks were also present, the gamma reflection was found at a lower 2θ value. Spectrometer traces for both materials exhibited broadened gamma peaks and indistinct patterns for alpha after annealing for 1000 hours at 360°C.

X-ray diffraction studies of the two U-10w/o Nb-Cr compositions showed the stabilizing effects of the increased amount of niobium at lower temperatures. Transformation of the gamma phase was considered to be complete after 100 hours at 600°C. However, after annealing at 550°C for 100 hours, the peaks for gamma were found at slightly lower 2θ values than those

for the 600°C annealing temperature. Although both materials exhibited similar behavior at the higher annealing temperatures, the alloy having the greater chromium content was the more stable after 1000 hours at 450°C. Both alloys were only partially transformed after this heat treatment, but the gamma peak for the U-10w/o Nb-0.78w/o Cr material had not shifted as far as the one for the U-10w/o Nb-0.13w/o Cr composition. Annealing for 1000 hours at 360°C produced only very slight shifts of the peaks for gamma from the solution treated values, and no alpha was detected.
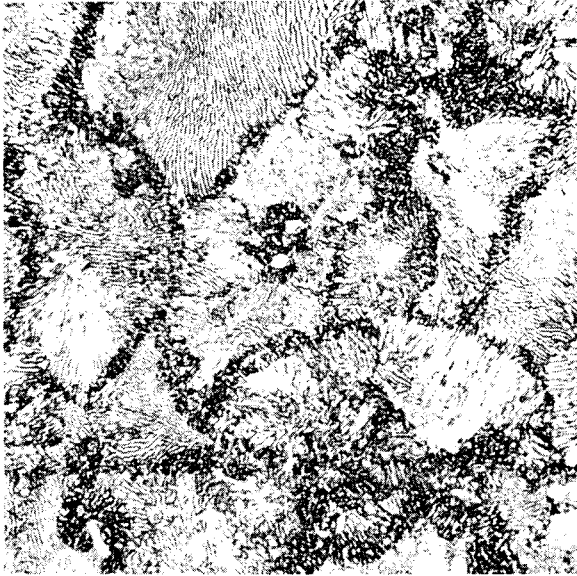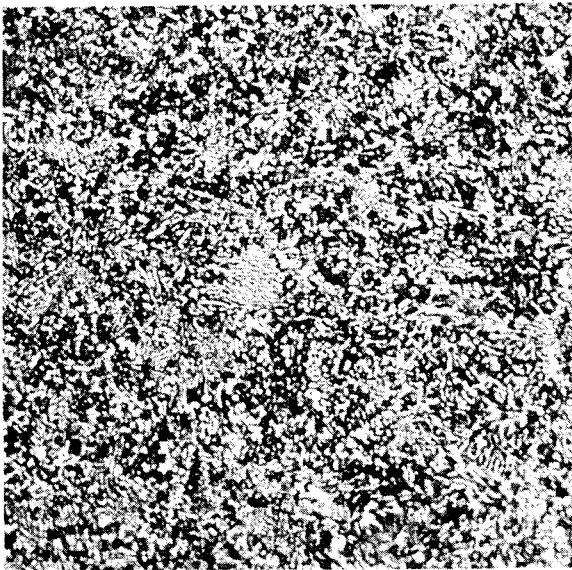
Neg. 13144   X 1000

Fig. 44

Alloy: U-10w/o Nb-0.13w/o Cr.
Treatment: 900°C-WQ; 600°C-10 hrs-WQ.
Lamellar transformation product.

Neg. No. 14725   X 1000

Fig. 45

Alloy: U-10w/o Nb-0.13w/o Cr.
Treatment: 900°C-WQ; 600°C-100 hrs-WQ.
Additional annealing at 600°C has
spheroidized the lamellar structure
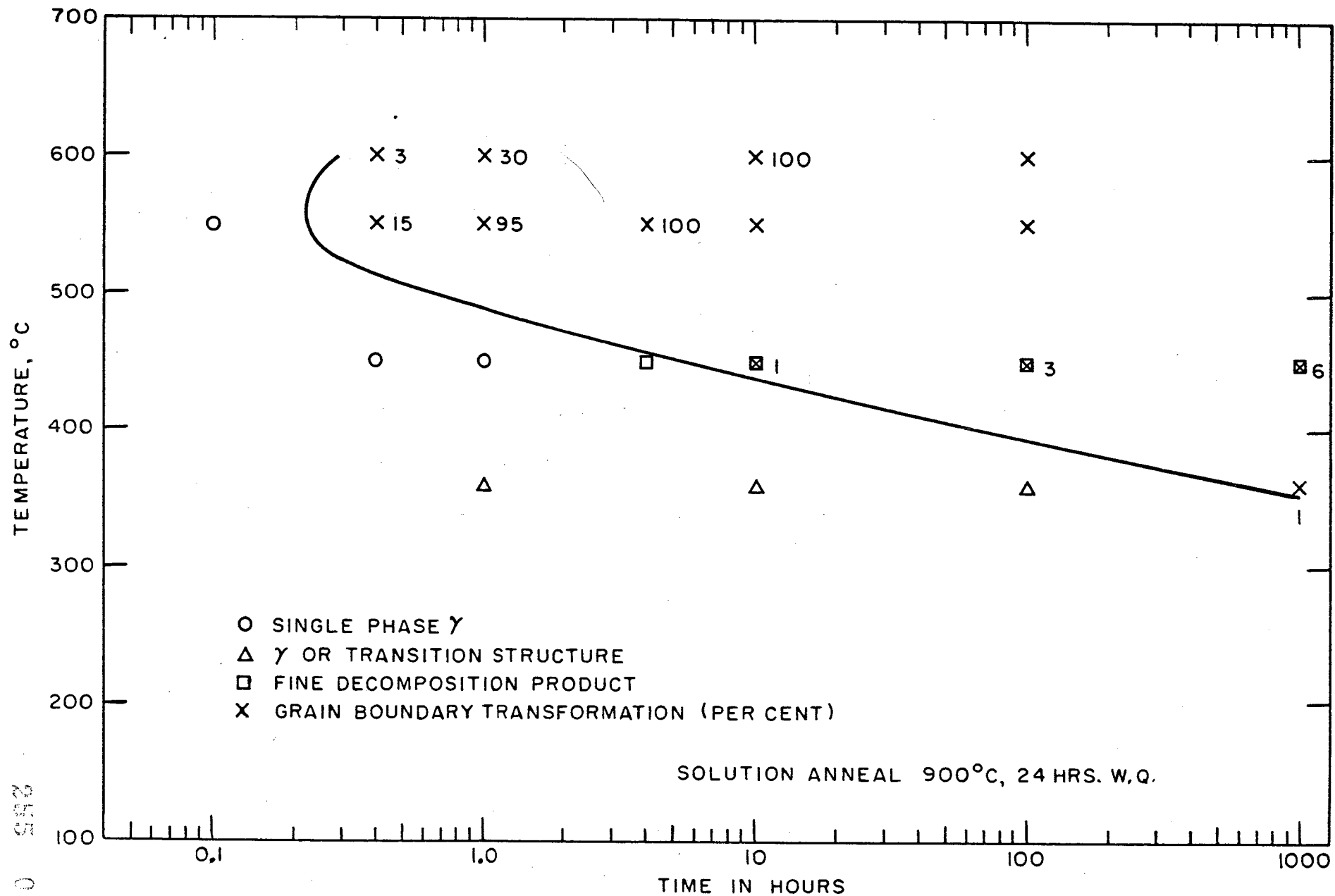shown in Fig. 44.

Etchant: 10% CrO_3 + 2% HF + H_2O.

- 57 -

255   063

FIG. 46 - TTT DIAGRAM FOR A U-8w/o Nb-0. 12w/o Cr ALLOY ILLUSTRATING INITIAL
METALLOGRAPHIC OBSERVATION OF GRAIN BOUNDARY TRANSFORMATION

FIG. 47 - TTT DIAGRAM FOR A U-8w/o Nb-0.74w/o Cr ALLOY ILLUSTRATING INITIAL
METALLOGRAPHIC OBSERVATION OF GRAIN BOUNDARY TRANSFORMATION

The figure shows a TTT diagram with TEMPERATURE, °C (100 to 700) on the vertical axis and TIME IN HOURS (0.1 to 1000) on the horizontal axis.

Legend:
O SINGLE PHASE γ
△ γ OR TRANSITION STRUCTURE
□ FINE DECOMPOSITION PRODUCT
X GRAIN BOUNDARY TRANSFORMATION (PER CENT)

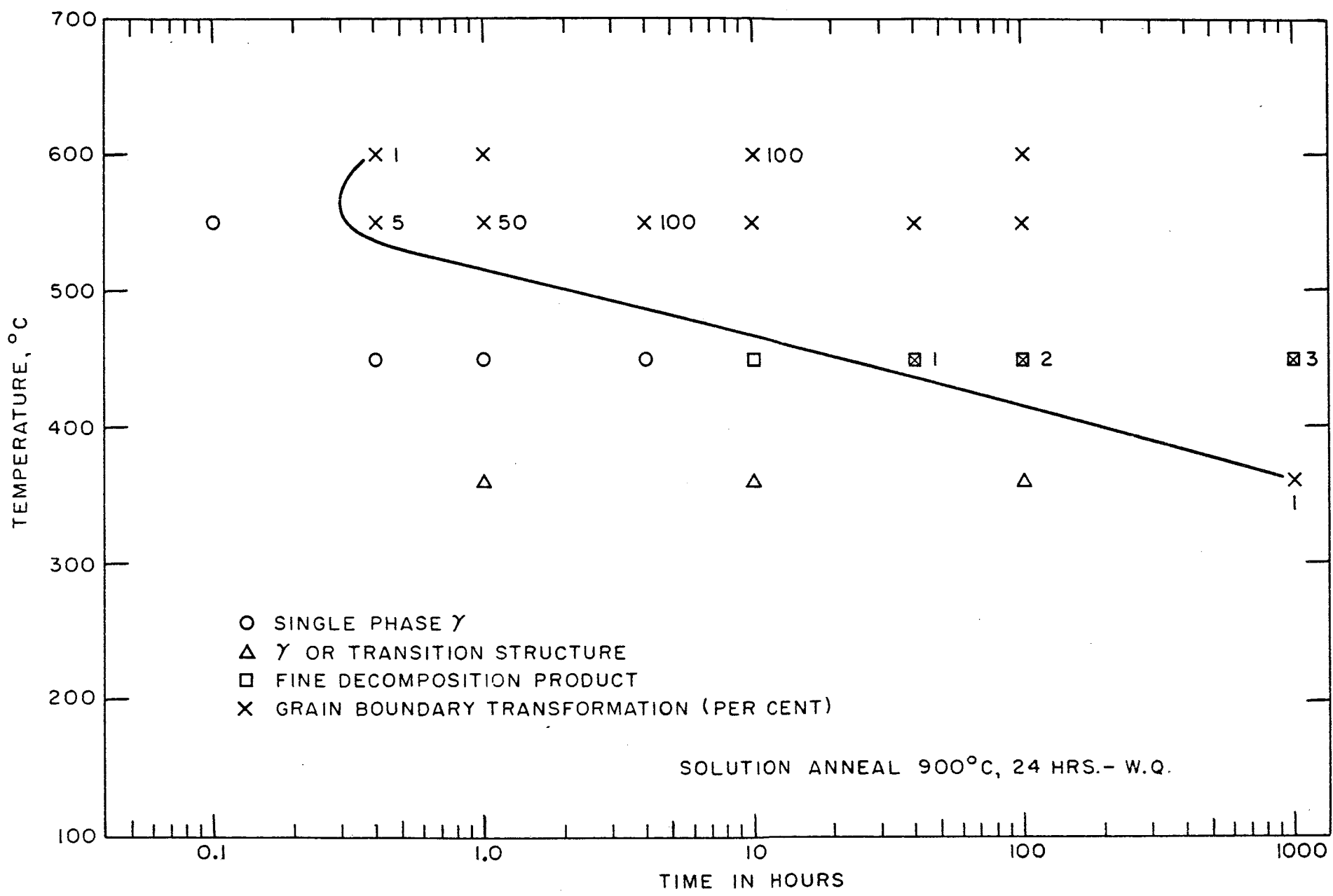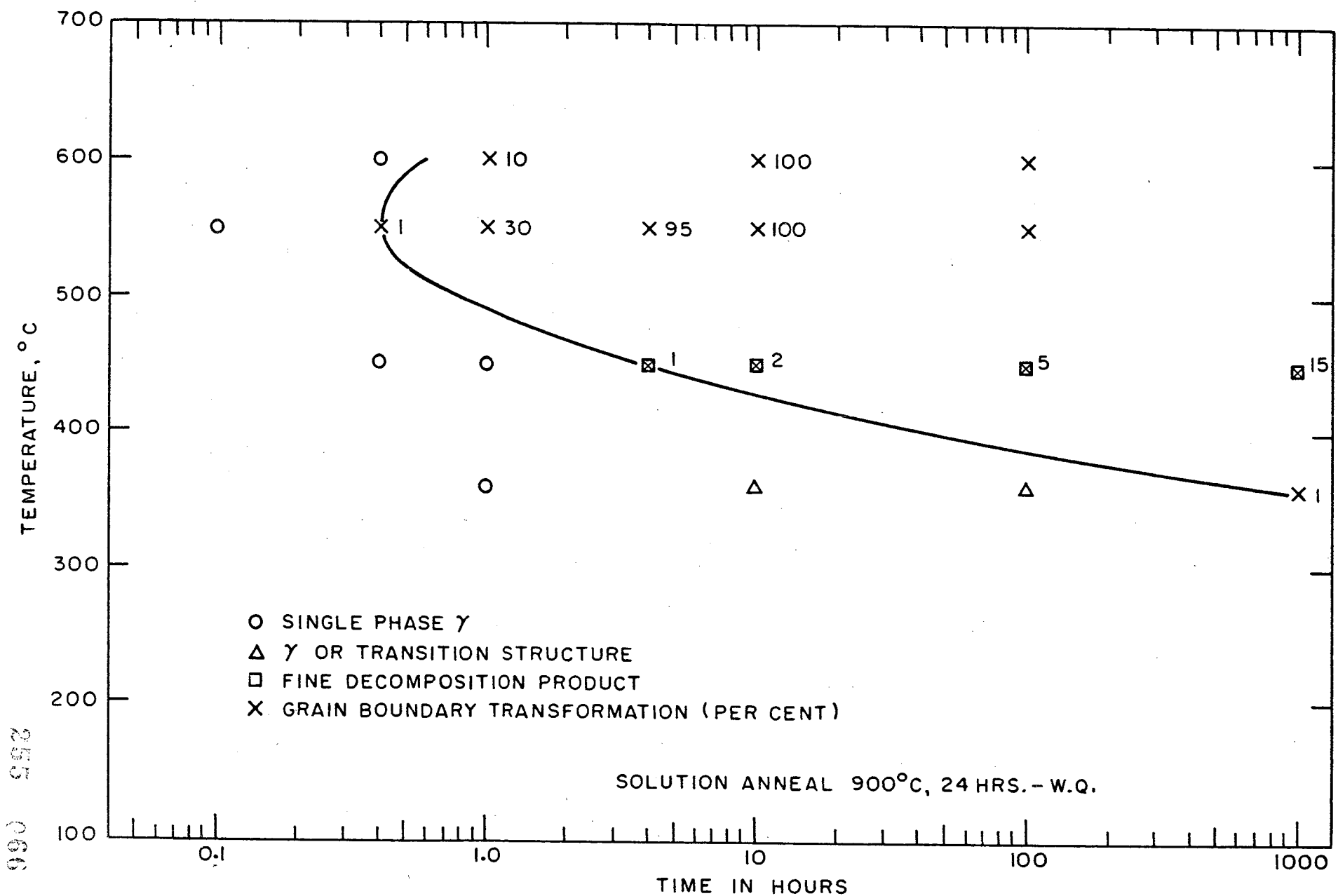SOLUTION ANNEAL 900°C, 24 HRS.- W.Q.

FIG. 48 - TTT DIAGRAM FOR A U-10w/o Nb-0.13w/o Cr ALLOY ILLUSTRATING INITIAL
METALLOGRAPHIC OBSERVATION OF GRAIN BOUNDARY TRANSFORMATION
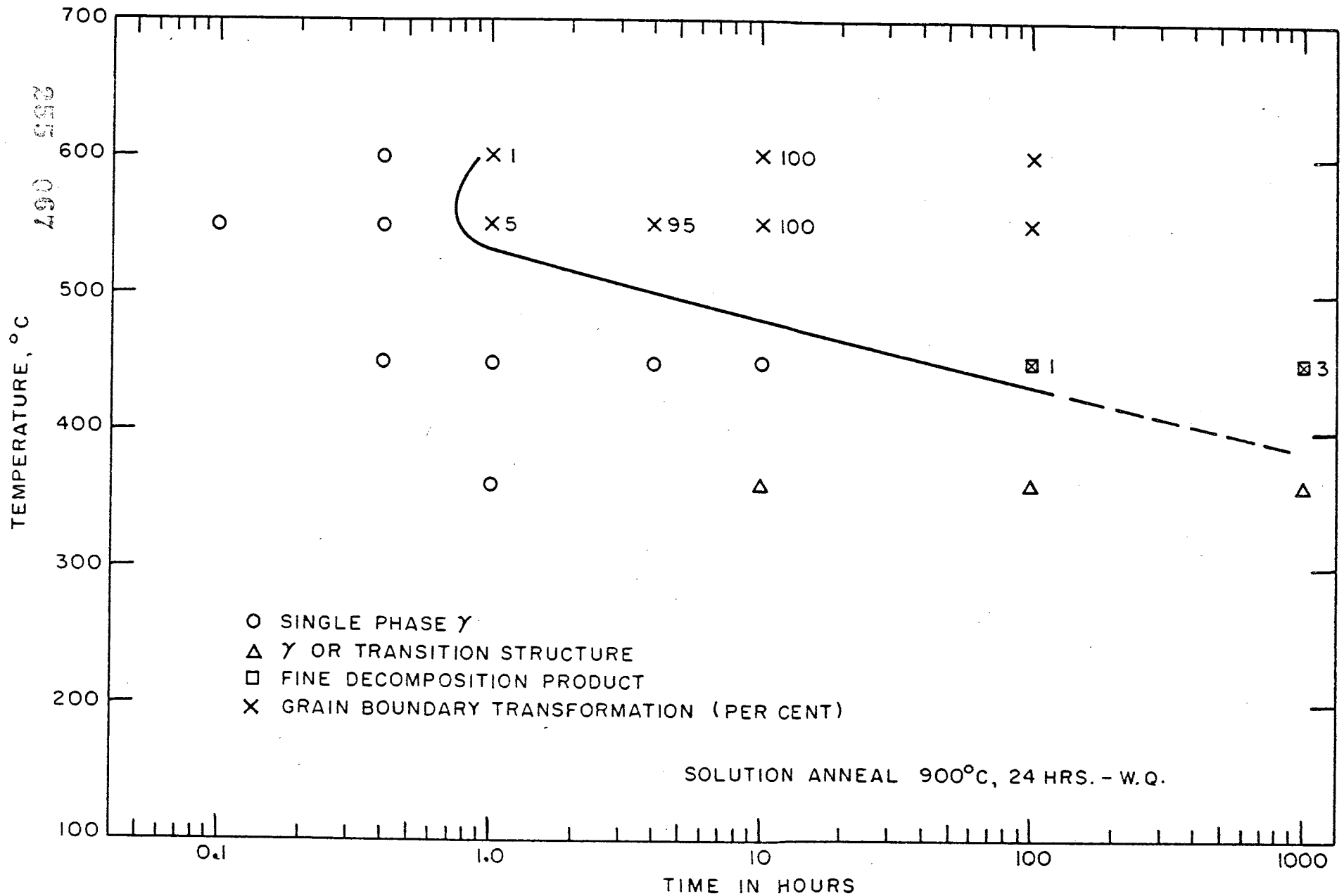
FIG. 49 - TTT DIAGRAM FOR A U-10w/o Nb-0.78w/o Cr ALLOY ILLUSTRATING INITIAL
METALLOGRAPHIC OBSERVATION OF GRAIN BOUNDARY TRANSFORMATION

FIG. 50 — HARDNESS DATA FOR AN ISOTHERMALLY ANNEALED U-8%Nb-0.12%Cr ALLOY
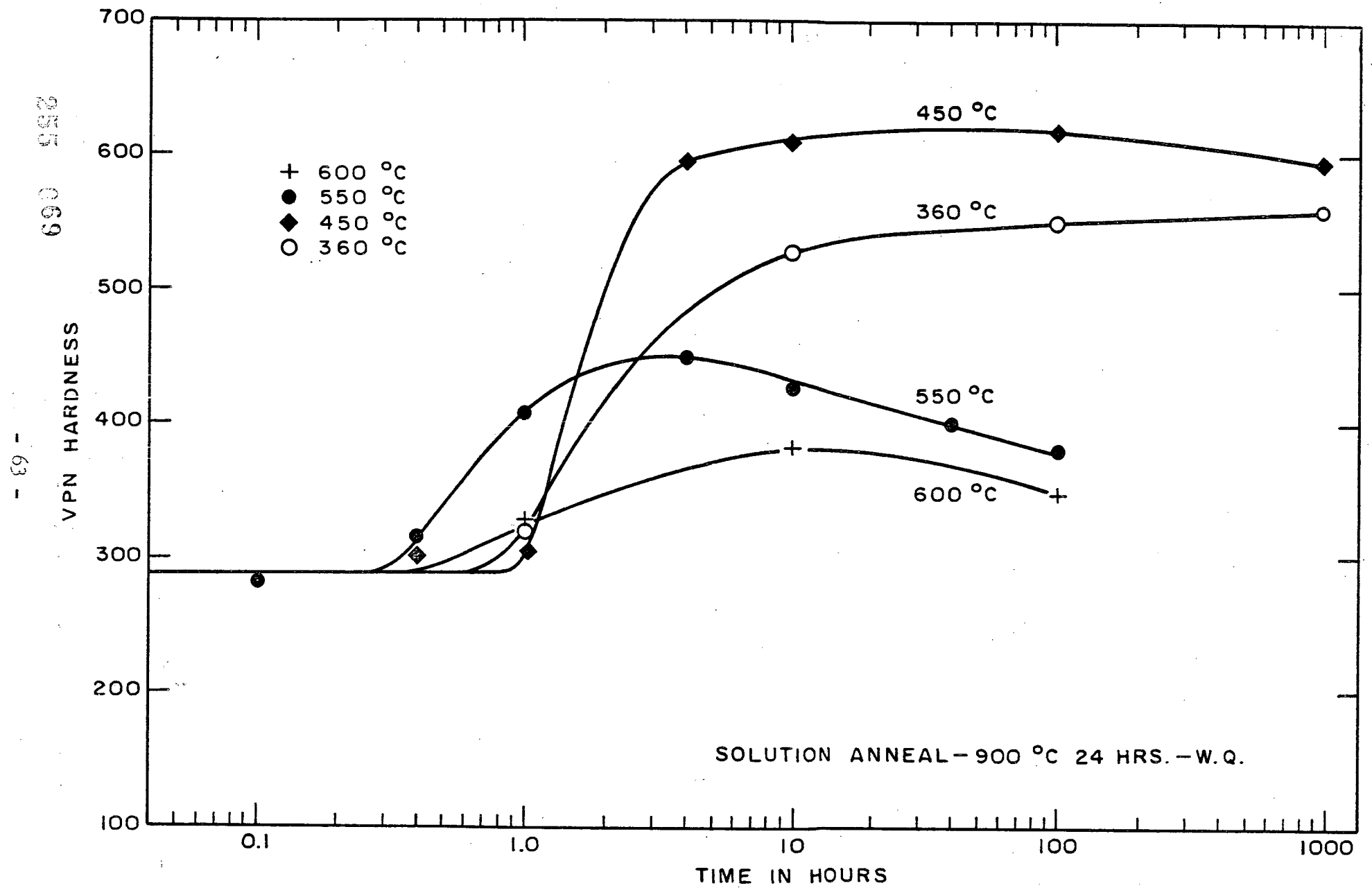
FIG. 51 - HARDNESS DATA FOR AN ISOTHERMALLY ANNEALED U-8 ^{W}/o Nb-0.74 ^{W}/o Cr ALLOY
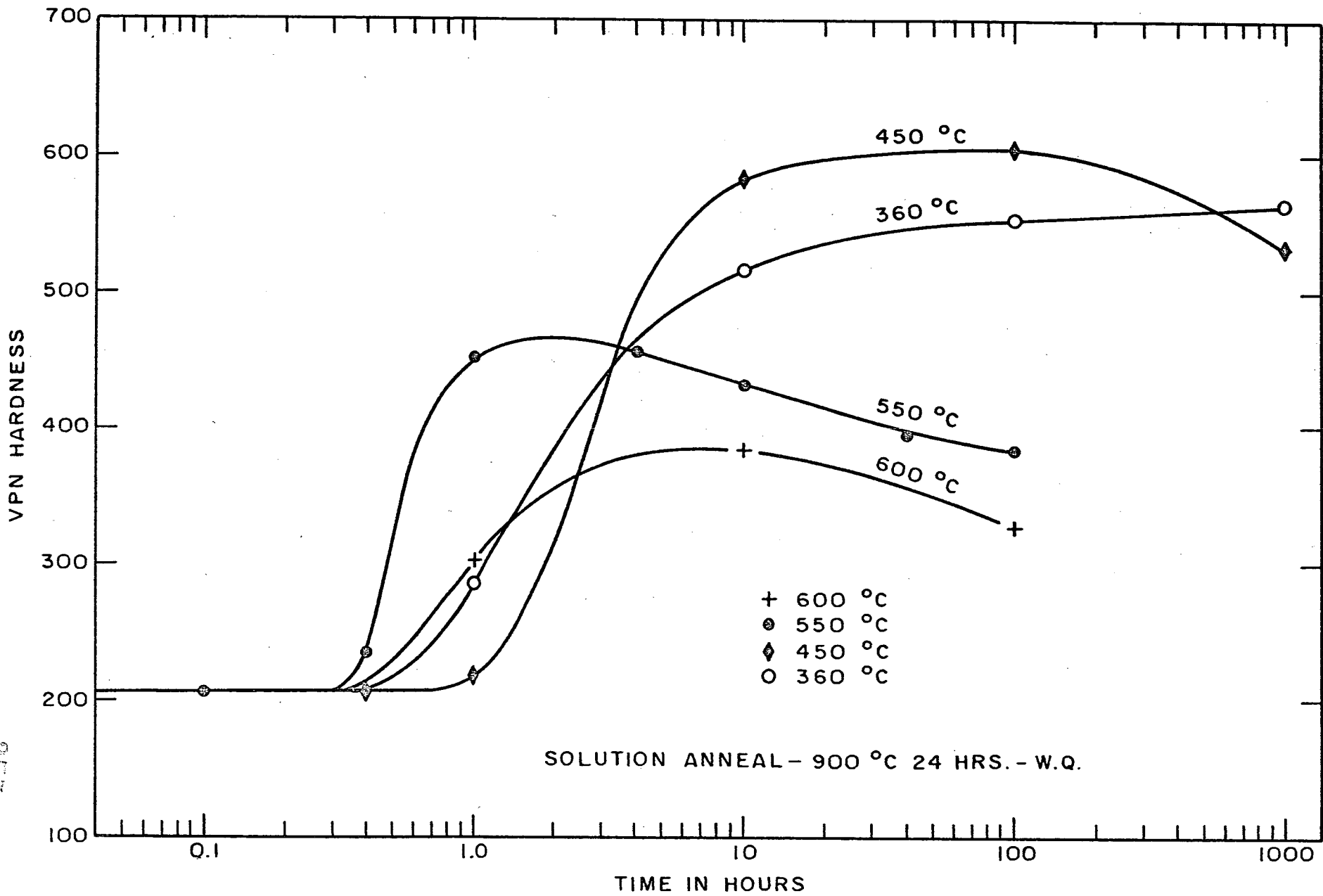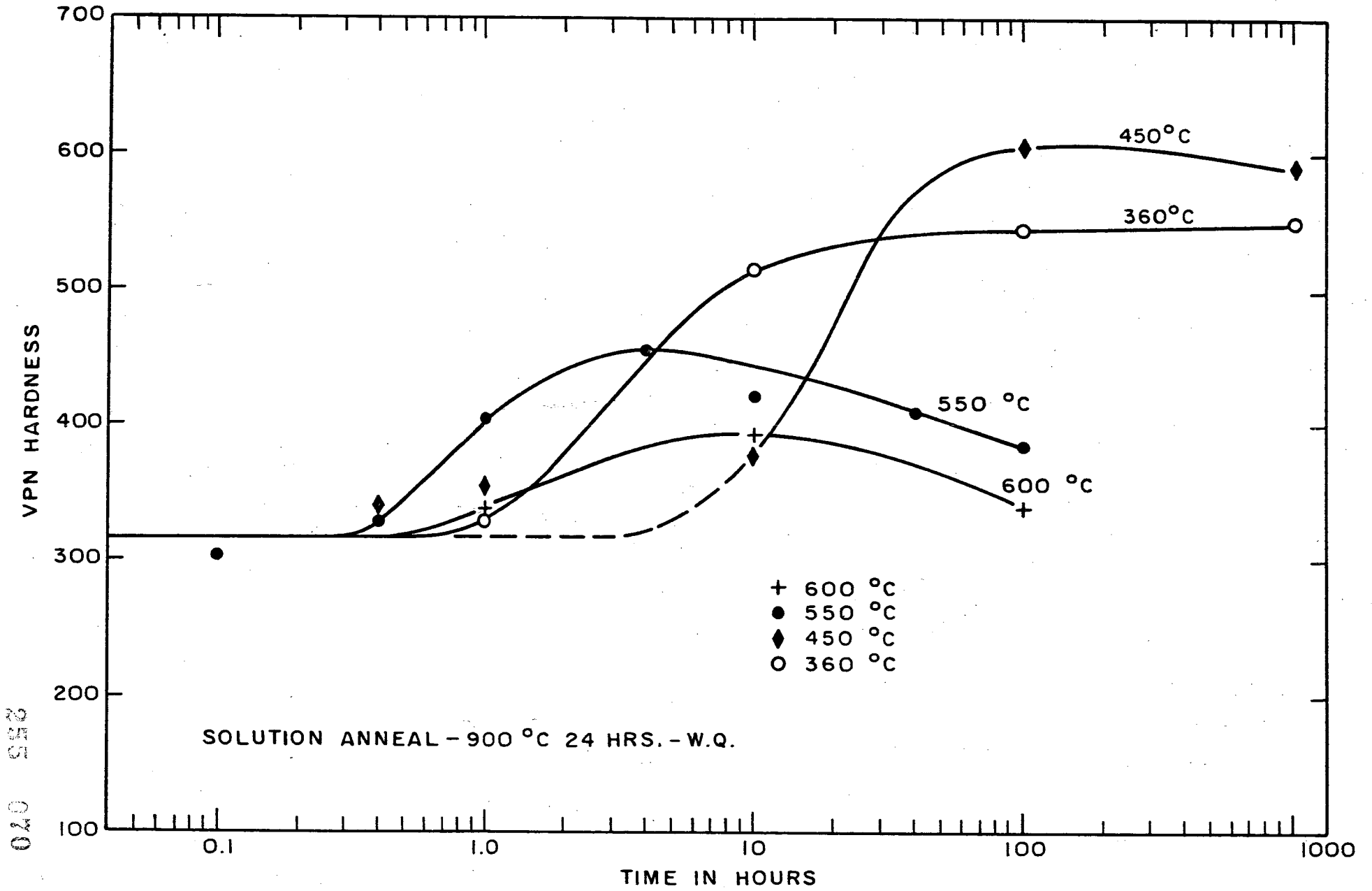
FIG. 52 - HARDNESS DATA FOR AN ISOTHERMALLY ANNEALED U-10% Nb-0.13%Cr ALLOY
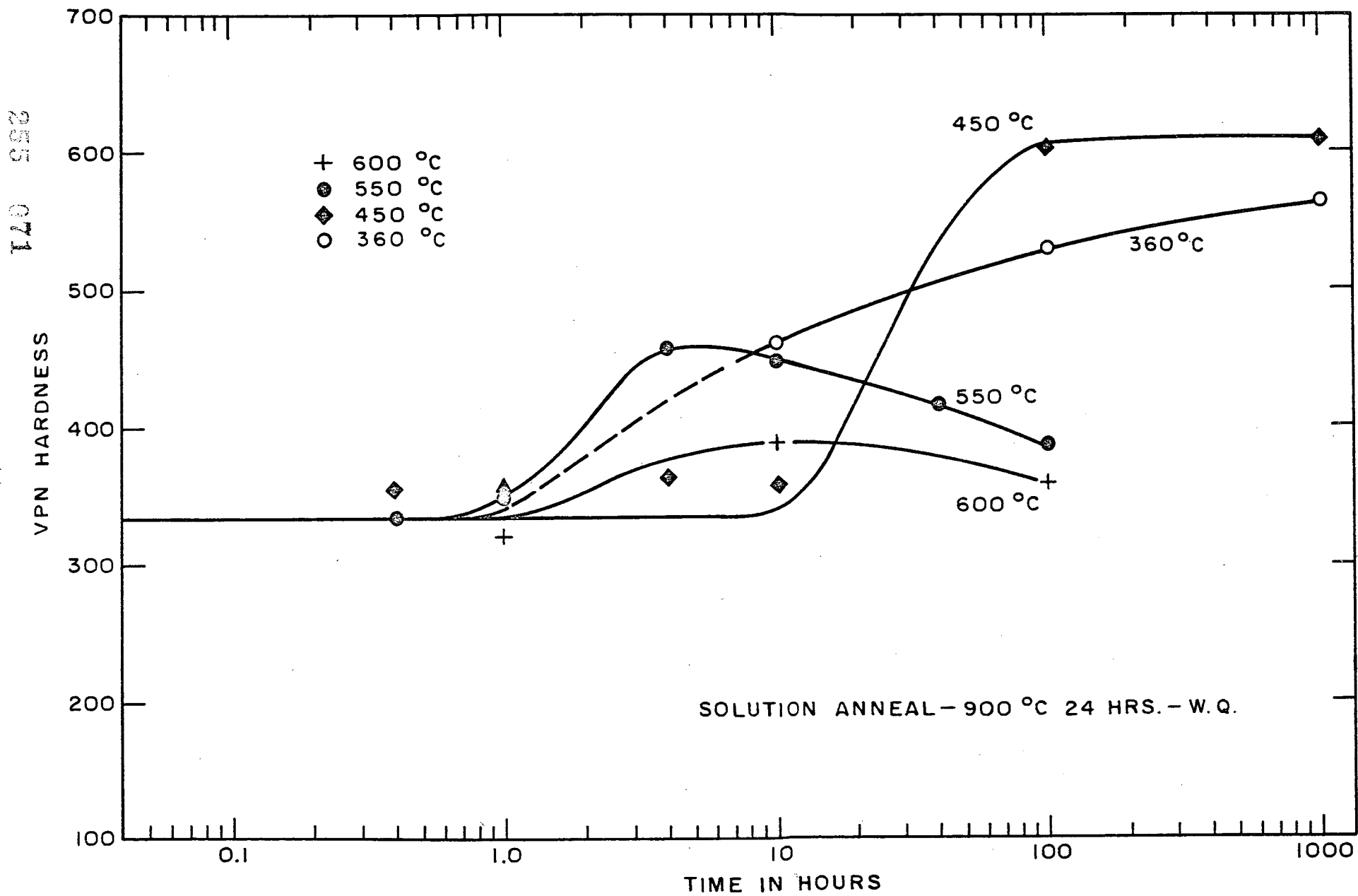
FIG. 53 - HARDNESS DATA FOR AN ISOTHERMALLY ANNEALED U-10^w/$_o$Nb-0.78^w/$_o$Cr ALLOY
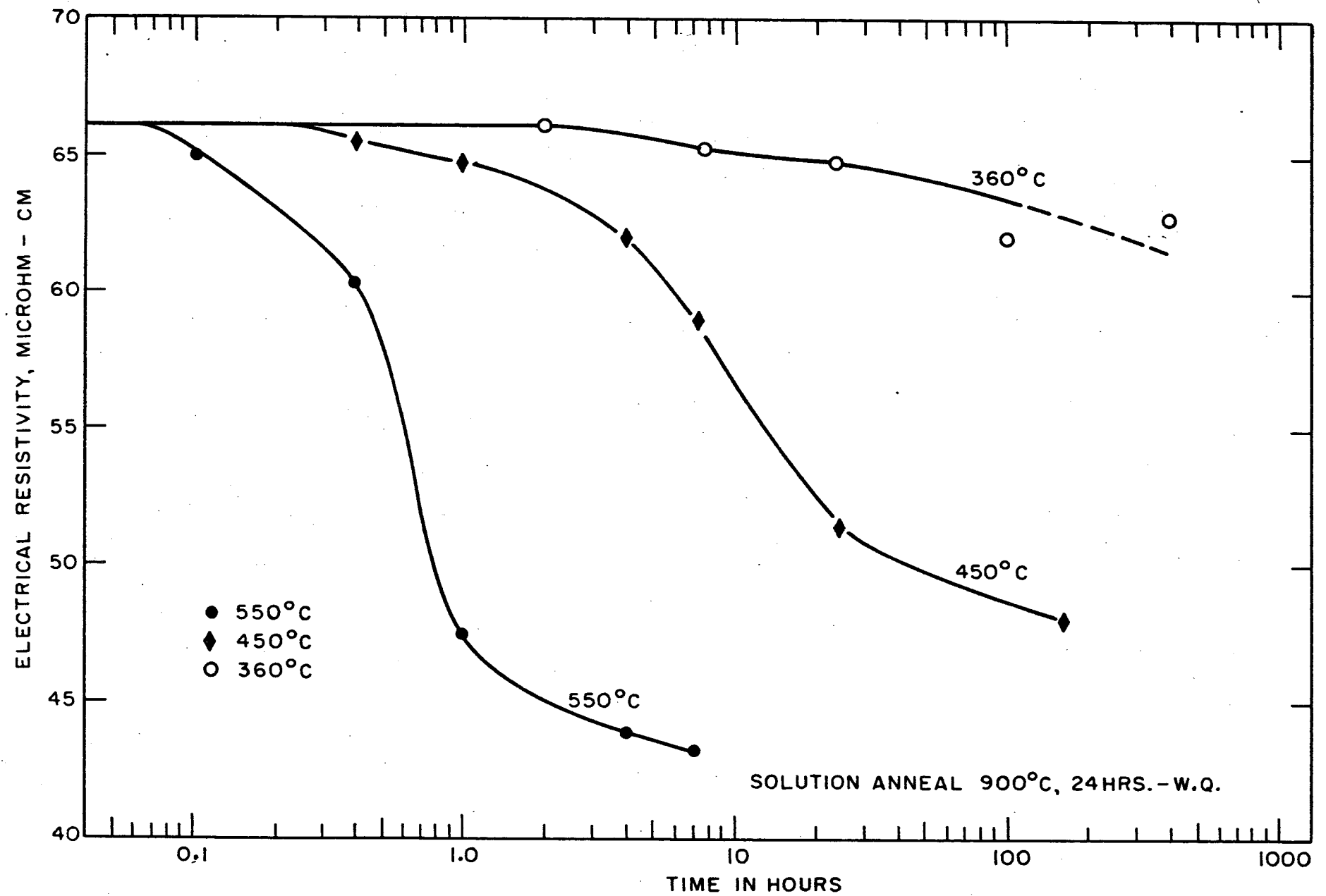
FIG. 54 - ROOM TEMPERATURE ELECTRICAL RESISTIVITY DATA FOR AN
ISOTHERMALLY ANNEALED U-8w/o Nb-0.12w/o Cr ALLOY
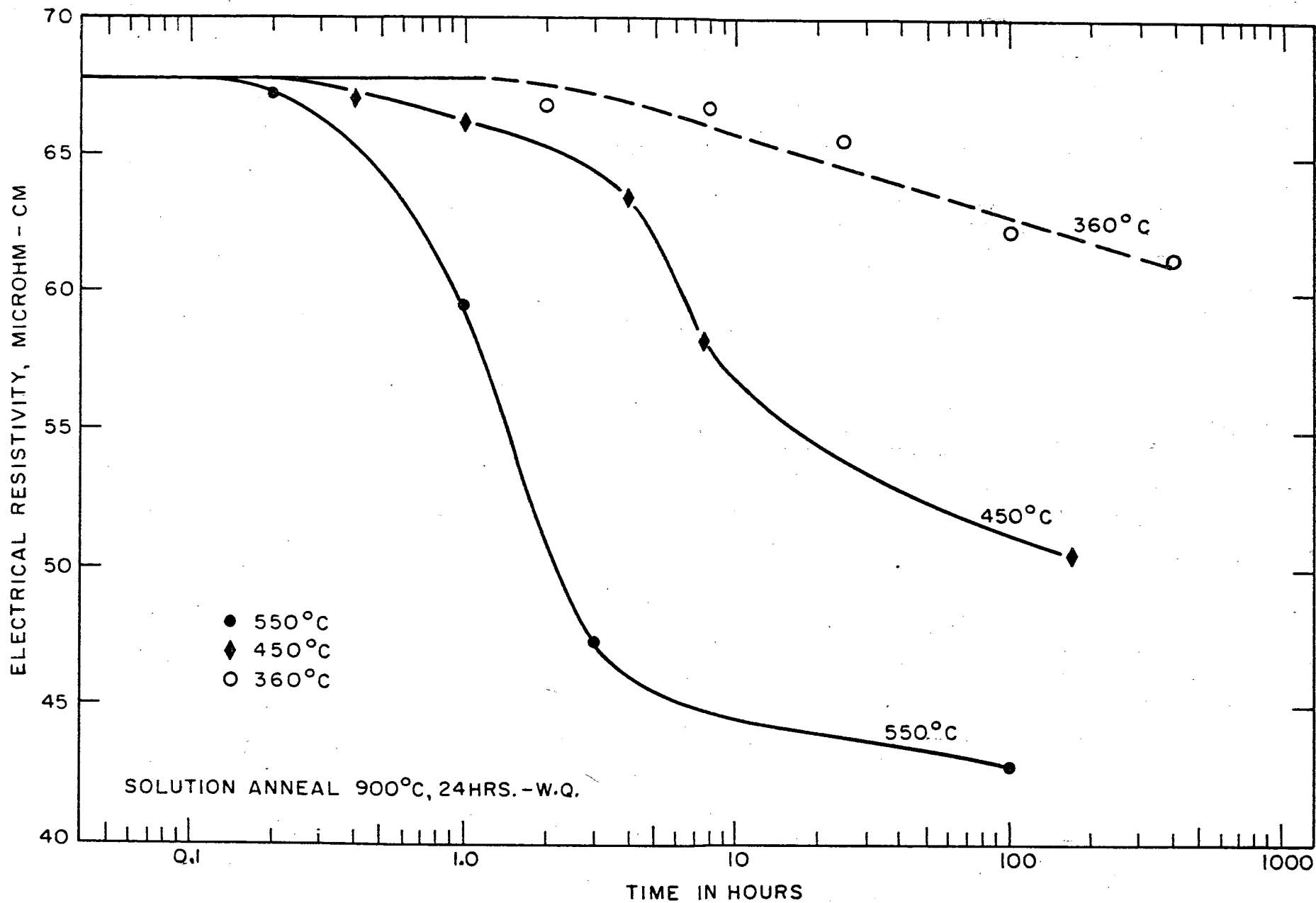
FIG. 55 - ROOM TEMPERATURE ELECTRICAL RESISTIVITY DATA FOR AN
ISOTHERMALLY ANNEALED U-8w/o Nb-0.74w/o Cr ALLOY
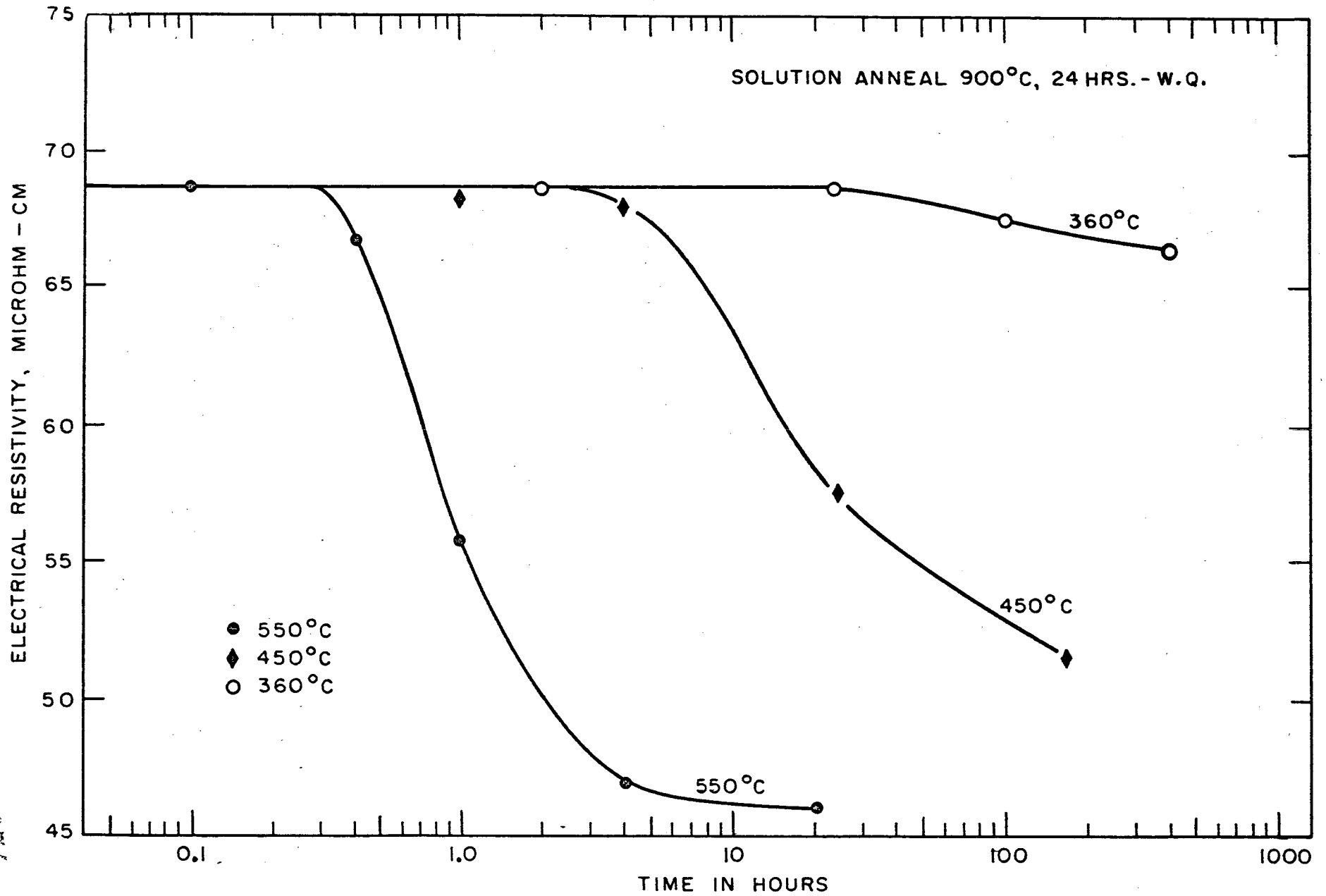
FIG. 56 - ROOM TEMPERATURE ELECTRICAL RESISTIVITY DATA FOR AN ISOTHERMALLY ANNEALED U-10w/o Nb-0.13w/o Cr ALLOY
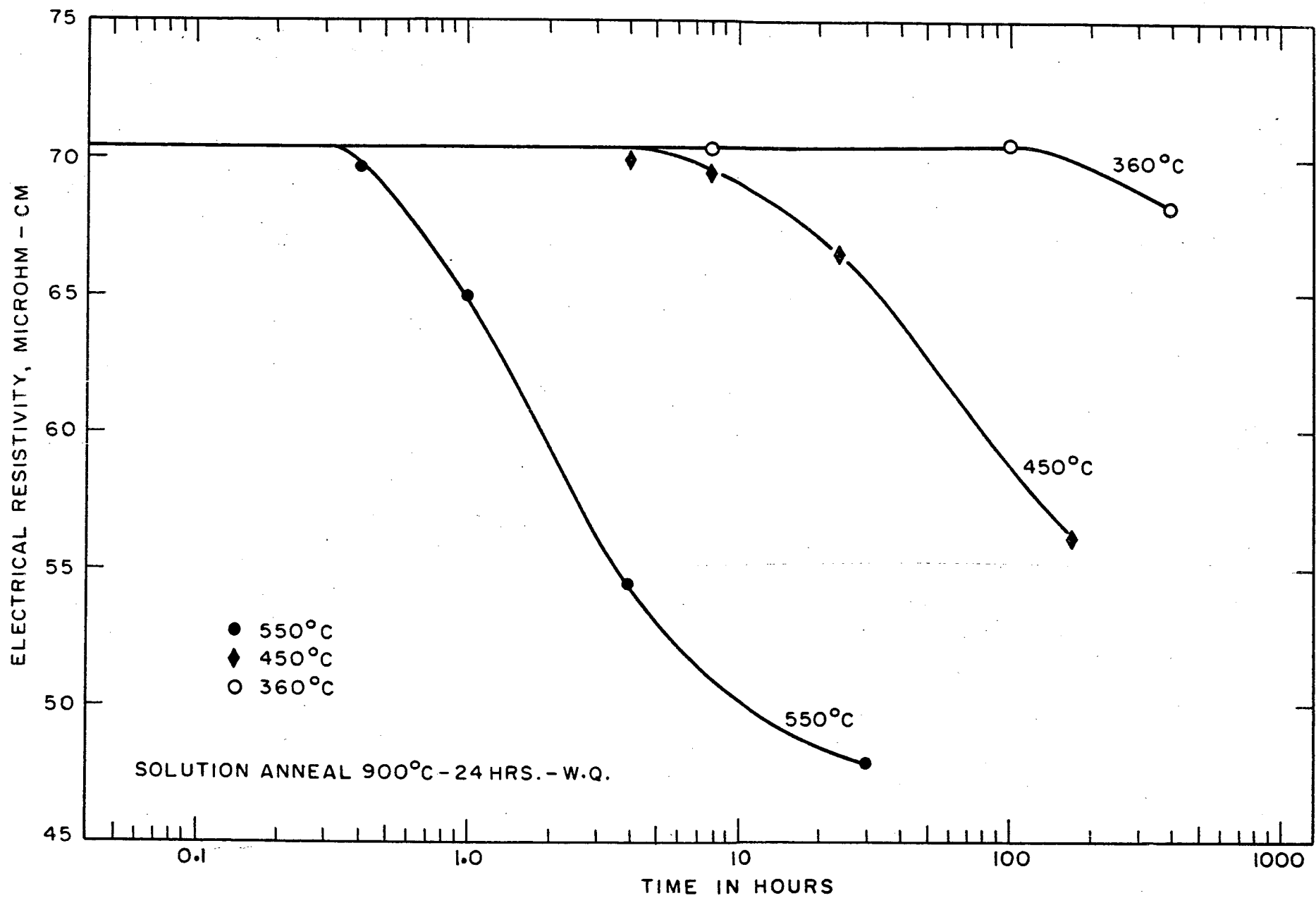
FIG. 57 - ROOM TEMPERATURE ELECTRICAL RESISTIVITY DATA FOR AN
ISOTHERMALLY ANNEALED U-10w/o Nb-0.78w/o Cr ALLOY
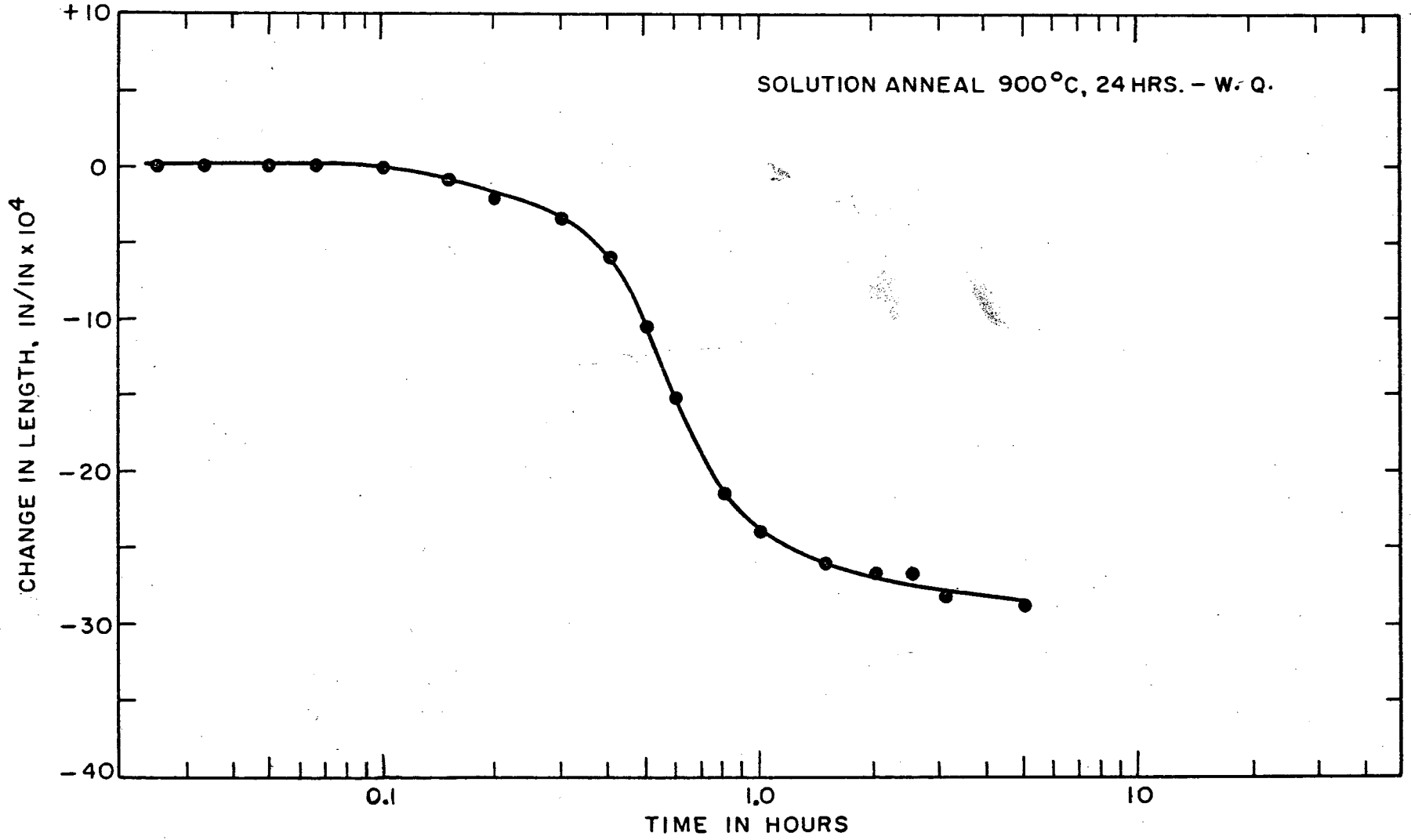
FIG. 58 - DILATOMETRIC DATA FOR A U-8w/o Nb-0.12w/o Cr ALLOY
ISOTHERMALLY ANNEALED AT 550°C

The figure shows a plot with axes:
- Y-axis: CHANGE IN LENGTH, IN/IN x 10^4, ranging from -40 to +10
- X-axis: TIME IN HOURS, ranging from about 0.1 to 10 (logarithmic)
- Annotation: SOLUTION ANNEAL 900°C, 24 HRS. — W. Q.

5. U-Nb-Ti Alloys

a. Metallographic Results

Titanium was added to a U-8w/o Nb base at the 4 and 8 a/o levels (0.90 and 1.94w/o, respectively). Microstructures of the U-8w/o Nb-0.90w/o Ti alloy at all annealing temperatures resembled those observed in most other compositions. At 600° and 550°C, the dark-etching product initiated at the grain boundaries, and as transformation proceeded, the areas of the light-etching gamma were consumed. Both the fine precipitate and grain boundary transformation were noted at 450°C after relatively short annealing times. Traces of grain boundary product were observed after 100 hours at 360°C, and microstructures at this annealing temperature exhibited the typical oriented patterns found in most of the materials under investigation.

Metallographic examination of the U-8w/o Nb-1.94w/o Ti composition showed structures which were not found in any other alloy. Annealing at 600° and 550°C produced decomposition products which originated not only at the grain boundaries as previously described but also throughout the grains as fine precipitate. This behavior occurred in other materials only at the 450°C temperature. Figure 59 is a photomicrograph of the U-8w/o Nb-1.94w/o Ti alloy which had been annealed for 10 hours at 600°C. The dark-etching matrix has the appearance of a fine precipitate. The lighter etching transformation at the grain boundaries is lamellar. Similar structures were observed at 550°C. Another unusual feature of the grain boundary decomposition at these temperatures is that although the product originates in very short annealing intervals, the growth is slow. After 10 hours at both 600° and 550°C, less than half of the surface area of the samples is occupied by this transformation product. For these annealing treatments, the transformation product initiating

at the grain boundaries covered the entire area in microstructures of most materials.

Annealing this U-8w/o Nb-1.94w/o Ti alloy at 450°C produced transformation at grain boundaries and as a fine product throughout the grains. These structures were observed after annealing for only 0.4 hour. Subsequent heat treatment at this temperature results in additional growth of the grain boundary product (Figure 60).

Microstructures of some of the samples annealed at 360°C exhibited evidence of this fine structure throughout the grains. None of the oriented pattern was noted at this annealing temperature, as had been observed in most of the other compositions. A small amount of transformation was present at the grain boundaries after 100 hours at 360°C.

TTT curves for the alloys containing titanium are illustrated in Figures 61 and 62. The material having the higher titanium content shows a more rapid initiation of grain boundary transformation at all annealing temperatures. Similar results were found using hardness measurements, indicating that addition of titanium to the U-8w/o Nb base has an adverse effect on stability of the gamma phase.

b. Hardness Results

Hardness data for the U-8w/o Nb-0.90w/o Ti alloy are presented in Figure 63. Hardness rises occurred in 0.4 hour or less at all annealing temperatures. The initial increase occurred at the 550°C temperature, as had been observed for other compositions under investigation. The peak hardness for the 550°C curve was unusually high; for most alloys, the maximum hardness values at 550°C were considerably lower than those obtained on annealing at 450°C and 360°C.

Increasing the titanium content to 1.94w/o resulted in extremely rapid hardening at all annealing temperatures. At 600°, 550° and 450°C, these rises occurred in considerably less than 0.1 hour, as shown in Figure 64. Maximum hardness values at 600° and 550°C exceeded those resulting from the lower temperature annealing treatments. This behavior was not observed in any other alloy being studied. Although hardness increases at these temperatures occurred rapidly, the peak hardness was not reached until about 4 hours. The curve for the 450°C annealing temperature exhibited double peaks to a minor extent, the first in one hour and the second in about 100 hours. Annealing at 360°C produced the smallest increases in hardness.

c. Electrical Resistivity Results

Resistivity curves for the U-8w/o Nb-0.90w/o Ti alloy are shown in Figure 65. A decrease occurred in less than 0.1 hour at 550°C, and changes in resistivity appeared to be complete in less than 10 hours. Data for other compositions studied continued to decrease slightly upon annealing for times up to 100 hours. The curve for 450°C shows a continued decrease at the 100-hour annealing interval. No decrease in resistivity occurred upon annealing at 360°C. This curve appeared to rise very slightly with increasing time; however, this increase was less than 1 microhm-cm above the value for the solution-treated material.

Electrical resistivity results for the U-8w/o Nb-1.94w/o Ti alloy (Figure 66) differed considerably from curves for other compositions. Annealing at 550°C produced large increases in resistivity as transformation proceeded. The curve reached a maximum in 0.4 hour, at a value which was 8 microhm-cm above the solution-treated value. After 0.4 hour, the resistivity decreased; in 20 hours, the value was 3 microhm-cm below that for solution-treated material. Even higher increases in resistivity occurred at the 450°C annealing

temperature. After 24 hours, a value of 84 microhm-cm was measured; this represents an increase of 13 microhm-cm over the value for untransformed specimens. A similar increase resulted from annealing for 24 hours at 360°C. The reason for these large increases is not known.

d.   Dilatometric Results

Dilatometric measurements at 550°C for the U-8w/o Nb-1.94w/o Ti alloy also showed the extremely rapid transformation which was found with the hardness, metallographic and resistivity determinations. A decrease in length occurred in less than 0.05 hour, as illustrated in Figure 67. The dilatometric data indicated that transformation was complete in about 0.3 hour; at this annealing interval, the resistivity value was near the maximum, although further rises in hardness occurred up to 4 hours (Figure 64).

This U-8w/o Nb-1.94w/o Ti material also exhibited rapid decreases in length upon annealing at 450°C. Dilatometric measurements show that transformation was initiated in less than 0.1 hour, and in 1 hour the change in length was over one half of the maximum value observed. After 1 hour the length decreased at a slower rate, and only slight changes were taking place at 72 hours, at which time the test was terminated. Dilatometric results at 360°C also demonstrated the rapid transformation of this alloy. The initial change in length occurred in less than 0.2 hour, although further decreases in length were not as rapid as those measured at higher annealing temperatures.

e.   X-Ray Diffraction Results

Studies of the mode of decomposition for the U-Nb-Ti alloys reveal a mechanism which differs from that of compositions previously described. Figures 68 to 70 show the spectrometer traces for the U-8w/o Nb-1.94w/o Ti material annealed at 550°C for increasing times; this series is typical of results

for both U-Nb-Ti alloys. Figure 68, after 0.1 hour, illustrates the pattern for the metastable gamma phase and also indicates the start of alpha precipitation. After 1 hour at 550°C (Figure 69), five distinct peaks are visible. The gamma reflection ($2\theta = 37.0°$) has shifted very slightly, and the four alpha peaks are well defined. A slight rise at a 2θ value of $37.9°$ is evident; this represents initial precipitation of the equilibrium niobium-rich γ_2. The microstructures for this heat treatment show the fine decomposition product plus small amounts of the grain boundary transformation. The strength of the alpha pattern indicates that the fine decomposition product contains the alpha phase. Figure 70 shows that after 4 hours at 550°C more γ_2 is present. Examination of this material was continued at annealing times up to 200 hours at this temperature, with only slight further changes in the spectrometer traces.

This series of X-ray diffraction patterns indicates that alpha may be the first to precipitate from the metastable gamma phase, and as transformation proceeds, γ_2 is precipitated. A similar behavior was noted at 450°C for both U-Nb-Ti compositions, although considerably longer annealing times were required for decomposition. After annealing for 1000 hours at 360°C, both materials exhibited slightly broadened peaks for gamma and no alpha was detected.
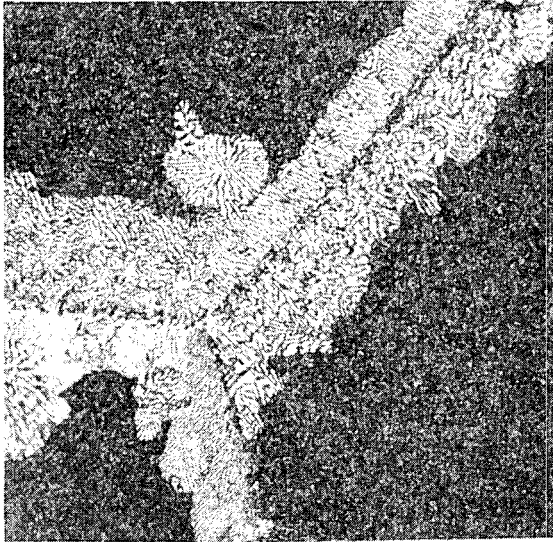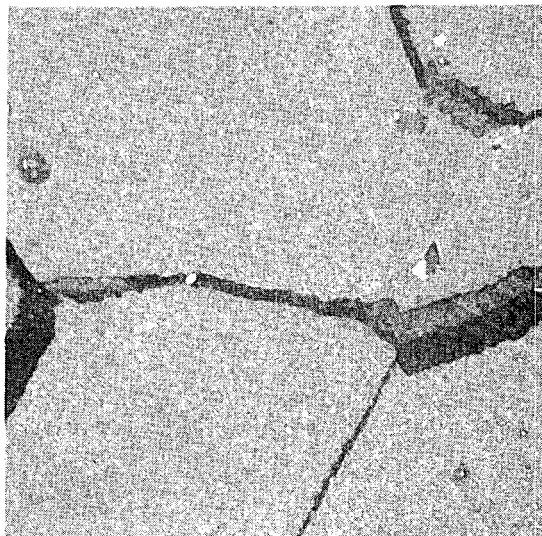
Neg. No. 13442   X 1000

Fig. 59

Alloy: U-8w/o Nb-1.94w/o Ti.
Treatment: 900°C-WQ; 600°C-10 hrs WQ.
Lamellar transformation at grain
boundaries; dark-etching fine precipi-
tate in matrix.

Neg. No. 13441   X 1000

Fig. 60

Alloy: U-8w/o Nb-1.94w/o Ti.
Treatment: 900°C-WQ; 450°C-10 hrs-WQ.
Dark-etching grain boundary transfor-
mation product with fine precipitate
in matrix.

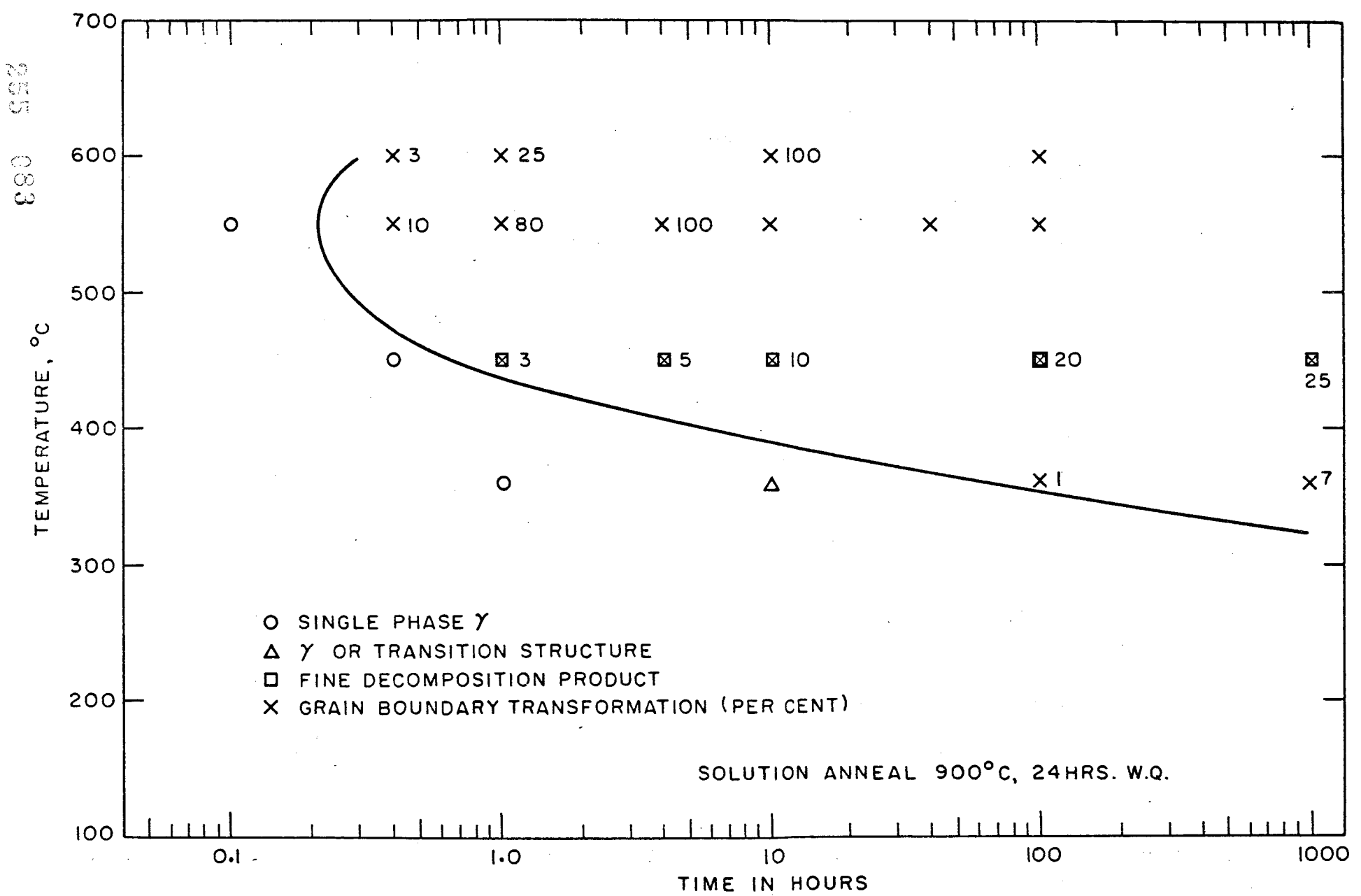Etchant: 10% CrO_3 + 2% HF + H_2O.

- 76 -

Project No. B 095
Summary Report

FIG. 61 - TTT DIAGRAM FOR A U-8w/o Nb-0.90w/o Ti ALLOY ILLUSTRATING INITIAL
METALLOGRAPHIC OBSERVATION OF GRAIN BOUNDARY TRANSFORMATION

700

600 ⊠ 2   ⊠ 5   ⊠ 8   ⊠ 35   ✕ 100

⊠ 2   ⊠ 8   ⊠ 10   ⊠ 20   ⊠ 45   ✕ 100

500

TEMPERATURE, °C

O   ⊠ 1   ⊠ 3   ⊠ 5   ⊠ 10   ⊠ 25   ✕ 100

400

O   □   ⊠ 1   ⊠ 8

300

O SINGLE PHASE γ
△ γ OR TRANSITION STRUCTURE
□ FINE DECOMPOSITION PRODUCT
✕ GRAIN BOUNDARY TRANSFORMATION (PER CENT)

200

SOLUTION ANNEAL, 900°C, 24 HRS. – W.Q.

100

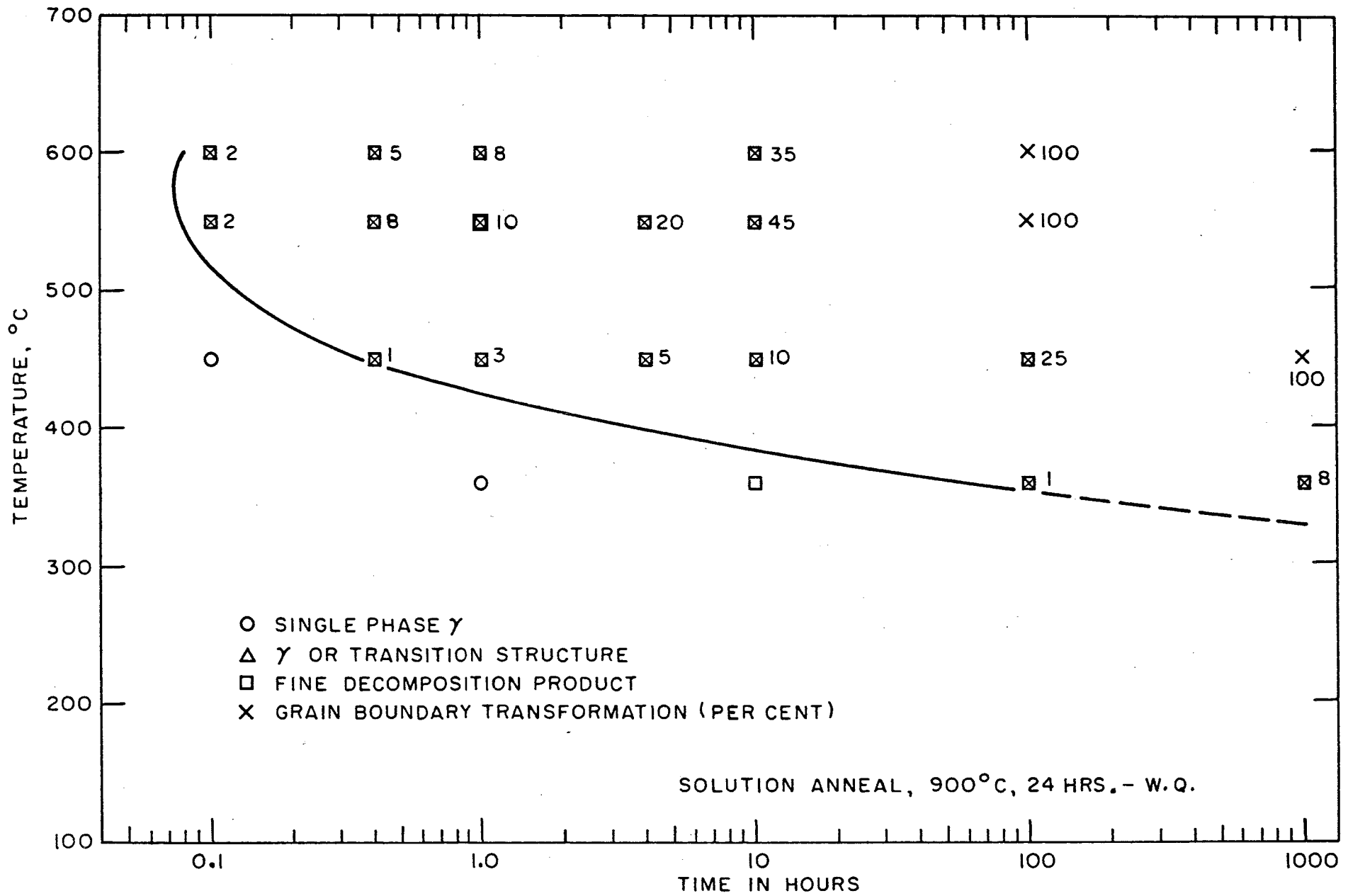0.1   1.0   10   100   1000

TIME IN HOURS

FIG. 62 – TTT DIAGRAM FOR A U-8w/o Nb-1.94w/o Ti ALLOY ILLUSTRATING INITIAL
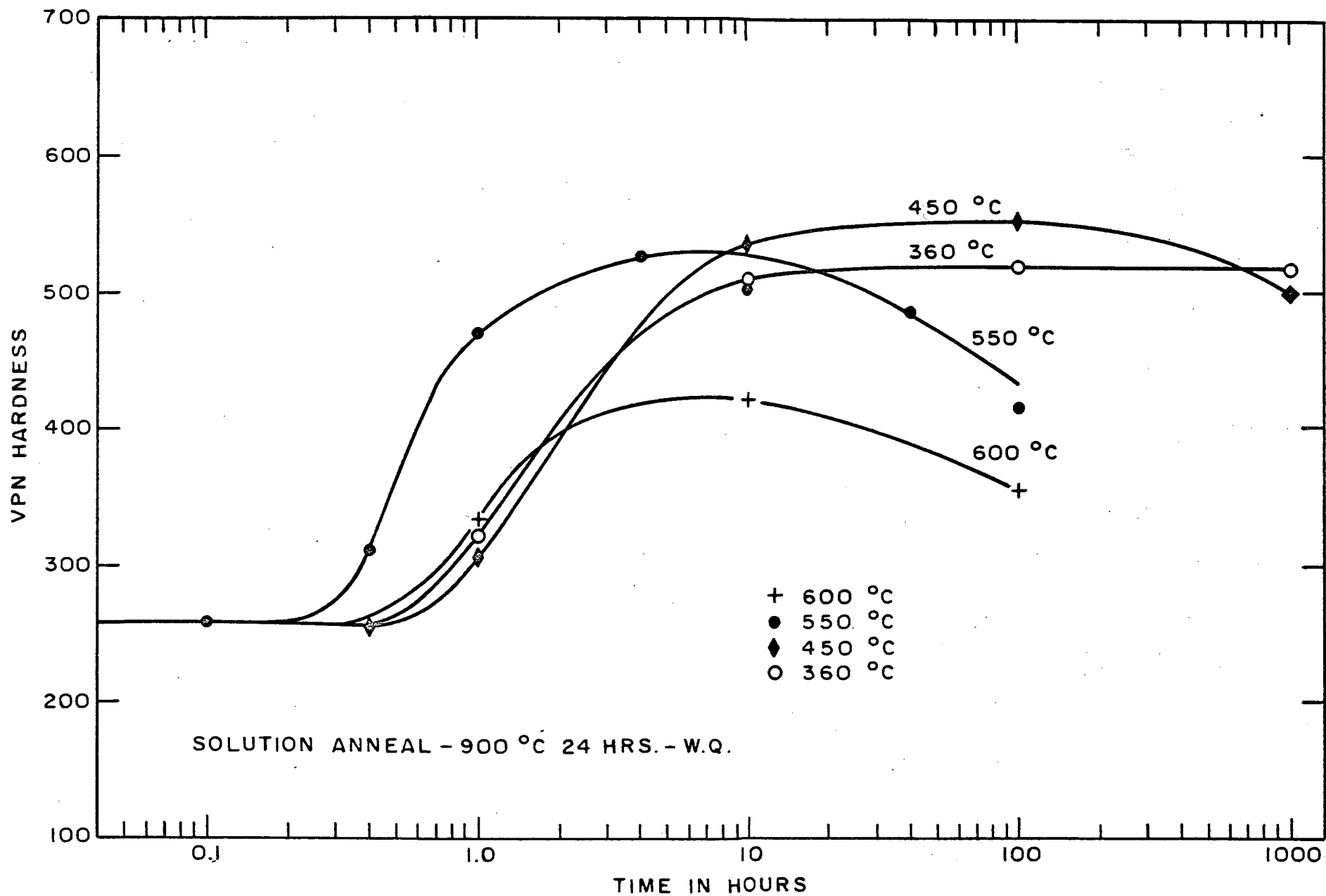METALLOGRAPHIC OBSERVATION OF GRAIN BOUNDARY TRANSFORMATION

FIG. 63 - HARDNESS DATA FOR AN ISOTHERMALLY ANNEALED U-8^{W}/o Nb-0.90^{W}/o Ti ALLOY
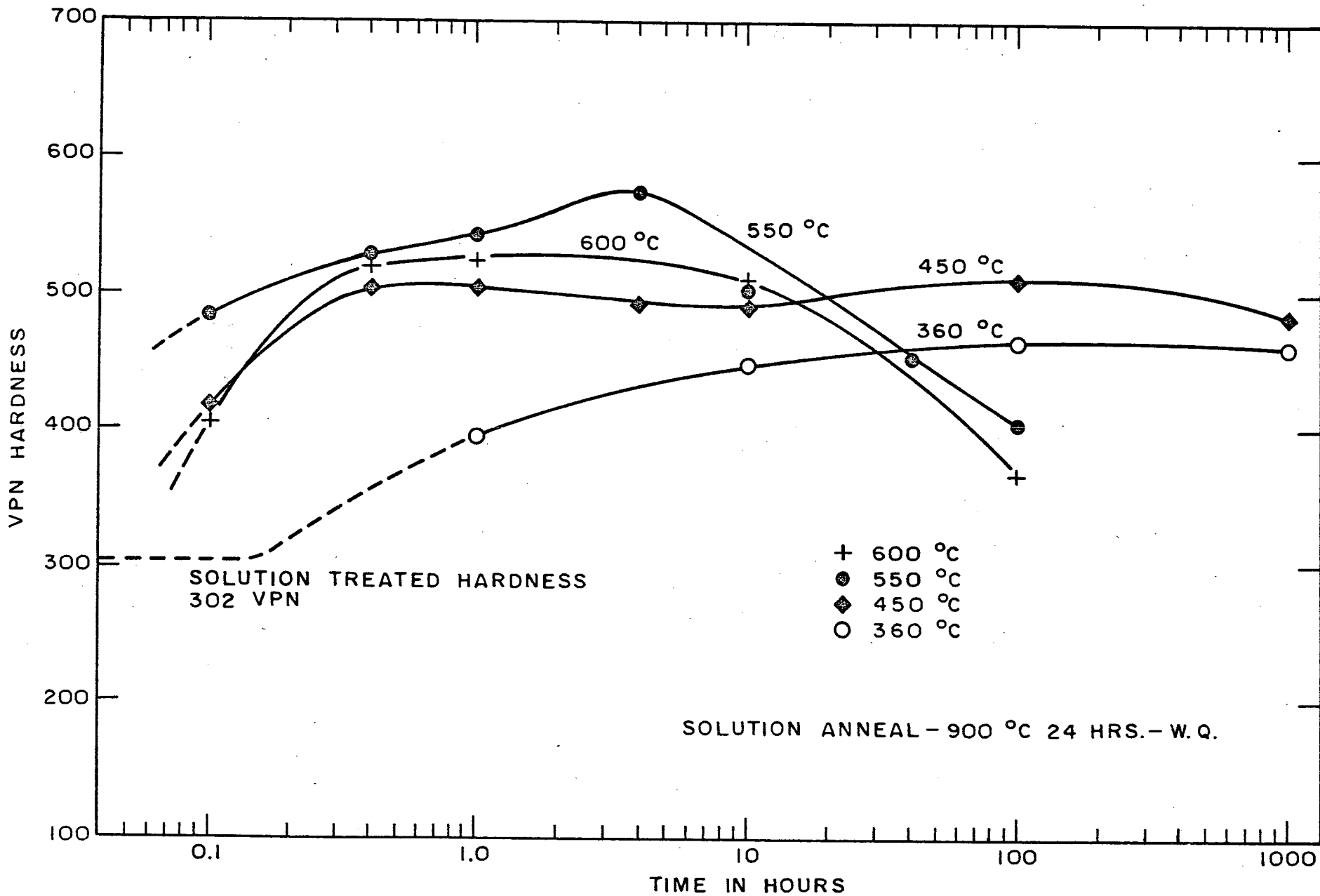
FIG. 64 - HARDNESS DATA FOR AN ISOTHERMALLY ANNEALED U-8 ^{W}/o Nb-1.94 ^{W}/o Ti ALLOY
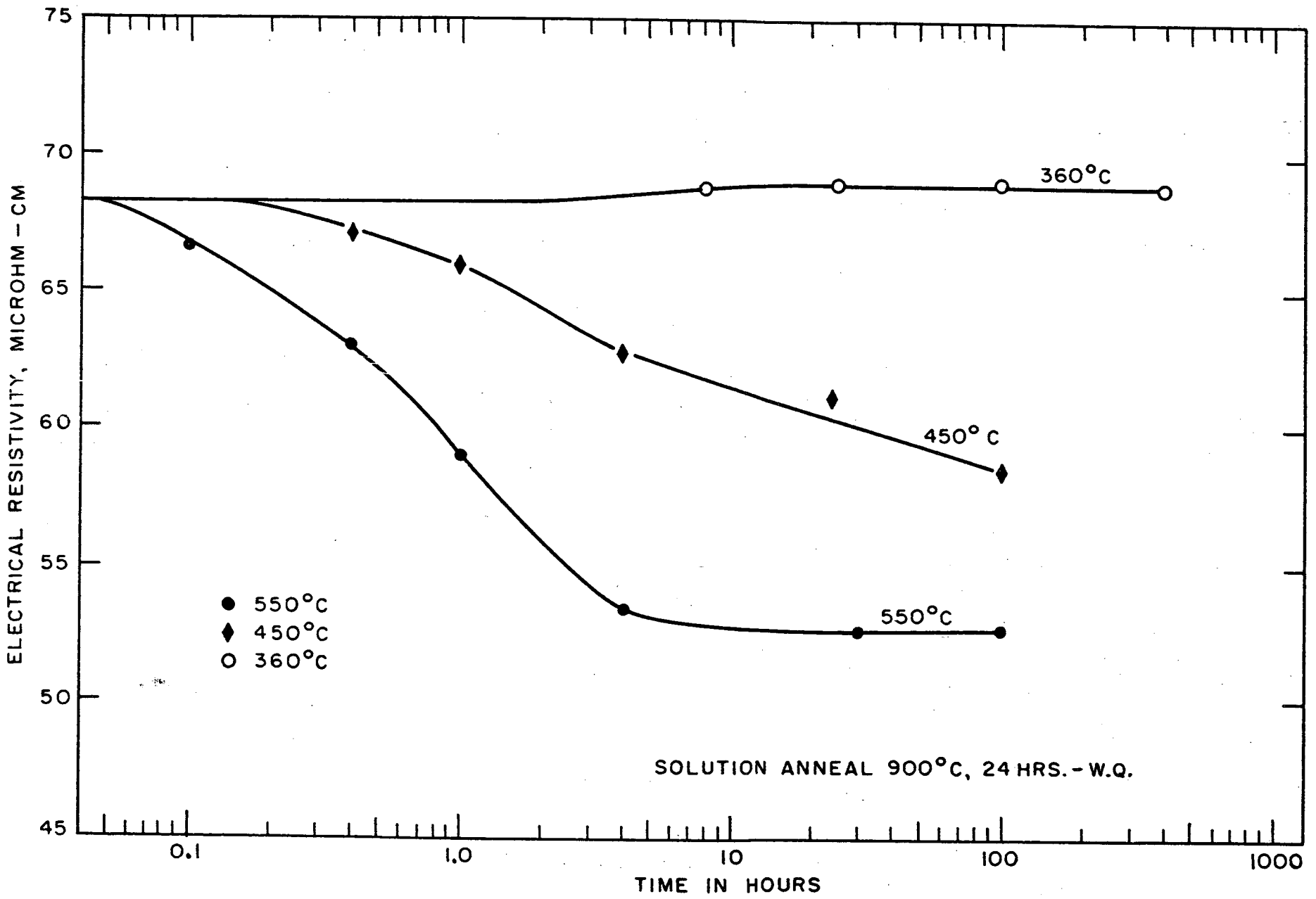
FIG. 65 - ROOM TEMPERATURE ELECTRICAL RESISTIVITY DATA FOR AN ISOTHERMALLY ANNEALED U-8w/o Nb-0.90w/o Ti ALLOY
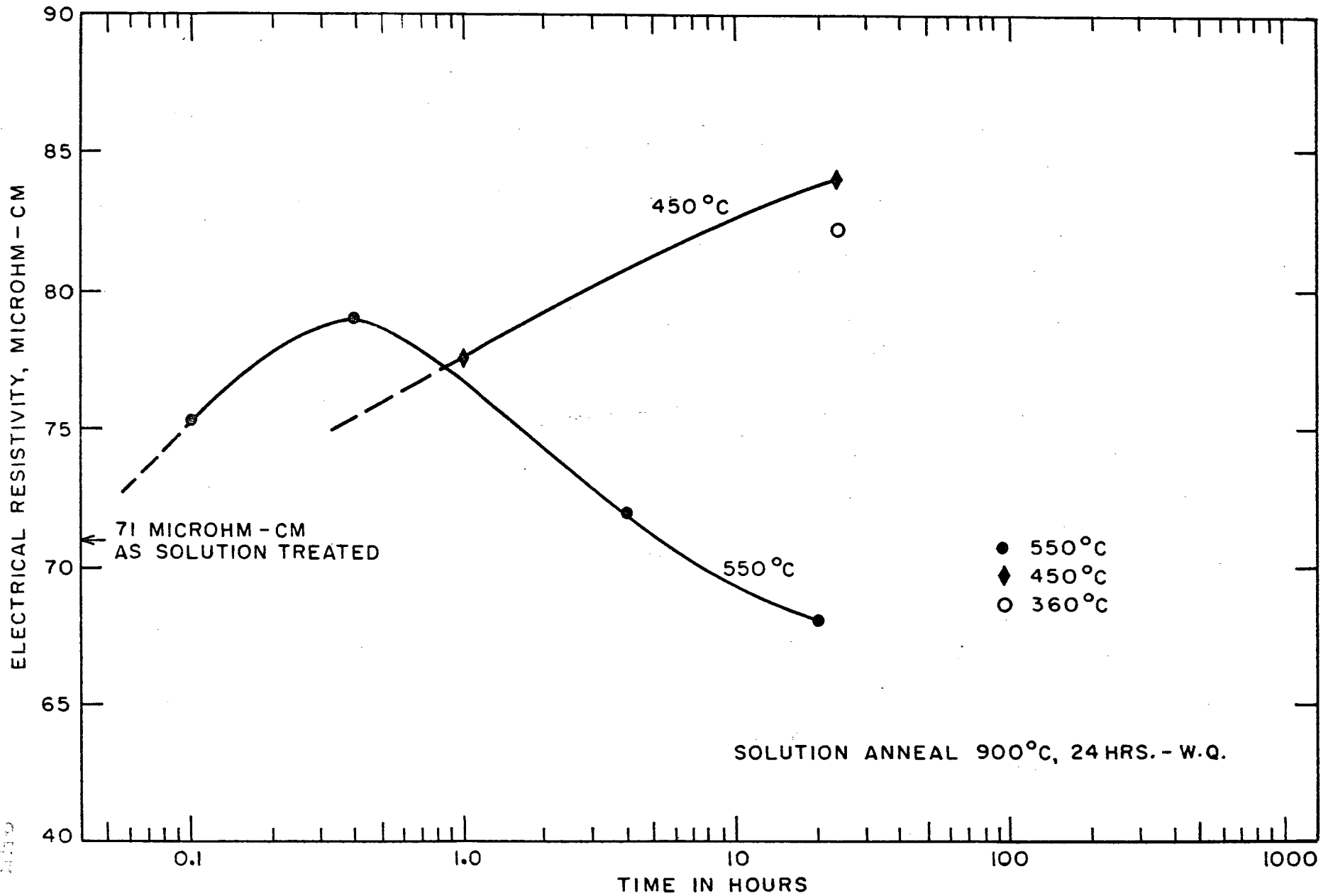
FIG. 66 - ROOM TEMPERATURE ELECTRICAL RESISTIVITY DATA FOR AN
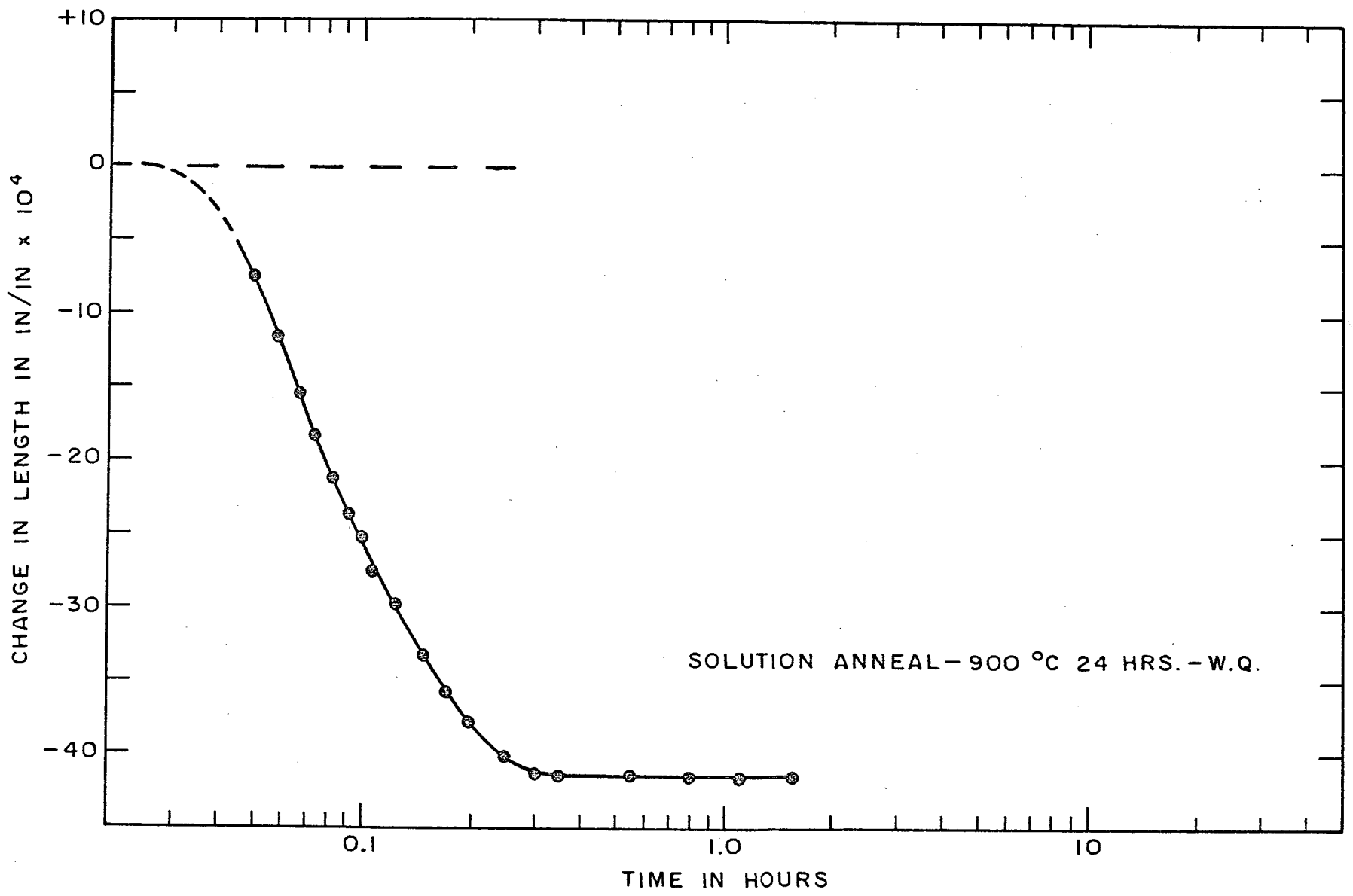ISOTHERMALLY ANNEALED U-8w/o Nb-1.94w/o Ti ALLOY

FIG. 67 - DILATOMETRIC DATA FOR A U-8 ^{W}/o Nb-1.94 ^{W}/o Ti ALLOY ISOTHERMALLY ANNEALED AT 550 °C
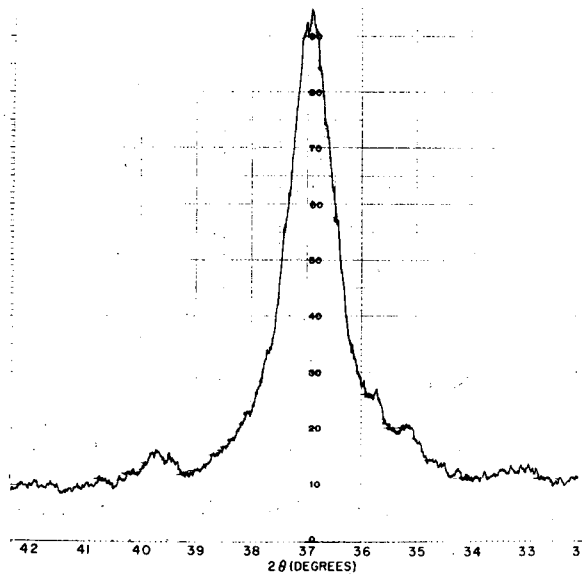
Fig. 68

X-ray diffractometer pattern.
Alloy: U-8w/o Nb-1.94w/o Ti.
Treatment: 900°C-WQ; 550°C-
0.1 hr-WQ. Retained γ ($2\theta = 36.9°$)
with traces of α.

Fig. 69

X-ray diffractometer pattern.
Alloy: U-8w/o Nb-1.94w/o Ti.
Treatment: 900°C-WQ; 550°C-
1 hr-WQ. γ_1, 4 peaks for α,
and incipient γ_2 at 37.9°.
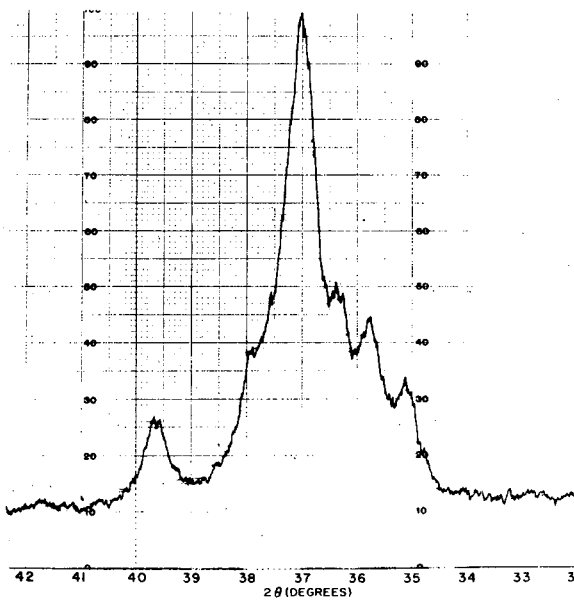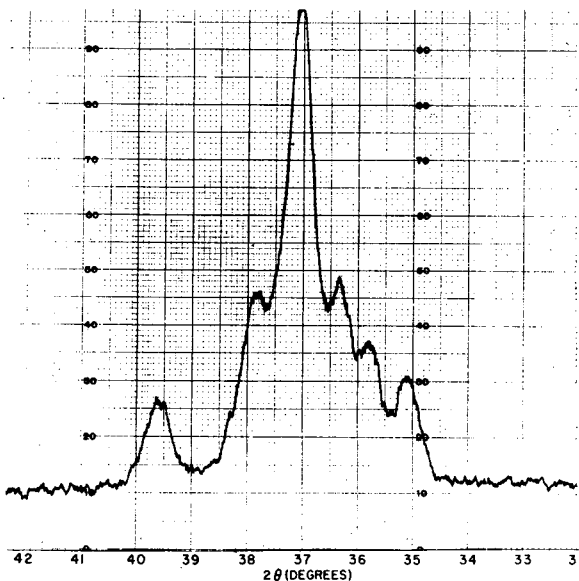

Fig. 70

X-ray diffractometer pattern.
Alloy: U-8w/o Nb-1.94w/o Ti.
Treatment: 900°C-WQ; 550°C-4
hrs-WQ. $\alpha + \gamma_1$ with increased
amount of γ_2.

255   090

- 84 -

6. U-Nb-Si Alloys

a. Metallographic Results

Silicon was added to a U-8w/o Nb base in amounts of 0.14w/o (1 atomic per cent) and 0.68w/o (5 atomic per cent). Both alloys were characterized by the presence of an intermetallic compound in the microstructures of all samples. Considerable amounts of this second phase were noted in the U-8w/o Nb-0.68w/o Si material. This composition exhibited very rapid transformation at all annealing temperatures. No gamma was detected after 4 hours at 450°C. Annealing at 360°C produced transformation at the grain boundaries in 10 hours, as illustrated in Figure 71. This photomicrograph shows the intermetallic compound and also the presence of decomposition within the grains. After 1000 hours at 360°C, Figure 72, the dark-etching grain boundary product occurs throughout the sample, together with the intermetallic compound. This annealing treatment produced only small amounts of the grain boundary transformation in other materials under study. TTT curves showing initiation of transformation in the U-Nb-Si alloys are presented in Figures 73 and 74. As the silicon content was increased, transformation occurred in much shorter annealing times.

An ingot of U-8w/o Nb-1.45w/o Si was prepared for the purpose of further investigating the intermetallic compound found in the U-Nb-Si alloys. Specimens of this composition were water-quenched from 900°C, and the gamma phase was not retained. A few grams of this alloy were dissolved in nitric acid until a finely divided material remained. This powder, when examined at high magnification, appeared metallic and resembled the intermetallic compound observed in the microstructures. Spectrographic analysis of this material was as follows: silicon, 15 ± 5%; uranium, 35 ± 10%; and niobium,

Project No. B 095
Summary Report

50 $\pm$ 10%. From these results it is evident that the silicon has combined with niobium as well as with uranium, thereby depleting the matrix of niobium. As niobium has been shown to be a gamma-phase stabilizer, a lower niobium content in the matrix would explain the rapid transformation in U-Nb-Si alloys.

b.   Hardness Results

Hardness curves for the U-8w/o Nb-0.14w/o Si alloy, Figure 75, show increases in less than 0.3 hour at all annealing temperatures. The initial rise occurred at 550°C, and a hardness peak was reached in less than 4 hours at this temperature and also at 600°C.

Increasing the silicon content to 0.68w/o resulted in extremely rapid hardness increases, as illustrated in Figure 76. At all annealing temperatures, hardness values were considerably above the solution-treated hardness in 0.1 hour, which was the shortest annealing interval used in these studies. The curves for 600° and 550°C show decreasing hardness values at 0.1 hour, indicating that overaging was occurring. Peak hardness was reached in less than 4 hours at 450°C; for most compositions, a maximum value occurred in 100 hours or more at this temperature.

c.   Electrical Resistivity Results

Measurements of electrical resistivity for the U-8w/o Nb-0.14w/o Si alloy show that transformation is initiated after relatively short annealing times (Figure 77). After 0.1 hour at 550°C, the resistivity had already decreased about 3 microhn-cm below the value for solution-treated material. Additional annealing at this temperature produced further rapid changes, and transformation appeared to be nearing completion after 4 hours. The curve for 450°C annealing treatments shows an initial decrease in about 0.25 hour,

and subsequent annealing resulted in rapidly decreasing resistivity values. Annealing at 360°C produced relatively small changes in resistivity.

Resistivity curves for the U-w/o Nb-0.68w/o Si alloy, Figure 78, demonstrate the extremely rapid transformation which was also detected by hardness and metallographic studies. In 0.1 hour at 550°C, the resistivity value was about 17 microhm-cm below the solution-treated value, and further annealing produced only slight additional decreases. The curve for 450°C shows that transformation was nearing completion in about 10 hours. Small resistivity changes occurred upon annealing at 360°C for times up to 24 hours; a sample annealed for 400 hours had a very low value, producing a sharp drop in the curve (Figure 78). This rapid decrease at 360°C may be the result of large amounts of decomposition at the grain boundaries.

d. Dilatometric Results

The rapid transformation in U-Nb-Si alloys is also verified by dilatometric data. Figure 79, for the U-8w/o Nb-0.14w/o Si material annealed at 550°C, shows an initial decrease in length in less than 0.1 hour. Transformation appears to be complete in about two hours. Annealing the same material at 450°C resulted in the curve shown in Figure 80. As in the previous illustration, the initial change in length occurred in about 0.1 hour. However, the length was decreasing after 6 hours, indicating that transformation was not complete. Data for the 360°C annealing temperature show slower changes in length than were noted at the higher temperature.

Dilatometric measurements on the U-8w/o Nb-0.68w/o Si composition were in general agreement with results of hardness, metallographic and resistometric studies. Very rapid changes in length occurred, especially at the 550° and 450°C annealing temperatures. Results at 360°C show that transformation is initiated in less than 0.2 hour.

ARMOUR RESEARCH FOUNDATION OF ILLINOIS INSTITUTE OF TECHNOLOGY

Project No. B 095
Summary Report

e.   X-Ray Diffraction Results

Decomposition of the gamma phase in the two U-Nb-Si alloys was studied by X-ray diffraction techniques. As transformation proceeded, alpha was precipitated, and the peak for gamma shifted to higher 2θ values as equilibrium was approached. Annealing for 100 hours at 600° and 550°C, and for 1000 hours at 450°C, resulted in substantially complete transformation in both materials containing silicon. After 1000 hours at 360°C, four alpha peaks were observed in the spectrometer traces for the U-8w/o Nb-0.14w/o Si composition, and the peak for gamma has shifted considerably from the solution-treated value. This annealing treatment produced additional transformation in the U-8w/o Nb-0.68w/o Si alloy; the four alpha peaks were well defined, and the gamma peak was low and broadened. All other compositions examined showed considerably less transformation after 1000 hours at 360°C.
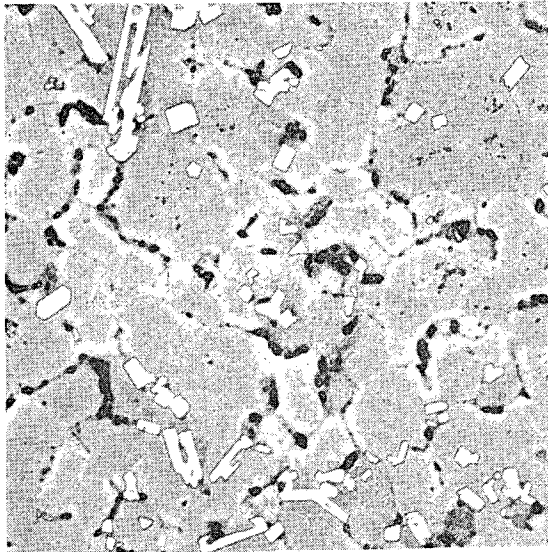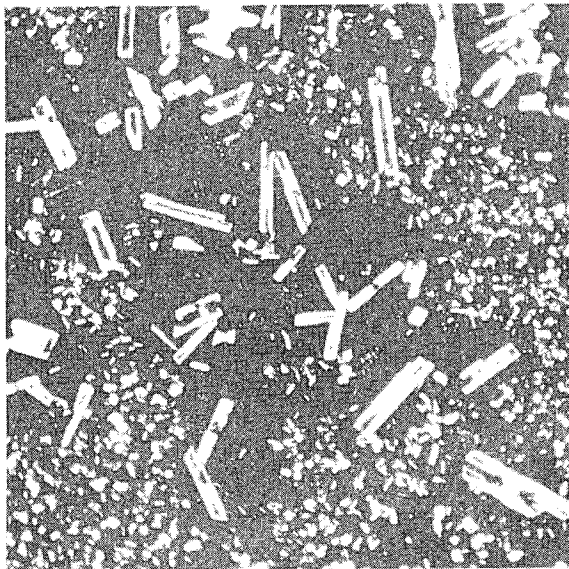
Neg. No. 13443   X 250

Fig. 71

Alloy: U-8w/o Nb-0.68w/o Si.
Treatment: 900°C-WQ; 360°C-10 hrs-
WQ. Dark-etching transformation at
the grain boundaries. Oriented
pattern within the grains, and
crystals of intermetallic compound
throughout sample.

Neg. No. 14708   X 150

Fig. 72

Alloy: U-8w/o Nb-0.68w/o Si.
Treatment: 900°C-WQ; 360°C-1000
hrs-WQ. The dark-etching decom-
position product occurs throughout
the sample, with crystals of the
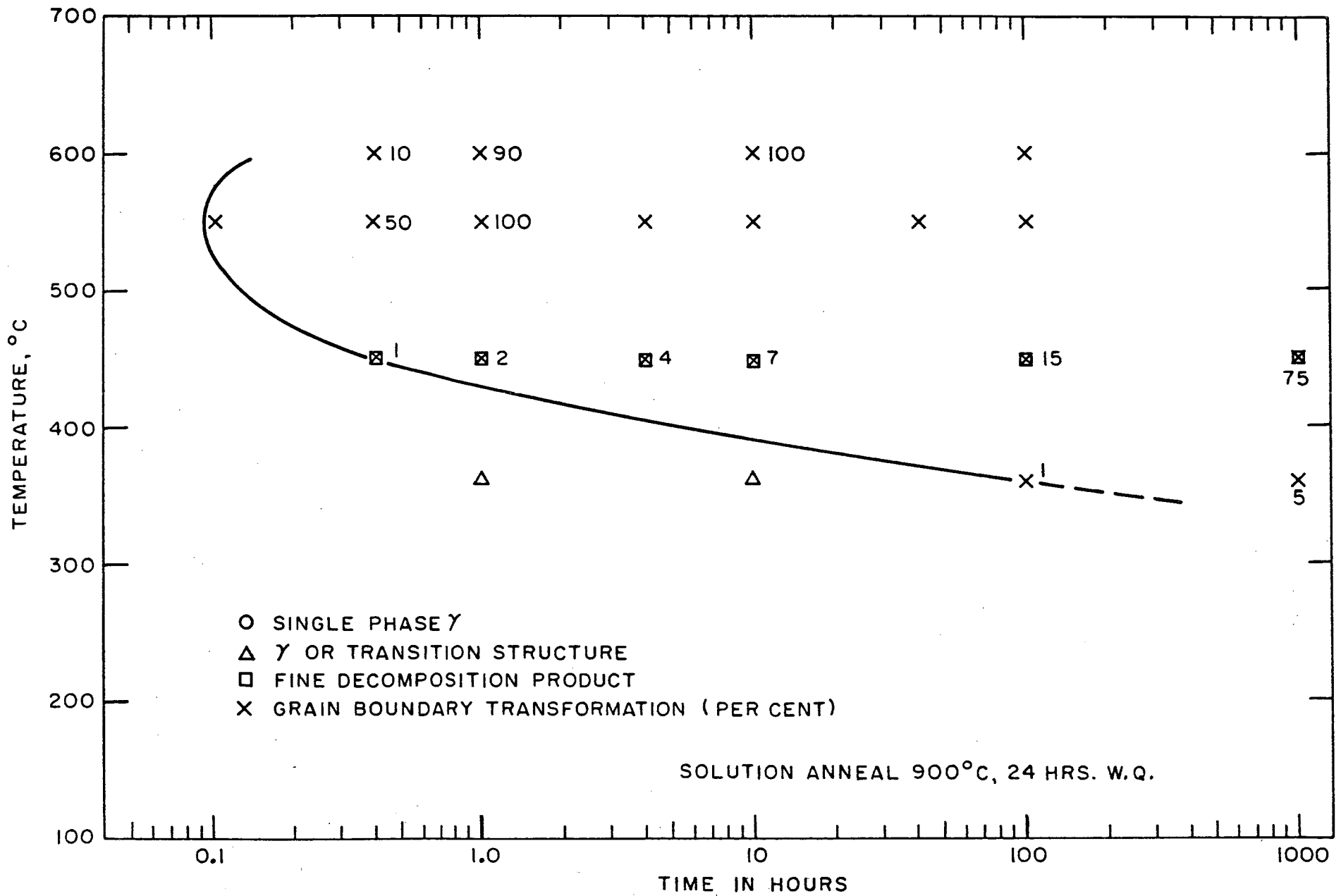intermetallic compound.

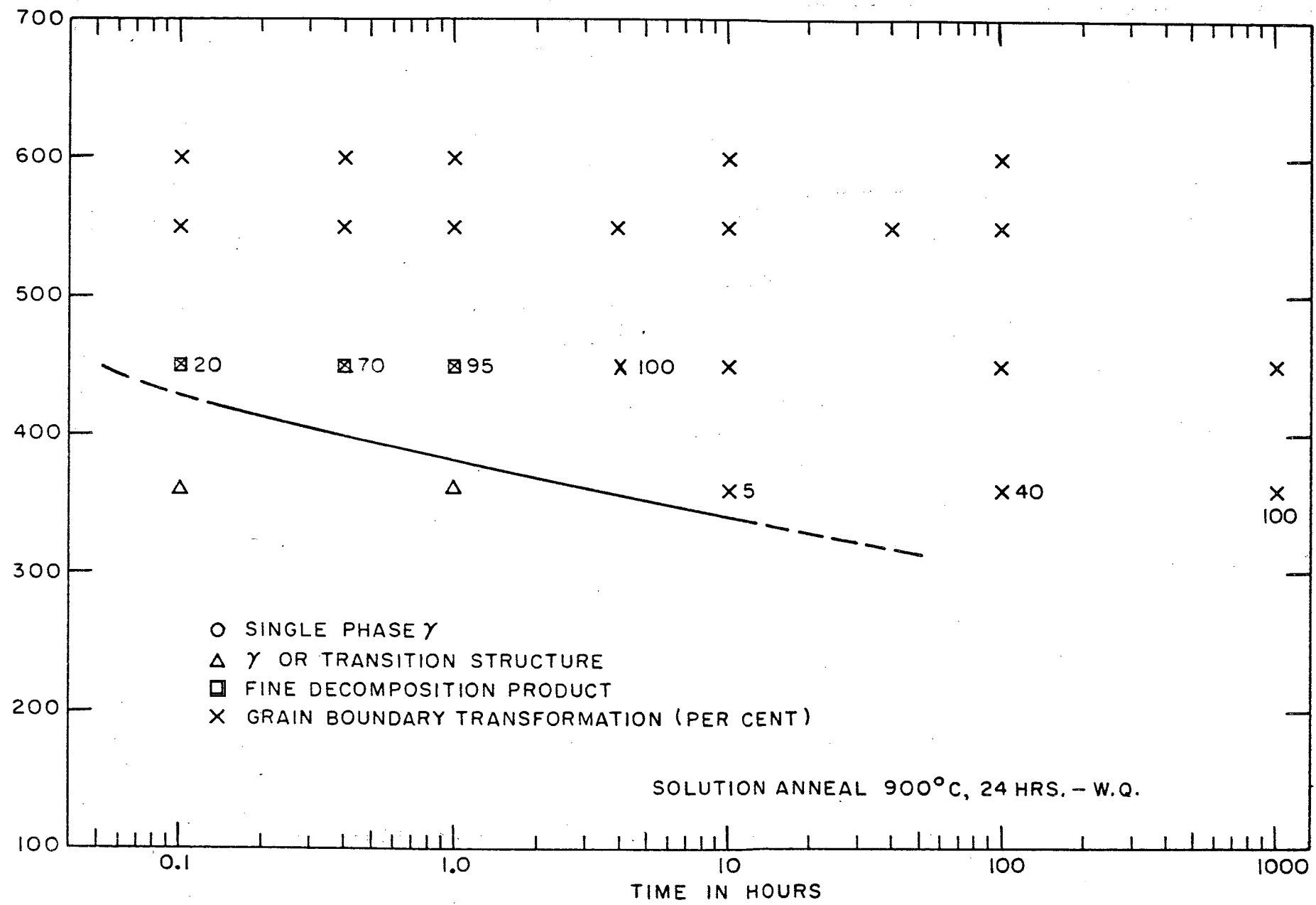Etchant: 10% CrO_3 + 2% HF + H_2O.

- 89 -

FIG. 73 - TTT DIAGRAM FOR A U-8w/o Nb-0.14w/o Si ALLOY ILLUSTRATING INITIAL
METALLOGRAPHIC OBSERVATION OF GRAIN BOUNDARY TRANSFORMATION

FIG. 74 - TTT DIAGRAM FOR A U-8w/o Nb-0.68w/o Si ALLOY ILLUSTRATING INITIAL
METALLOGRAPHIC OBSERVATION OF GRAIN BOUNDARY TRANSFORMATION
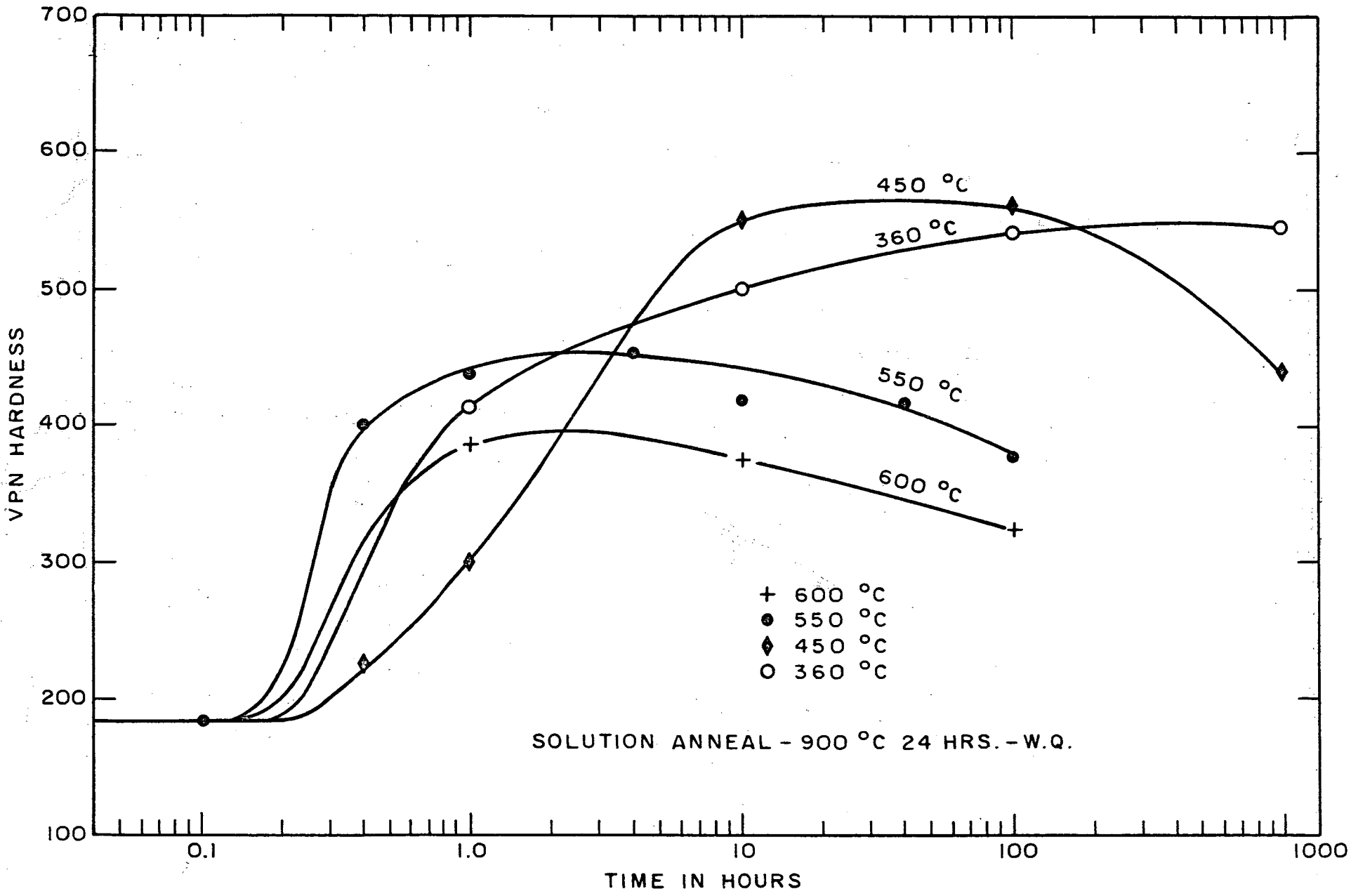
FIG. 75 - HARDNESS DATA FOR AN ISOTHERMALLY ANNEALED U-8^W/o Nb-0.14^W/o Si ALLOY
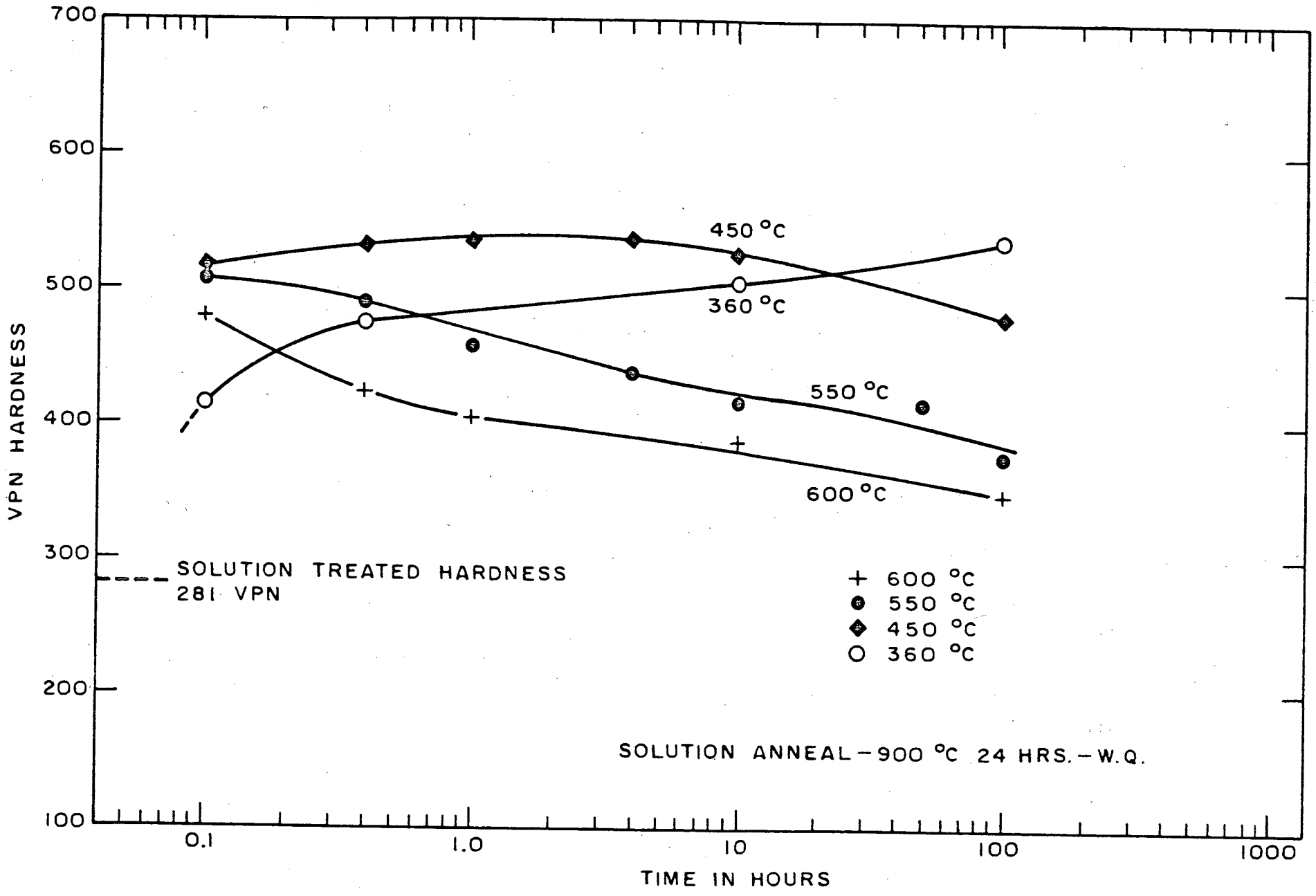
FIG. 76 - HARDNESS DATA FOR AN ISOTHERMALLY ANNEALED U-8w/o Nb-0.68w/o Si ALLOY

FIG. 77 - ROOM TEMPERATURE ELECTRICAL RESISTIVITY DATA FOR AN
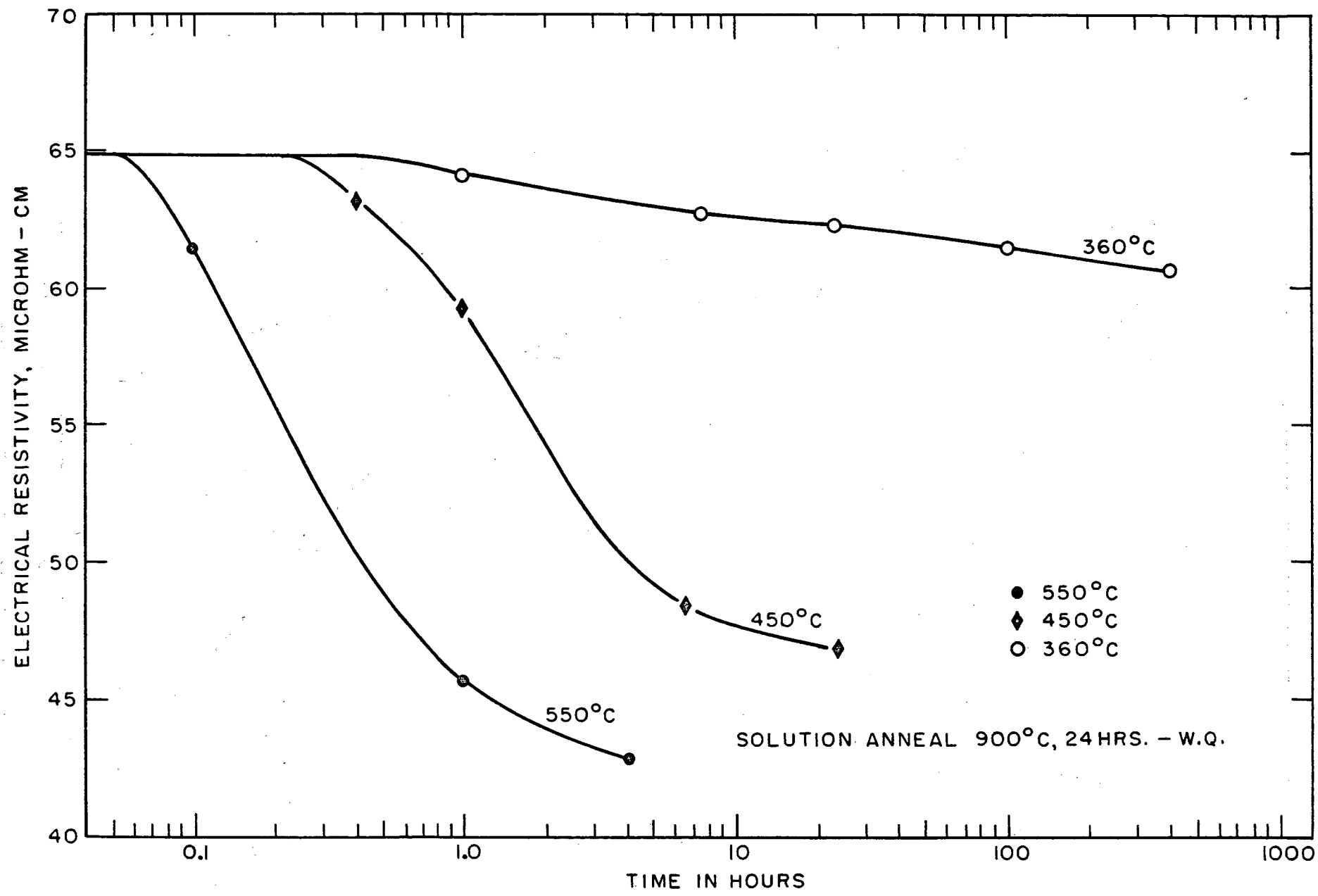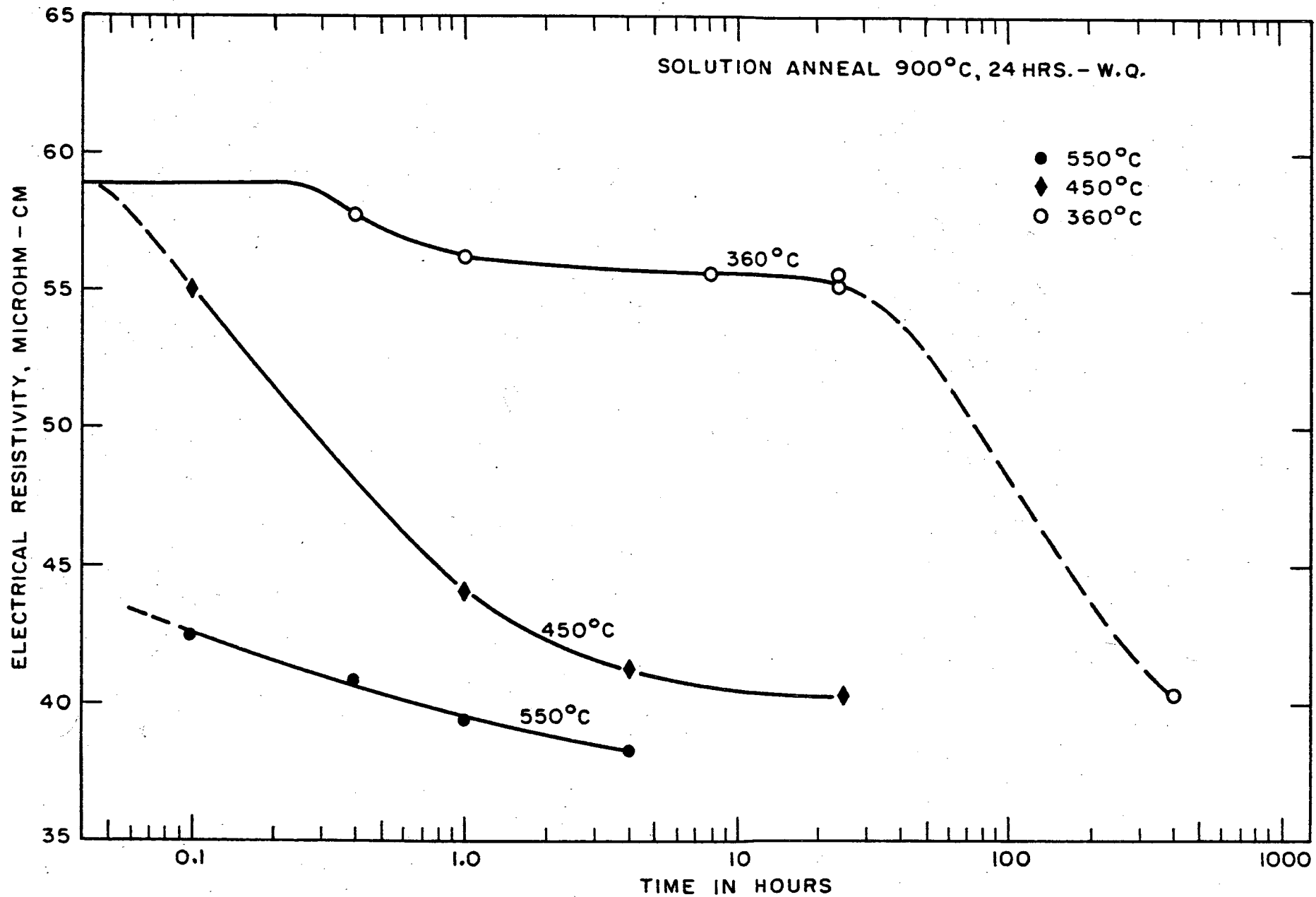ISOTHERMALLY ANNEALED U-8w/o Nb-0.14w/o Si ALLOY

FIG. 78 - ROOM TEMPERATURE ELECTRICAL RESISTIVITY DATA FOR AN
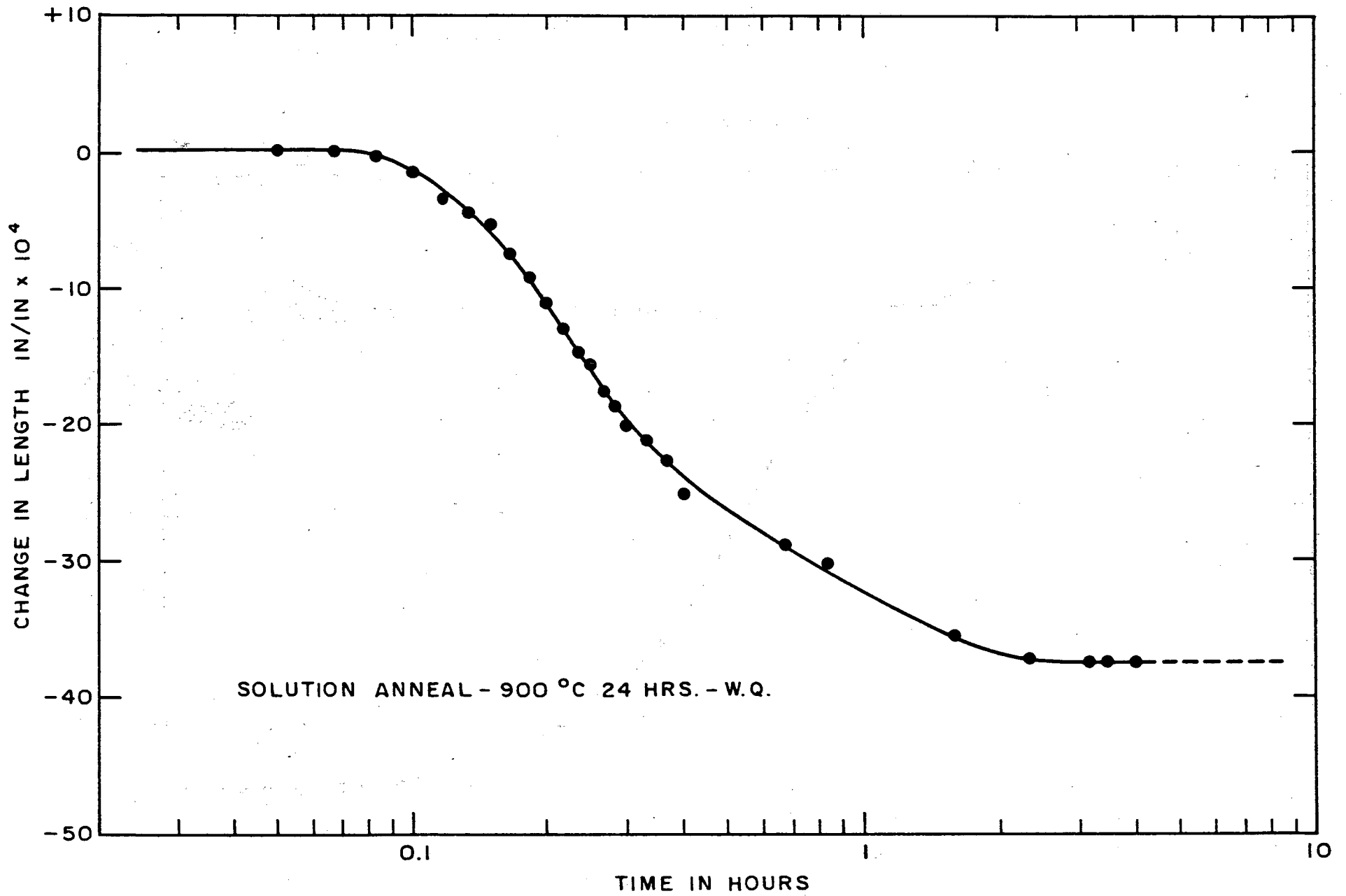ISOTHERMALLY ANNEALED U-8w/o Nb-0.68w/o Si ALLOY

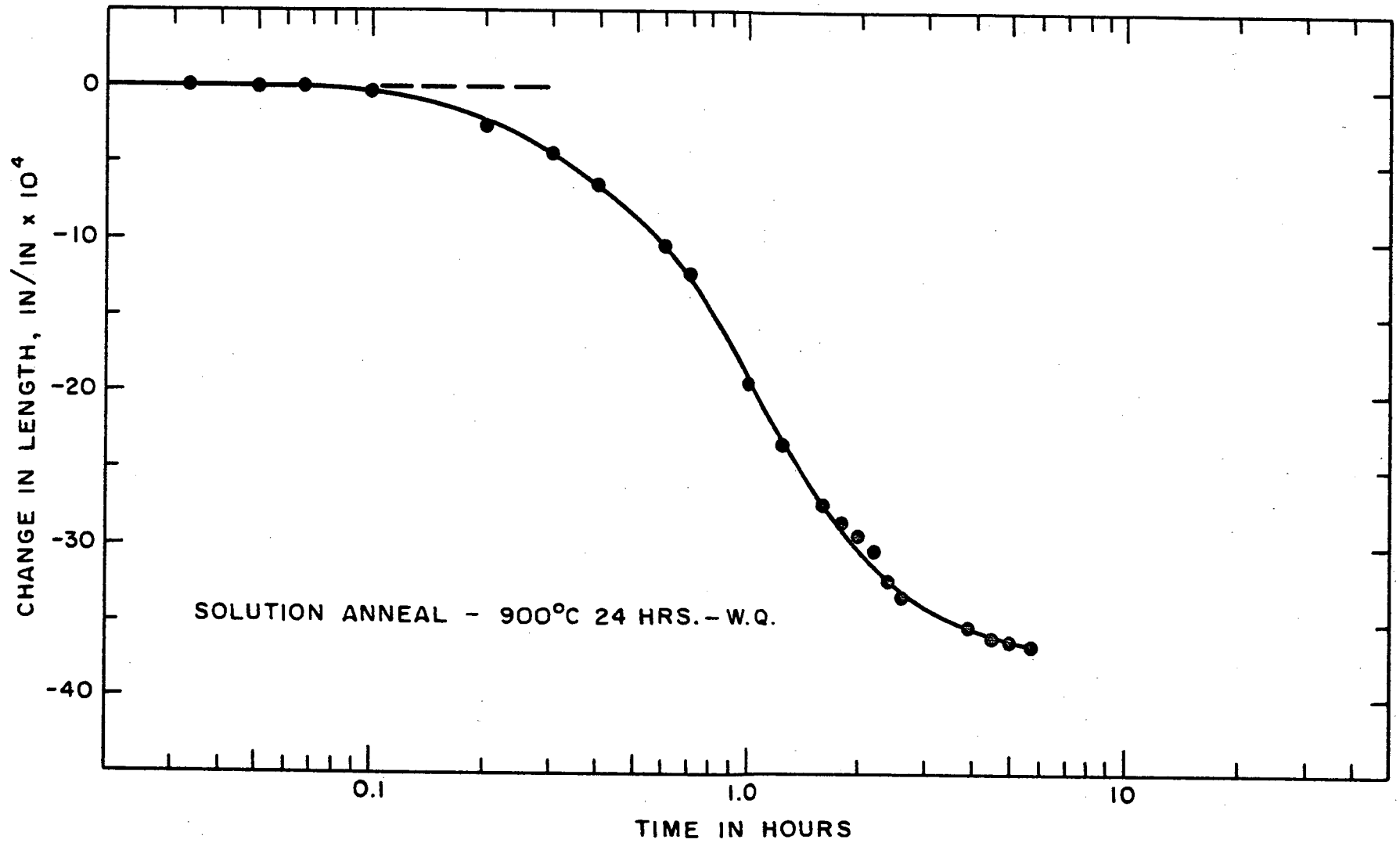FIG. 79 - DILATOMETRIC DATA FOR A U-8^W/o Nb-0.14^W/o Si ALLOY ISOTHERMALLY ANNEALED AT 550°C

FIG. 80 - DILATOMETRIC DATA FOR A U-8 ^{W}/o Nb-0.14 ^{W}/o Si ALLOY
ISOTHERMALLY ANNEALED AT 450°C

- 97 -

7.   U-Nb-Ni Alloys

a.   Metallographic Results

Two U-Nb base compositions containing nickel were included in the program. Difficulties were encountered in homogenizing the alloy having the higher nickel content. This material, U-8w/o Nb-0.84w/o Ni, exhibited incipient melting at the 1100°C homogenization temperature. In addition, the material appeared to react with the molybdenum sheet in which the specimens were wrapped. This reaction was evidenced by the visual appearance of the wrapped specimens after heat treating and by metallographic examination. Similar results were observed after homogenization at 900°C. Figure 81 is a photomicrograph showing the structure resulting after 48 hours at 900°C. A low-melting constituent is present both within the gamma grains and in the grain boundaries. The distribution of this material throughout the sample was not uniform. Several lower temperature homogenization treatments were attempted but the results were not satisfactory. Annealing the cast material for 72 hours at 750°C produced the microstructure shown in Figure 82. In addition to producing incipient melting, this lower annealing temperature did not eliminate coring. As in other samples of this composition, the second-phase constituent was not uniformly distributed, and variations in hardness occurred within the specimens. No further investigations were conducted on this alloy.

The second-phase material was not detected in microstructures of the U-8w/o Nb-0.14w/o Ni composition which were annealed at 1100°C. However, samples of this alloy were characterized by nonuniform hardness which indicated some variations in composition.

Transformation structures in this material were similar to those observed in most of the compositions. Annealing at 600° and 550°C produced

the typical dark-etching grain boundary decomposition. This product was
detected after relatively short annealing times, as indicated by the TTT
curve presented in Figure 83. The presence of the fine decomposition product
(stained matrix) was observed after 0.4 hour at 450°C, indicating rapid trans-
formation. Microstructures of samples annealed at 360°C exhibited the lightly
stained, oriented pattern after annealing for 1 hour.

b. Hardness Results

Hardness data for the U-8w/o Nb-0.14w/o Ni alloy are shown in
Figure 84. Increases occurred in less than 0.2 hour at all annealing temper-
atures. The hardness curve at 550°C reached a maximum in the comparatively
short time of two hours. The peak hardness at 450°C occurred in less than
100 hours. Although the alloy having a higher nickel content was not tested
for comparison, these results indicate that the additions of nickel to a
U-8w/o Nb base accelerate initiation of transformation. This will be demon-
strated in the "Comparative Data" section.

c. Electrical Resistivity Results

Results of electrical resistivity measurements on the U-8w/o Nb-
0.14w/o Ni alloy also show rapid initiation of transformation at all annealing
temperatures (Figure 85). A decrease occurred at 550°C in considerably less
than 0.1 hour, and although resistivity values dropped sharply upon further
annealing, the curve shows that small changes were taking place at 100 hours.
A similar initial decrease was noted at 450°C; longer annealing times were
required to produce further changes. Annealing at 360°C resulted in an
initial decrease in about 0.3 hour. Further annealing caused relatively
slight changes; after 400 hours, the resistivity was only 6 microhm-cm below
the value for solution-treated material.

Project No. B 095
Summary Report

d.   Dilatometric Results

A dilatometric curve for the U-8w/o Nb-0.14w/o Ni composition annealed at 550°C is illustrated in Figure 86. An initial change in length occurred in less than 0.1 hour. This value is in agreement with results of metallographic, hardness and electrical resistivity determinations of initial property changes. The findings indicate that transformation was essentially complete in two hours. Dilatometric data at lower annealing temperatures show the rapid transformation of this alloy which was detected by other methods of examination.

e.   X-Ray Diffraction Results

X-ray diffraction studies of this alloy were limited. After 1000 hours at 450°C four alpha peaks were present in the spectrometer pattern, and the peak for gamma had shifted from the solution-treated 2θ value of 36.7° to 37.6°, indicating that transformation was approaching completion. The spectrometer trace for a sample annealed at 360°C for 1000 hours showed incipient alpha precipitation and a broadened, poorly defined peak for gamma.
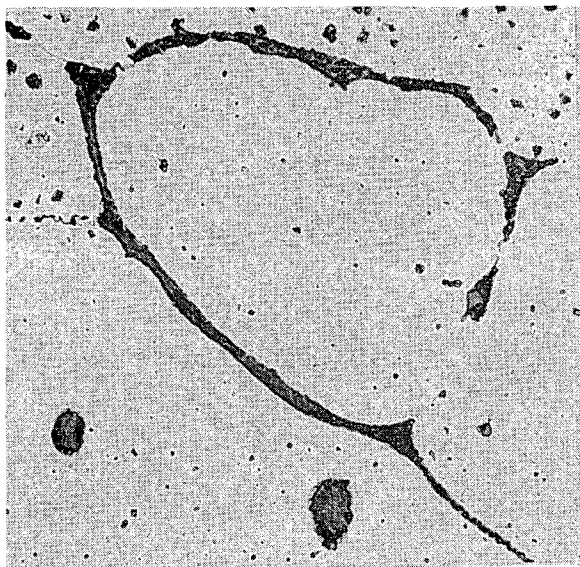
Neg. No. 13635   X 250

Fig. 81

Alloy: U-8w/o Nb-0.84w/o Ni.
Treatment: 900°C-48 hrs-WQ.
γ and incipient melting at grain
boundaries and within grains.
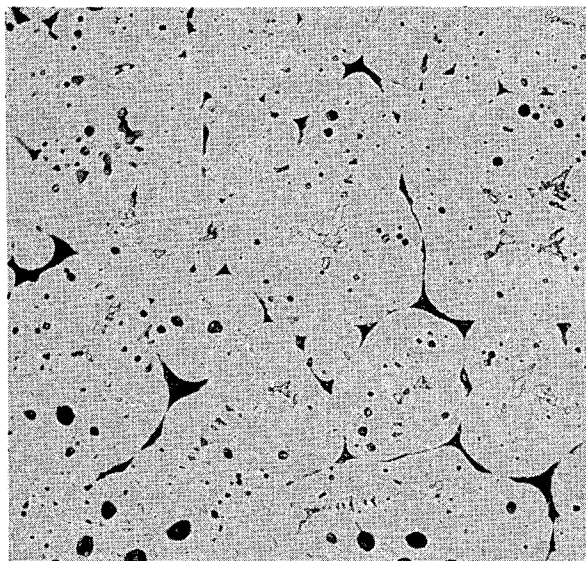
Neg. No. 13634   X 250

Fig. 82

Alloy: U-8w/o Nb-0.84w/o Ni.
Treatment: 750°C-72 hrs WQ.
The lower temperature heat treatment
did not eliminate the melting ob-
served in Fig. 81. In addition, a
residual dendritic structure is
present.

Etchant: 10% CrO$_3$ + 2% HF + H$_2$O.

- 101 -

FIG. 83 - TTT DIAGRAM FOR A U-8w/o Nb-0.14w/o Ni ALLOY ILLUSTRATING INITIAL
METALLOGRAPHIC OBSERVATION OF GRAIN BOUNDARY TRANSFORMATION

FIG. 84 - HARDNESS DATA FOR AN ISOTHERMALLY ANNEALED U-8w/o Nb-0.14w/o Ni ALLOY

FIG. 85 - ROOM TEMPERATURE ELECTRICAL RESISTIVITY DATA FOR AN
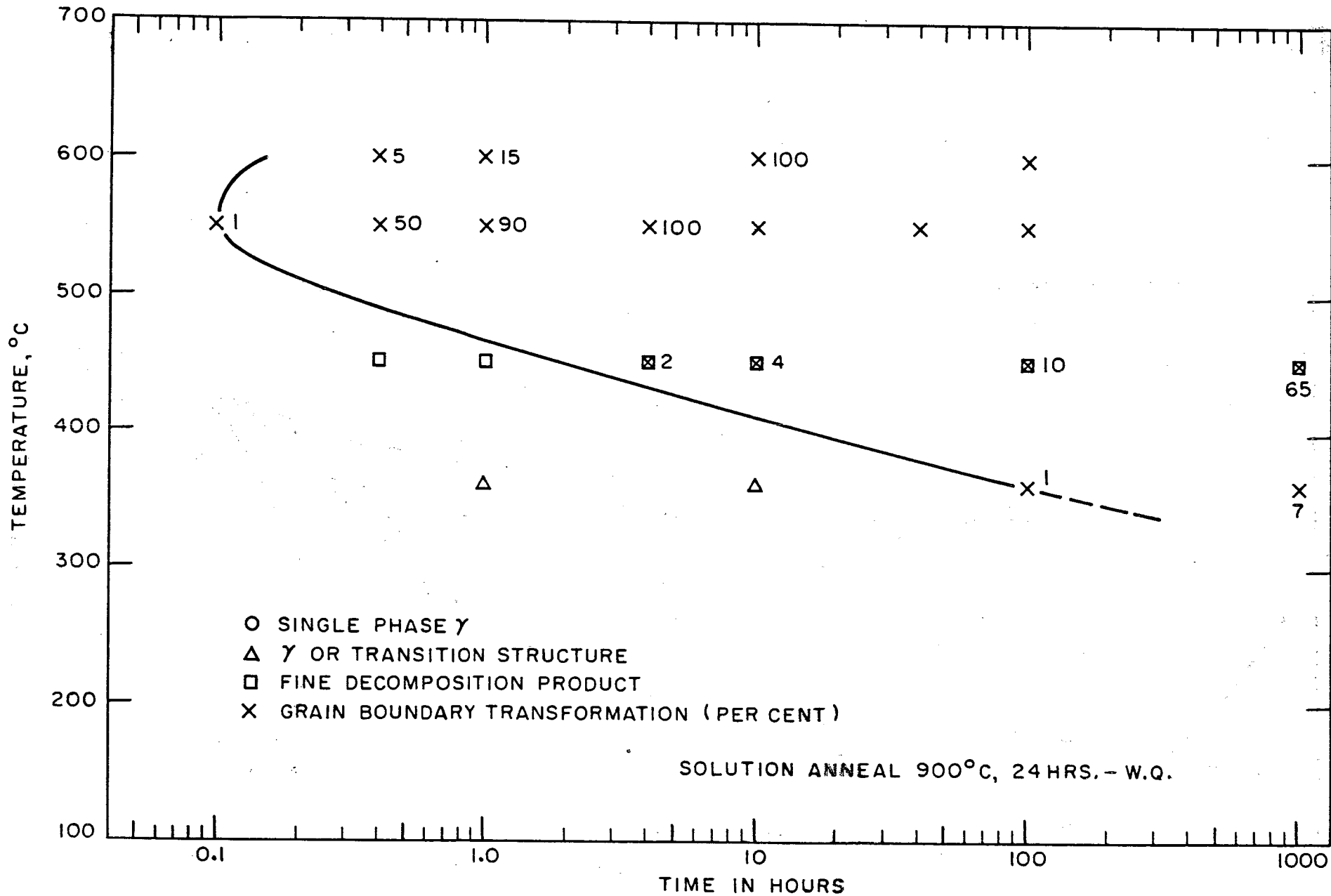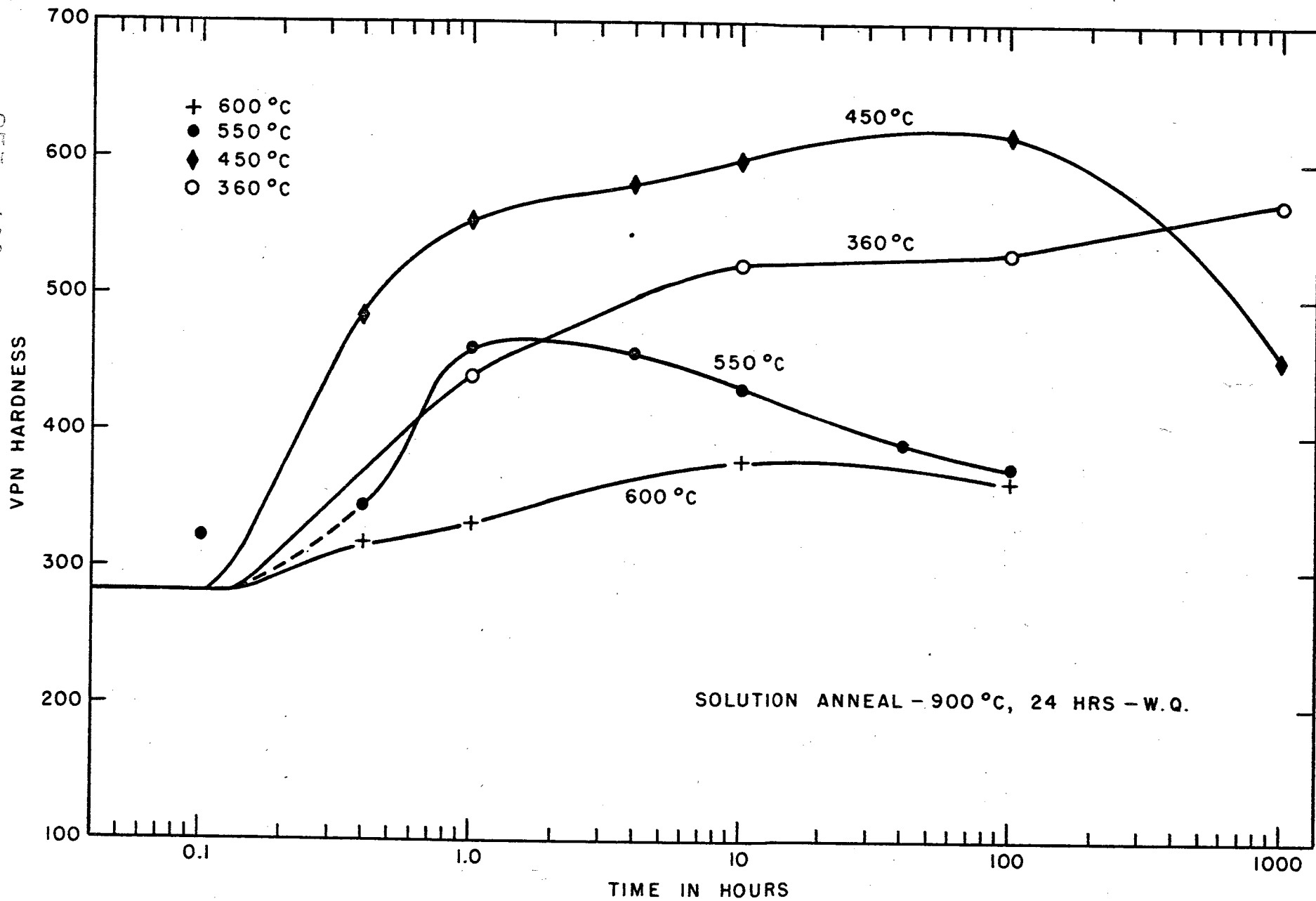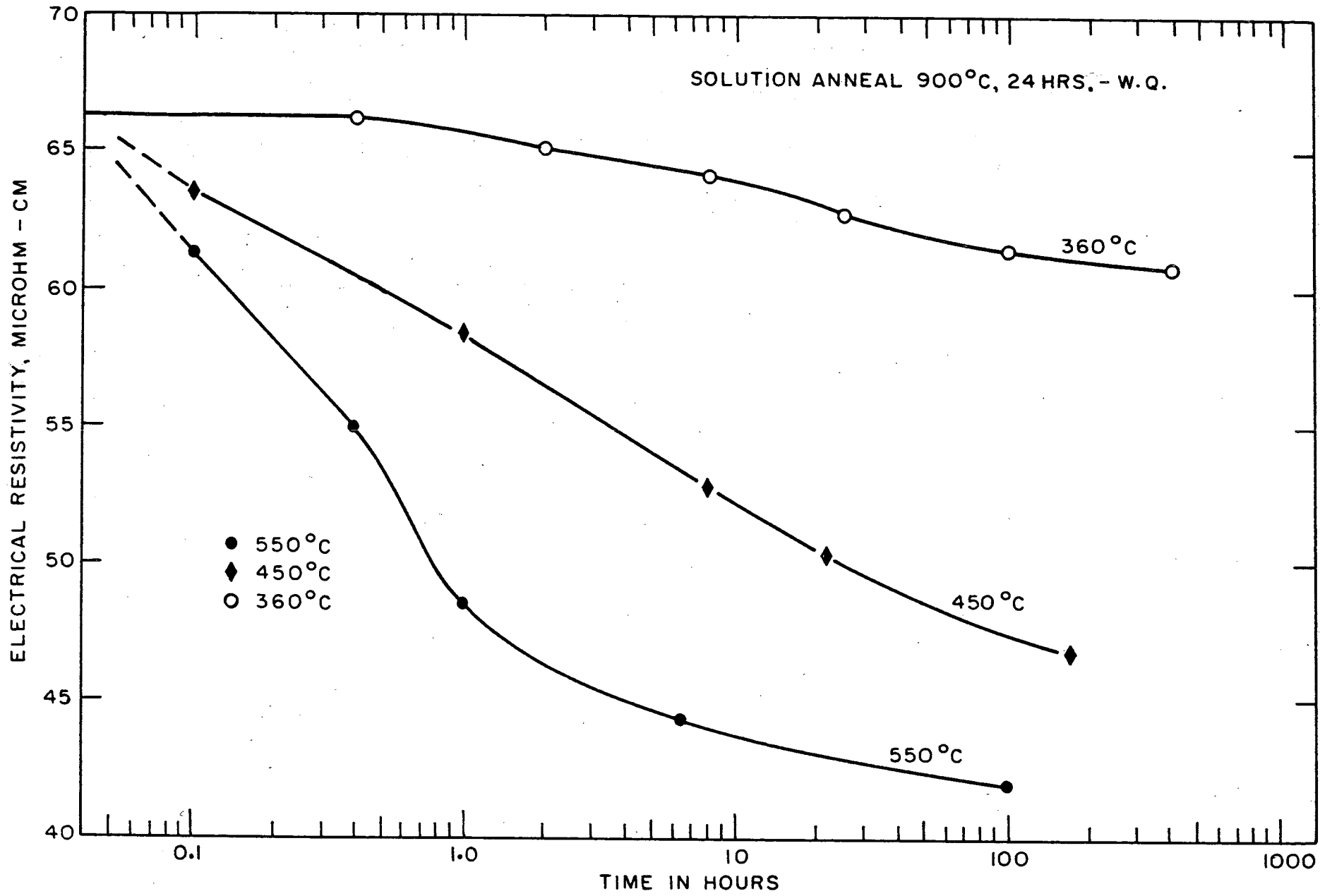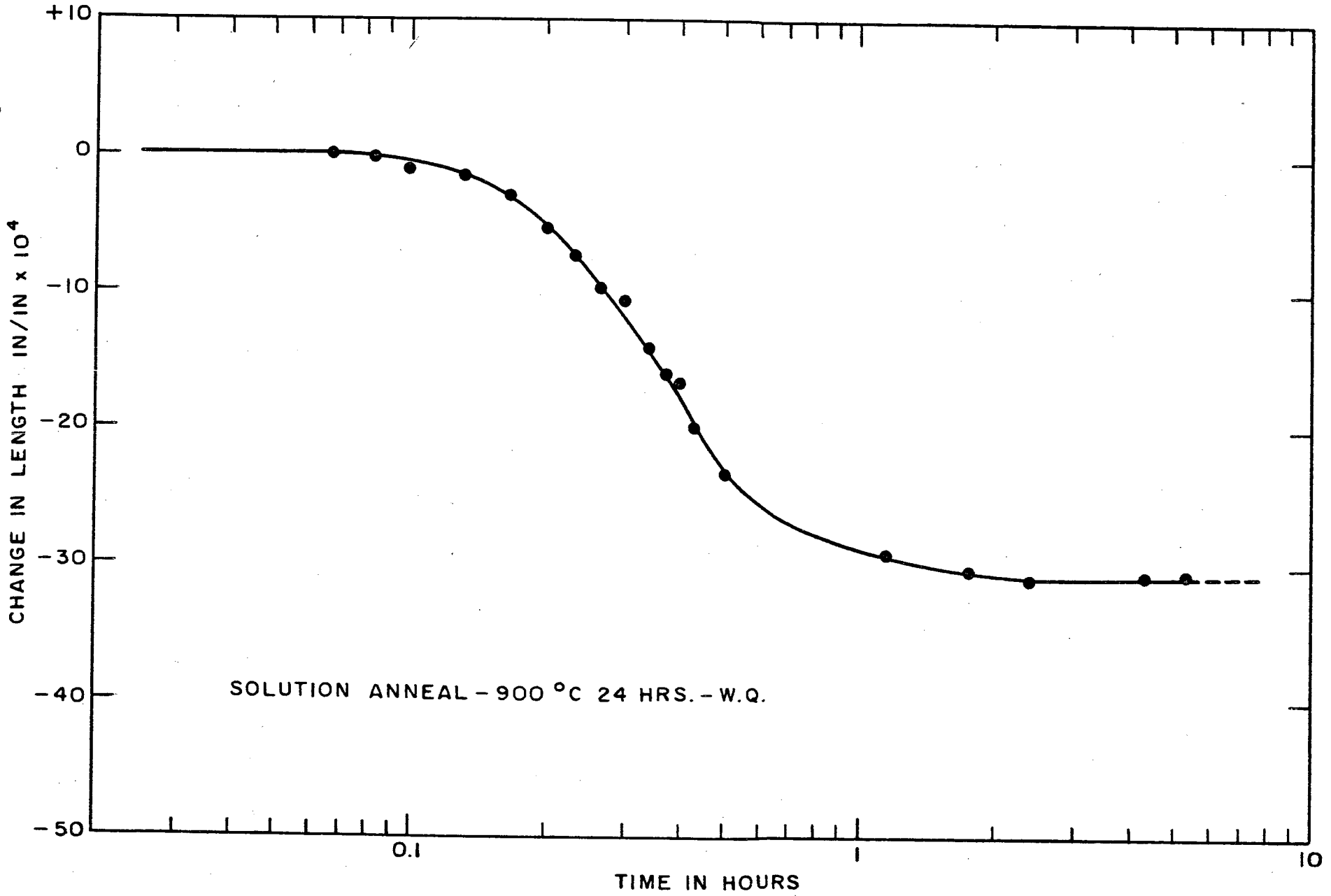ISOTHERMALLY ANNEALED U-8w/o Nb-0.14w/o Ni ALLOY

FIG. 86 - DILATOMETRIC DATA FOR A U-8w/o Nb-0.14w/o Ni ALLOY ISOTHERMALLY ANNEALED AT 550°C

8.   U-Nb-Ru Alloy

a.   Metallographic Results

Transformation structures in the U-8w/o Nb-0.49w/o Ru alloy at 600° and 550°C exhibited the typical dark-etching product which originated at grain boundaries. At 450°C small amounts of grain boundary transformation and also the fine decomposition product were observed in the microstructure of a sample annealed for 10 hours. Further annealing produced slow growth of the grain boundary product; about 8 per cent was present after 1000 hours at 450°C. The oriented structure was detected after annealing for 10 hours at 360°C, and a small amount of transformation at the grain boundaries was found after 1000 hours. The TTT diagram and other metallographic data for this composition are shown in Figure 87.

b.   Hardness Results

Results of hardness measurements, Figure 88, show that the initial increase occurred at 550°C in about 0.4 hour. Longer annealing times were required to produce initial hardness rises at the other annealing temperatures. The effect of this element on the stability of the gamma phase is more difficult to determine here, where only one composition containing ruthenium was studied, than when the ternary addition was made at two levels. These hardness data, however, show that this alloy was more stable than the U-8w/o Nb base compositions having additions of silicon, titanium, nickel and chromium.

c.   Electrical Resistivity Results

Resistivity curves for the U-8w/o Nb-0.49w/o Ru alloy are presented in Figure 89. Annealing at 550°C produced the initial decrease in less than 0.1 hour, a much shorter time than was required to initiate decomposition at the grain boundaries and an increase in hardness. This effect has been noted

in other compositions and will be discussed under the "Comparative Data"
section. A resistivity decrease at 450°C was observed after annealing for
0.3 hour, and values continued to decrease at 100 hours at this temperature.
Annealing at 360°C produced a small decrease in 1 hour. After 400 hours at
360°C, relatively slight further changes occurred, indicating that only a
small amount of transformation had taken place.

d. Dilatometric Results

Initiation of transformation, as determined by dilatometric
measurements, was in fair agreement with results from other techniques used
to study decomposition of the gamma phase. Changes in length at 550° and
450°C occurred after the initial resistivity decrease but before an increase
was noted in hardness. Measurements at 360°C showed small density changes
in less than 8 hours; this annealing interval produced a large increase in
hardness, and the oriented pattern was observed in the microstructure of a
sample annealed for 10 hours.

e. X-Ray Diffraction Results

Annealing the U-8w/o Nb-0.49w/o Ru alloy at 550°C for 100 hours
resulted in substantially complete transformation, as indicated by X-ray
diffraction studies. The four peaks for alpha were well defined, and the
peak for gamma had shifted from the solution-treated 2θ value of 36.8 to
37.9°. Less transformation resulted from annealing at 450°C for 1000 hours;
the four alpha reflections were present, but the gamma peak was located at a
2θ value of 37.5°, considerably below that for equilibrium γ_2. The dif-
fraction pattern for a sample heat-treated for 1000 hours at 360°C showed a
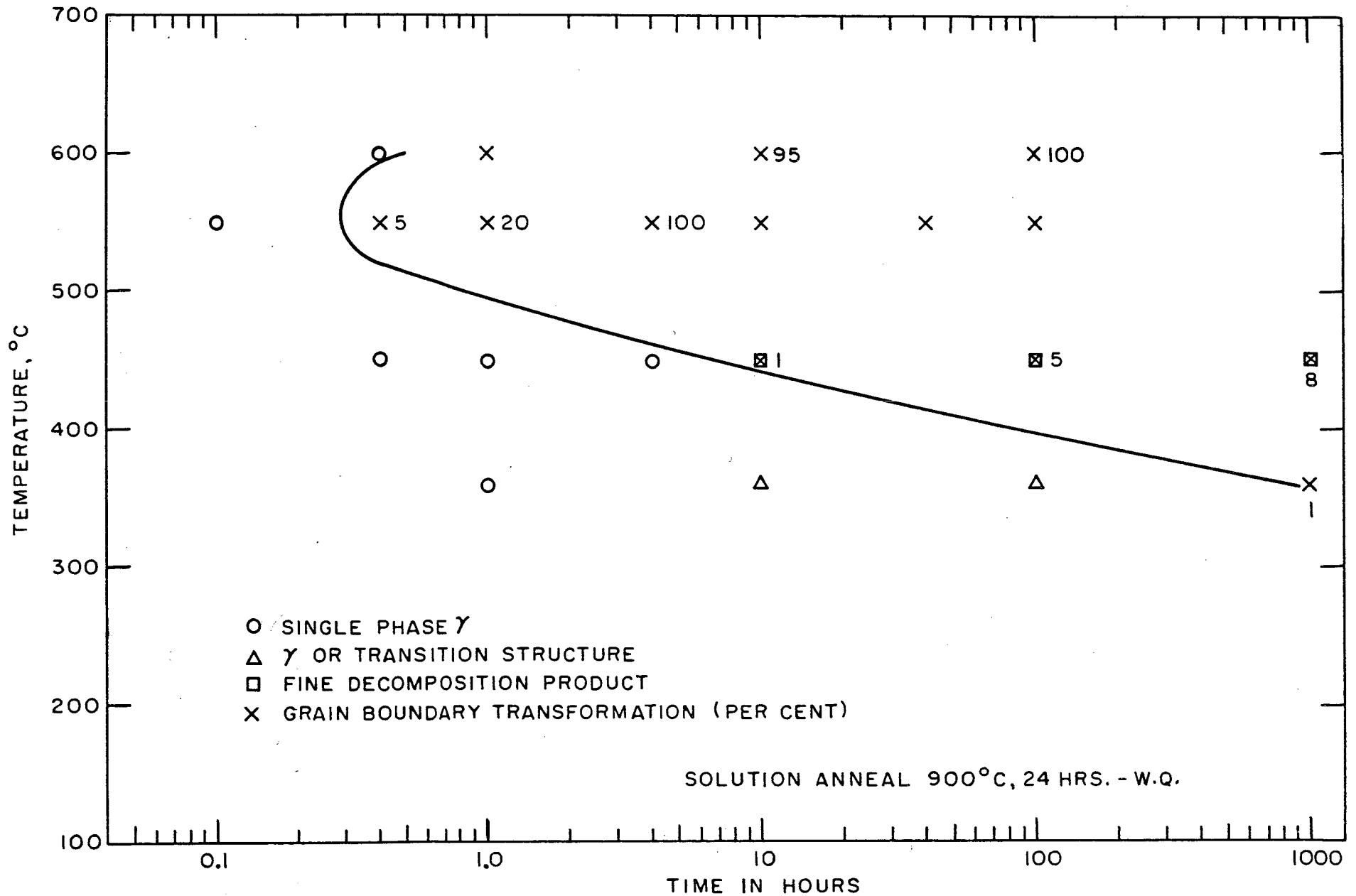slightly broadened gamma peak and indications of one of the alpha peaks.

FIG. 87 - TTT DIAGRAM FOR A U-8w/o Nb-0.49w/o Ru ALLOY ILLUSTRATING INITIAL
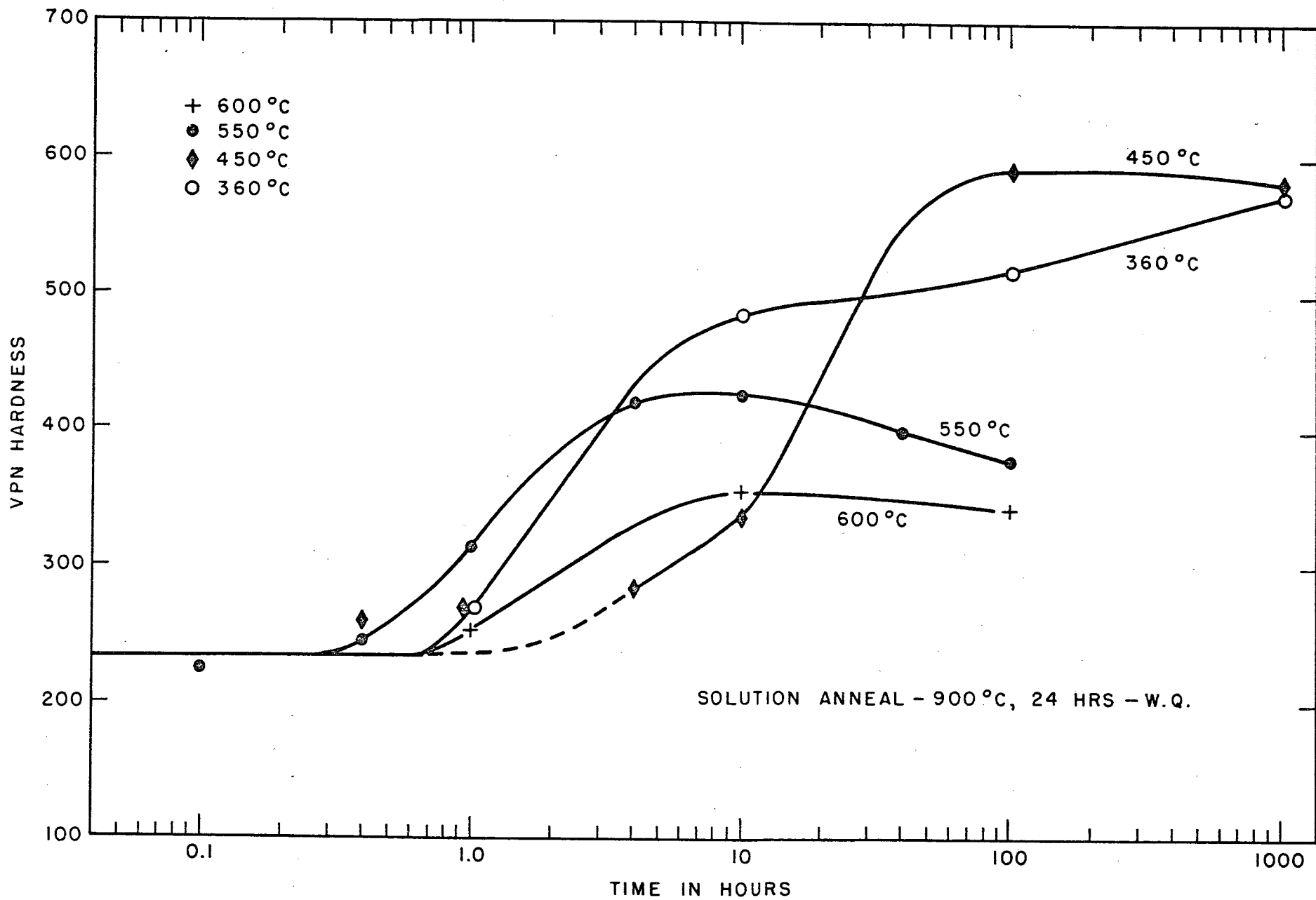METALLOGRAPHIC OBSERVATION OF GRAIN BOUNDARY TRANSFORMATION

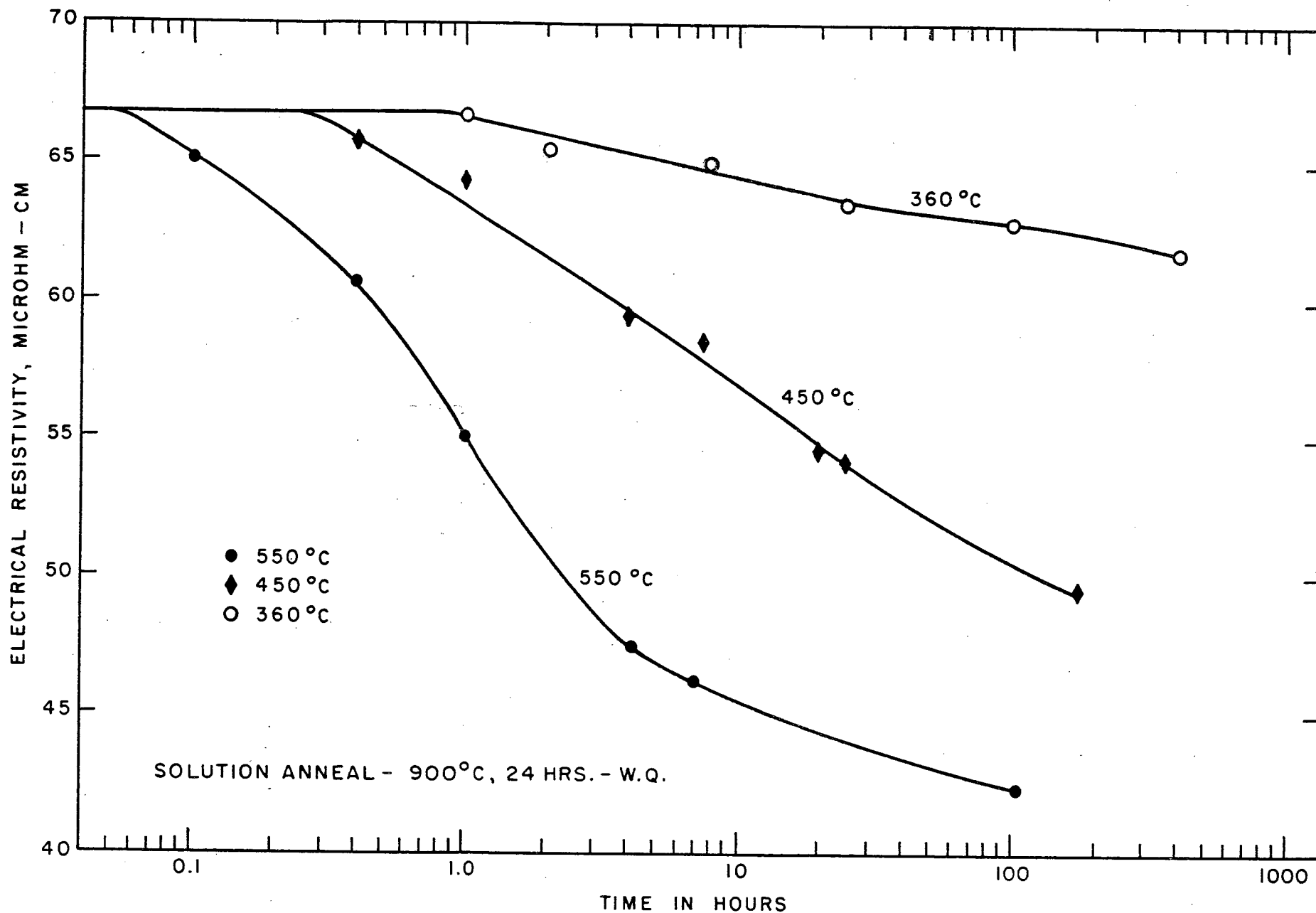FIG. 88 - HARDNESS DATA FOR AN ISOTHERMALLY ANNEALED U-8w/o Nb-0.49w/o Ru ALLOY

FIG.89 - ROOM TEMPERATURE ELECTRICAL RESISTIVITY DATA FOR AN
ISOTHERMALLY ANNEALED U-8w/o Nb-0.49w/o Ru ALLOY

9. U-Nb-V Alloys

a. Metallographic Results

Vanadium was added to a U-8w/o Nb base at levels of 0.98w/o
(4a/o) and 2.02w/o (8a/o). Annealing these compositions at 600° and 550°C
produced transformation at the grain boundaries and around impurity particles.
This structure etched lighter than decomposition products for other alloys.
As transformation proceeded, it was sometimes difficult to distinguish between
areas of this light-etching material and patches of retained gamma. A typical
example is illustrated in Figure 90. This U-8w/o Nb-2.02w/o sample was annealed
at 600°C for 10 hours, and shows the light-etching decomposition product and
also former gamma grain boundaries. Subsequent annealing at 600°C produced
structures which differed considerably from those of other compositions having
the same heat treatment. After 100 hours, Figure 91, the material has a dark-
etching phase which in most areas is completely surrounded by the lighter
matrix. X-ray diffraction results for this material show that α, γ_1, and γ_2
are present. Most compositions annealed at 600° or 550°C for 100 hours show
more of the darker etching product, and the lighter etching phase is not
continuous. Such a structure is illustrated in Figure 45.

In the case of the alloy containing vanadium, the small particles
of alpha are somewhat rounded; it is possible that further annealing would
result in additional spheroidization of this dispersed phase. Such a structure
may be of interest if the matrix of $\gamma_1 + \gamma_2$ is sufficiently corrosion resistant.
A former gamma grain boundary may be seen in Figure 91; the precipitated alpha
does not form a continuous network along these grain boundaries.

Annealing the U-Nb-V alloys at 450°C produced both the fine decom-
position product and grain boundary transformation. In the case of the

ARMOUR RESEARCH FOUNDATION OF ILLINOIS INSTITUTE OF TECHNOLOGY

255 117

U-8w/o Nb-0.98w/o V material, both types of decomposition appeared simultaneously after annealing for 10 hours. The microstructure is illustrated in Figure 92. The dark-etching transformation is present at some grain boundaries and around impurity particles. The lighter etching fine decomposition product appears at a few grain boundaries and is initiated within the gamma grains. Further annealing results in the merging of these areas into a uniformly stained matrix.

Microstructures of both compositions annealed at 360°C showed initiation of transformation at the grain boundaries after 1000 hours. Samples of the U-8w/o Nb-2.02w/o V alloy exhibited only very small amounts of the oriented structures at the 360°C annealing temperature.

Metallographic data, including TTT curves based on initiation of grain boundary transformation, are presented in Figures 93 and 94. Curves for the two alloys are almost identical, indicating that increasing the vanadium content from 4 to 8a/o had little effect on initiation of transformation. Both compositions were considerably more stable than the U-8w/o Nb material, which demonstrates that addition of vanadium to a U-Nb base retards transformation of the gamma phase.

b. Hardness Results

Hardness data for the U-Nb-V alloys (Figures 95 and 96) indicate that the U-8w/o Nb-0.98w/o V composition was more stable at all annealing temperatures than the material having the higher vanadium content. Both alloys required much longer annealing times to initiate hardness changes than were noted for any other U-8w/o Nb base ternary composition.

The initial hardness increase in the U-8w/o Nb-0.98w/o V material occurred in 1 hour at 550°C; changes in hardness at other annealing temperatures

required two to three hours. The U-8w/o Nb-2.02w/o V alloy transformed in somewhat shorter annealing times, especially at the higher temperatures.

c.   Electrical Resistivity Results

Resistivity curves for the U-8w/o Nb-0.98w/o V composition are shown in Figure 97. As observed in other alloys, the most rapid decrease occurred at the 550°C annealing temperature. The initial change at 450°C required almost 4 hours; this annealing interval also produced the first hardness increase, and small amounts of decomposition were observed in the microstructure. Annealing at 360°C resulted in a very small decrease in resistivity after 100 hours.

Results of resistivity measurements of the U-8w/o Nb-2.02w/o V alloy were considerably different, as illustrated in Figure 98. The curve for 550°C was similar to that of the previously described material. However, annealing at 450°C resulted in an initial increase of resistivity; in 0.4 hour, the value was 1.5 microhm-cm above the solution-treated measurement. From 1 hour to 4 hours the resistivity decreased to about 2 microhm-cm below the solution-treated value. Another, and more significant, decrease occurred after 24 hours at 450°C. The reason for this behavior is not known. Annealing at 360°C produced gradually increasing electrical resistivity after about 10 hours; in 400 hours, the resistivity was 3.5 microhm-cm above the value for solution-treated material.

d.   Dilatometric Results

Annealing the U-w/o Nb-0.98w/o V alloy at 550°C produced the dilatometric curve shown in Figure 99. A change in length was initiated in slightly less than 1 hour and was approaching completion in 5 hours. Similar results were obtained from hardness measurements. Dilatometric data for the

U-8w/o Nb-2.02 V composition at 550°C show an initial decrease in length after 0.5 hour which was nearly complete in 6 hours. These values are also in close agreement with hardness curves for this material.

Annealing both U-Nb-V alloys at 450°C produced very small initial decreases in length in 4 hours. After 24 hours at this temperature, large changes in length had taken place, indicating that transformation was partially complete. Annealing for 400 hours at 360°C also produced a considerable increase in density, as determined by measurements taken on samples before and after this heat treatment.

e. X-Ray Diffraction Results

The mechanism of transformation in the U-Nb-V alloys was examined at several annealing temperatures using X-ray diffraction techniques. For each annealing temperature, a sample was reheated for progressively longer times, and a spectrometer pattern was obtained at each interval.

Results of these studies show a mode of decomposition which resembled that found in the U-Nb-Ti alloys. A series of diffraction patterns for the U-8w/o Nb-2.02w/o V material annealed for varying lengths of time at 450°C, is shown in Figures 100, 101 and 102. After 1 hour (Figure 100) only the single peak for gamma is present. Annealing for 10 hours at 450°C resulted in the pattern shown in Figure 101. The gamma peak is unchanged, and small amounts of alpha are present. In addition, the indistinct rise at a 2θ value of 38.2° indicates incipient precipitation of γ_2. After 100 hours (Figure 102) the diffraction pattern shows evidence of increased amounts of both alpha and γ_2, and the peak for γ_1 is unchanged. Additional annealing at 450°C produced relatively slight further changes although after 1000 hours the peaks for alpha and γ_2 were sharper.

Project No. B 095
Summary Report

Similar investigations were conducted for the U-8w/o Nb-0.98w/o V alloy at 450°C, and for both compositions at higher annealing temperatures. The mode of transformation in both materials at 550°C and 600°C was found to be similar to the results illustrated in Figures 100 to 102. These studies show that both alpha and γ_2 are co-precipitated from the metastable gamma phase. It appears that at equilibrium both alloys are located in the three-phase space $\gamma_1 + \gamma_2$ and α. These three phases were also present in both compositions after annealing for 50 hours at 625°C. Data from samples annealed for 100 hours at 660°C indicate that the U-8w/o Nb-0.98w/o V alloy is in the single-phase γ_1 region, and that the material containing 2.02w/o vanadium is in the two-phase $\gamma_1 + \gamma_2$ space.

The composition having the higher vanadium content was found to be more stable after 1000 hours at 360°C. Spectrometer traces for this heat treatment showed only a slight broadened gamma peak for the U-8w/o Nb-2.02w/o V alloy, whereas small amounts of alpha were detected in the pattern for the U-8w/o Nb-0.98w/o V material.
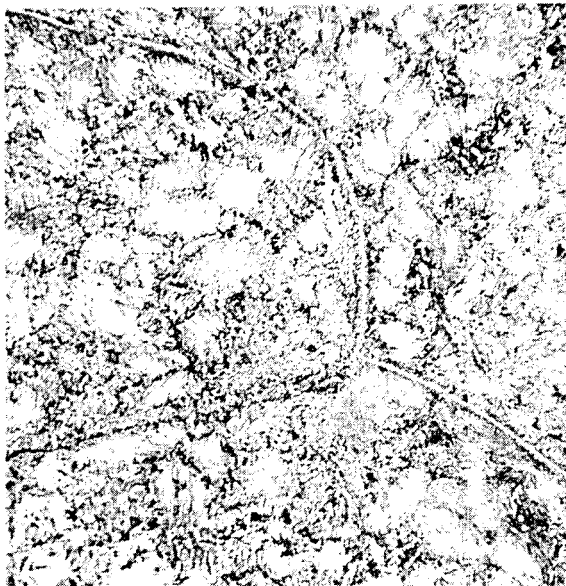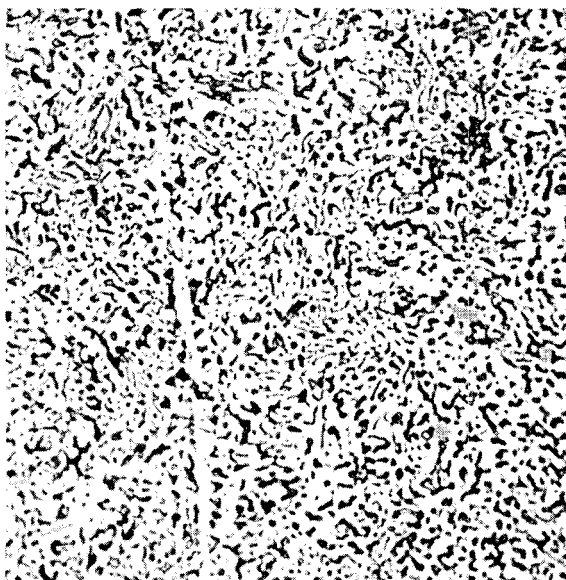
Neg. No. 14083   X 500

Fig. 90

Alloy: U-8w/o Nb-2.02w/o V.
Treatment: 900°C-WQ; 600°C-10 hrs-
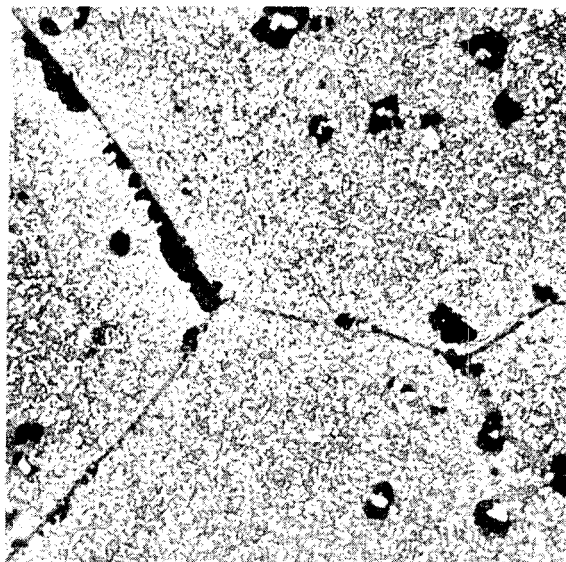WQ. Relatively light-etching
decomposition product.

Neg. No. 13951   X 1000

Fig. 91

Alloy: U-8w/o Nb-2.02w/o V.
Treatment: 900°C-WQ; 600°C-100 hrs-
WQ. Fine structure with the dark-
etching alpha as a dispersed phase.
The matrix is probably a mixture of
γ_1 and γ_2.

Neg. No. 13642   X 500

Fig. 92

Alloy: U-8w/o Nb-0.98w/o V.
Treatment: 900°C-WQ; 450°C-10 hrs-
WQ. Fine decomposition product
originating within gamma grains.
The dark-etching transformation
product is present at some grain
boundaries and around impurity
particles.

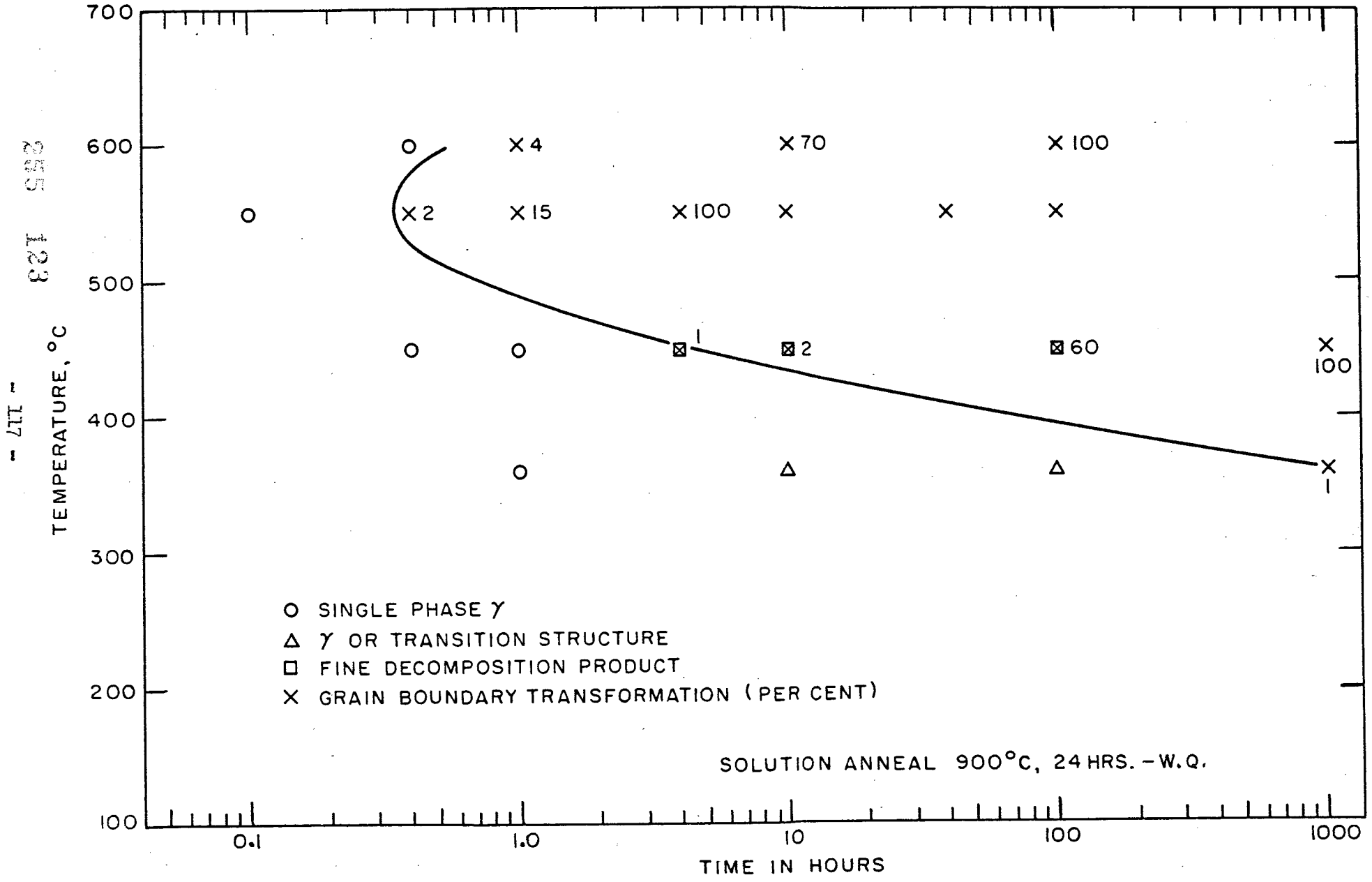Etchant: 10% CrO_3 + 2% HF + H_2O.

- 116 -

255 122

FIG. 93 - TTT DIAGRAM FOR A U-8w/o Nb-0.98w/o V ALLOY ILLUSTRATING INITIAL
METALLOGRAPHIC OBSERVATION OF GRAIN BOUNDARY TRANSFORMATION

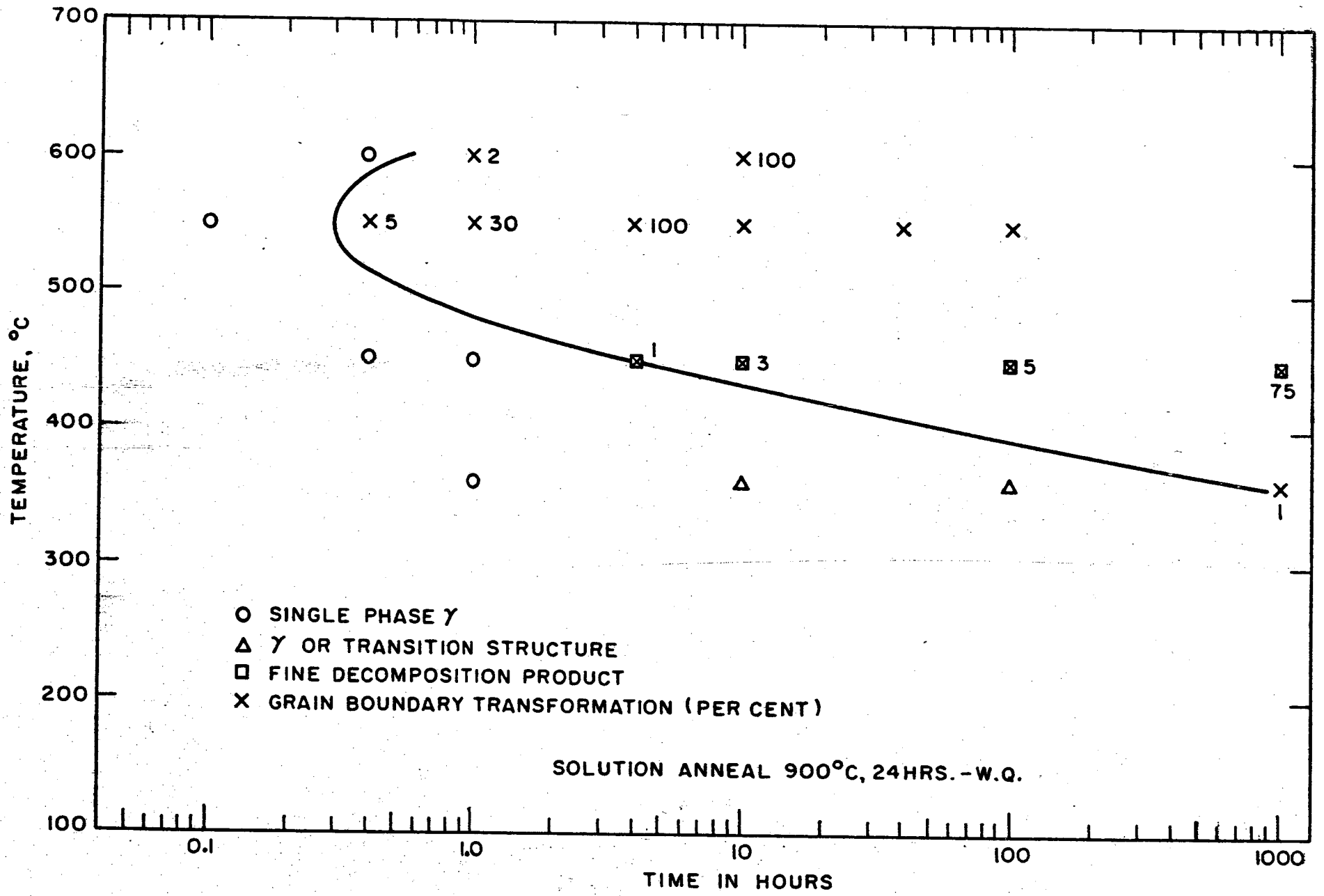FIG. 94 - TTT DIAGRAM FOR A U-8w/o Nb-2.02w/o V ALLOY ILLUSTRATING INITIAL
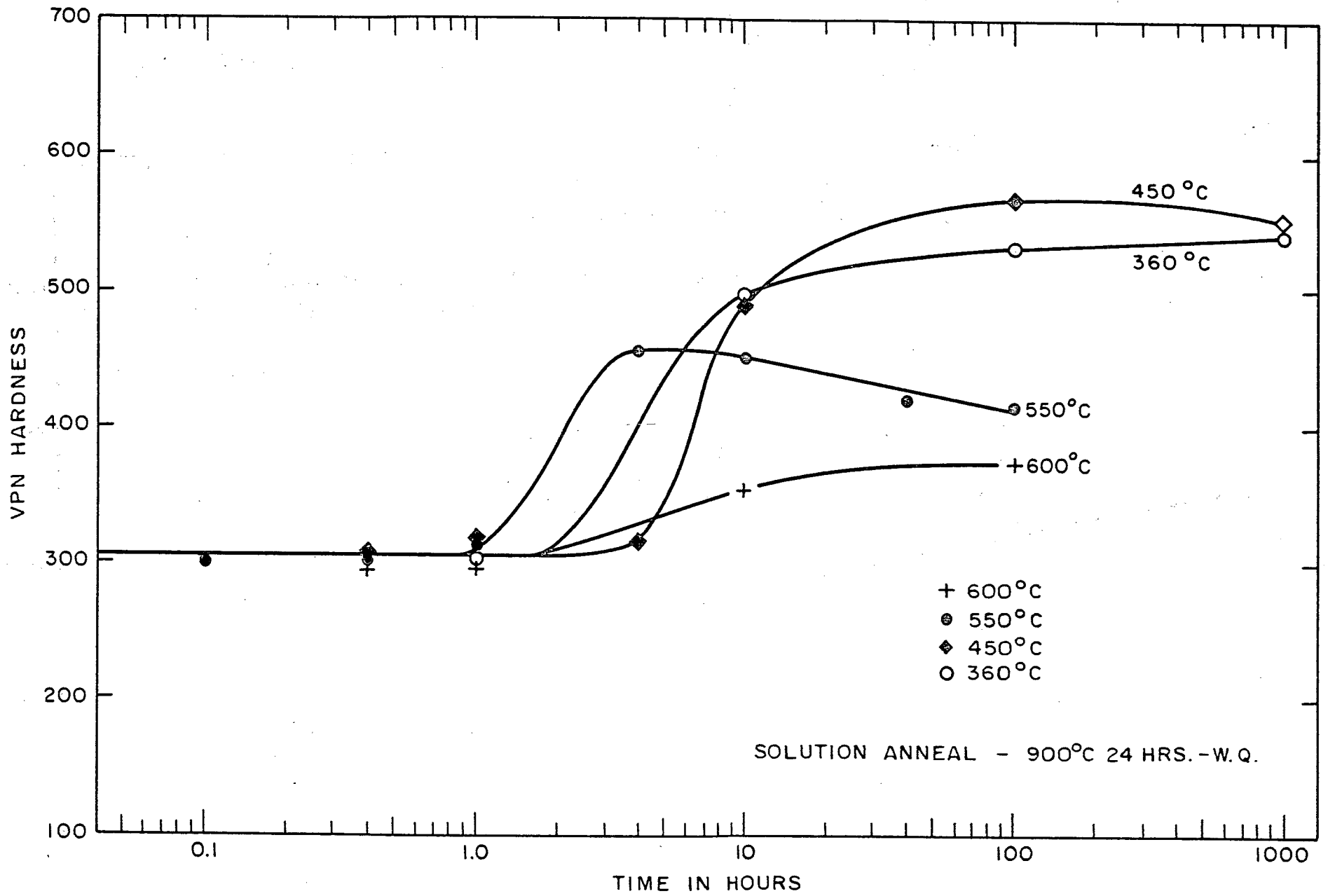METALLOGRAPHIC OBSERVATION OF GRAIN BOUNDARY TRANSFORMATION

FIG. 95 — HARDNESS DATA FOR AN ISOTHERMALLY ANNEALED U-8 ^{W}/o Nb-0.98 ^{W}/o V ALLOY

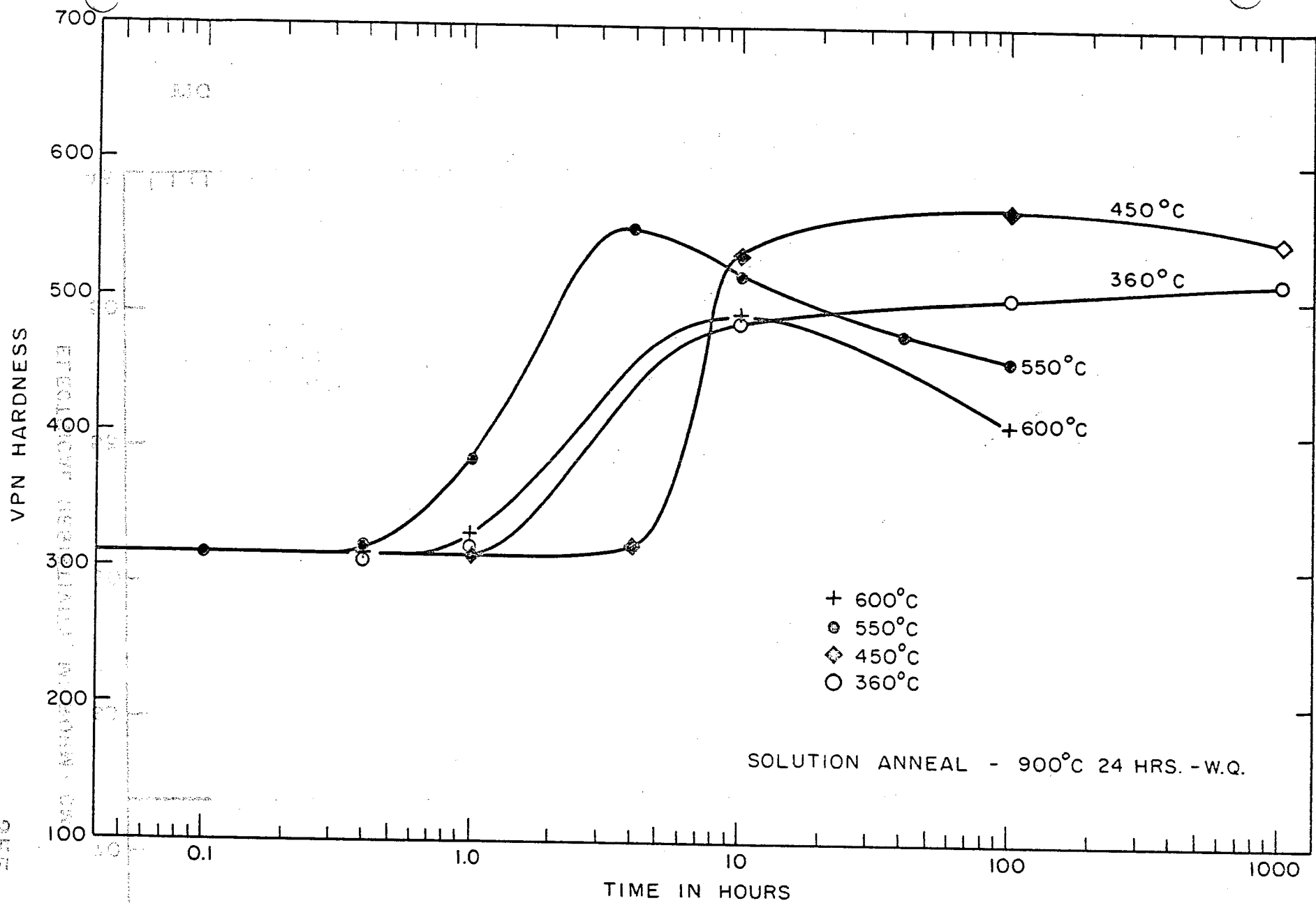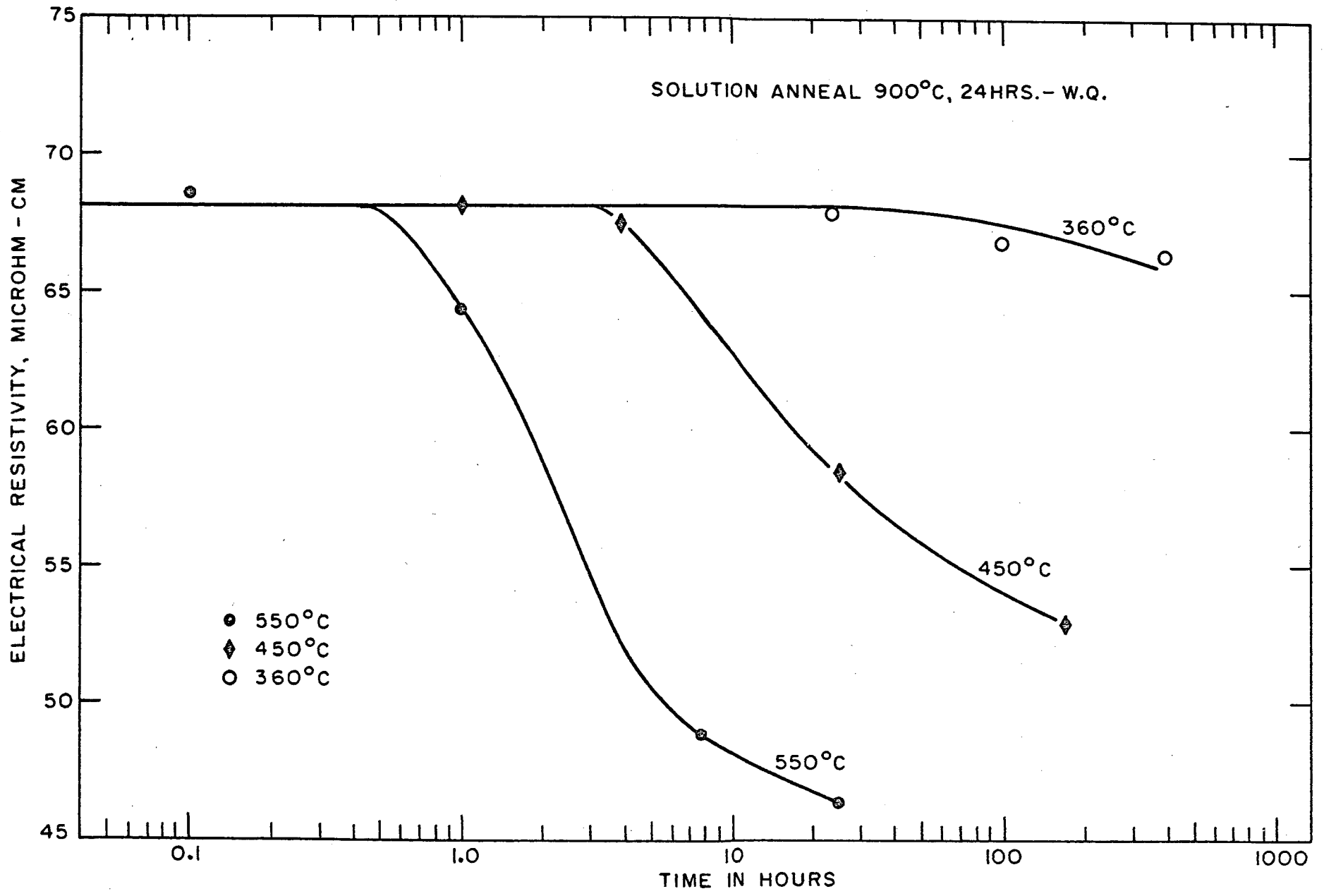FIG. 96 - HARDNESS DATA FOR AN ISOTHERMALLY ANNEALED U-8 $^W/o$ Nb-2.02 $^W/o$ V ALLOY

FIG. 97 - ROOM TEMPERATURE ELECTRICAL RESISTIVITY DATA FOR AN
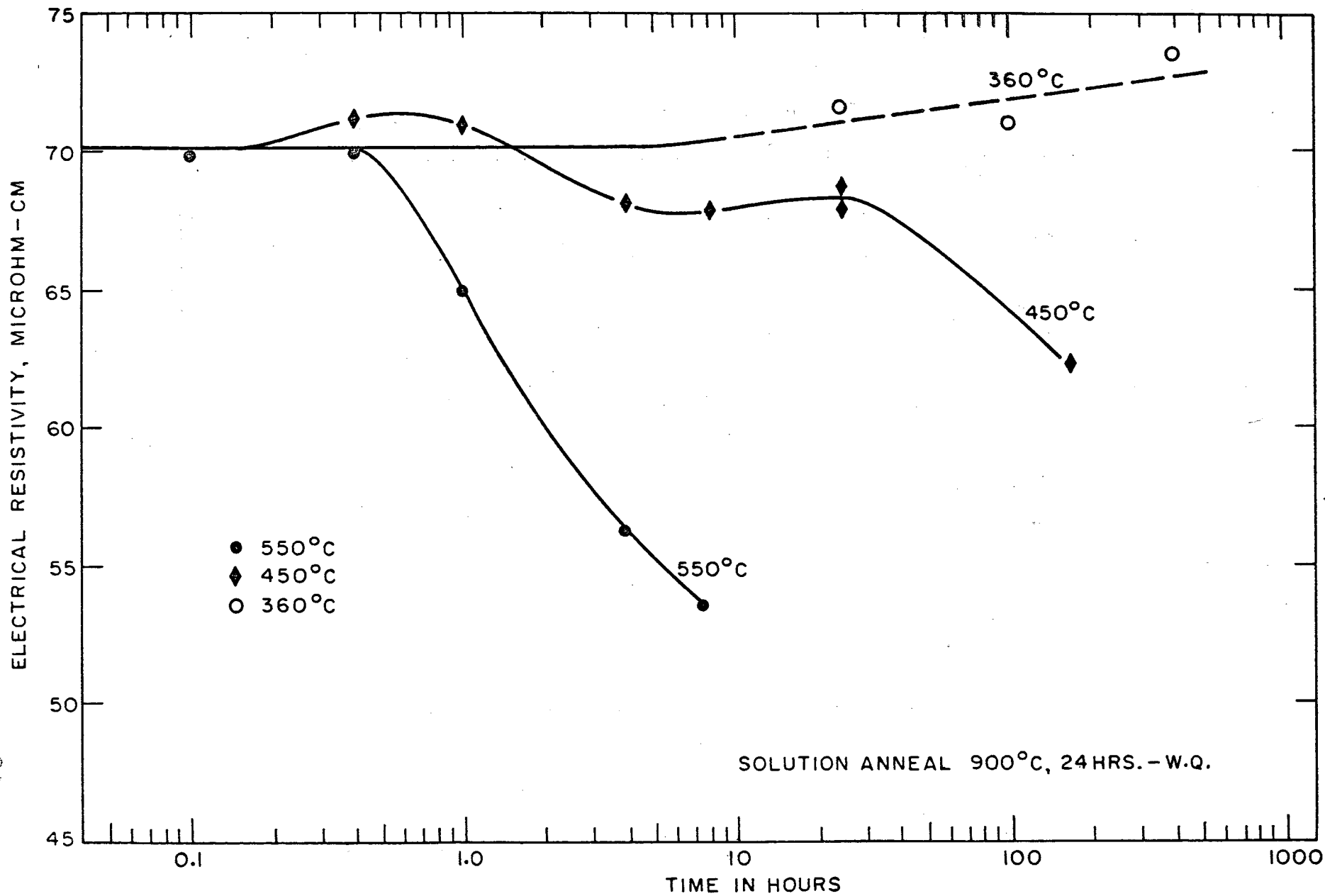ISOTHERMALLY ANNEALED U-8w/o Nb-0.98w/o V ALLOY

FIG. 98 - ROOM TEMPERATURE ELECTRICAL RESISTIVITY DATA FOR AN
ISOTHERMALLY ANNEALED U-8w/o Nb-2.02w/o V ALLOY
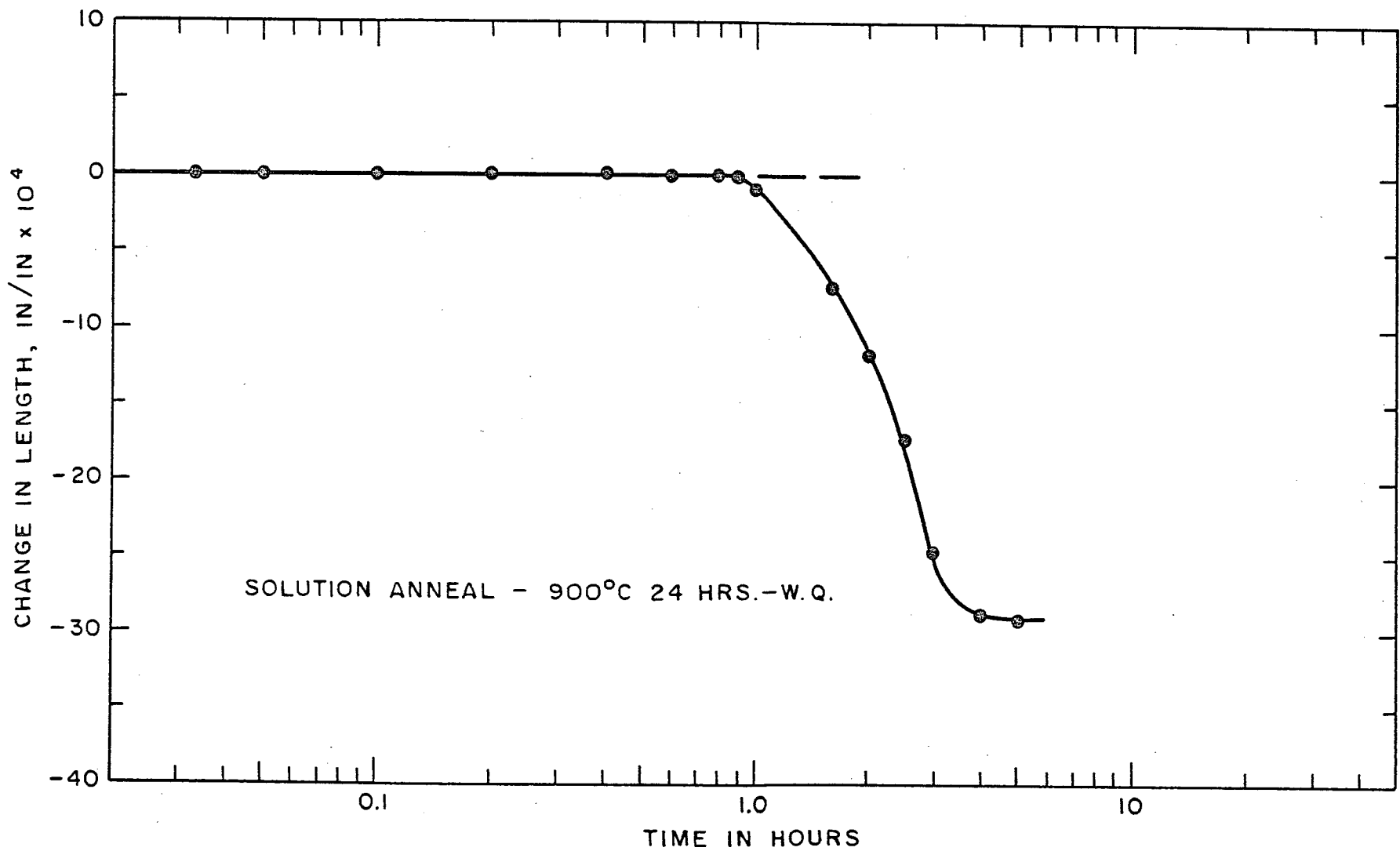
FIG. 99- DILATOMETRIC DATA FOR A U-8 $^W/o$ Nb-0.98 $^W/o$ V ALLOY
ISOTHERMALLY ANNEALED AT 550°C
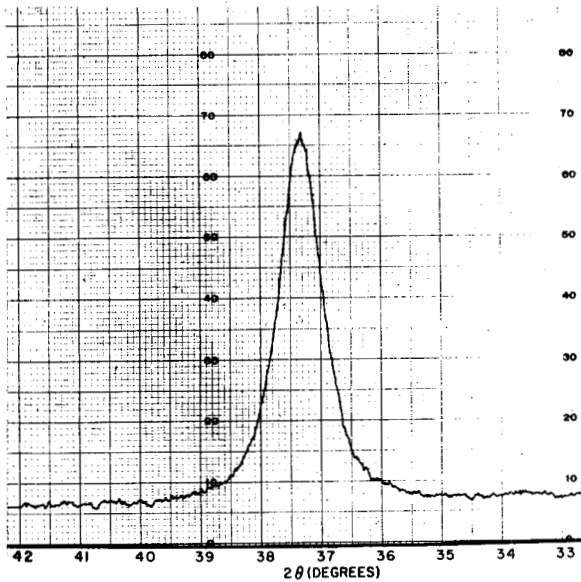
Fig. 100

X-ray diffractometer pattern.
Alloy: U-8w/o Nb-2.02w/o V.
Treatment: 900°C-WQ; 450°C-1 hr-
WQ. γ_1.
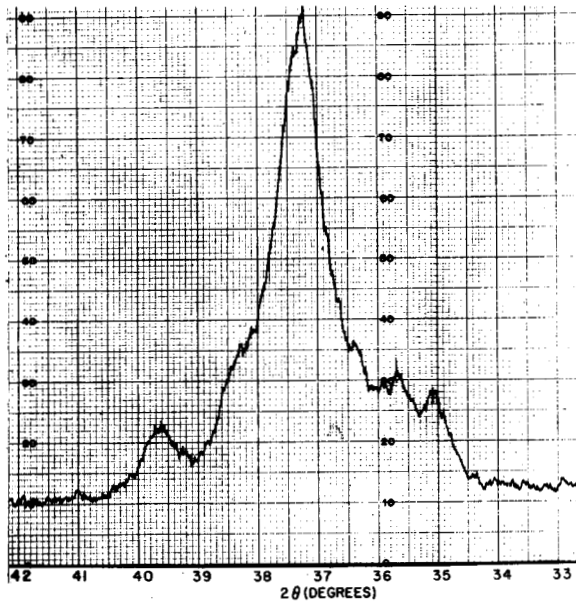
Fig. 101

X-ray diffractometer pattern.
Alloy: U-8w/o Nb-2.02w/o V.
Treatment: 900°C-WQ; 450°C-10 hrs
WQ. γ_1 is unchanged and α is
present. Incipient γ_2 peak in
vicinity of 38.2°.

Fig. 102

X-ray diffractometer pattern.
Alloy: U-8w/o Nb-2.02w/o V.
Treatment: 900°C-WQ; 450°C-100 hrs-
WQ. Location of γ_1 peak is un-
changed. Amount of α has increased
and γ_2 more predominant than in
Fig. 101.

255   130

- 124 -

10. Effects of Cold Work on Transformation

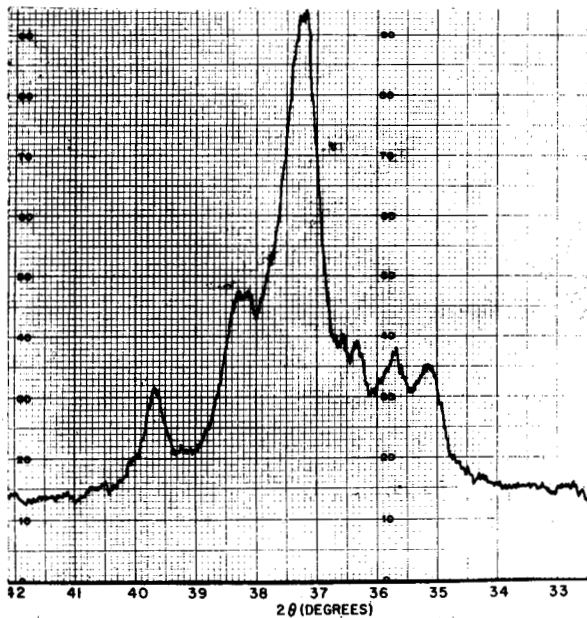The effects of two levels of reduction by cold rolling on the transformation kinetics of the U-7w/o Nb-2w/o Zr alloy were studied by metallographic examination and hardness tests. The ingot was first reduced about 60 per cent in area by hot rolling at 830°C. After a 900°C solution treatment and water quench, one portion of the slab was cold rolled to 17 per cent reduction of area and another section was rolled to 42 per cent RA. Samples from each of these worked bars were annealed for varying lengths of time at 450° and 360°C. In addition, a sample of the hot-worked material which had been solution-treated but not cold worked was annealed with the reduced specimens for purposes of comparison.

The results of Vickers (10 Kg) hardness tests on the samples are shown in Figures 103 and 104. Strain accelerated hardness changes in the metastable gamma structure. Both levels of cold working increased the hardness to about 260 VPN compared to 200 VPN for the solution-treated material. After 0.1 hour at 360°C (see Figure 103) the hardness of both cold-worked samples was over 100 VPN higher than the value for the material which had not been cold rolled. From 0.4 hour to 100 hours at 360°C, the hardness difference between worked and unworked samples remained fairly constant at about 50 VPN. In addition, hardness values for the two cold-worked materials were nearly the same at all annealing times.

Figure 104 shows the hardness curves at the 450°C annealing temperature. In 0.1 hour both cold-worked samples exhibited a substantial rise in hardness above the value for the solution-treated material. At 0.4 hour the difference was less marked, and in 1 hour the curves were separated only slightly. Further annealing resulted in a greater hardness increase in the

255 131

17 per cent RA samples than was noted for the 42 per cent RA material.

A comparison of hardness curves for this hot-worked ingot with previously reported results for the thermally homogenized U-7w/o Nb-2w/o Zr material shows very close agreement at both 450° and 360°C. Initial hardness increases occurred in approximately the same annealing time for both materials, and the hardness values were slightly lower for the hot-worked ingot. This material had a much finer grain size than was observed in the thermally homogenized alloy.

The microstructures of the cold-worked materials were considerably different from the structures observed in the sample which had been solution-treated. No decomposition was noted in the grain boundaries in any of the specimens annealed at 360°C. However, the cold-worked materials exhibited an appreciable amount of transformation as evidenced by banding within the grains. This product was more pronounced as the 450°C annealing temperature. Figure 105 is photomicrograph of the material which had been hot rolled, solution-treated at 900°C, and annealed for 24 hours at 450°C. A small amount of grain boundary transformation is present, and the matrix is lightly stained. Cold rolling the solution-treated material to 17 per cent RA, followed by 24 hours at 450°C, results in the microstructure illustrated in Figure 106. Oriented banding is present in many of the grains. With an increasing amount of cold work (42 per cent RA) followed by the same annealing treatment (24 hours at 450°C), more of the product is present, as shown in Figure 107. In many of the grains this material has a Widmanstätten structure. Microhardness tests reveal that the darker etching grains are somewhat softer than the lighter areas of the sample. The hardness curves (Figure 104) show that this material (42% RA) was softer than the material which had been cold worked to 17% RA. This effect was not noted at the 360°C annealing temperature.
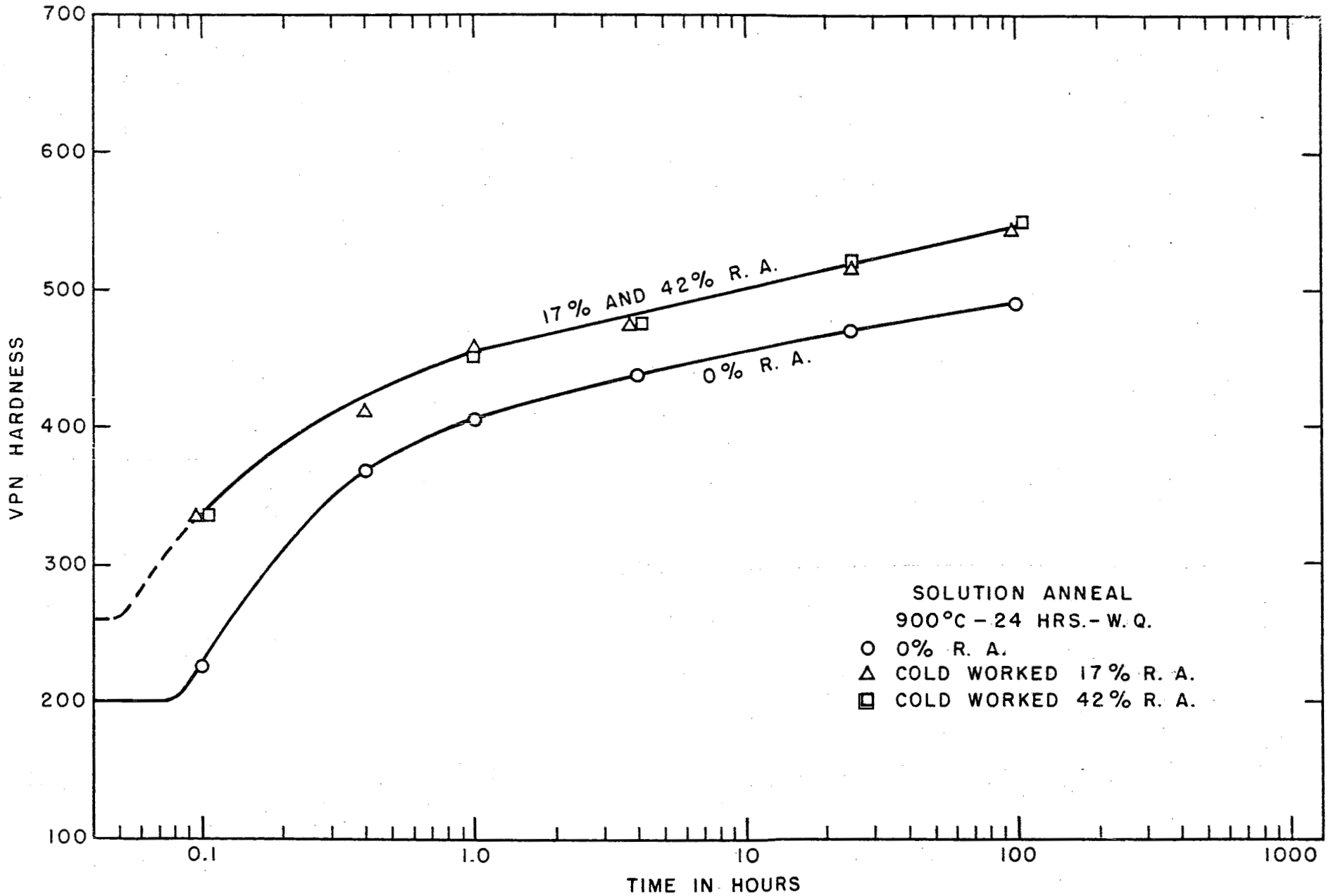
FIG. 103 - HARDNESS DATA FOR A U-7w/o Nb-2w/o Zr ALLOY ANNEALED AT 360°C.
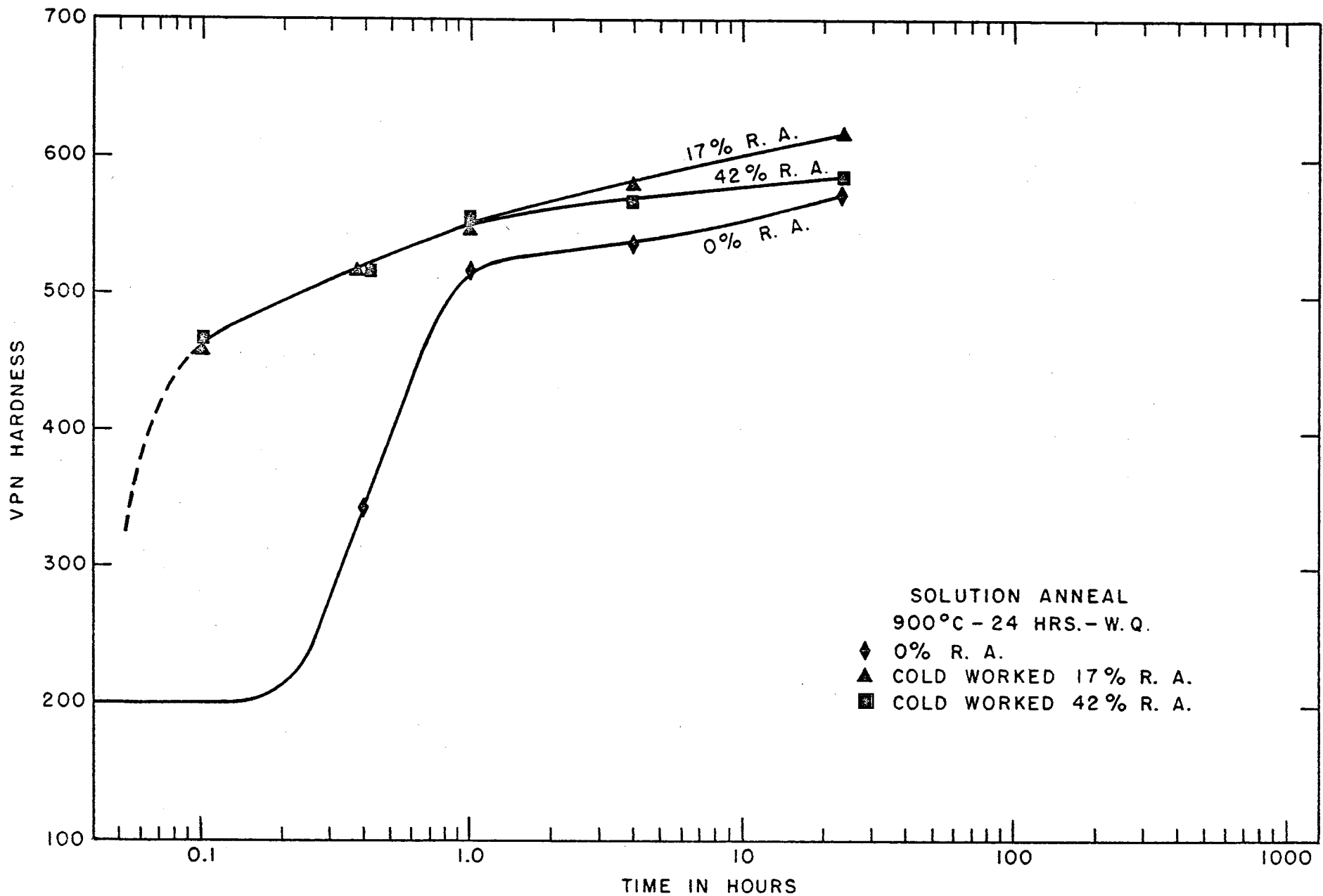
FIG. 104 - HARDNESS DATA FOR A U-7w/o Nb-2w/o Zr ALLOY ANNEALED AT 450°C
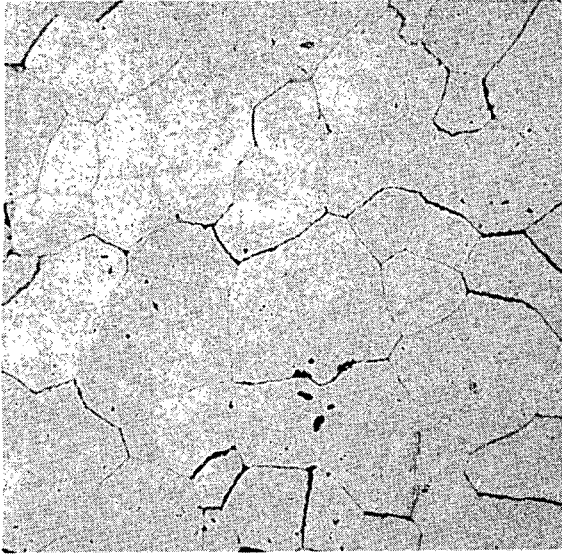
Neg. No. 14468   X 500

Fig. 105

Alloy: U-7w/o Nb-2w/o Zr.
Treatment: 900°C-WQ; 450°C-24 hrs-WQ.
Small amount of transformation in the
grain boundaries and within the grains,
indicated by staining.
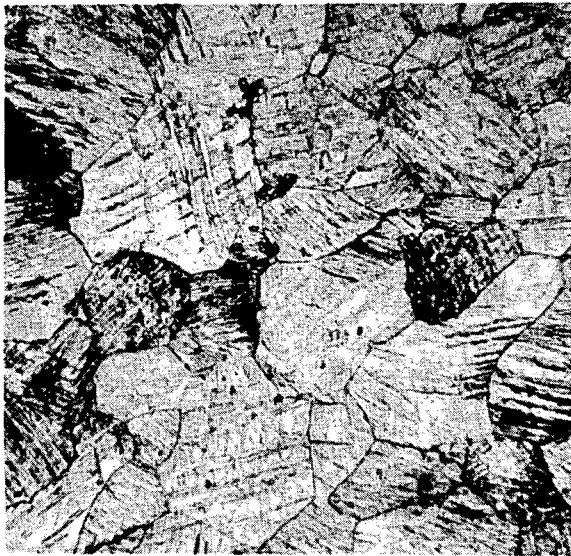
Neg. No. 14453   X 500

Fig. 106

Alloy: U-7w/o Nb-2w/o Zr.
Treatment: 900°C-WQ; cold worked-
17% RA; 450°C-24 hrs-WQ. Transformation
as a banded structure.

Neg. No. 14454   X 500

Fig. 107

Alloy: U-7w/o Nb-2w/o Zr.
Treatment: 900°C-WQ; cold worked-
42% RA; 450°C-24 hrs-WQ. Increased
amount of decomposition.

Etchant: Electrolytic - 8 parts orthophosphoric acid, 5 parts ethylene
          glycol, 5 parts ethyl alcohol.

255   135   - 129 -

11. Comparative Data

a, TTT Curves

The results of metallographic, hardness and resistometric studies of the alloys under investigation are summarized in the series of TTT diagrams, Figures 108 to 115. The curves are grouped according to alloy composition as outlined in the preceding sections. With the exception of zirconium, the ternary elements were added to a U-8w/o Nb base, and available data for this binary alloy are included to clearly show the effects of ternary additions to this base. Similarly, curves for the U-7w/o Nb alloy are presented with curves for the U-7w/o Nb-(1,2)w/o Zr materials. TTT diagrams for materials containing nickel and ruthenium are combined, as only one alloy was studied for each.

These curves readily demonstrate the merits of the various elements on stabilizing the gamma phase. Niobium, zirconium, chromium, ruthenium and vanadium were found to retard transformation, whereas titanium, silicon and nickel increased the initiation of transformation.

Observation of TTT diagrams for each composition shows that metallographic, hardness and resistometric results were in agreement concerning the relative stabilizing ability of the various alloy additions. However, the annealing times required to produce initial changes varied with the method of investigation used. This effect is illustrated in Figure 116 for the U-8w/o Nb-0.12w/o Cr alloy, where curves for the three methods are presented. At 600° and 550°C, initiation of grain boundary transformation and an increase in hardness are in fair agreement, and an initial decrease in resistivity occurred in a slightly shorter annealing time at 550°C. The results at 450°C show that hardness and resistivity changes are in approximate agreement, while a considerably longer annealing time was required to initiate transformation

at the grain boundaries. At this temperature the fine decomposition product

was noted in the microstructures at annealing times more closely corresponding

to changes in other properties. Because of the structural evidence of this

product, the times required for its initiation are difficult to determine

accurately. Close correlation was generally observed between this mode of

transformation and resistivity findings at 450°C. The three curves in

Figure 116 are more widely separated at 360°C. A pre-precipitation hardness

increase occurred in about 0.4 hour, whereas grain boundary transformation

was not detected until 1000 hours. The microstructure of a sample annealed

for 1 hour at 360°C exhibited the oriented pattern which in most materials

is associated with hardening at this temperature. A decrease in resistivity

required a somewhat longer annealing time.It has been shown previously that

at 450°C and 360°C, changes in other properties including density occur long

before transformation is observed at the grain boundaries. These results

have been confirmed by X-ray diffraction studies which indicate that the fine

decomposition product associated with other property changes is a precipitate

of the alpha phase.

Although initiation of grain boundary decomposition does not

necessarily denote initial transformation, this property affords one method

of comparing the relative stability of alloys under investigation. Some

precipitation also occurs around impurity particles; the effects of small

amounts of impurities on decomposition of the gamma phase are considered

negligible. TTT diagrams based on metallographically observed grain boundary

transformation in a number of compositions are shown in Figure 117.

Decomposition was most rapid at all annealing temperatures in the U-8w/o Nb-

0.68w/o Si alloy, followed by U-8w/o Nb-1.94w/o Ti, indicating that silicon

and titanium accelerate transformation of the gamma phase. The most stable were the U-15w/o Nb, U-12.5w/o Nb and U-10w/o Nb-0.78w/o Cr materials. Additions of zirconium to a U-7w/o Nb base resulted in increased stability.

A similar series of TTT diagrams based on initial hardness changes in thirteen compositions is illustrated in Figure 118. These curves also demonstrate the stability of the U-15w/o Nb and U-12.5w/o Nb alloys, and the rapid transformation in the materials containing silicon and titanium. Of the U-8w/o base ternary alloys, the most stable were those containing vanadium, ruthenium and chromium in the order listed. The addition of 0.14w/o nickel to this base resulted in more rapid hardness increases. The curve for the U-7w/o Nb-2w/o Zr alloys shows good stability at 600° and 550°C, whereas more rapid hardness changes were noted at the lower temperatures, especially 450°C. This behavior was not observed in other compositions.

The relative stability as determined by initial changes in electrical resistivity is shown in Figure 119. Resistivity measurements probably afford the best single method of determining initiation of transformation. As observed in the two preceding sets of TTT diagrams, the U-15w/o Nb and U-12.5w/o Nb materials required the longest annealing times to initiate transformation. The U-8w/o Nb-0.98w/o V and U-10w/o Nb-0.13w/o Cr alloys also exhibited relatively good stability. Considerably shorter annealing intervals produced changes in resistivity in other compositions illustrated in Figure 119. Materials containing additions of silicon and nickel to a U-8w/o Nb base were the most rapid to transform, and somewhat increased stability was shown by alloys containing ruthenium and chromium. A curve

for the U-8w/o Nb-1.94w/o Ti composition has not been shown in the figure
as the rapid transformation in this material was accompanied by an increase
rather than a decrease in resistivity.

b.   Hardness Results

The hardness values of some U-Nb and U-Nb-X alloys, as solution-
treated and quenched from 900°C, are presented in Figure 120. These results
are expressed as atomic per cent additions to a U-8w/o Nb base in order to
show the relative effect of the ternary additions on hardness. The effects
of increasing amounts of niobium are also illustrated and Figure 120 shows
that this element, and also vanadium, produced extremely rapid increases in
hardness when added to the U-8w/o Nb base. It has been observed that these
two elements are the most effective in stabilizing the gamma phase among the
materials under investigation. Additions of chromium, titanium and silicon
cause a more gradual rise in hardness.

The hardness values previously reported for the alloys under
investigation were obtained with a diamond pyramid indenter using a 10 Kg
load. In partially transformed samples, these indentions were too large to
permit determination of the hardness of areas of retained gamma. A series of
microhardness readings, using a 200-gram load, was taken on samples of
several compositions which had been partially transformed at 550°C. The
results presented in Table II completely corroborate the findings based on
other techniques.

TABLE II

MICROHARDNESS DATA

Material (w/o)	Heat Treatment	Grain Boundary Transformation (%)	Location of Hardness Test	VPN (200 g)
U-7 Nb-2 Zr	Solution treated	0	γ	218
	550°C-0.4 hr	5	γ	224
	550°C-1 hr	20	γ	234
U-8 Nb-0.90 Ti	Solution treated	0	γ	280
	550°C-0.4 hr	10	γ	308
	550°C-1 hr	80	γ	342
			Grain boundary area	473
U-8 Nb-1.94 Ti	Solution treated	0	γ	313
	550°C-1 hr	10	Fine product in matrix	575
			Grain boundary area	570
	550°C-4 hrs	20	Fine product in matrix	603
			Grain boundary area	580
	550°C-10 hrs	45	Fine product in matrix	620
			Grain boundary area	534
U-8 Nb-0.98 V	Solution treated	0	γ	321
	550°C-1 hr	15	γ	320
U-8 Nb-2.02 V	Solution treated	0	γ	326
	550°C-1 hr	30	γ	329
			Grain boundary area	494

For the U-Nb-Zr material the areas of gamma showed a rise in hardness as the amount of transformation at the grain boundaries increased. X-ray diffraction analysis of this composition showed that as alpha is precipitated, the gamma phase is enriched in niobium with the resultant shift of the peak for gamma to higher 2θ values. The higher niobium content of the matrix would account for the increased hardness of these untransformed areas.

Microhardness examination of the U-8w/o Nb-0.90w/o Ti alloy also revealed that the hardness of the matrix increased with additional precipitation in the grain boundaries. X-ray diffraction studies of this material show that after 1 hour at 550°C the gamma peak had shifted to a higher 2θ value, and that a considerable amount of alpha was present.

A different behavior was noted in the U-8w/o Nb-1.94w/o Ti composition. Metallographic samples of this material showed both the fine product in the matrix and decomposition at the grain boundaries after relatively short annealing times at 550°C. Growth of the grain boundary transformation was very slow; after 10 hours at 550°C this product covered only about 45 per cent of the sample and was lighter etching than the matrix. Table II shows that after 1 hour both the matrix and the grain boundary areas were approximately the same hardness. Subsequent annealing resulted in a considerably higher hardness in the matrix than was found in the grain boundary transformation. From the X-ray diffraction studies of this material, alpha was present after 1 hour at 550°C and in 4 hours both alpha and γ_2 were noted

255 141

Project No. B 095
                                        Summary Report

in the spectrometer traces. The lower hardness of this lighter etching grain boundary transformation product may result from the agglomeration of increasing amounts of γ_2 in these areas.

Examination of the alloys containing vanadium revealed no significant increase in hardness of the gamma matrix as increasing amounts of grain boundary transformation product are formed. X-ray diffraction studies of these materials indicate that both alpha and γ_2 are precipitated simultaneously from the metastable gamma phase. The peak for γ_1, as transformation proceeds, remains at approximately the same 2θ value as that for the solution-treated sample, indicating that the matrix was not becoming richer in niobium content. The microhardness of these retained gamma areas verifies the X-ray diffraction findings.

c.   Electrical Resistivity Results

The effects of some of the ternary additions to the U-8w/o Nb base on electrical resistivity are illustrated in Figure 121. As expected, the resistivity values of solution-treated materials are increased by all of the alloying elements except silicon. Although not shown in Figure 121 increasing amounts of zirconium and niobium also result in higher resistivity values. The decrease in electrical resistivity resulting from silicon additions appears to be due to the depletion of niobium from the matrix in the formation of the intermediate phase.

d. X-Ray Results

Examination of diffractometer traces taken from samples annealed
for increasing times at various temperatures indicates that the decomposition
of the metastable gamma phase occurred in several different ways. Results of
these investigations were discussed under the preceding alloy sections. The
modes of decomposition may be classified according to two general types. In
one type, as the alpha phase is precipitated the gamma matrix is enriched in
niobium, resulting in a continuous shifting of the peak for gamma to higher
2θ values (lower a_0). The phases present at equilibrium are alpha and the
niobium-rich γ_2. All compositions except those containing titanium and
vanadium exhibited this method of transformation. Some variations in this
mechanism have been noted in several alloys. At lower temperatures($450°C$ and
below) the initial gamma peak becomes broadend and poorly defined and the
spectrometer trace exhibits rises in the vicinity of the three alpha peaks
having lower 2θ values than γ_1. This pattern is believed to represent an
intermediate transition structure or the incipient precipitation of alpha.
As annealing continues, the four alpha peaks become more clearly defined, and
the peak for gamma shifts to higher angles. Another variation of this mecha-
nism of decomposition occurs at $550°C$ and above, as described under the section
on U-Nb-Zr alloys. In this case the gamma peak weakens in intensity and be-
comes broad during intermediate stages of precipitation. Some alloys may
evidence both variations at different temperatures.

The second general type of decomposition was found in materials
containing titanium and vanadium. As transformation proceeded, both alpha
and γ_2 were co-precipitated from the metastable γ_1 phase. In the case of the
U-Nb-V alloys, both phases were precipitated simultaneously, whereas alpha
appeared to be the first to precipitate in the materials containing titanium.

ARMOUR RESEARCH FOUNDATION OF ILLINOIS INSTITUTE OF TECHNOLOGY

Table III presents the phases found at various annealing temperatures by X-ray diffraction examination. The notation γ_2 refers to the gamma phase having an α_0 value which is approximately that for equilibrium. The metastable phase retained on water-quenching from 900°C is γ_1. If values of the lattice spacing for gamma have not reached the minimum value for the alloy, the notation γ is used. The structure denoted by α' is characterized in spectrometer traces by the indistinct broadening of the gamma peak over the range of 2θ values for most of the alpha peaks and probably is characteristic of an intermediate transition structure. When only very small traces of a phase were detected, the phase designation is placed in brackets.

The results shown in Table III offer some means of comparing relative stability of the gamma phase in the various alloys, although it must be realized that the X-ray diffraction technique is relatively insensitive to incipient transformation. After 1000 hours at 360°C, no alpha was detected in five compositions: U-15w/o Nb, U-12.5w/o Nb, U-10w/o Nb - (0.13, 0.78)w/o Cr and U-8w/o Nb-1.94w/o Ti. The least stable materials were those containing silicon, as considerable amounts of alpha were noted in the diffraction patterns. Figures 122 to 125 illustrate spectrometer traces of four materials with varying degrees of transformation after this thermal treatment. Only the peak for gamma was found for the U-15w/o Nb material (Figure 122). A well-defined gamma peak and also very small rises in the vicinity of the alpha peaks are noted in Figure 123 for the U-8w/o Nb-0.49w/o Ru alloy. Annealing at 360°C for 1000 hours produced the pattern for α' in the U-8w/o Nb-0.14w/o Ni composition (Figure 124), indicating further decomposition than in the previous sample. Figure 125 shows the spectrometer trace for the U-8w/o Nb-0.14w/o Si. The strength of the pattern for alpha demonstrates that this heat treatment

TABLE III

X-RAY DIFFRACTOMETER ANALYSIS-PHASES OBSERVED

Composition (w/o)	Annealing Treatment						
	360°C 1000 hrs	450°C 1000 hrs	550°C 100 hrs	600°C 100 hrs	620°C 100 hrs	625°C 50 hrs	660°C 100 hrs
U-7 Nb	α'	$\alpha + \gamma_2$	$\alpha + \gamma_2$				
U-12.5 Nb	γ	$\alpha + \gamma$	$\alpha + \gamma_2$				
U-15 Nb	γ	$\alpha + \gamma$	$\alpha + \gamma_2$				
U-7 Nb-1 Zr	α'	$\alpha + \gamma$	$\alpha + \gamma_2$	$\alpha + \gamma$			
U-7 Nb-2 Zr	α'	$\alpha + \gamma$	$\alpha + \gamma_2$	$\alpha + \gamma$			
U-8 Nb-0.12 Cr	α'	$\alpha + \gamma$	$\alpha + \gamma_2$	$\alpha + \gamma_2$			
U-8 Nb-0.74 Cr	α'	$\alpha + \gamma$	$\alpha + \gamma_2$	$\alpha + \gamma_2$	$\alpha + \gamma_2$		
U-10 Nb-0.13 Cr	γ	$\alpha + \gamma$	$\alpha + \gamma$	$\alpha + \gamma_2$			
U-10 Nb-0.78 Cr	γ	$\alpha + \gamma$	$\alpha + \gamma$	$\alpha + \gamma_2$	$\alpha + \gamma_2$		
U-8 Nb-0.90 Ti	γ (+ α)	$\alpha + \gamma_1 + \gamma_2$	$\alpha + \gamma_1 + \gamma_2$	$\alpha + \gamma_1 + \gamma_2$			
U-8 Nb-1.94 Ti	γ	$\alpha + \gamma_1 + \gamma_2$	$\alpha + \gamma_1 + \gamma_2$	$\alpha + \gamma_1 + \gamma_2$			
U-8 Nb-0.14 Si	$\alpha + \gamma$	$\alpha + \gamma_2$	$\alpha + \gamma_2$	$\alpha + \gamma_2$			
U-8 Nb-0.68 Si	$\alpha + \gamma$	$\alpha + \gamma_2$	$\alpha + \gamma_2$	$\alpha + \gamma_2$			
U-8 Nb-0.14 Ni	α'	$\alpha + \gamma$					
U-8 Nb-0.49 Ru	γ (+ α)	$\alpha + \gamma$	$\alpha + \gamma_2$				
U-8 Nb-0.98 V	α'	$\alpha + \gamma_1 + \gamma_2$	$\alpha + \gamma_1 + \gamma_2$	$\alpha + \gamma_1 + \gamma_2$ (50 hrs)		$\alpha+\gamma_1+\gamma_2$	γ
U-8 Nb-2.02 V	γ (+ α)	$\alpha + \gamma_1 + \gamma_2$	$\alpha + \gamma_1 + \gamma_2$	$\alpha + \gamma_1 + \gamma_2$ (50 hrs)		$\alpha+\gamma_1+\gamma_2$	$\gamma_1+\gamma_2$

Note: Refer to text page 136 for description of phases.

produced a large amount of transformation. Only the U-7w/o Nb and the

U-8w/o Nb-(0.14, 0.68)w/o Si alloys were completely transformed after 1000

hours at 450°C. Annealing for 100 hours at 600° and 550°C resulted in com-

plete transformation in most of the compositions; 2θ values for a few materials

were slightly below maximum equilibrium values and were not considered com-

pletely transformed.

The atomic radii for the elements included in these studies are

tabulated according to decreasing size in Table IV. The only element having

a larger radius than gamma uranium is zirconium. Titanium and niobium have

slightly smaller radii, while the remainder have considerably smaller radii

than uranium.

The effects of various additions to uranium on a_o values for the

solution-treated materials are shown in Table V. The addition of zirconium,

having a larger atomic radius, to the U-Nb base produces an increase of the

interatomic spacing. Increasing additions of niobium, chromium, titanium and

vanadium result in lower a_o values. These elements have smaller atomic radii

than gamma uranium. Very slight changes are noted for additions of nickel and

ruthenium. However, these elements were present in amounts of only 0.5 and

1 atomic per cent respectively. The addition of 0.68w/o Si to the U-8w/o Nb

base resulted in a substantial increase in the interatomic spacing of the

solution-treated material. The atomic radius of silicon is relatively small

and falls well outside of the range favorable for solid solubility in gamma

uranium. Previous work has shown that this element combines with niobium to

form an intermediate phase, thereby lowering the niobium content of the matrix.

This would result in some increase of the interatomic spacing of the matrix

material. However, the value reported in Table V is higher than that which

TABLE IV

ATOMIC RADII OF ELEMENTS

Element	Atomic Radius (Å)*
Zr	1.58
Gamma U	1.50
Ti	1.44
Nb	1.43
Ru	1.32
V	1.31
Cr	1.25
Ni	1.24
Si	1.17

*"Theory of Alloy Phases", ASM, 1956, by F. Laves.

TABLE V

LATTICE PARAMETERS OF γ_1 FOR URANIUM-BASE ALLOYS

Alloy Additions		
(w/o)	(a/o)	a_o (Å)
7 Nb	16.2 Nb	3.460
7 Nb-1 Zr	16.0 Nb-2.32 Zr	3.465
7 Nb-2 Zr	15.7 Nb-4.57 Zr	3.475
8 Nb	18.2 Nb	3.450
8 Nb-0.12 Cr	18.2 Nb-0.5 Cr	3.450
8 Nb-0.74 Cr	17.8 Nb-3.0 Cr	3.435
8 Nb-0.90 Ti	17.7 Nb-4.0 Ti	3.445
8 Nb-1.94 Ti	17.1 Nb-8.0 Ti	3.440
8 Nb-0.14 Si	18.1 Nb-1.0 Si	3.450
8 Nb-0.68 Si	17.4 Nb-5.0 Si	3.505
8 Nb-0.14 Ni	18.2 Nb-0.5 Ni	3.460
8 Nb-0.49 Ru	18.1 Nb-1.0 Ru	3.450
8 Nb-0.98 V	17.7 Nb-4.0 V	3.435
8 Nb-2.02 V	17.1 Nb-8.0 V	3.420
10 Nb-0.13 Cr	22.1 Nb-0.5 Cr	3.435
10 Nb-0.78 Cr	21.7 Nb-3.0 Cr	3.420
12.5 Nb	26.8 Nb	3.435
15 Nb	31.2 Nb	3.420

would be expected from a depletion of niobium from the matrix. No definite correlation was observed between the atomic radii of the elements and their relative effect upon stabilizing the gamma phase.

e.   Conclusions

The relative stability of the various alloys has been discussed in the previous sections. Results of the several methods of transformation study are in good agreement concerning the effects of the alloying elements as gamma-phase stabilizers. Silicon, titanium and nickel additions to a U-Nb base were found to accelerate decomposition upon isothermal annealing. For most annealing treatments, the elements zirconium, chromium and ruthenium increased the stability of the gamma phase. Additions of 12.5 and 15w/o niobium to uranium, and additions of vanadium to a U-8w/o Nb base produced the greatest stabilizing effects.

Upon annealing at 600° and 550°C transformation of the gamma phase in most compositions originated at the grain boundaries, and continued annealing resulted in a niobium enrichment of the gamma matrix as more alpha was precipitated. Data from metallographic, hardness, resistometric and dilatometric studies were generally in good agreement for showing initiation of transformation at these higher annealing temperatures. X-ray diffraction results showed that additional decomposition occurred after no significant property changes were noted using other methods. Metallography indicates that the precipitation of alpha covers all of the structure at an early stage even though considerable amounts of gamma may remain in the structure. For this reason, the apparent completion of transformation may vary to some extent depending upon the technique.

Annealing times required to initiate transformation at 450° and 360°C varied according to the method used. Annealing at 450°C produced a fine precipitate of alpha throughout the gamma grains in addition to the decomposition at the grain boundaries. The highest hardness values were usually found at this temperature, and changes in other properties were closely associated with the appearance of the fine decomposition product in the microstructures. Annealing at 360°C resulted in rapid hardness increases which are beleived to be pre-precipitation hardening effects. Microstructures of samples annealed at this temperature often exhibited an oriented structure within the grains, although most compositions showed only small amounts of transformation at the grain boundaries after 1000 hours. Electrical resistivity measurements at 360°C placed initiation of transformation at annealing intervals between those for the initial hardness rise and the appearance of grain boundary decomposition.
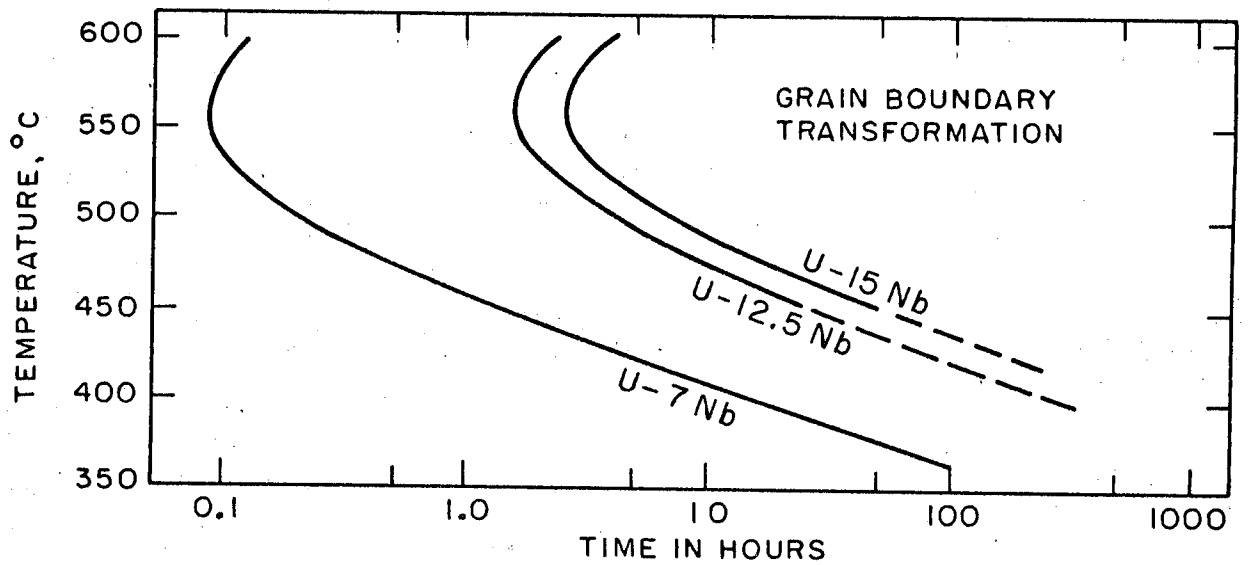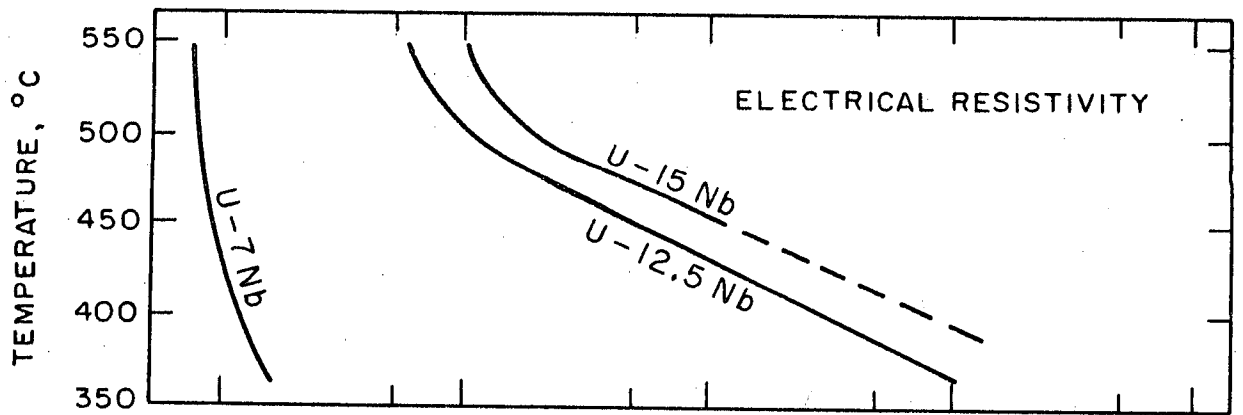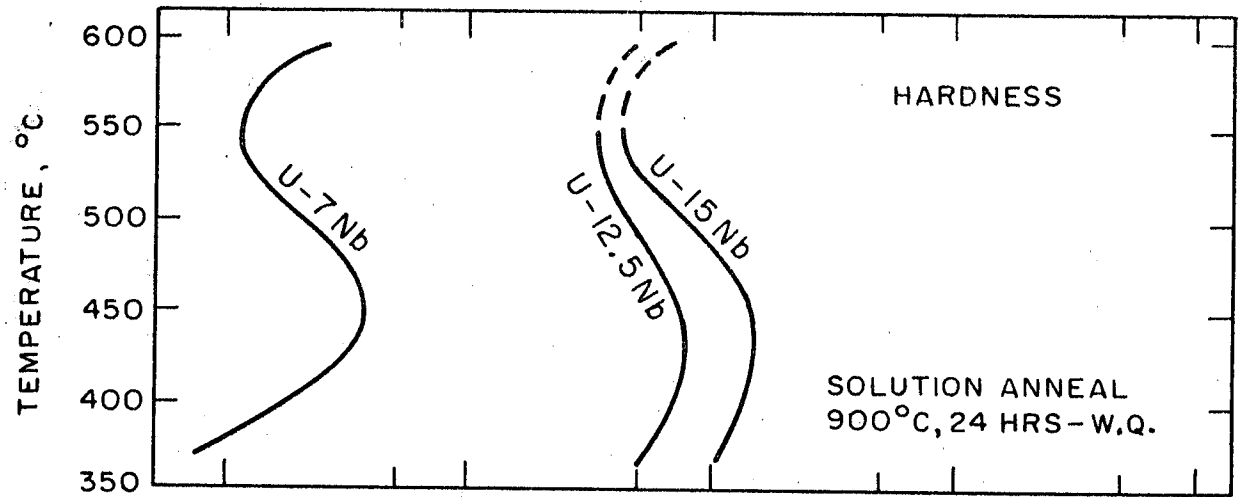
FIG. 108 – TTT DIAGRAMS ILLUSTRATING INITIAL PROPERTY CHANGES FOR U-Nb ALLOYS
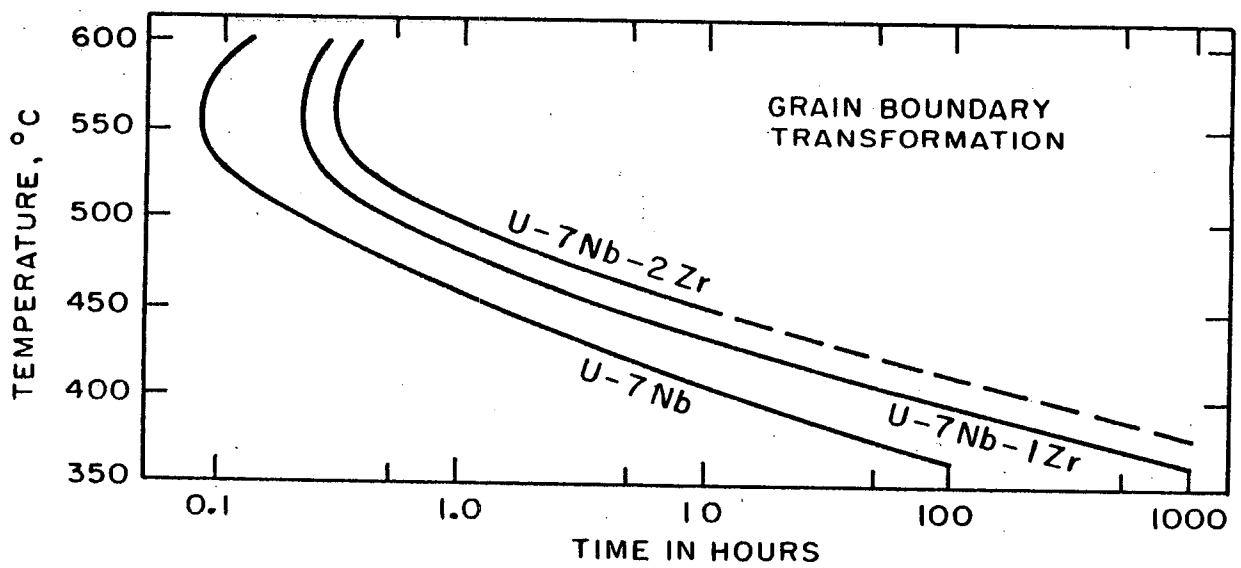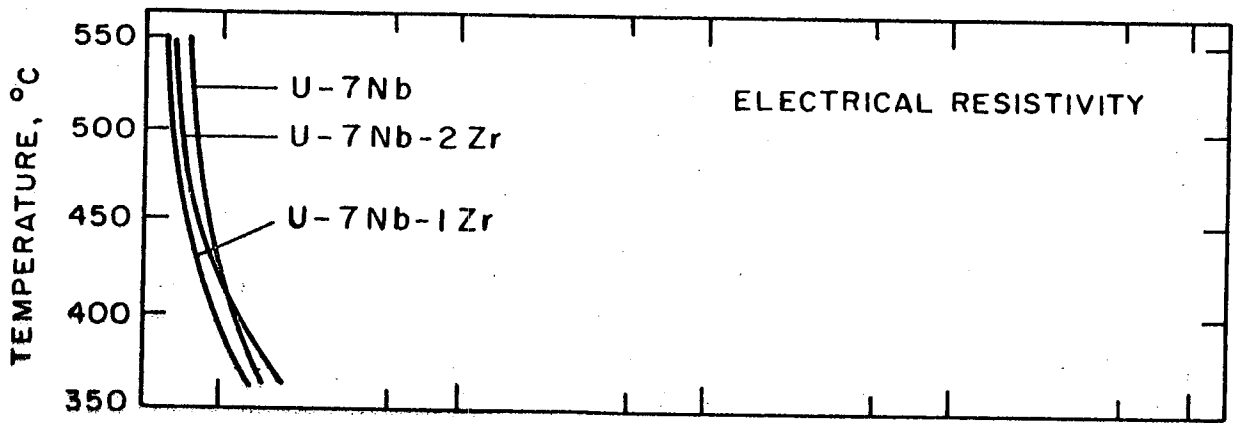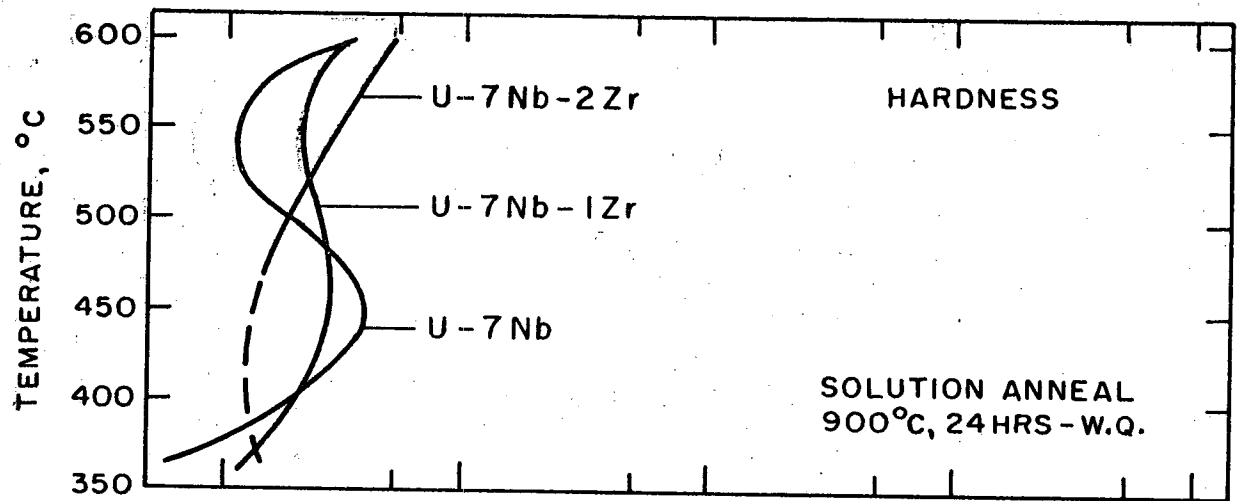
FIG. 109 - TTT DIAGRAMS ILLUSTRATING INITIAL PROPERTY
CHANGES FOR U-7w/o Nb-Zr ALLOYS
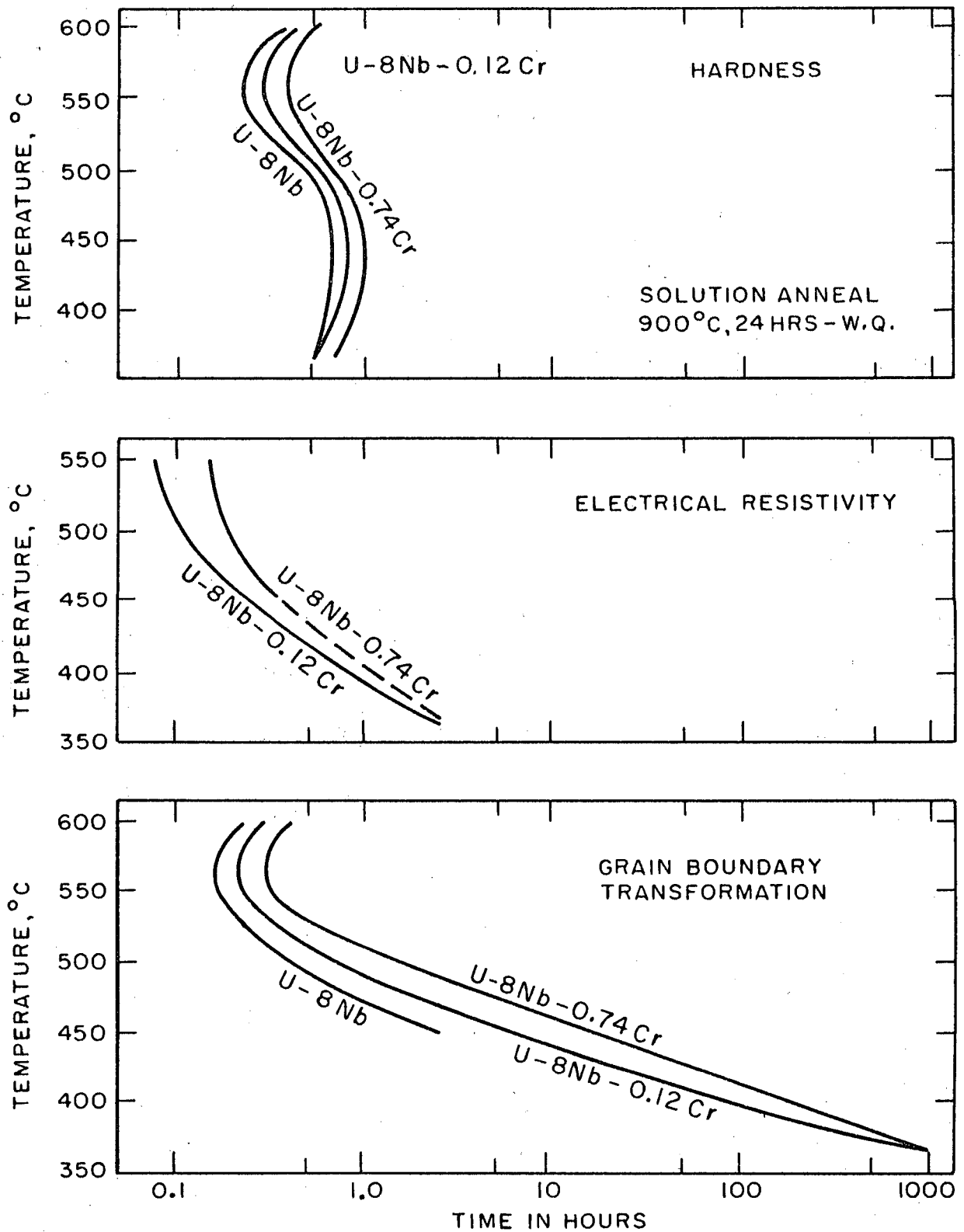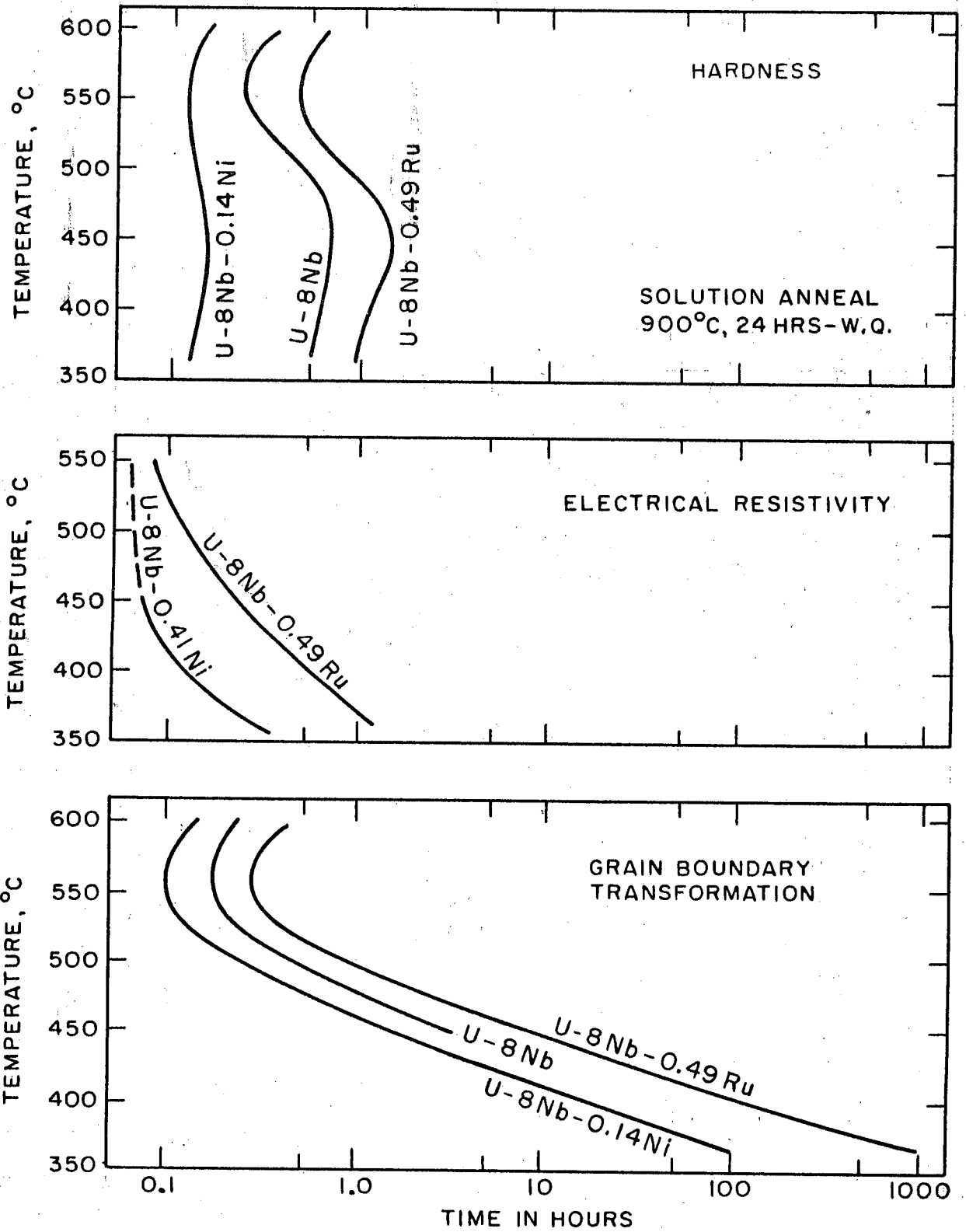
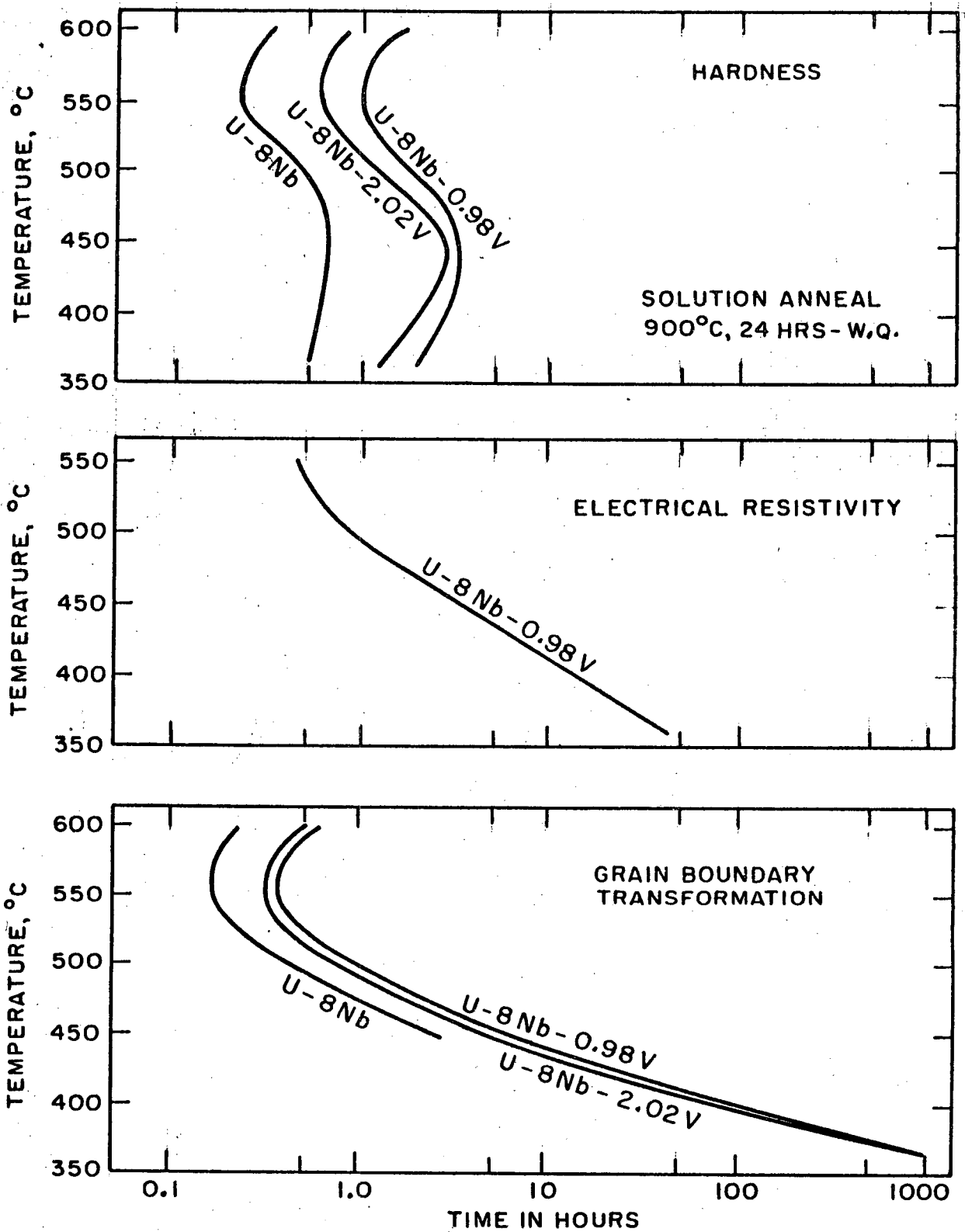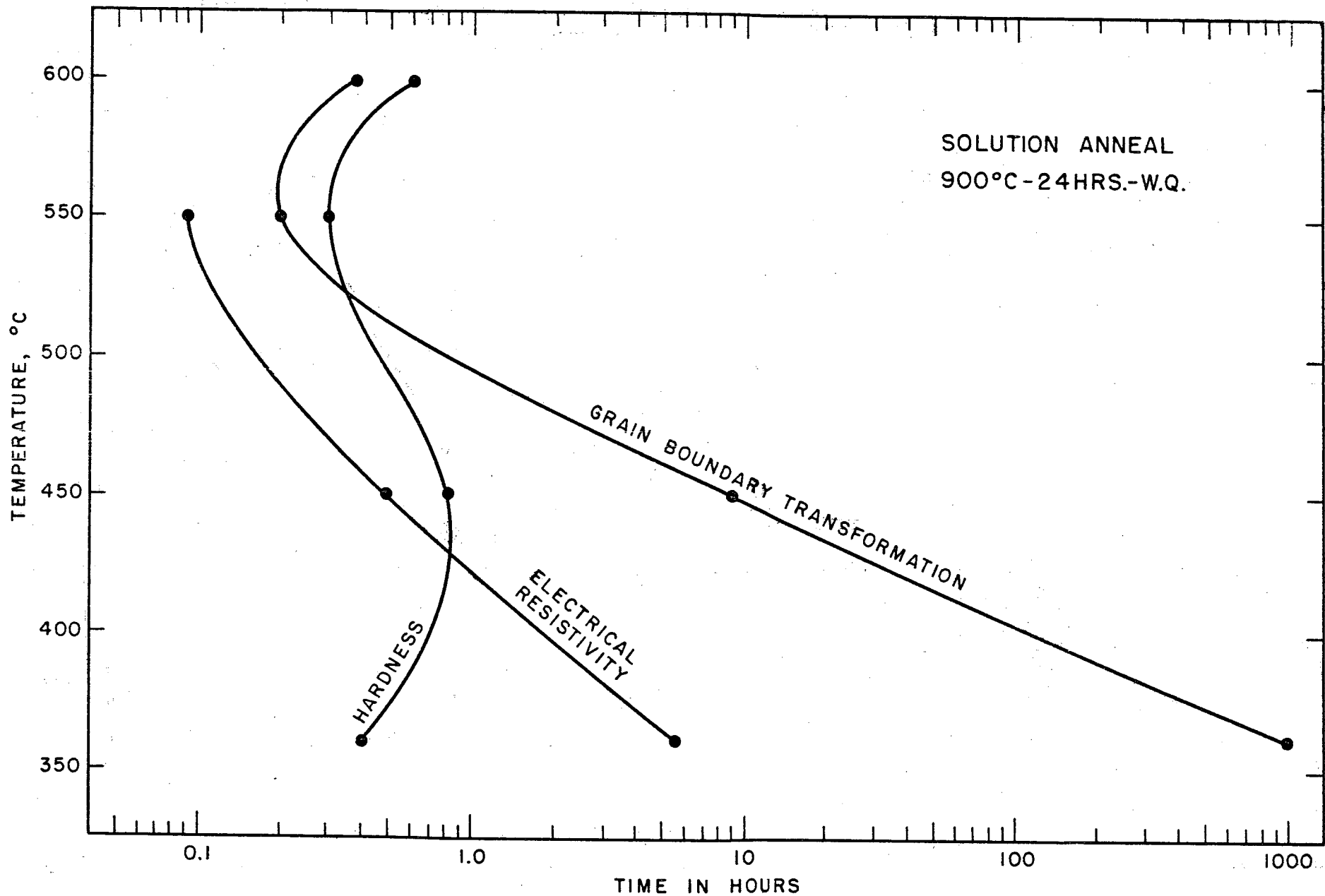FIG. 110 - TTT DIAGRAMS ILLUSTRATING INITIAL PROPERTY
CHANGES FOR U-8w/o Nb-Cr ALLOYS
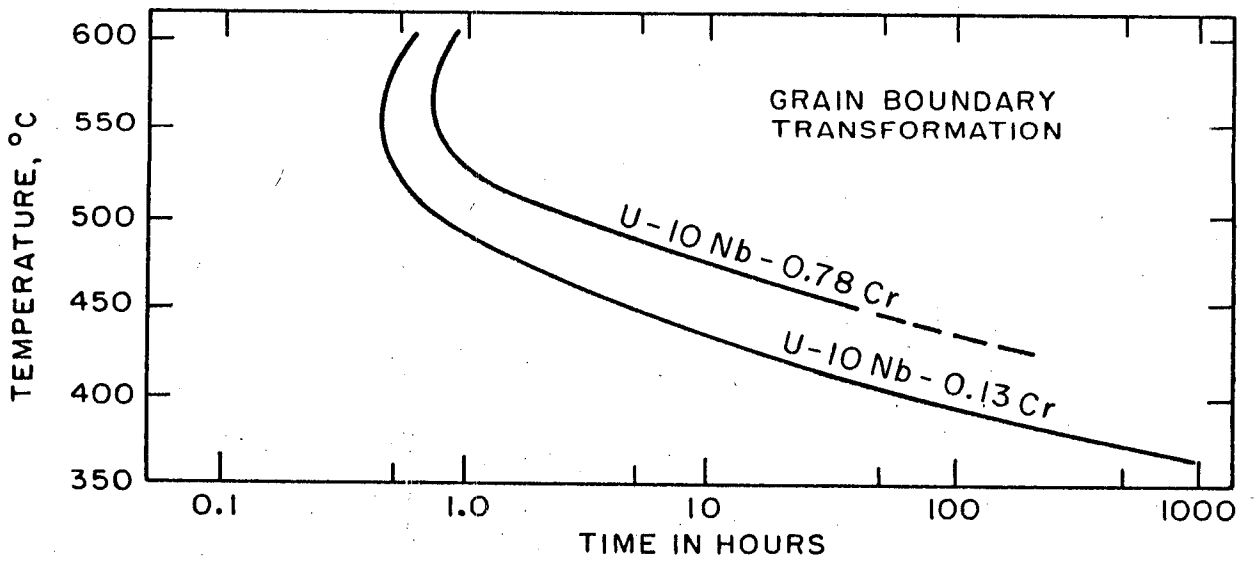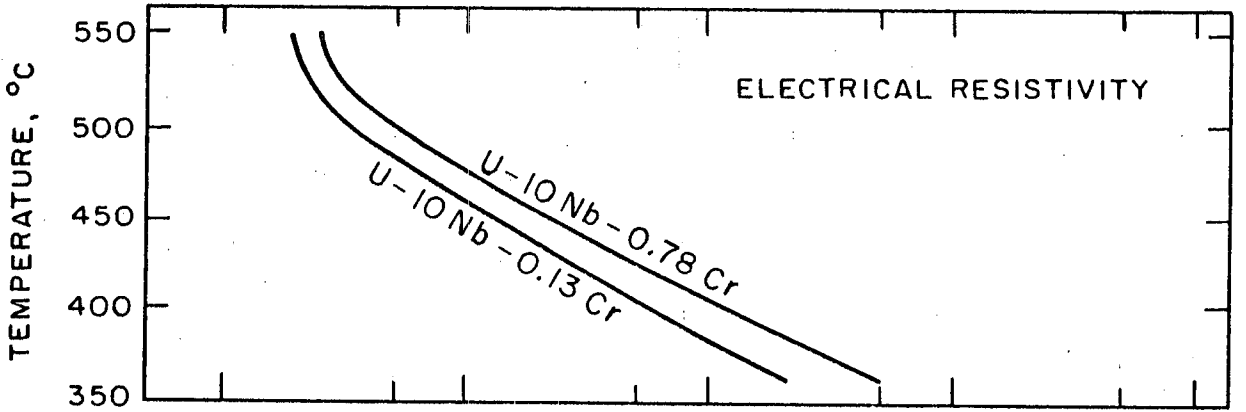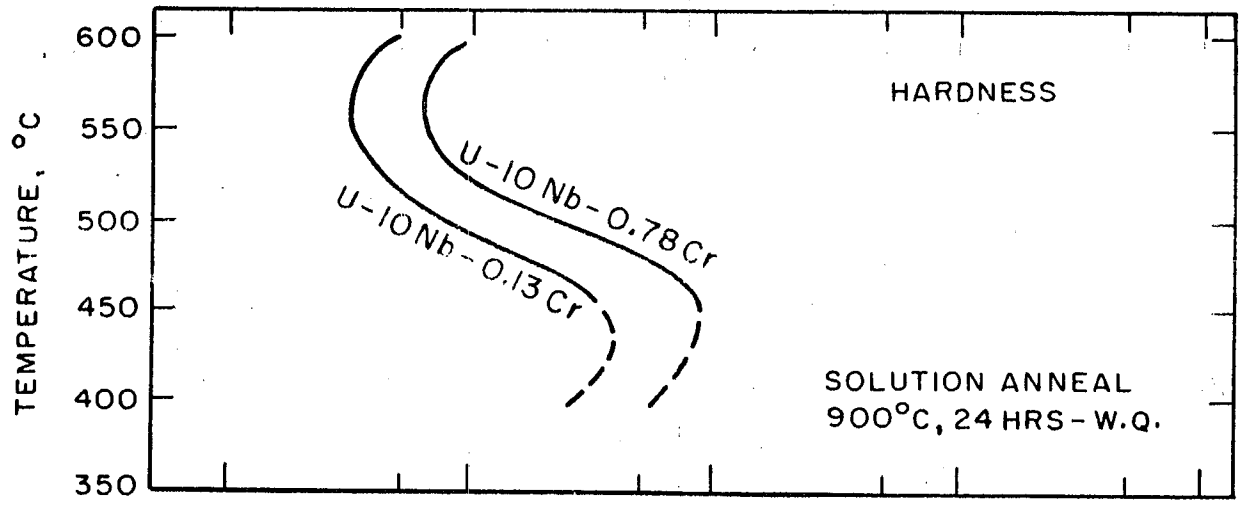
FIG. 111 - TTT DIAGRAMS ILLUSTRATING INITIAL PROPERTY
CHANGES FOR U-10w/o Nb-Cr ALLOYS

148 -
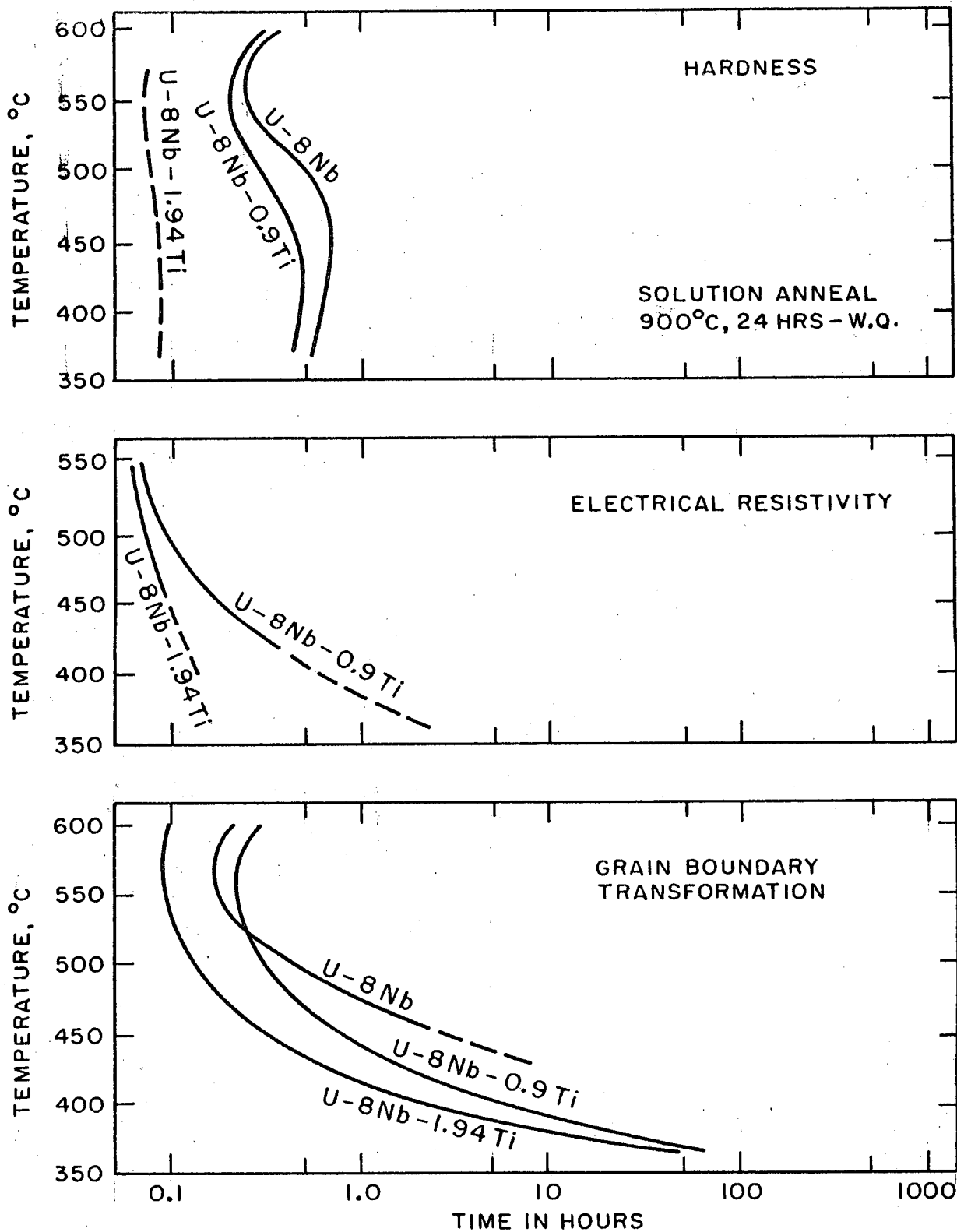
FIG. 112 - TTT DIAGRAMS ILLUSTRATING INITIAL PROPERTY
CHANGES FOR U-8w/o Nb-Ti ALLOYS
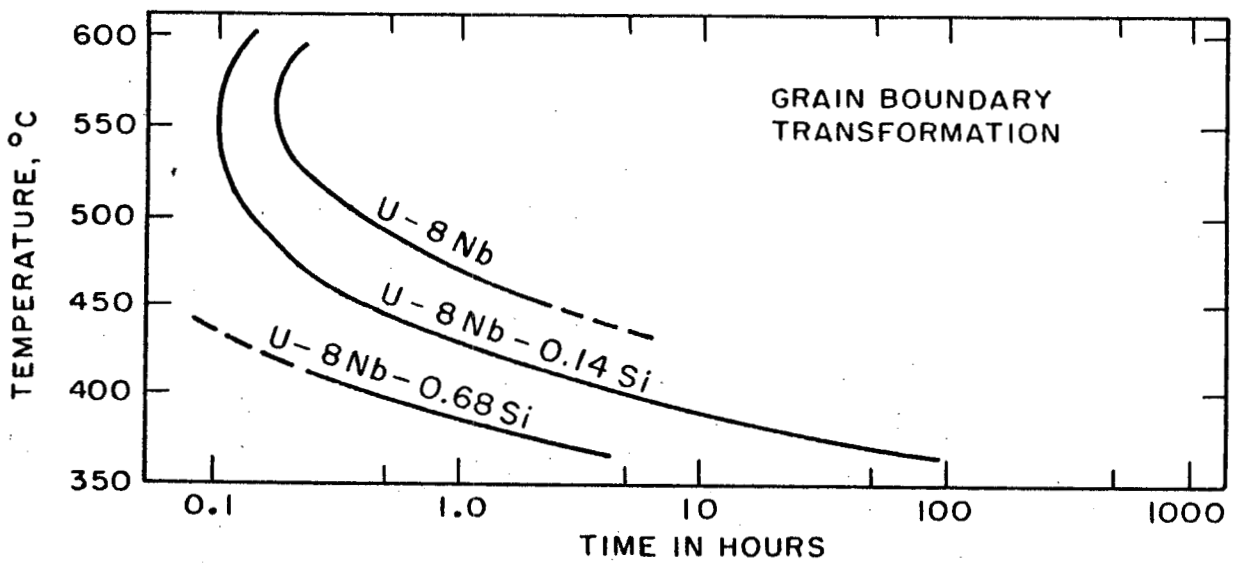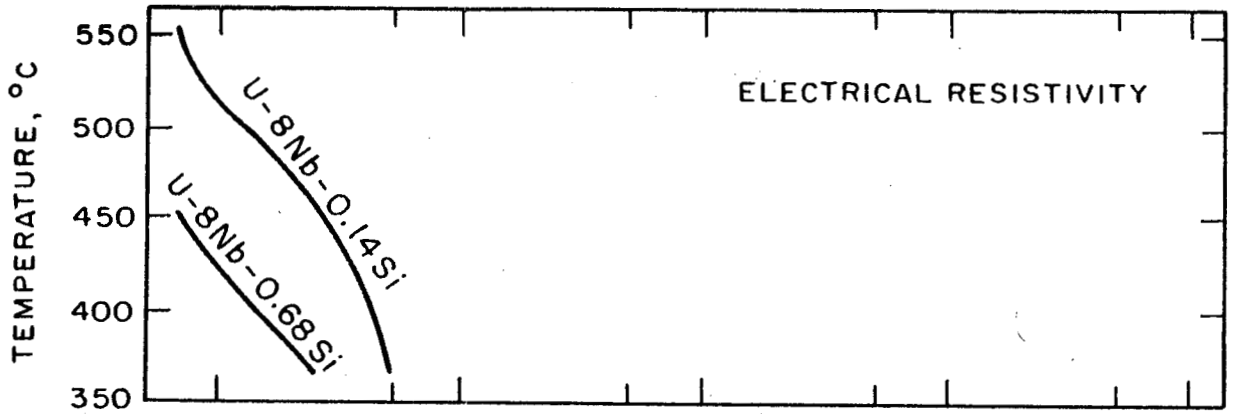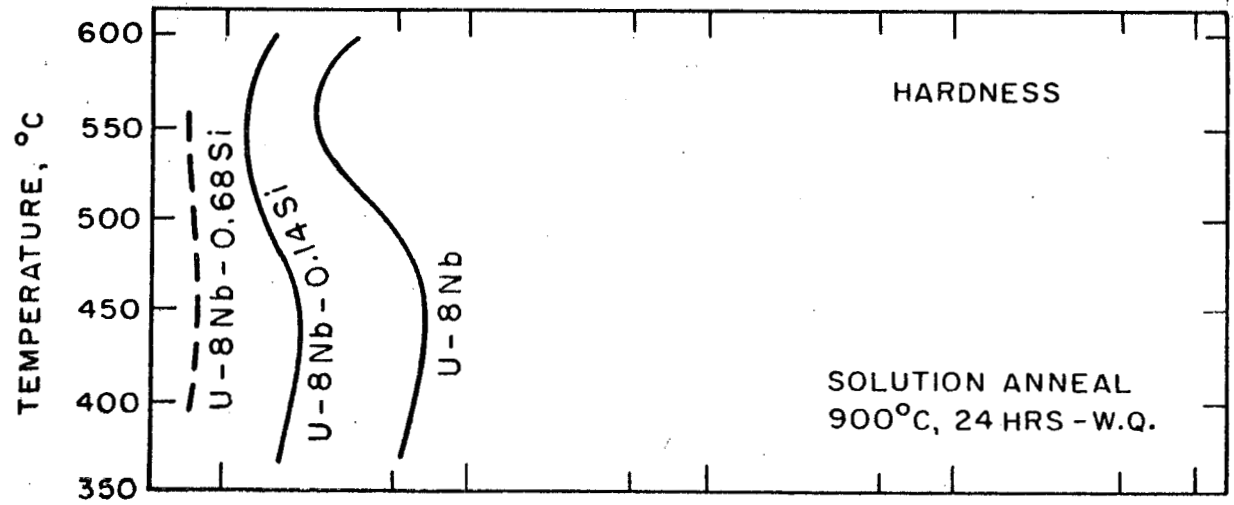
FIG. 113 - TTT DIAGRAMS ILLUSTRATING INITIAL PROPERTY
CHANGES FOR U-8w/o Nb-Si ALLOYS

FIG. 114 – TTT DIAGRAMS ILLUSTRATING INITIAL PROPERTY
CHANGES FOR U-8w/o Nb-Ni AND U-8w/o Nb-Ru ALLOYS

FIG. 115 - TTT DIAGRAMS ILLUSTRATING INITIAL PROPERTY
CHANGES FOR U-8w/o Nb-V ALLOYS

- 152 -

FIG. 116 - TTT DIAGRAMS FOR A U-8w/o Nb-0.12w/o Cr ALLOY
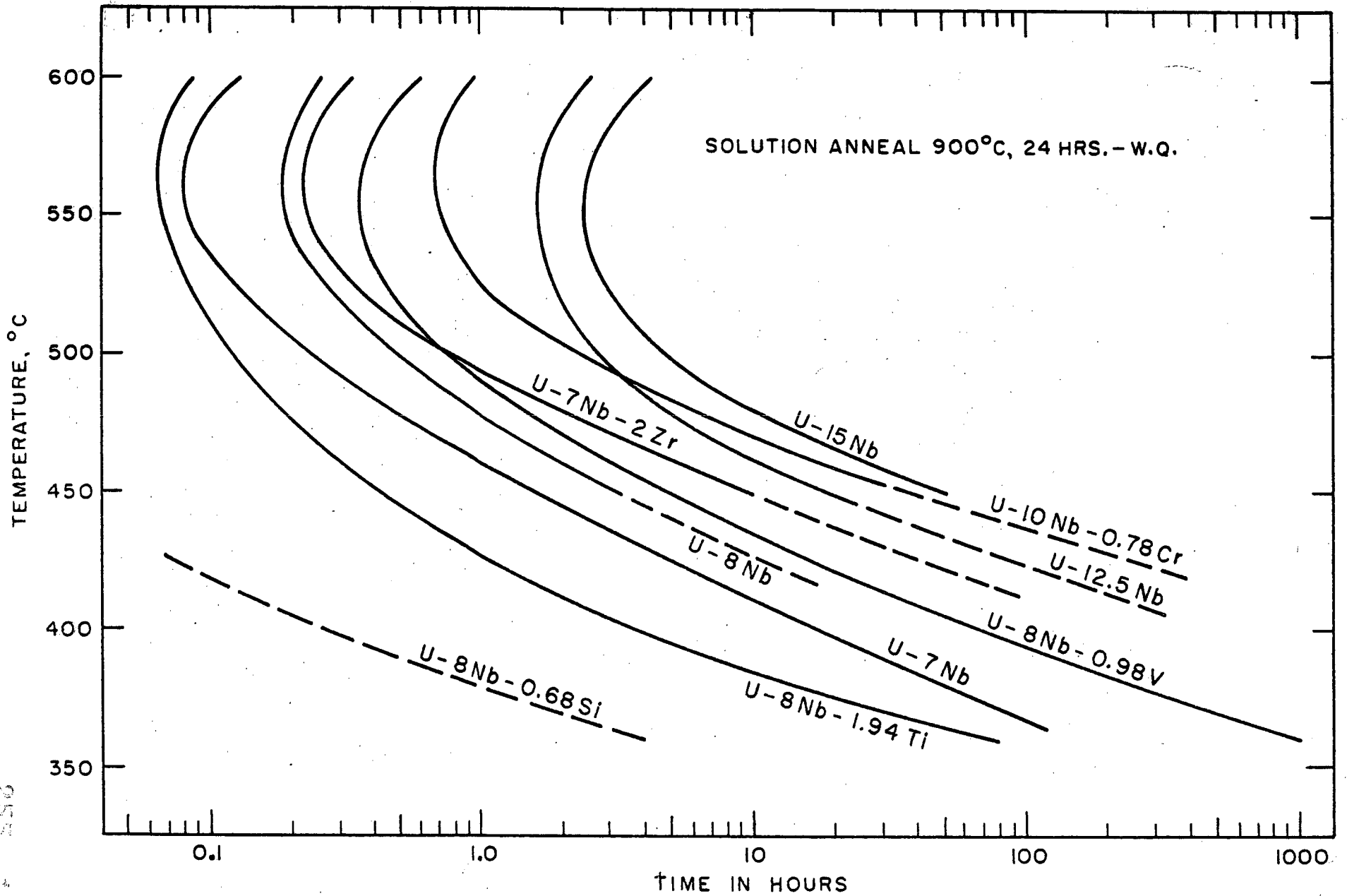
FIG. 117 - TTT DIAGRAMS ILLUSTRATING INITIAL METALLOGRAPHIC OBSERVATION OF
GRAIN BOUNDARY TRANSFORMATION FOR U-Nb AND U-Nb-X ALLOYS

SOLUTION ANNEAL
900°C, 24 HRS — W.Q.
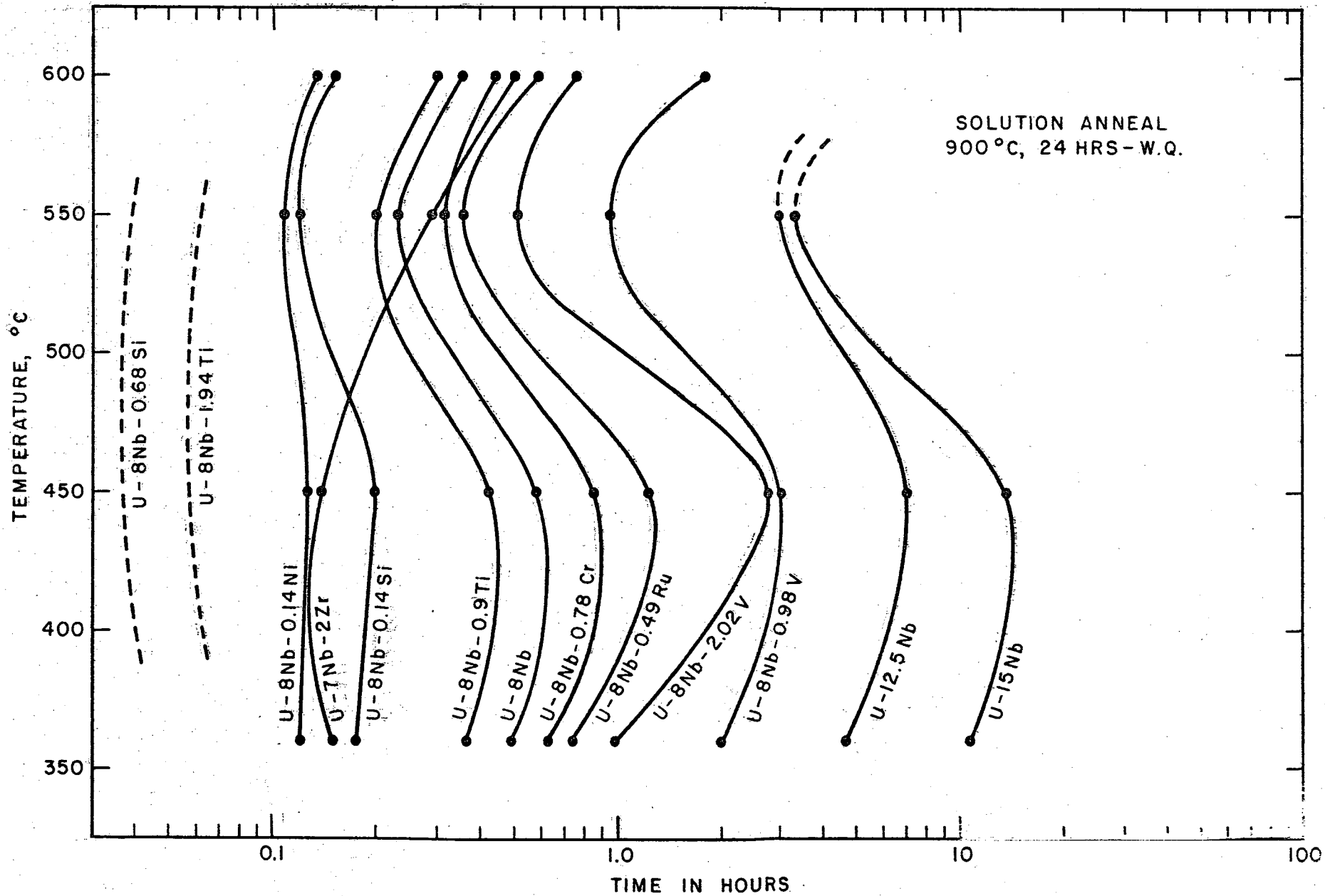
FIG. 118 — TTT DIAGRAMS ILLUSTRATING INITIAL HARDNESS CHANGE
FOR U-Nb AND U-Nb-X ALLOYS
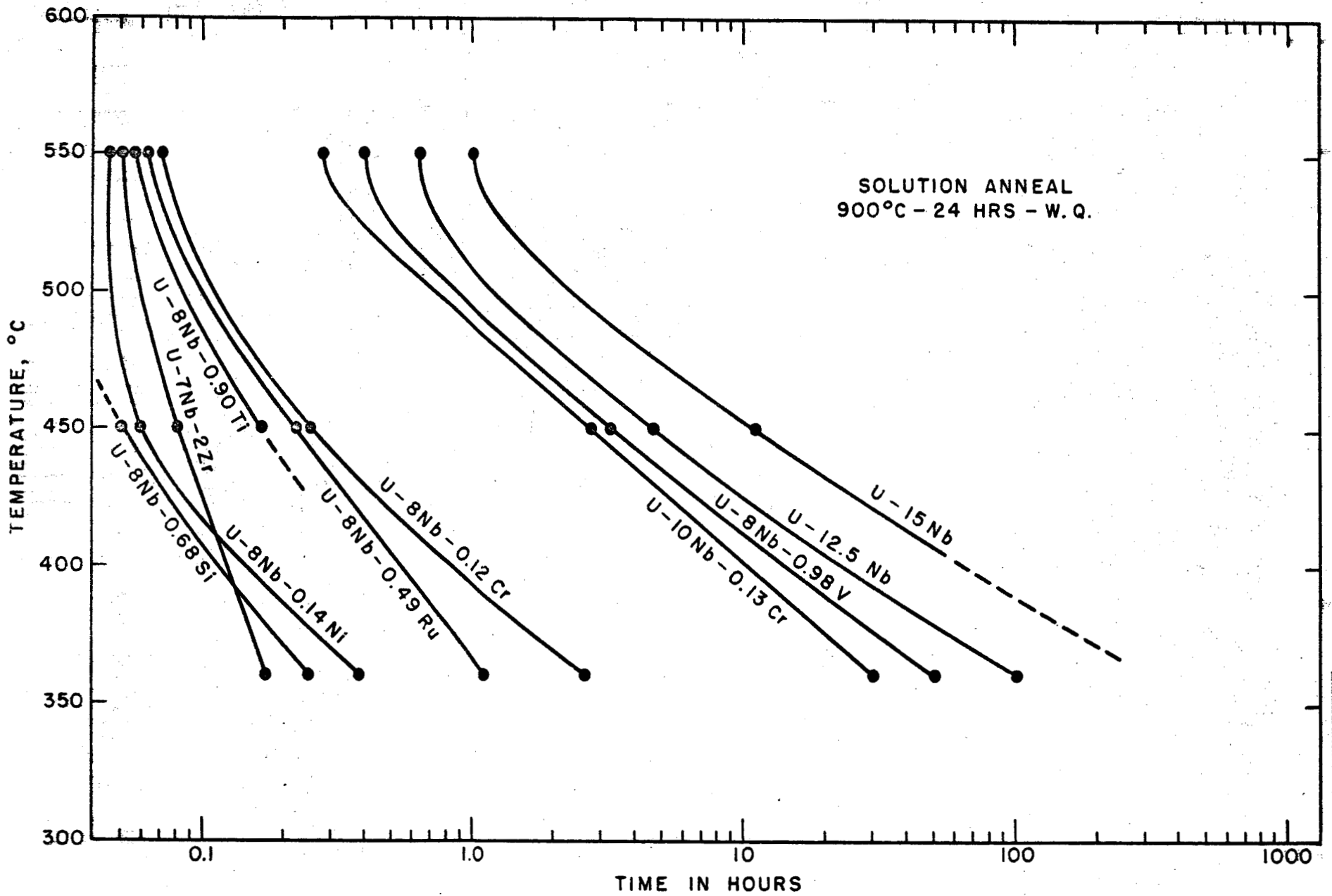
FIG. 119 - TTT DIAGRAMS ILLUSTRATING INITIAL RESISTIVITY CHANGE FOR U-Nb AND U-Nb-X ALLOYS
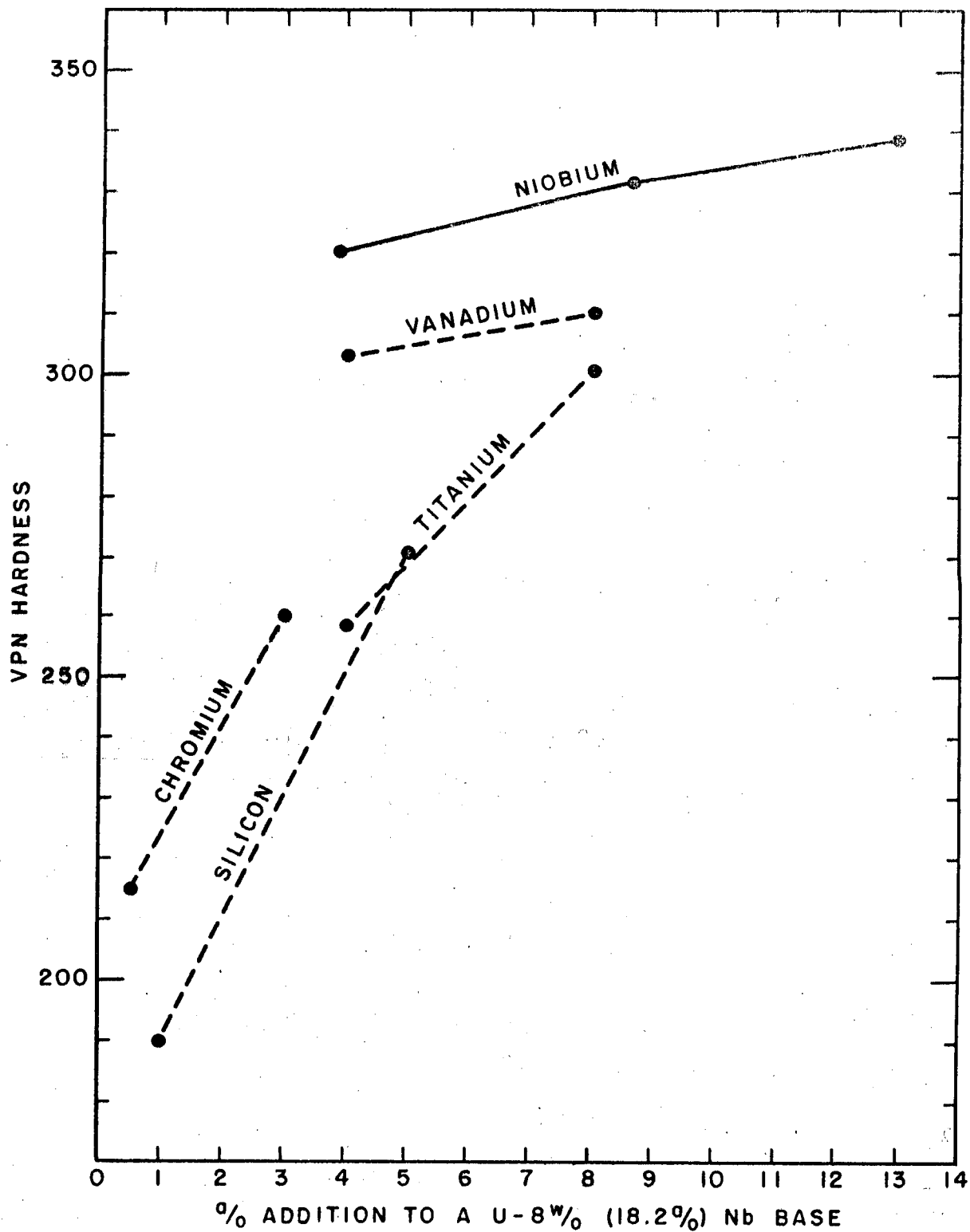
FIG. 120 - EFFECTS OF ADDITIONS TO A U-8w/o Nb BASE ALLOY
ON HARDNESS AS WATER QUENCHED FROM 900°C
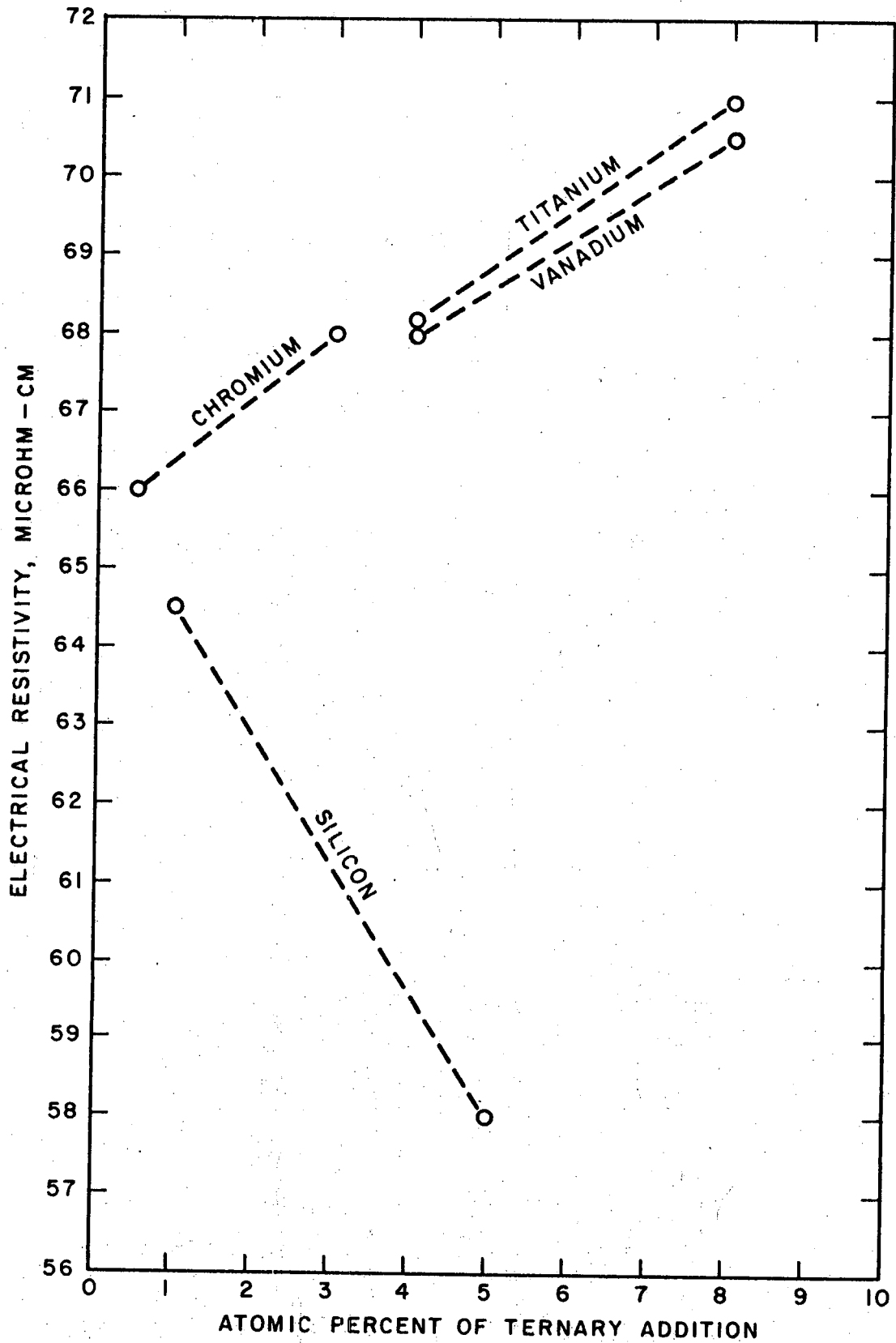
FIG. 121 - EFFECT OF TERNARY ADDITION TO U-8w/o Nb BASE
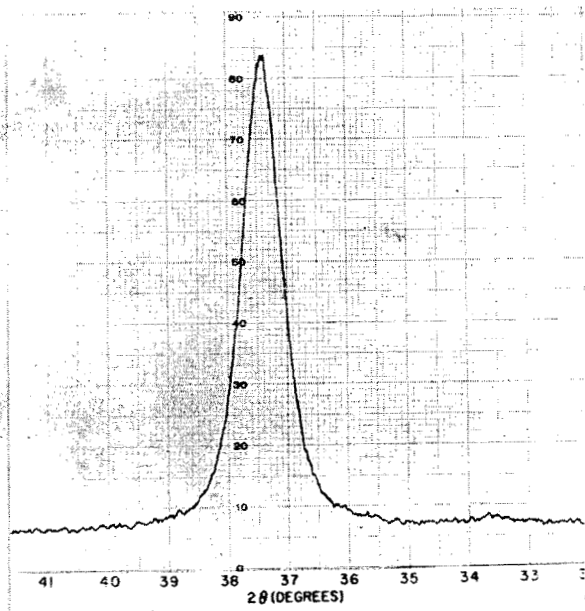ALLOY ON SOLUTION TREATED ELECTRICAL RESISTIVITY

Fig. 122

X-ray diffractometer pattern.
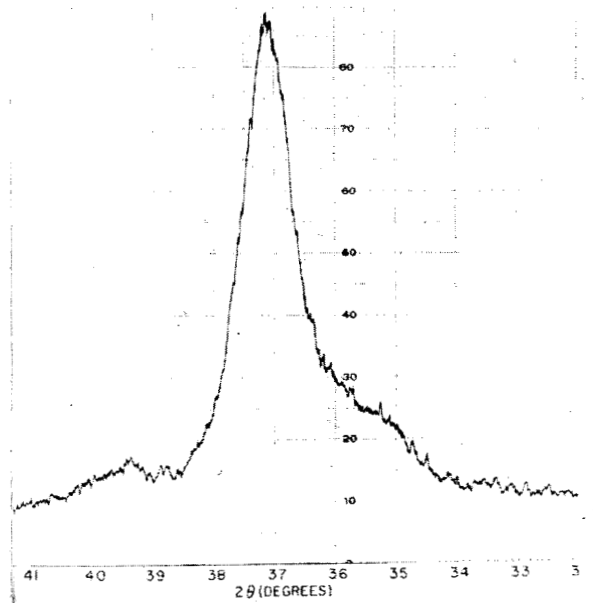Alloy: U-15w/o Nb.
Treatment: 900°C-WQ; 360°C-
1000 hrs-WQ. γ_1.

Fig. 123

X-ray diffractometer pattern.
Alloy: U-8w/o Nb-0.49w/o Ru.
Treatment: 900°C-WQ; 360°C-
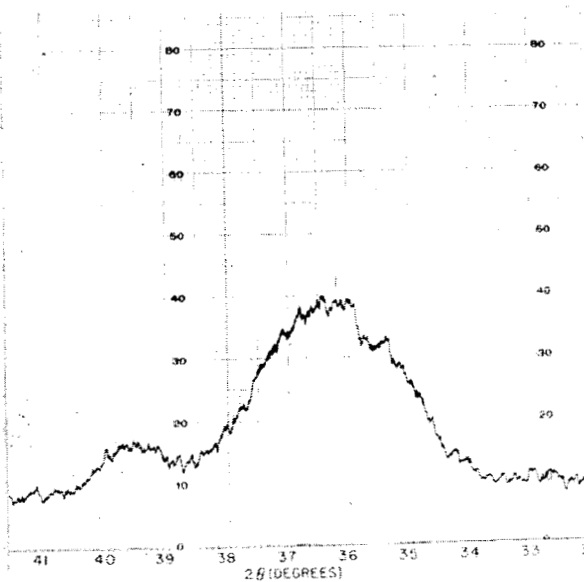1000 hrs-WQ. γ_1 with traces
of α.

Fig. 124

X-ray diffractometer pattern.
Alloy: U-8w/o Nb-0.14w/o Ni.
Treatment: 900°C-WQ; 360°C-
1000 hrs-WQ. Broadened γ peak
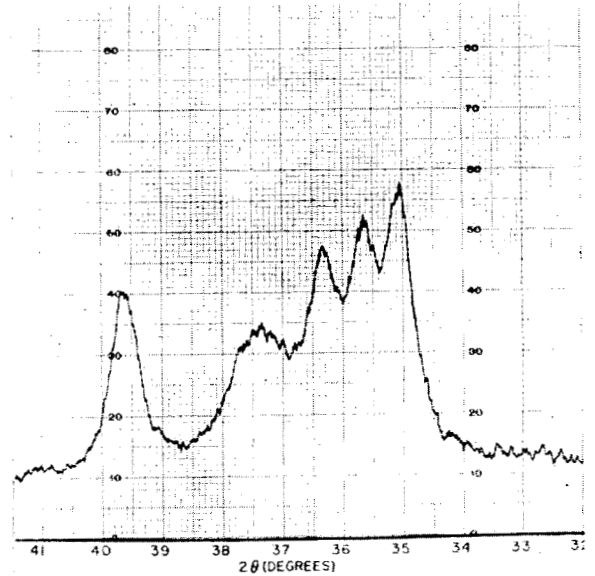and rises in the vicinity of
peaks for α.

Fig. 125

X-ray diffractometer pattern.
Alloy: U-8w/o Nb-0.14w/o Si.
Treatment: 900°C-WQ; 360°C-1000
hrs-WQ. Predominant α. The peak
for γ has shifted from a solution
treated value of 36.8° to 37.4°,
indicating a considerable amount
of transformation.

255   165   - 159 -

B. Continuous Cooling Transformation Studies For The U-10w/o Nb Alloy

Transformation kinetics are reported for samples solution-annealed in the gamma field at 950°C for 1 hour. A solution treatment of 1 or 4 hours 700°C was also employed to determine the effect of various holding times in the $\gamma + \gamma_2$ field. Samples were cooled at linear rates and quenched from temperatures between 600° and 300°C. A cursory investigation was performed to determine the effect of other melting and fabrication techniques upon the transformation kinetics.

1. Experimental Techniques

The preparation of samples has been previously described, with the exception of hot-worked material which was obtained from the Westinghouse Electric Corporation. Following induction melting, this material was forged at 980°C and rolled at 790°C or extruded at 870°C and then rolled at 925°C and air cooled. All the samples were solution-annealed at 950°C for 1 hour, prior to continuous cooling. The results of chemical analyses of all materials are given in Table VI.

Metallography and hardness determinations were used to follow transformation. The metallographic findings are more accurate since hardness data may be insensitive or misleading due to pre-precipitation hardening. However, the hardness results do give a measure of the mechanical property changes as transformation proceeds.

The temperature was always monitored by means of a chromel-alumel thermocouple attached to the samples. A program controller yielded linear cooling rates and a special furnace without insulation was constructed to permit cooling rates approaching 30°C per minute. Rapid quenching at the desired temperature was obtained by direct water quenching from the vertical

TABLE VI

CHEMICAL ANALYSES OF U-10w/o Nb ALLOY SAMPLES

Sample	(w/o)				
	C	Nb	O	N	H
ARF (thermally homogenized)	0.015	9.82	0.029	0.017	0.0014
WAPD (extruded, rolled)	0.010	9.78	0.022	0.016	0.0051
WAPD (forged, rolled)	0.012	9.41	0.21	0.017	not detectable

tube furnace. For some of the results, the samples were contained in tubes illustrated in Figure 126. Upon completion of the solution treatment, the power to the furnace was turned off and the tube slowly withdrawn manually so as to maintain a predetermined cooling rate.

2. Discussion of Results

a. Solution-Annealed at 950°C for 1 Hour

The metallographic data for arc-cast and thermally homogenized samples annealed at 950°C for 1 hour are summarized in Figure 127. The estimated amount of transformation is plotted as a function of log time for the various temperatures investigated. The time coordinate on the graph represents the time required to cool the specimen from the solution-annealing temperature (950°C) to the indicated quenching temperatures. The temperature difference divided by the time yields the average cooling rate. The decomposition ($\gamma \rightarrow \alpha + \gamma_2$) structure was similar to that obtained by isothermal annealing. Many heat treatments were performed and the microstructures contained up to 80% transformation. Decomposition was observed at all temperatures except 600°C. The gamma structure was metastable upon cooling to this temperature at a rate of 2°C per minute.

Vickers hardness data (10 kg) obtained from the metallographic specimens are presented in Figure 128. Upon transformation at temperatures between 400° and 300°C, the hardness shows a sharp increase. The hardness of the retained gamma structure has been corroborated by additional data not shown because the cooling rates were sufficiently rapid that the data points did not fit on Figure 128.

Figures 129 to 132 are photomicrographs of samples cooled at rates of 10°, 7°, 4° and 2.2°C per minute to 400°C and water quenched. Retained gamma is illustrated in Figure 129; incipient transformation is present in

ARMOUR RESEARCH FOUNDATION OF ILLINOIS INSTITUTE OF TECHNOLOGY

Figure 130. A progressive increase in the amount of transformation is demonstrated in Figures 131 and 132.

With the data from Figures 127 and 128 a continuous cooling transformation diagram was constructed (Figure 133). Two linear cooling rates are indicated as dashed lines for comparison. A "c-curve" is not obtained, as the transformation curve should become asymptotic with the critical cooling rate at the lower temperatures. The data points represent the temperature-time relationships for an initial hardness increase or incipient metallographic decomposition. Some minor amount of foreign phase has been observed at the grain boundaries of samples cooled at fast rates. However, no increase in the amount of this material was detected until the cooling rate was slower than 10°C per minute. Accordingly, the critical cooling rate data were taken from the curves of Figure 127.

The hardness and metallographic results are in close agreement. As expected, the nose of the transformation curves based on continuous cooling lie at longer times than those shown previously for isothermal treatments. For both hardness and metallographic data, the nose of the curve was placed near 500°C and 60 minutes. Unlike the previous TTT investigation, it appears that pre-precipitation hardening did not occur, and hardness increases were due to observable transformation only. The critical cooling rates to avoid transformation based on metallographic and hardness findings are 8.5° and 7.5°C per minute, respectively.

b.   Solution-Annealed at 700°C For 1 and 4 Hours

The purpose of annealing at 700°C was to observe the effect of annealing samples in a two-phase region on the continuous cooling characteristics of the alloy. An early phase diagram of the U-Nb system[2] indicates

Project No. B 095
                                                Summary Report

, that the U-10w/o Nb composition is within a two-phase area up to about 860°C. Later work[3] has shown that this composition is not within the $\gamma_1 + \gamma_2$ field above 695°C. It is therefore doubtful that the true effect of annealing in the two-phase area was observed by treating at 700°C. A very slight effect was noticed; it might be attributed to the fact that the annealing temperature was very close to $\gamma_1/\gamma_1+\gamma_2$ boundary or could result from experimental error since the differences were so small.

Only gamma was detected in the microstructure of specimens annealed at 700°C in the $\gamma + \gamma_2$ field. Upon transformation following this solution treatment, the structures were similar to those obtained with the 950°C solution anneal. Figure 134 illustrates the retained gamma structure. Upon cooling at 8°C per minute some transformation has resulted (Figure 135). Curves illustrating the amount of transformation vs cooling time were constructed for both solution treatments at 700°C (Figures 136 and 137). The data for initiation of decomposition were obtained from these drawings and are summarized as continuous cooling transformation diagrams in Figure 138.

Similar to the findings for the 950°C solution treatment, the nose of the transformation curves occurs near 500°C. The critical cooling rates for the solution treatments at 700°C for 1 and 4 hours are approximately 9° and 11°C per minute, respectively. These results indicate that longer holding time at 700°C may accelerate the monotectoid decomposition.

Vickers hardness data (10 kg) obtained on the metallographic samples solution annealed at 700°C for 1 hour were plotted as a function of time as in Figure 128. Isothermal curves connecting the equitemperature data points exhibited multiple peaking and were difficult to interpret. This was probably a result of solution annealing at 700°C.

Figure 139 is an isometric line drawing of the three-dimensional surface obtained upon plotting hardness data vs. temperature and log time. The exact hardness values cannot readily be interpreted from the figure, so the data are detailed in Table VII. The various cooling rates are marked by lightly dashed lines and the isothermal data are connected by heavy lines in Figure 139. A peak hardness was obtained at a cooling rate of about 10°C per minute. Following this peak there is a hardness minimum at cooling rates of approximately 4 to 6°C per minute. Hardness values lower than the solution-annealed hardness were obtained for some treatments. After this softening, there is a general rise in hardness that is associated with the additional decomposition of the gamma phase. From this data it seems injudicious to assign a critical cooling rate for the hardness results. It should be noted that, although a definite trend in the double peaks was noted, the actual changes in hardness were small. A three-dimensional drawing (Figure 140) was also required to interpret the hardness findings for the solution treatment of 4 hours at 700°C presented in Table VIII.

c.   Alloy Material Evaluation

Metallographic examination showed that some of the induction-melted and fabricated stock was somewhat cored; and a check of the hardness, which varied throughout the samples, verified this finding. The worked material appeared to contain more inclusions although the chemical analyses showed no gross differences. Because of hardness variations it was difficult to obtain reliable hardness data upon transformation and only metallographic data are reported. Since only a cursory check was to be made on the worked material, only two temperatures, 350° and 450°C, were investigated.

TABLE VII

HARDNESS AS A FUNCTION OF TEMPERATURE AND COOLING RATE
FOR A SOLUTION ANNEAL AT 700°C FOR 1 HOUR

Temperature (°C)	VPN (10 Kg) Cooling Rate (°C/min)									
	20	14	12	10	8	6	5	4	3	2
550	310	298	304	300	310	318	302	295	311	314
500	325	296	327	300	333	317		298	313	336
450	315	319	337	312	339	322	309	302	336	392
400	318	317	329	348	342	331		302	337	364
350	310	313	351	338	327	288	314	337	349	379
300	321	325	323	345	325	274	308	317	337	375

TABLE VIII

HARDNESS AS A FUNCTION OF TEMPERATURE AND COOLING RATE FOR A SOLUTION ANNEAL AT 700°C FOR 4 HOURS

Temperature (°C)	VPN (10 Kg)				
	Cooling Rate (°C/min)				
	14	12	8	4	3
550		314	322	303	309
500		316	308	329	306
450	301	330	319	336	
400	312	339	319	364	334
350	312	330	325	343	333
300	305	327	254	327	335

255 173

Photomicrographs of forged and rolled samples after solution annealing, cooling to 450°C and quenching, are given in Figures 141 to 144. Figure 141 illustrates retained gamma upon cooling at 25°C per minute. A similar structure is shown in Figure 142. Figures 143 and 144 present increased amounts of transformation obtained at cooling rates of 10° and 5°C per minute, respectively. Similar microstructures were observed with samples that had been extruded and rolled. On the basis of similar data, Figures 145 and 146 were constructed and the data summarized in Figure 147. The critical cooling rates for the extruded or forged specimens are approximately 14.5° or 13°C per minute, respectively.

Critical cooling rates for all solution treatments and materials are given in Figure 148. The curves indicate the start of metallographically observed transformation. The time ordinate refers to the time spent cooling from 700°C; that is, the data points for the 950°C for 1 hour solution treatment have been adjusted for comparative purposes. Linear cooling rates are shown for comparison. On the basis of these data, it is apparent that the thermally homogenized arc-cast material transforms less rapidly than the induction-melted and hot-worked samples. The annealing treatments at 700°C seem to have a slight detrimental effect on the critical rates.
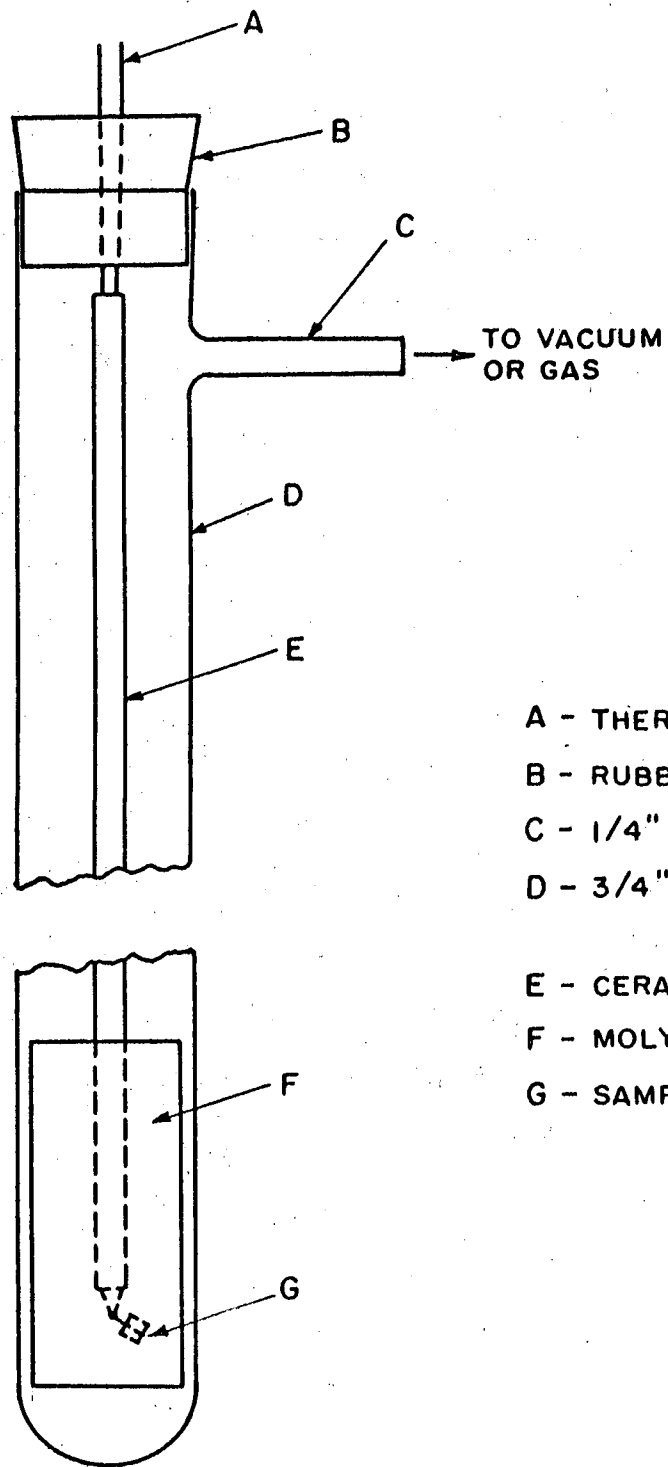
A - THERMOCOUPLE LEADS

B - RUBBER STOPPER

C - 1/4" VYCOR SIDE ARM

D - 3/4" VYCOR TUBE - ONE END CLOSED, 24" LONG

E - CERAMIC INSULATOR

F - MOLYBDENUM SHIELD

G - SAMPLE WIRED TO BEAD

FIG. 126 - SCHEMATIC DIAGRAM OF VYCOR TUBE USED IN CONTINUOUS COOLING DETERMINATIONS
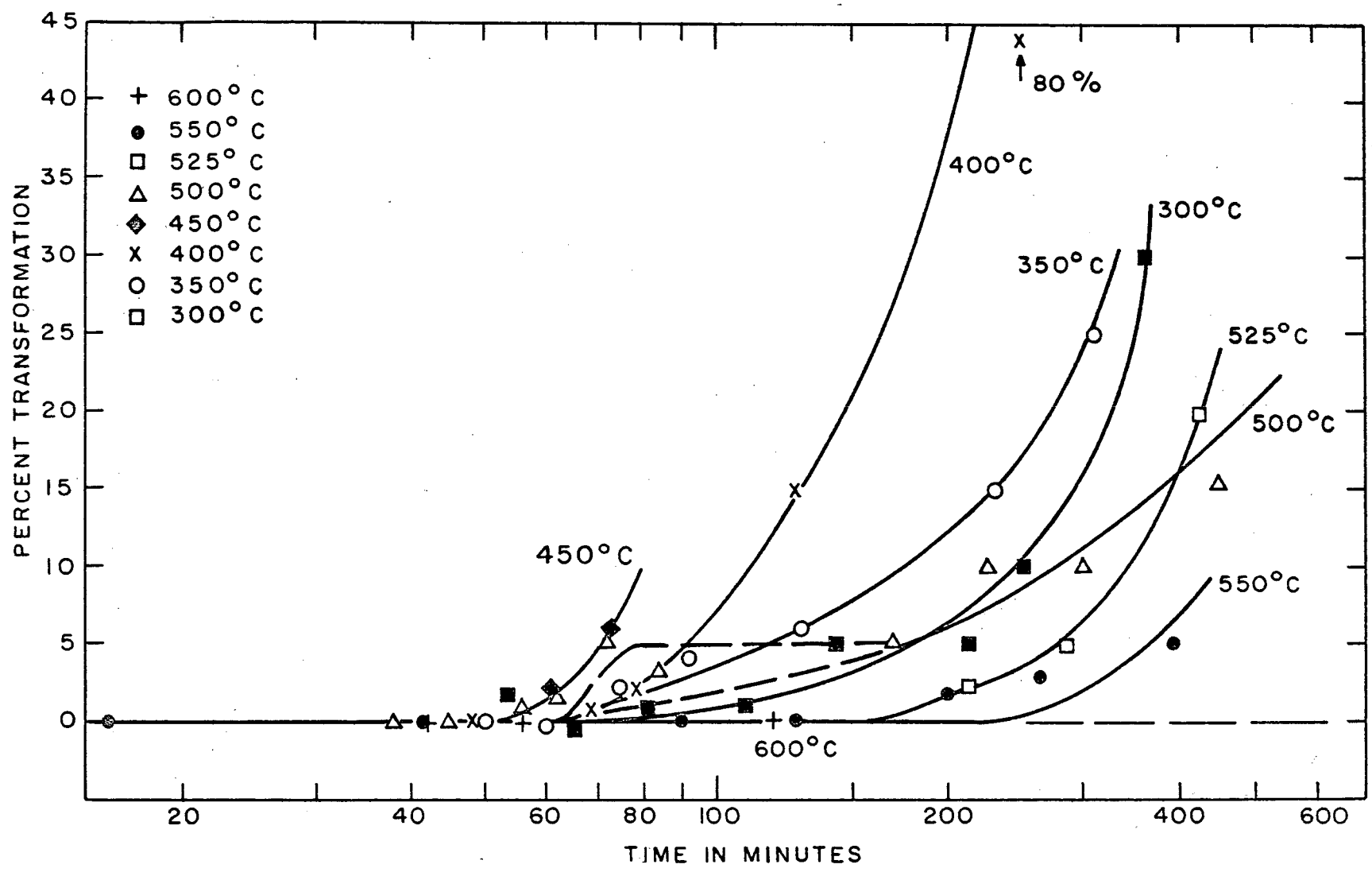
FIG. 127 - AMOUNT OF METALLOGRAPHICALLY OBSERVED TRANSFORMATION VS. COOLING TIME FOR A U-10 W/o Nb ALLOY SOLUTION TREATED FOR 1 HOUR AT 950°C
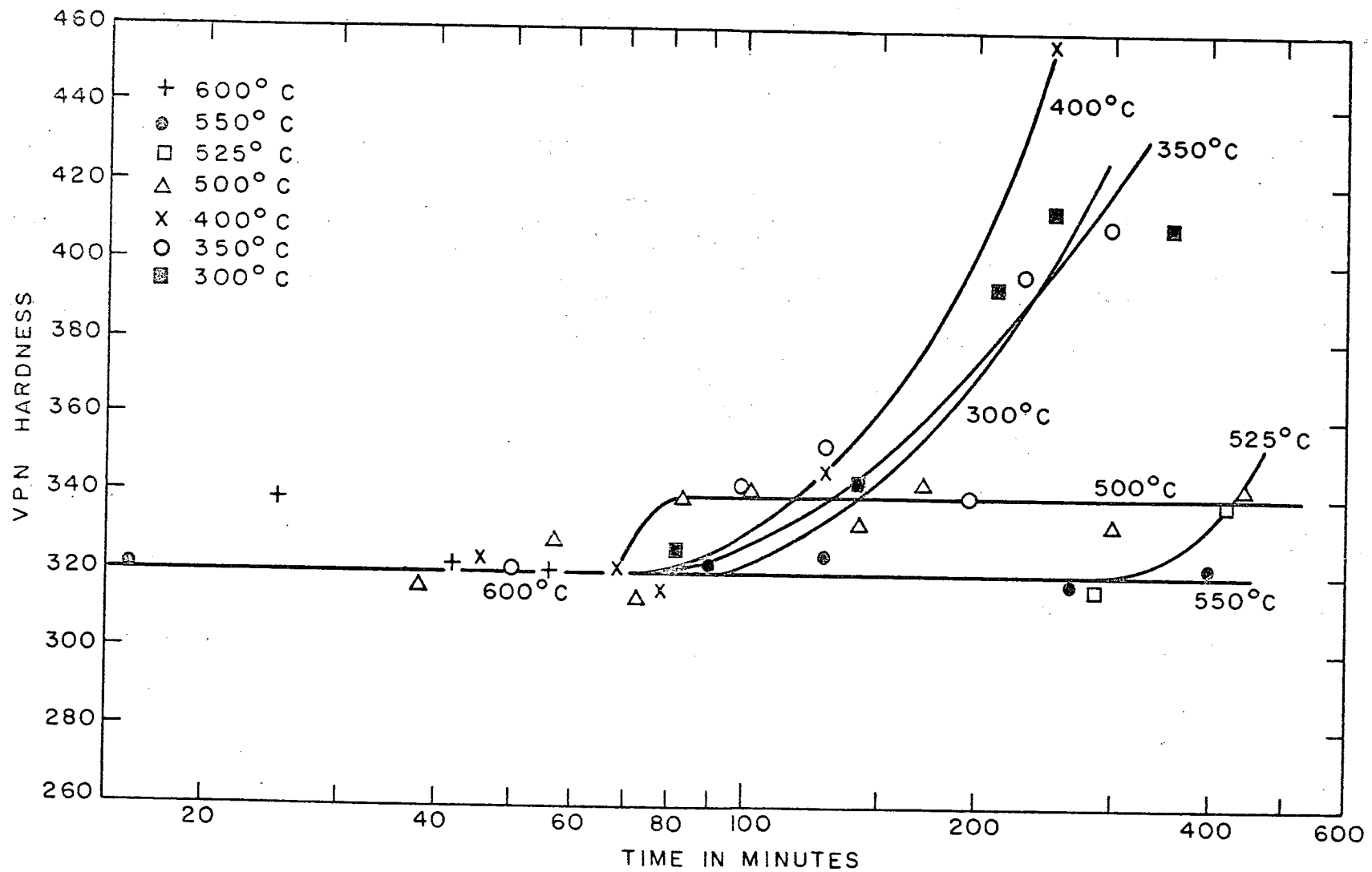
FIG. 128 - HARDNESS DATA FOR A CONTINUOUSLY COOLED U-10 w/o Nb ALLOY
SOLUTION TREATED FOR 1 HOUR AT 950°C
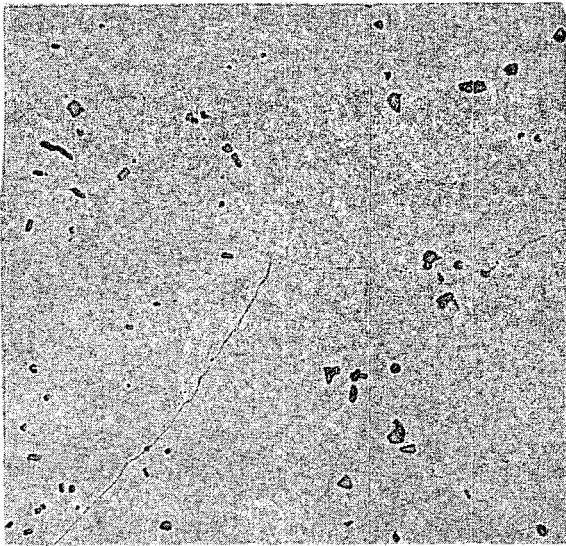
Neg. No. 13463   X 250

Fig. 129

U-10w/o Nb alloy solution treated
at 950°C for 1 hour, cooled at 10°C
per minute to 400°C and water
quenched. Retained γ with impuri-
ties evident.
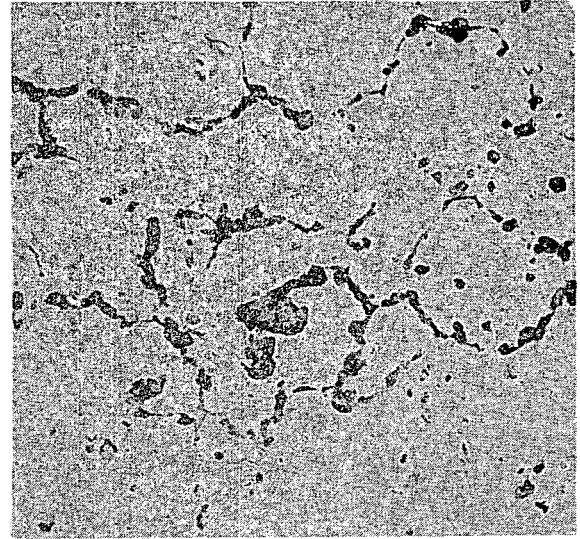
Neg. No. 12374   X 250

Fig. 130

U-10w/o Nb alloy solution treated at
950°C for 1 hour, cooled at about
7°C per minute to 400°C and water
quenched. Initial transformation in
γ.
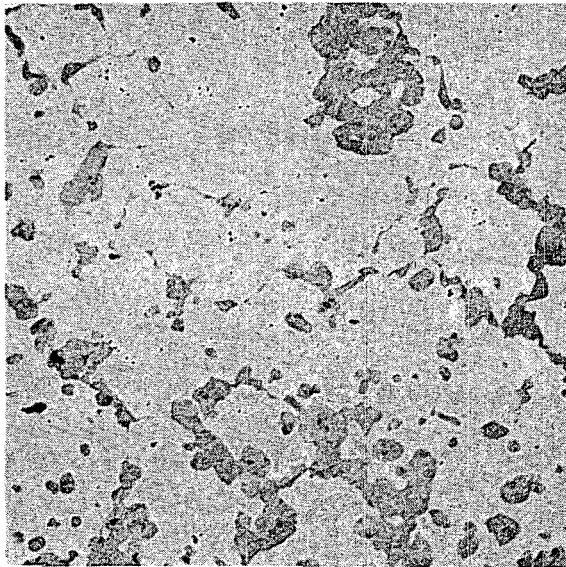
Neg. No. 12373   X 250

Fig. 131

U-10w/o Nb alloy solution treated
at 950°C for 1 hour, cooled at
approximately 4.4°C per minute to
400°C and water quenched. Ad-
ditional decomposition of γ.

Etchant: 4% CrO$_3$ + 1% HF + H$_2$O
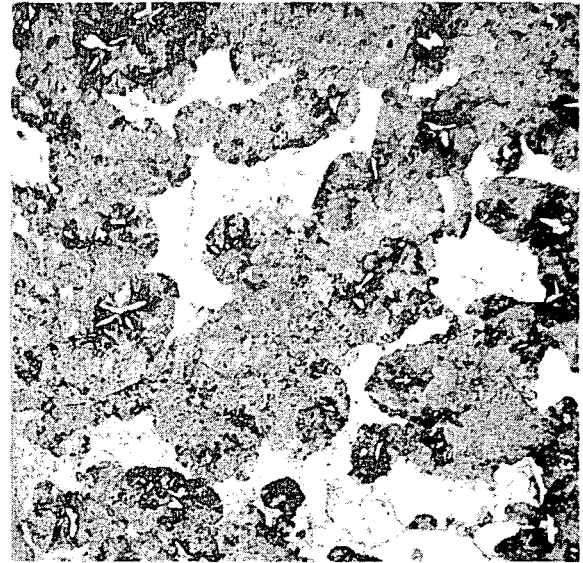
Neg. No. 12372   X 250

Fig. 132

U-10w/o Nb alloy solution treated at
950°C for 1 hour, cooled at about
2.2°C per minute to 400°C and water
quenched. Transformation now covers
most of microstructure. Impurity
phase is evident.
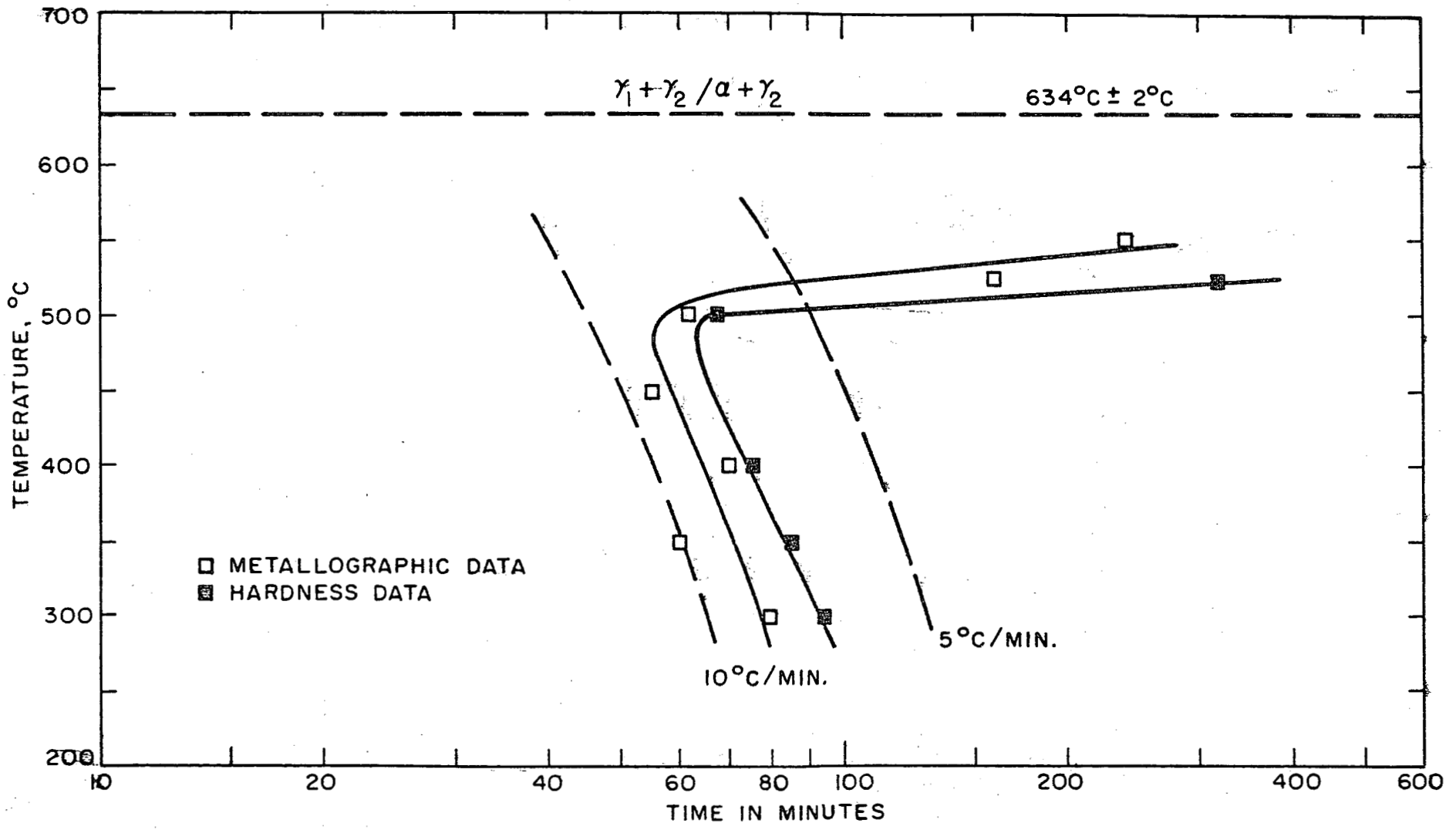
FIG. 133-CONTINUOUS COOLING TRANSFORMATION DIAGRAMS FOR U-10w/o Nb ALLOYS BASED
ON HARDNESS AND METALLOGRAPHIC DATA (SOLUTION TREATED FOR 1 HOUR AT 950°C)
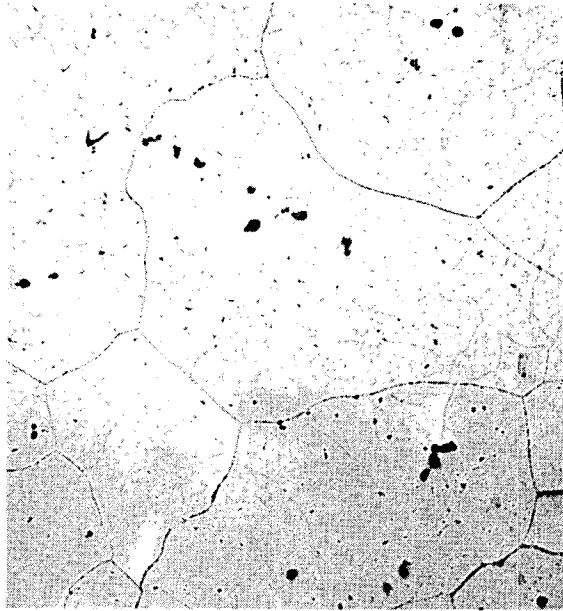
Neg. No. 13960   X 250

Fig. 134

U-10w/o Nb alloy solution treated
at 700°C for 4 hours, cooled at
400°C at 14°C per minute and water
quenched. Retained γ structure
similar to Fig. 129.

Neg. No. 13961   X 250

Fig. 135

U-10w/o Nb alloy solution treated
at 700°C for 4 hours, cooled to
400°C at 8°C per minute and water
quenched. Transformation has
initiated.

Etchant: $4\% \ CrO_3 + 1\% \ HF + H_2O$

- 174 -

245   180
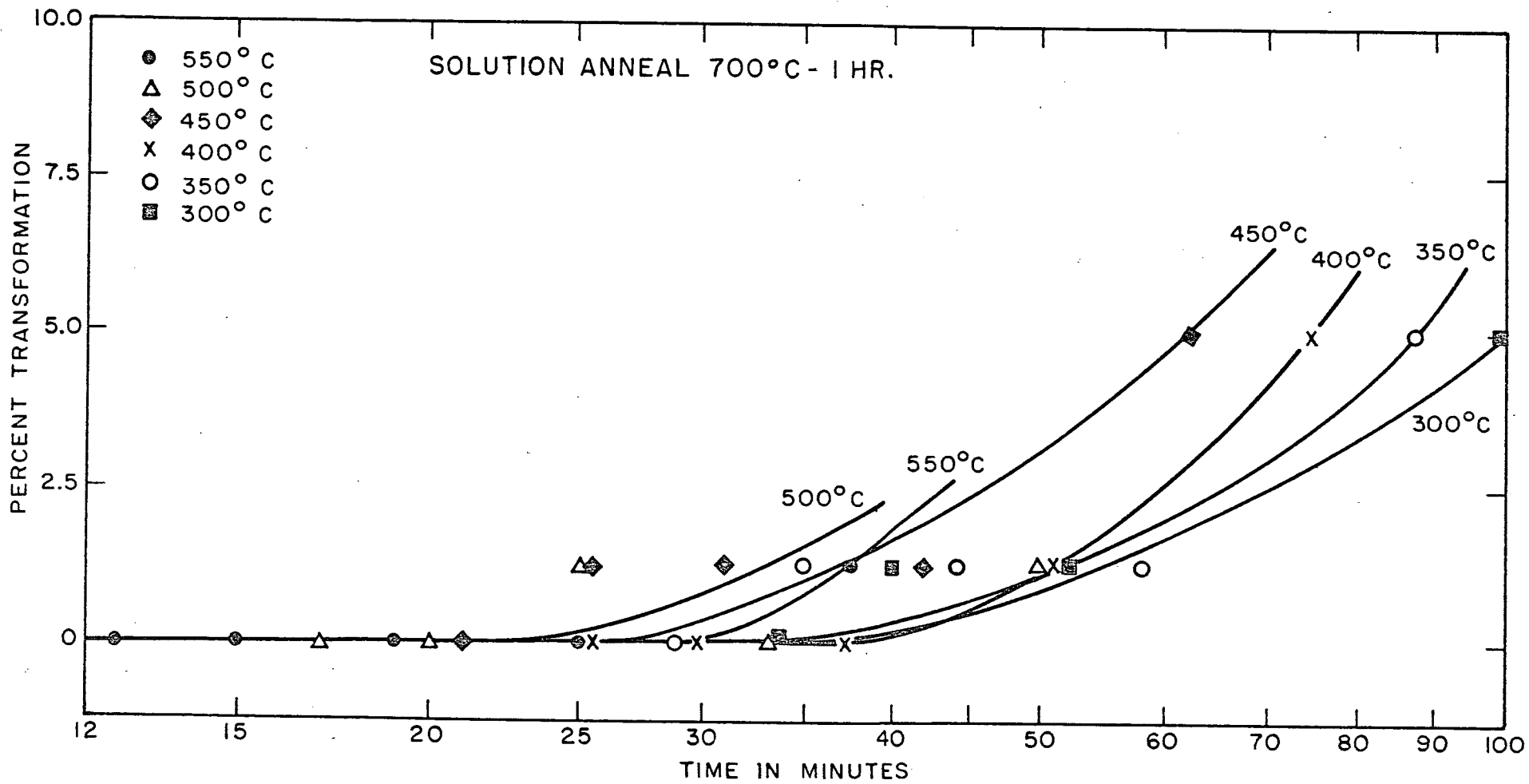
FIG. 136 - AMOUNT OF METALLOGRAPHICALLY OBSERVED TRANSFORMATION VS. COOLING TIME FOR A U-10 W/o Nb ALLOY SOLUTION TREATED FOR 1 HOUR AT 700°C
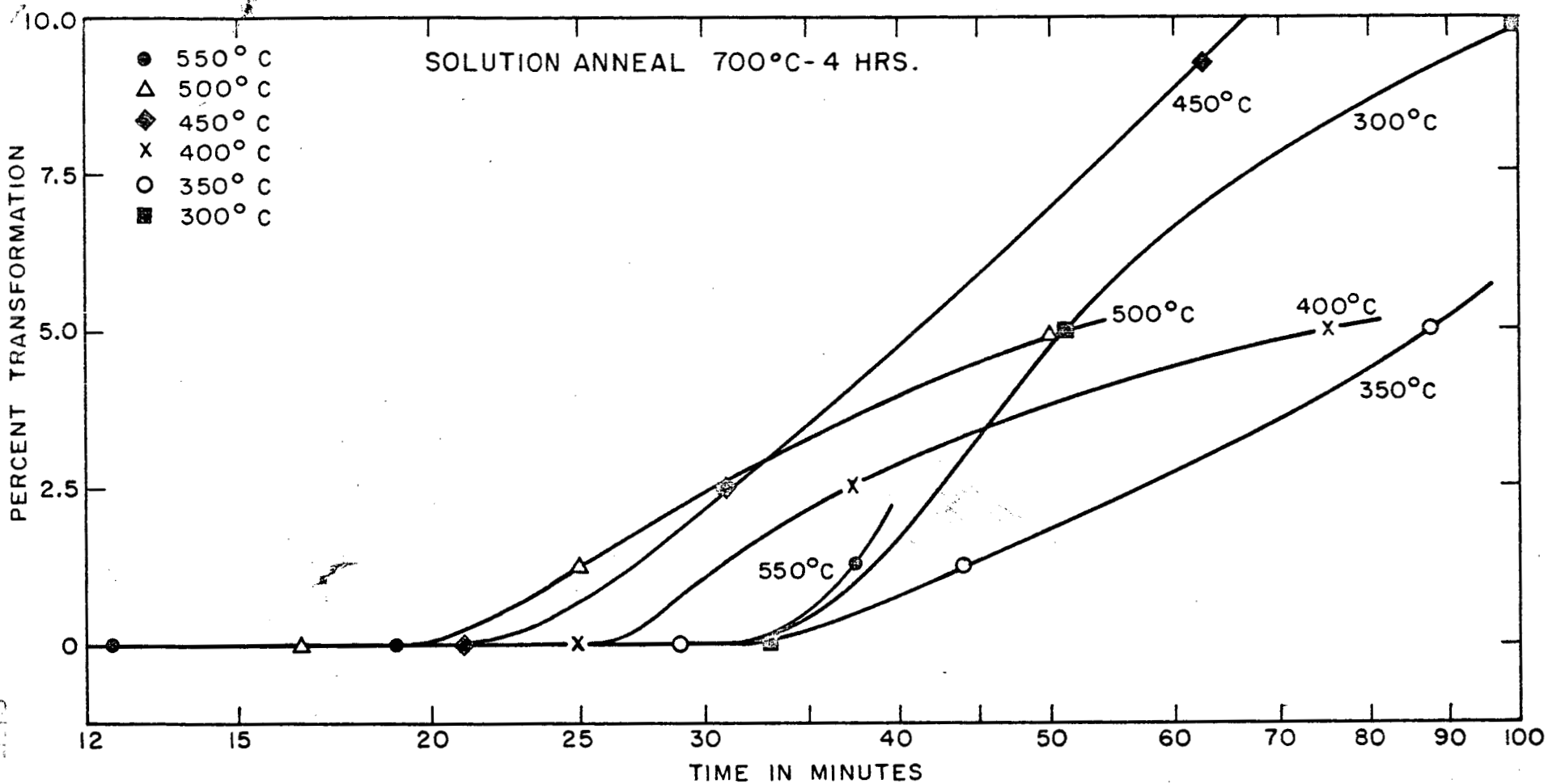
FIG. 137 - AMOUNT OF METALLOGRAPHICALLY OBSERVED TRANSFORMATION VS. COOLING TIME FOR A U-10 ^{W}/o Nb ALLOY SOLUTION TREATED FOR 4 HOURS AT 700 °C
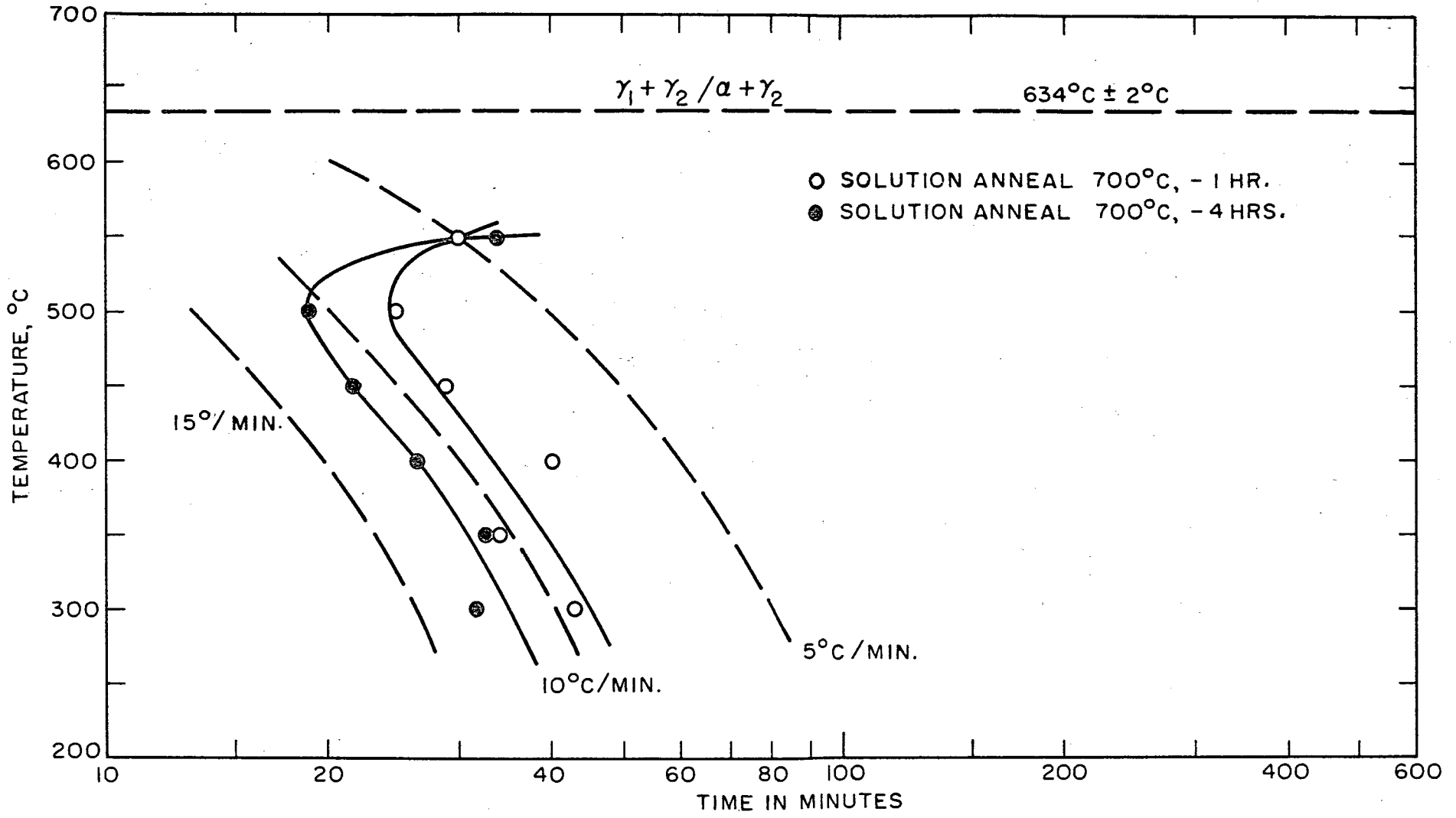
FIG. 138 - CONTINUOUS COOLING TRANSFORMATION DIAGRAM FOR U-10w/o Nb ALLOY SOLUTION TREATED AT 700°C FOR 1 AND 4 HOURS (BASED ON METALLOGRAPHIC DATA)
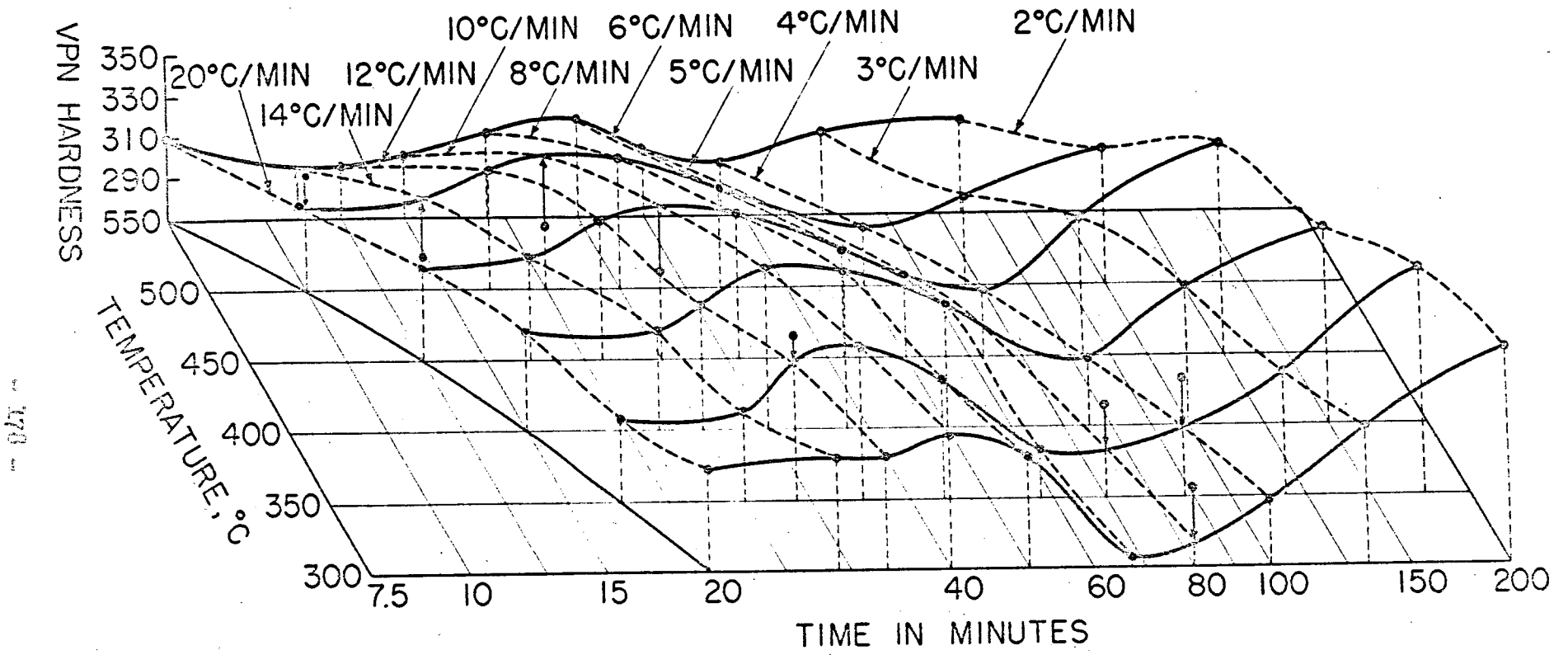
FIG. 139 - ISOMETRIC DRAWING SHOWING HARDNESS OF THE U-10% Nb ALLOY (SOLUTION TREATED FOR 1 HOUR AT 700°C) AS A FUNCTION OF TEMPERATURE AND TIME
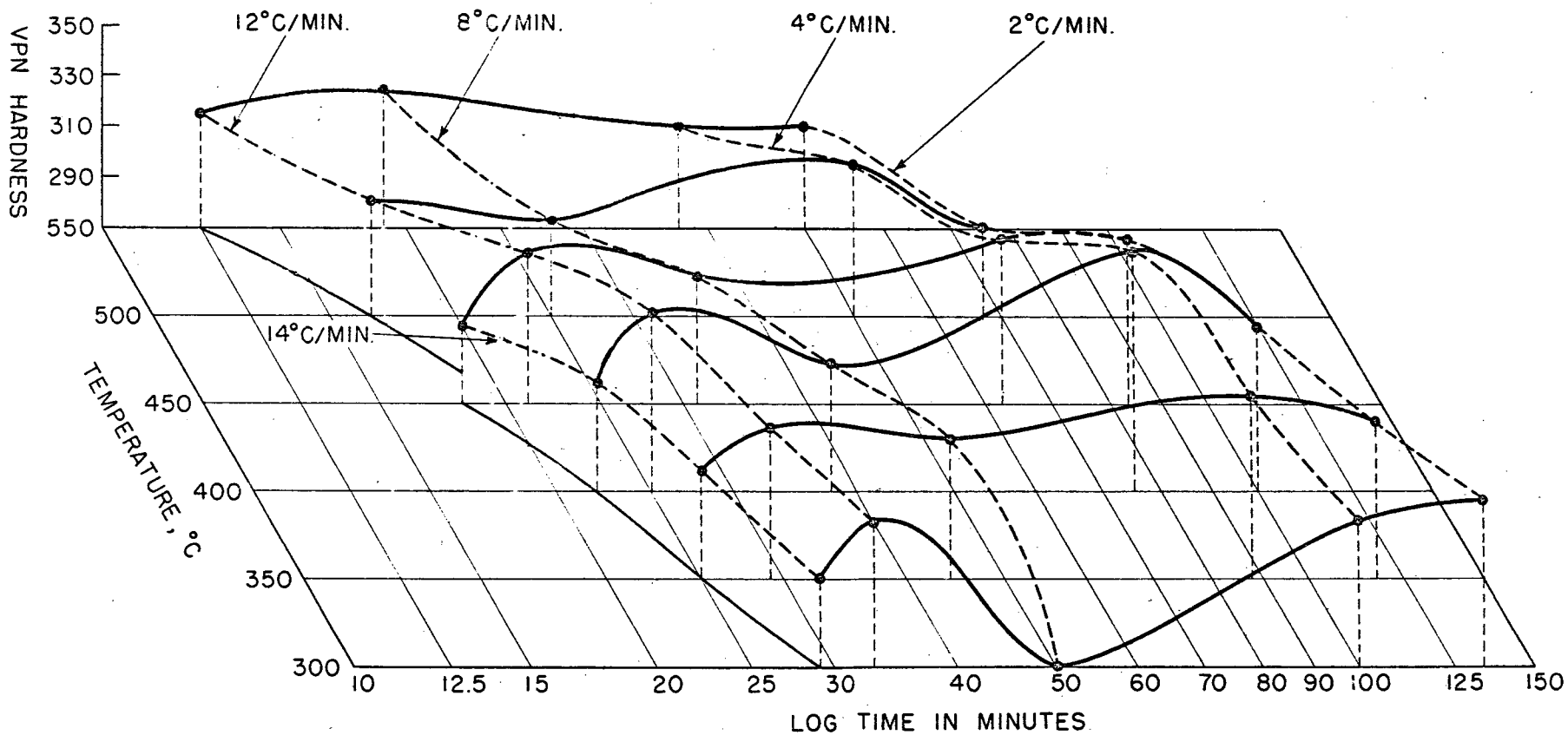
FIG. 140 - ISOMETRIC DRAWING SHOWING HARDNESS AS A FUNCTION OF TEMPERATURE
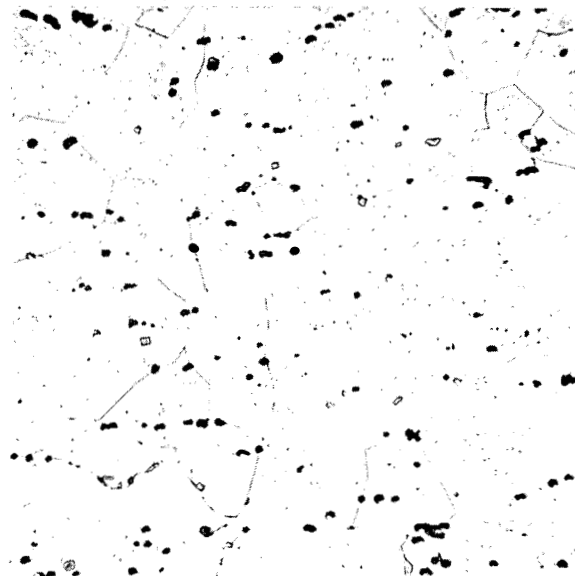AND LOG TIME FOR A SOLUTION ANNEAL OF 700 °C FOR 4 HOURS
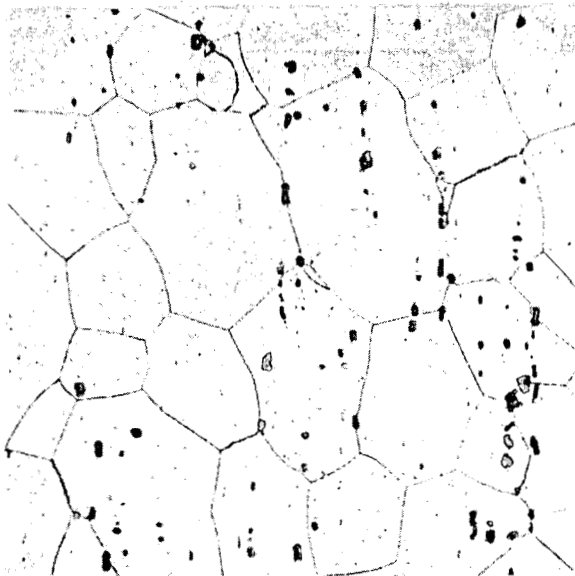
Neg. No. 13194   X 250

Fig. 141

U-10w/o Nb alloy forged and rolled,
solution treated at 950°C-1 hr,
cooled at 25°C per minute to 450°C-
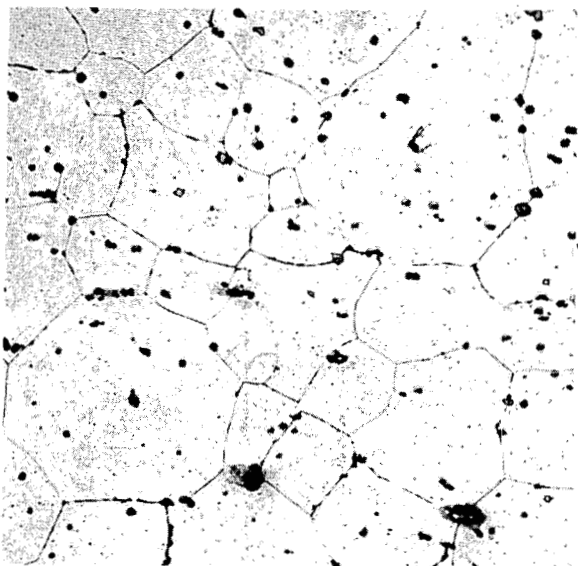WQ. Retained γ with banded im-
purities.

Neg. No. 13195   X 250

Fig. 142

U-10w/o Nb alloy forged and rolled,
solution treated at 950°C-1 hr,
cooled at 15°C per minute to 450°C-
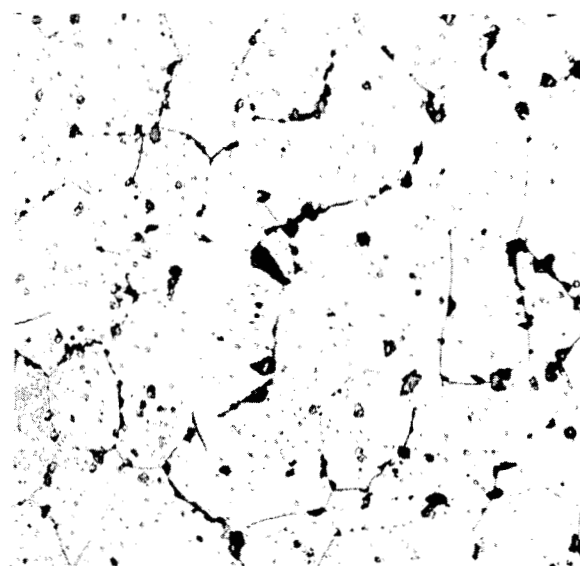WQ. Similar to Fig. 141.

Neg. No. 13196   X 250

Fig. 143

U-10w/o Nb alloy forged and rolled,
solution treated at 950°C-1 hr,
cooled at 10°C per minute to 450°C-
WQ. Retained γ with incipient trans-
formation.

Etchant: 4% CrO_3 + 1% HF + 0.5% HNO_3 + H_2O

Neg. No. 13111   X 250

Fig. 144

U-10w/o Nb alloy forged and rolled,
solution treated at 950°C-1 hr,
cooled at 5°C per minute to 450°C-
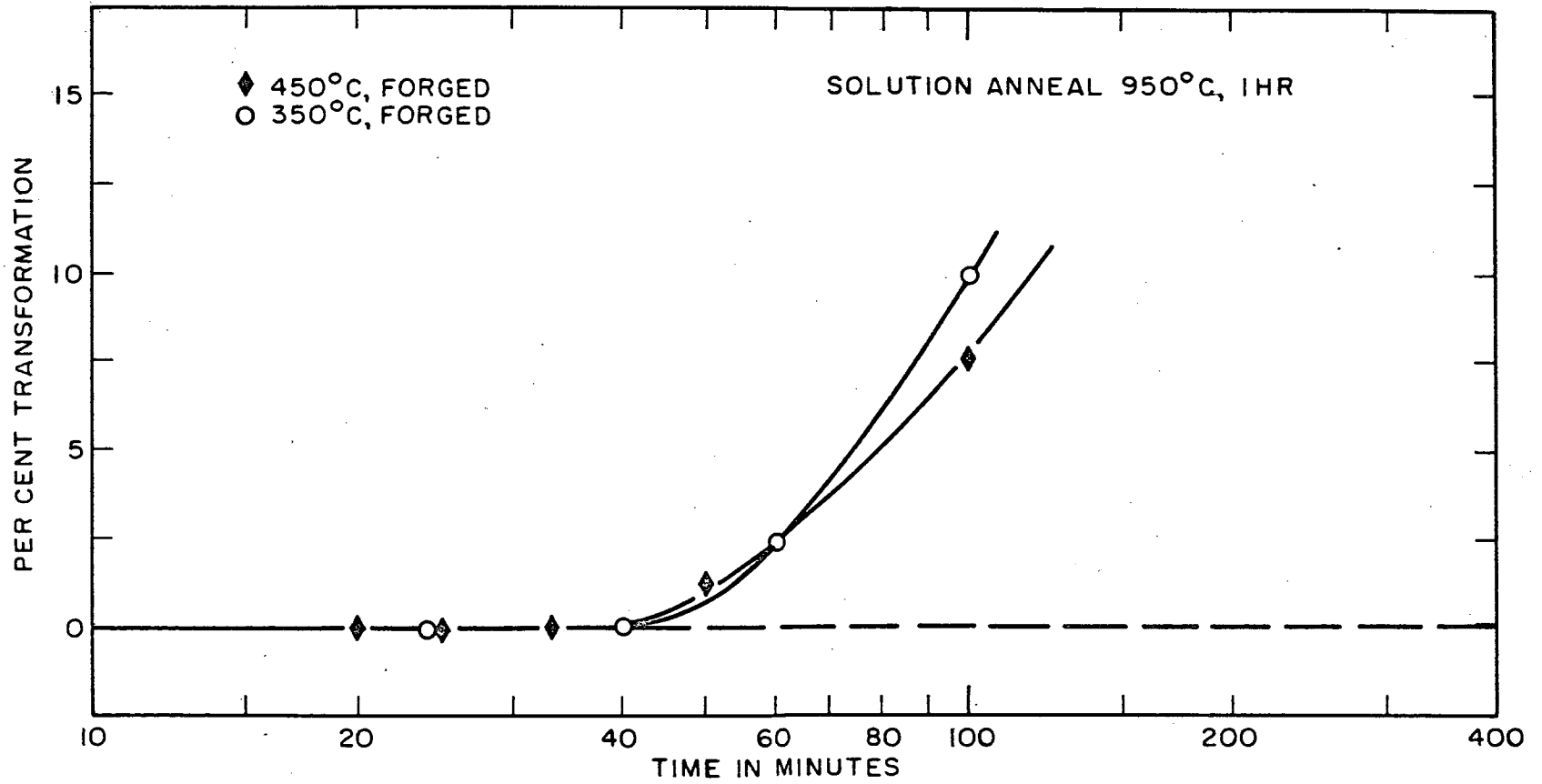WQ. Retained γ with increased
amount of transformation.

FIG. 145-AMOUNT OF METALLOGRAPHICALLY OBSERVED TRANSFORMATION VS
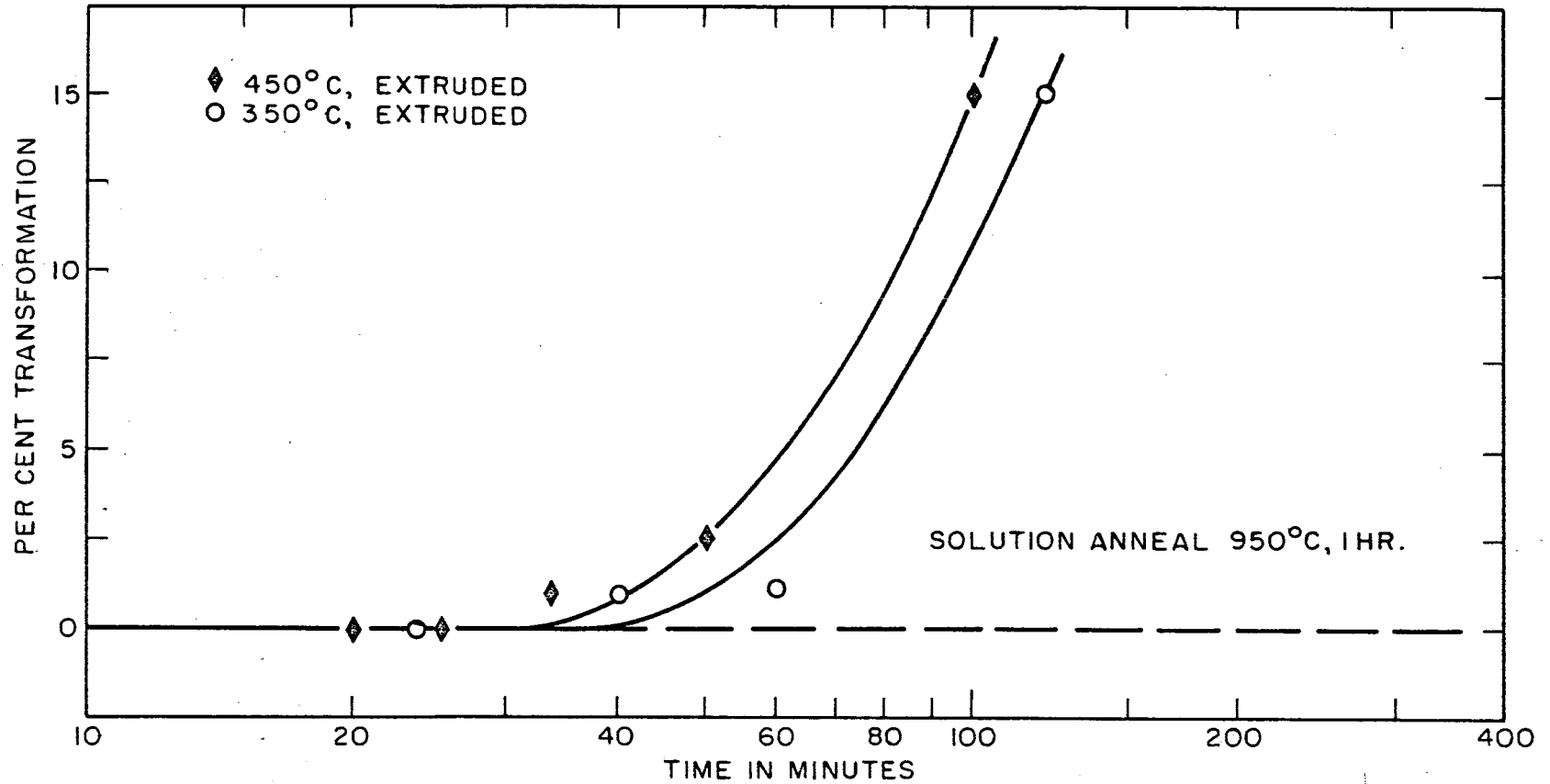COOLING TIME FOR A FORGED U-10w/o Nb ALLOY

FIG. 146-AMOUNT OF METALLOGRAPHICALLY OBSERVED TRANSFORMATION VS
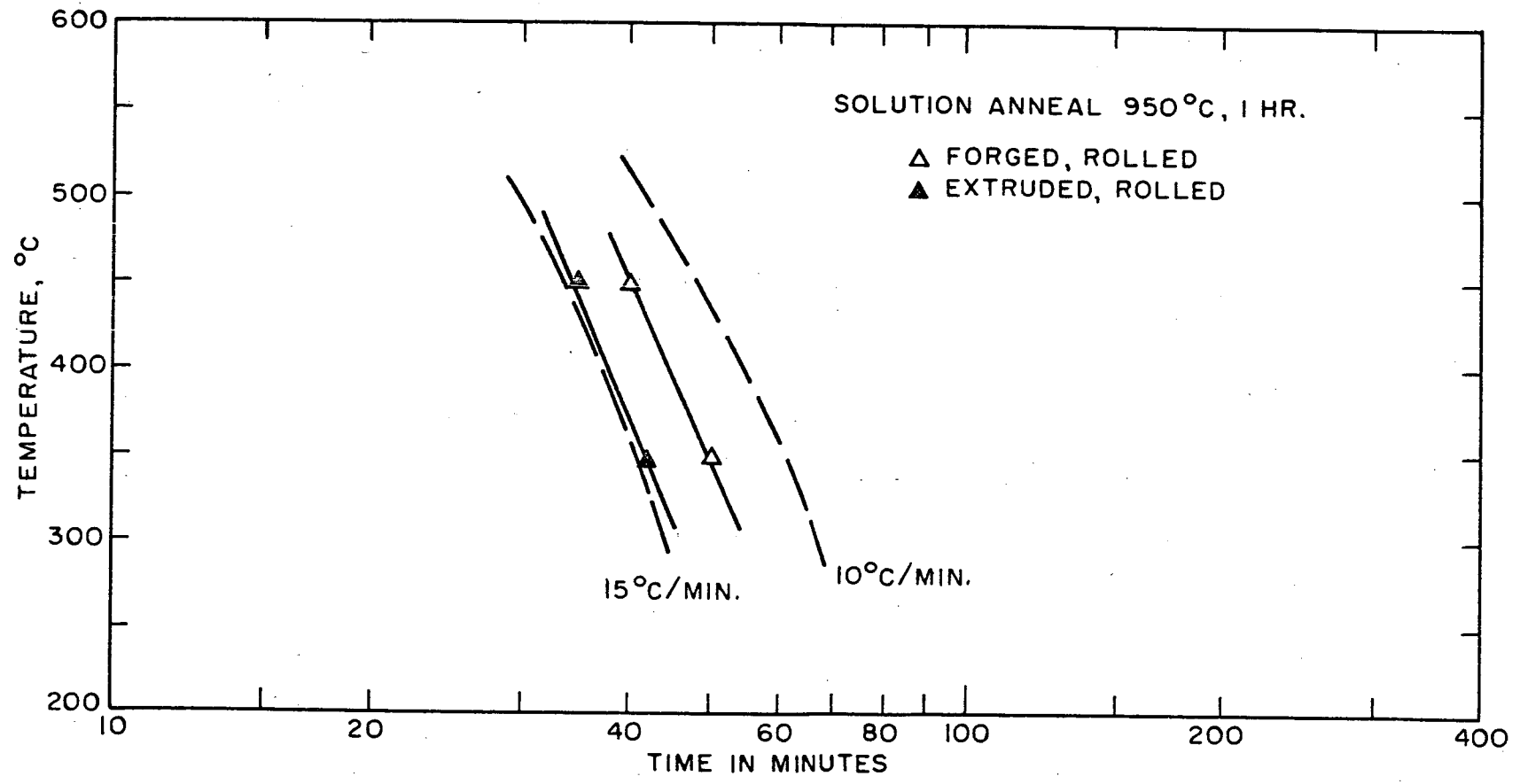COOLING TIME FOR EXTRUDED U-10w/o Nb ALLOYS

FIG. 147–PARTIAL CONTINUOUS COOLING TRANSFORMATION DIAGRAMS FOR FORGED
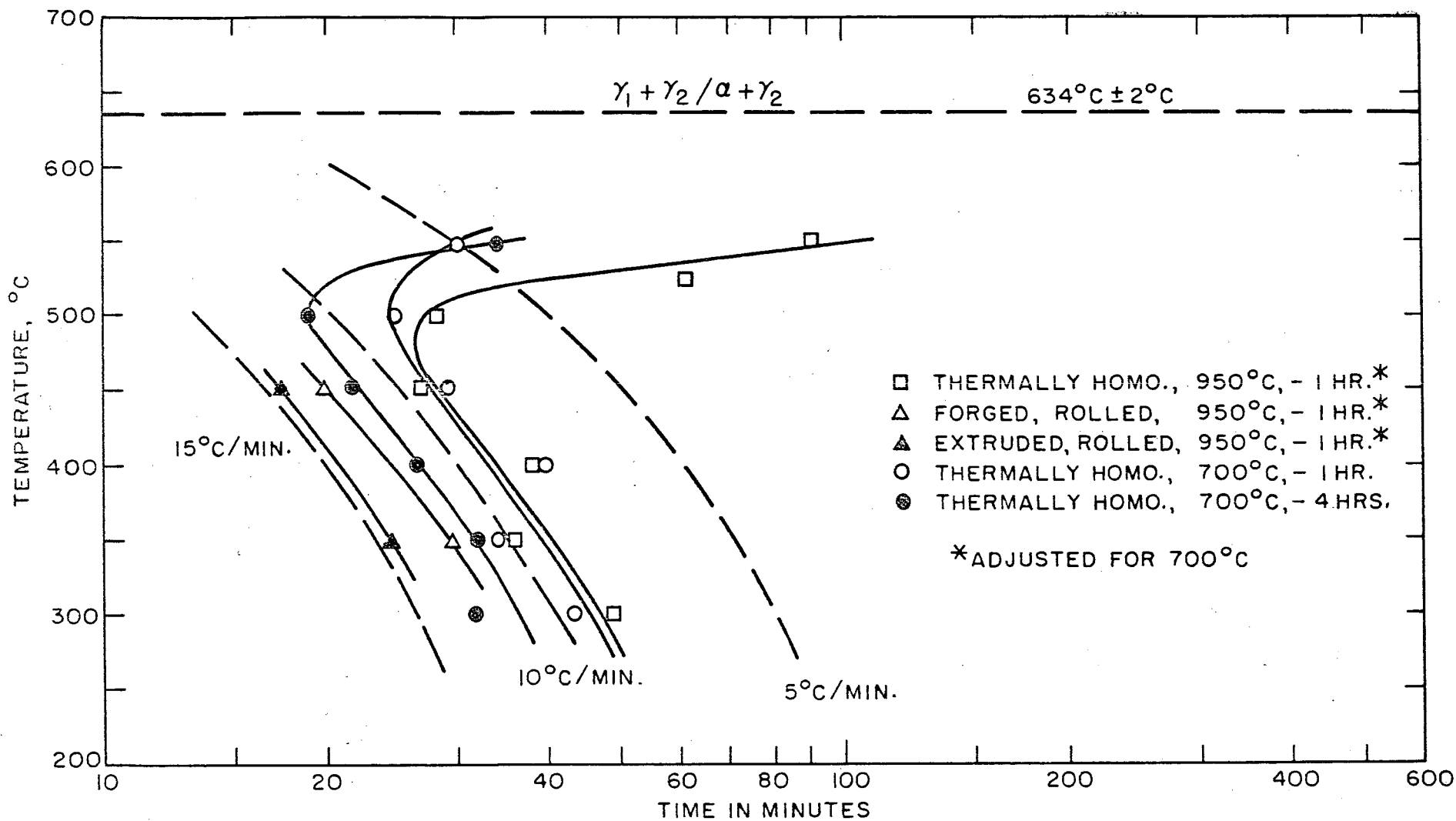AND EXTRUDED U-10w/o Nb ALLOY BASED ON METALLOGRAPHIC DATA

FIG. 148-COMPARATIVE CONTINUOUS COOLING TRANSFORMATION DIAGRAMS FOR U-10w/o Nb MATERIALS BASED ON METALLOGRAPHIC DATA

IV. SUMMARY

The transformation kinetics of eighteen U-Nb and U-Nb-X alloys have been investigated under this program. A nonconsumable tungsten electrode arc furnace was used to prepare 200-gram ingots of each composition. After a homogenization anneal, the samples were solution-treated at 900°C for 24 hours and water-quenched to retain the gamma phase. Isothermal annealing treatments were conducted in the range of 360° to 600°C for lengths of time up to 1000 hours. Specimens for thermal treatments were wrapped in molybdenum foil and encapsulated in Vycor bulbs.

The decomposition of the metastable gamma phase was studied by metallographic, hardness, electrical restivity, dilatometric and X-ray diffraction techniques. TTT curves based on metallograhpic, hardness and resistometric results show initiation of property changes at the various annealing temperatures. A number of dilatometric tests were conducted, and results were in general agreement with other techniques used to determine initiation of transformation. X-ray diffraction studies were used to identify the phases present in the decomposition products and to compare the different mechanisms of transformation.

The stability of the gamma phase as determined by the various techniques was improved by several of the alloy additions. In the binary U-Nb system, increasing the niobium content from 7w/o to 15w/o resulted in greatly increased stability; the U-15w/o Nb material was found to be the most stable of the alloys under investigation. Additions of zirconium, chromium, ruthenium and vanadium to a U-Nb base produced increased stability of the gamma phase. The elements titanium, nickel and silicon, added to a U-8w/o Nb base, produced alloys which transformed rapidly upon annealing. An intermetallic compound

Project No. B 095
Summary Report

was formed in the U-Nb-Si compositions; analyses showed that this compound contained a substantial amount of niobium. A low-melting compound was formed in the U-8w/o Nb-0.84w/o Ni alloy; incipient melting was observed at temperatures as low as 750°C.

For most of the compositions, X-ray diffraction studies showed that as the alpha phase was precipitated, the gamma matrix was continuously enriched in niobium, producing a shift of the peak for gamma to higher 2Θ values. Alloys exhibiting different mechanism of transformation included the U-Nb-Ti and U-Nb-V materials. In these compositions, both alpha and the equilibrium, niobium-rich γ_2 phase were co-precipitated.

Initiation of transformation, as determined by metallographic, hardness, resistivity and dilatometric techniques, showed some variation in each alloy at the various annealing temperatures. These variations were due to pre-precipitation hardening effects at the 360°C annealing temperature and to the precipitation of finely dispersed product throughout the matrix upon annealing at 450°C. Annealing all of the compositions at this temperature also produced transformation products at the grain boundaries; at higher temperatures, decomposition initiated only at the grain boundaries except in the U-8w/o Nb-1.94w/o Ti material where the fine decomposition in the matrix was also observed.

For most materials, the nose of TTT curves was at about 550°C, where property changes usually occurred in 1 hour or less. Considerably longer annealing times were required to produce changes at the lower temperatures. Strain resulting from cold rolling was shown to accelerate transformation of a U-7w/o Nb-2w/o Zr composition. Decomposition appeared in the microstructures as an oriented banding.

Project No. B 095
Summary Report

Continuous cooling studies were conducted with samples of the U-10w/o Nb alloy solution-annealed at 700° and 950°C, using metallographic and hardness techniques. The critical cooling rate for the thermally homogenized material solution annealed at 950°C for 1 hour was approximately 8.5°C per minute. A similar finding was obtained for the material solution-annealed at 700°C for 1 hour; but after 4 hours at this temperature, a critical cooling rate of 11°C per minute resulted. In addition to the arc-cast, thermally homogenized material produced at the Foundation, critical cooling rates were determined for induction-melted, hot-worked U-10w/o Nb alloys supplied by the Westinghouse Electric Corporation. Alloys which had been forged and rolled or extruded and rolled required cooling rates in the range of 13°C to 14.5°C per minute to retain the metastable gamma phase after a solution anneal of 950°C for 1 hour.

V. CONTRIBUTING PERSONNEL AND LOGBOOKS
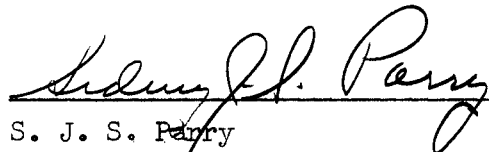
The following personnel contributed to the work reported herein:
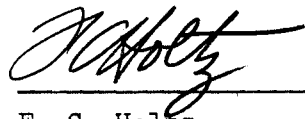
G. M. Blair   Technician - heat treating
R. F. Dragen   Technician - metallography
W. A. Dupraw   Chemical analyses
A. L. Hess   Technician - material preparation
F. C. Holtz   Project Leader
T. L. Marion   Technician - equipment construction
S. J. S. Parry   X-ray diffraction & continuous cooling
J. J. Rausch   Project Engineer (until May, 1956)
R. J. Van Thyne   Supervisor
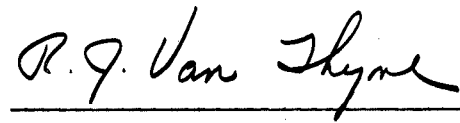B. Zajada   X-ray diffraction patterns

Data relating to the work reported herein are recorded in the following Foundation Logbooks: C-5305, -5306, -5413, -5642, -5735, -5736, -5737, -6041, -6038, and -6413.
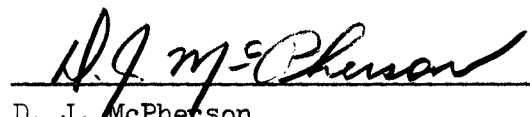
Respectfully submitted,

ARMOUR RESEARCH FOUNDATION
OF ILLINOIS INSTITUTE OF TECHNOLOGY

S. J. S. Parry
Assistant Metallurgist
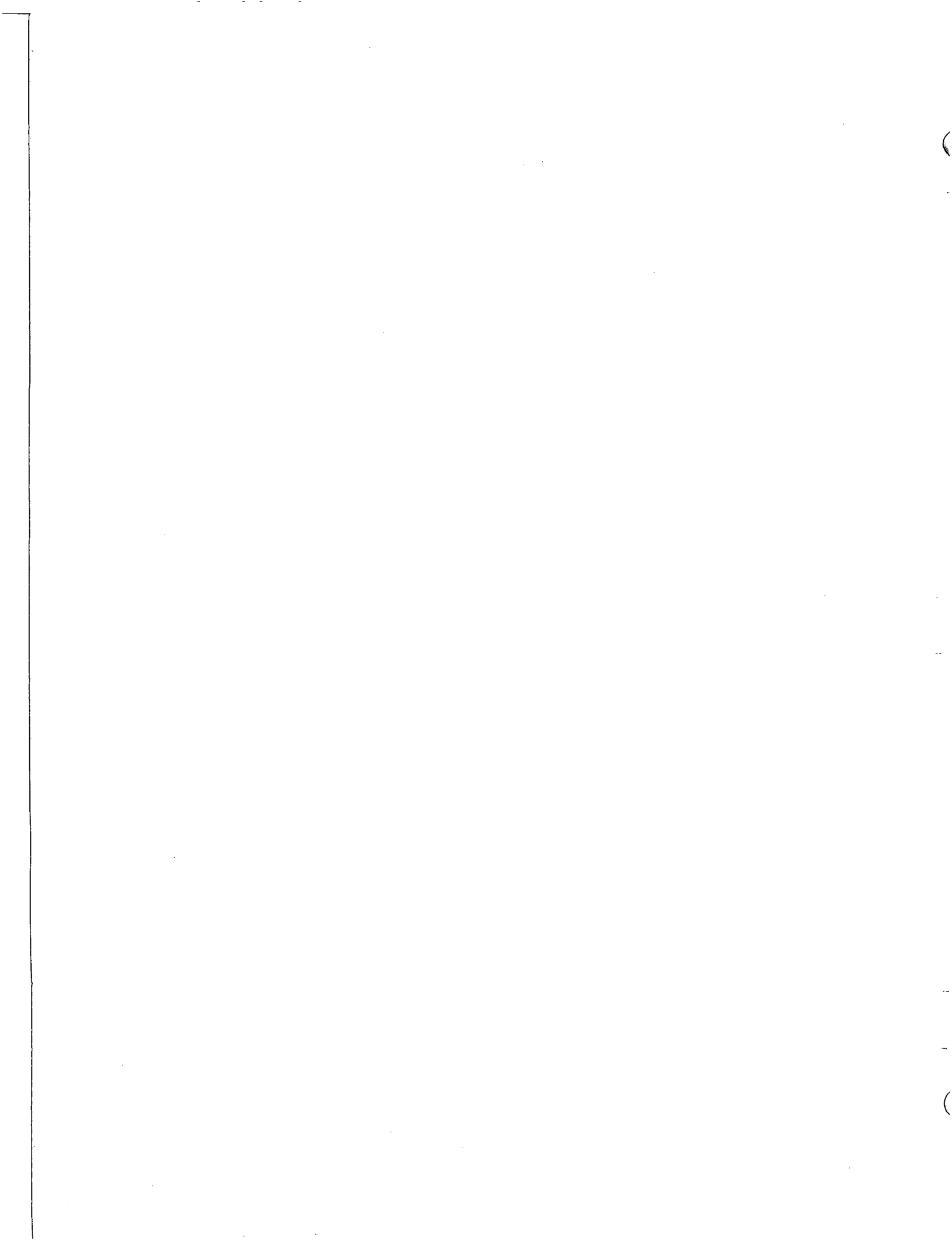

F. C. Holtz
Research Metallurgist

R. J. Van Thyne
Supervisor
Reactor Metallurgy

D. J. McPherson
Assistant Manager
Metals Research

rmh

REFERENCES

1. R. J. Van Thyne and D. J. McPherson, "Transformation Kinetics of Uranium-Base Alloys", Armour Research Foundation Final Report, Part I, to WAPD, Pittsburgh, Pennsylvania under Task 6 - Subcontract No. 73-(14-309).

2. H. A. Saller and F. A. Rough, "Compilation of United Stated and United Kingdom Uranium and Thorium Constitution Diagrams", BMI 1000, June, 1955.

3. Private communication with Dr. A. E. Dwight, Argonne National Laboratory, December, 1956.

255   195